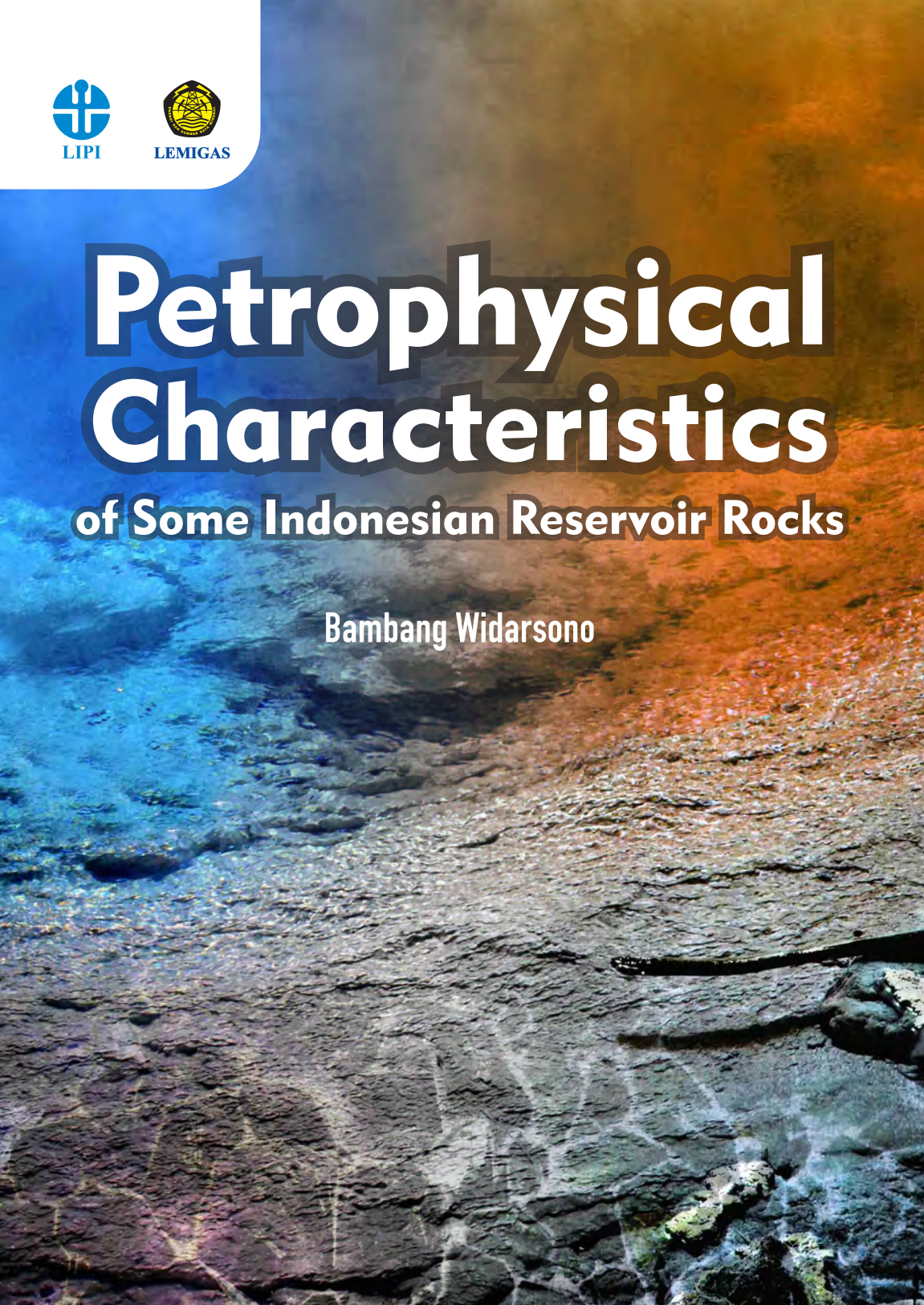
LIPI
LEMIGAS
Petrophysical Characteristics
of Some Indonesian Reservoir Rocks
Bambang Widarsono

Petrophysical Characteristics

of Some Indonesian Reservoir Rocks

Petrophysical Characteristics

of Some Indonesian Reservoir Rocks

Bambang Widarsono

LIPI Press

Cataloging-in-Publication Data

Petrophysical Characteristics of Some Indonesian Reservoir Rocks/Bambang Widarsono.–
Jakarta: LIPI Press, 2016.

xxxi + 257 pp.; 14,8 x 21cm

ISBN 978-979-799-840-0

1. Petrophysical 2. Reservoir rocks
3. Indonesian

553.28

Copy editor : Annisa W.
Proofreader : Martinus Helmiawan and Sarwendah Puspita Dewi
Layouter : Erna Rumbiati and Prapti Sasiwi
Cover Designer : Rusli Fazi
Cover Pic. Source : https://pixabay.com

First Edition : February 2016

Published by :
LIPI Press, member of Ikapi
Jln. Gondangdia Lama 39, Menteng, Jakarta 10350
Phone. (021) 314 0228, 314 6942. Fax.: (021) 314 4591
E-mail: press@mail.lipi.go.id

CONTENTS

LIST OF FIGURE

LIST OF TABLE

EDITORIAL NOTE

As a scientific publisher, LIPI Press holds on high responsibility to provide high-quality scientific publication. The provision of qualified publication is the epitome of our works to participate in enlightening society intelligence and awareness as stated in The 1945 Constitution of the Republic of Indonesia.

The book *Petrophysical Characteristics of Some Indonesian Reservoir Rocks* offers a solution to answer the ever rising demand of Indonesia's national oil and gas demands. Keeping the oil and gas reserves' production is important for our energy supply, and reservoir characterization is crucial for reservoir's further development. The book will cover petrophysical characterization of some of the most important reservoirs in Indonesia.

We surely hope this book could give new insights and information, especially about importance of petrophysical properties in petroleum industry. As a final note, we would like to deliver our heartfelt gratitude to everyone taking part in the process of this book.

LIPI Press

PREFACE

The need to maintain and improve Indonesia's national oil and gas reserves and production requires support from various sectors of the industry. Apart from the need to discover new reserves, efforts have also to be spent in optimizing and maximizing reserves of the generally mature producing oil and gas fields. In doing so, reservoir characterization is an integral part in modeling and planning for field's further developments, production optimization, and any other activities that are aimed at production and reserves improvements. In reservoir characterization, petrophysical properties play a pivotal role in understanding how reservoirs may react under various production schemes.

Petrophysical properties of reservoir rocks are normally acquisitioned through both direct (laboratory tests and field survey) and indirect methods (geophysical interpretations), of which results of the direct approach are usually taken as sources of comparison and validity. This volume is made up of five published works that present results of studies on petrophysical characteristics of various Indonesia's reservoir rocks derived from laboratory tests. This underlines that all data values were directly measured on rock samples from fields, hence emphasizing representative and originality of data. For this, I would like to express my gratitude to PPPTMGB "LEMIGAS" as the administrator of the laboratory and the Ministry of Energy and Mineral Resources of the Republic of Indonesia as the overseeing authority of all subsurface data for permitting to use the data.

Through the use of the data—and the ensuing analyses and published articles—I sincerely hope that this volume will serve as

a contribution to the understanding over Indonesia's reservoir rocks characteristics. This in turn will assist many activities in scientific/ research areas and in engineering-related applications at various scales through introduction of local knowledge into the universally known standard methods and approaches. Trying to make this book easily understood, I use illustrations as well. Some of them are taken from my previous publications, and the rests are purposedly made for completing this book. Being aware that the amount of data involved in the making of the volume is most likely to be just a minor part of the entire data available nationally, I also hope that this will encourage others to conduct similar studies using other sets of relevant data in order to improve further our comprehension over Indonesia's reservoir rock characteristics.

Upon completion of this book, I also wish to express my gratitude to Professor Pudji Permadi from Petroleum and Mining Engineering Faculty of The Bandung Institute of Technology and Dr. Hermes Panggabean from The Geological Agency-Ministry of Energy and Mineral Resources for providing technical advises and suggestions. Special thanks are also expressed to co-authors of the technical papers used as parts of this book, Mr. Ari Muladi and Mr. Indra Jaya. Valuable supports have also been provided by many LEMIGAS colleagues; amongst others are Ms. Junita Musu and Mr. Ridwan for supporting in geology-related information and material, as well as Mr. Daru Siswanto, Mr. Bagus Aribowo, and others at LEMIGAS' Afilliation and Information Division for the book's preparation and editorial works. All those supports are highly appreciated.

Jakarta, March 2015

Writer

FOREWORD

This is the first textbook ever treating comprehensively the petrophysical data of Indonesian geologic formations, mainly the productive ones. It contains a huge volume of the related data and information presented in the forms of materials that have been carefully analyzed, interpreted, and discussed.

The author, based on his experiences of doing researches in the petrophysics area at the PPPTMGB "Lemigas" and serving the petroleum industry in the fields of petrophysics and reservoir engineering, shares his knowledge delivered in the form of this book. All the materials contained in this book are undoubtedly needed for those who are involved in the related research areas and the petroleum industry.

It is expected that publishing this book is an important step toward provision of the petrophysic reference in the effort of developing and improving the Indonesian oil and gas reserves.

Bandung, May 2015

Prof. Pudji Permadi

CHAPTER I
INTRODUCTION

A. General

Petrophysics is a scientific branch of applied physics that was closely associated with geology and geophysics. It has developed from the need to understand between rock's states of solid, lithology, mineral composition, and structure and their physical properties. For sedimentary rocks, the need has expanded further to physical properties that also reflect rock's pore features such as pore types, structures, filling, and surface characteristics. The concept of petrophysics actually encompasses a wide area of scientific studies that include activities such as direct observations of rocks in geological field surveys, geophysical surveys (e.g. gravity, magnetic, resistivity, and velocity), and laboratory tests and observations (e.g. rock mechanics and rock hydraulic property measurements). Laboratory petrophysics in its development has also been very closely related to other geological laboratory activities as in mineralogy, petrography, and geochemistry. Attentions have also been given to studying petrophysical aspects of lunar and other extraterrestrial rocks with their relevant to other sciences such as astronomy.

The petrophysical studies have established in understanding the relations between rock physical feature and its property, and in return

have enabled to present the model. Equations, correlations, formulas and other forms of mathematical models have been produced to represent the relationships, claimed to be valid for either general or local applications. Rapid developments in computational capacity encourage extensive and intensive use of numerical methods for 3D rock models at various scales.

Applications of petrophysics encompass various fields of activity. At macro scales, petrophysics has contributed in large scales studies such as studies on earth's crust deep mantle, earth's history, continental drifts, and tectonics. At meso scales, studies in volcanology, regional geology, and geophysical prospecting benefit much from petrophysics. At lower levels, various geological and engineering applications rely heavily on petrophysical properties produced by petrophysical studies and testing. Applications of petroleum engineering, geological modeling, hydrology, mining, and underground storage are exemplary traditional users of petrophysical properties. The last decade of the previous century up to present has witnessed extensive use of petrophysics in new areas such as exploitation of unconventional hydrocarbon (shale oil/gas, bitumen, and coal bed methane) and carbon capture and storage (CCS).

In petroleum industry, however, applied petrophysics has been narrowed in its definition and scope. Common understanding over petrophysical properties is limited to properties that mostly represent storage capacity, flow capacity, fluid contents, clay contents, wetting tendency, and pore structure of formation/sedimentary rocks. The term of petrophysical properties is often used to differentiate it from other rock properties obtained from geomechanical and other geological rock data acquisition methods. Basic rock properties, such as porosity, permeability, wettability, density, fluid saturation, and special/advanced rock properties, such as relative permeability, capillary pressure, and electrical properties are in general categorized

as petrophysical properties. These properties are traditionally acquisitioned from direct laboratory tests on core samples, but a considerably large volume of studies and research have also been waged to find and establish methods to retrieve such information from less direct techniques such as from well logging, well testing, inter-well tracer, and even seismic field survey.

In Indonesia's petroleum industry, the place and role that are played by petrophysics are not different from any other places in the world. Petrophysics plays a crucial role in various applications in petroleum industry. One aspect that differs Indonesia's petroleum industry from similar industry in other countries, especially in developed countries, is the general rarity in publications that present aspects of Indonesian reservoir rocks petrophysical properties. This book is hoped to some extent fill this absence. By no means that all petrophysical properties are presented here, and works contained in this volume do not have any pretension to represent all reservoir rocks in Indonesia.

B. Role of Petrophysical Properties in Petroleum Industry

Petrophysics plays very important part in studies or activities aimed at understanding nature and characteristics of a potential oil/gas reservoir as a part of a big scheme for field development. The activities, commonly known as reservoir description or reservoir characterization, include retrieving information regarding petrophysical properties is through both direct (i.e. core analysis, mud logging and cutting logging) and indirect (i.e. core analysis/measurement while drilling, well pressure transient analysis and seismic attribute analysis) techniques (Figure 1.1). The role of petrophysical properties and other information derived from core analysis is that apart from providing

formation rocks physical features, it also serves as means of comparison/calibration for the indirect techniques. The main objective of the comparison/calibration is certainly to improve quality of quantitative values provided by the indirect techniques.

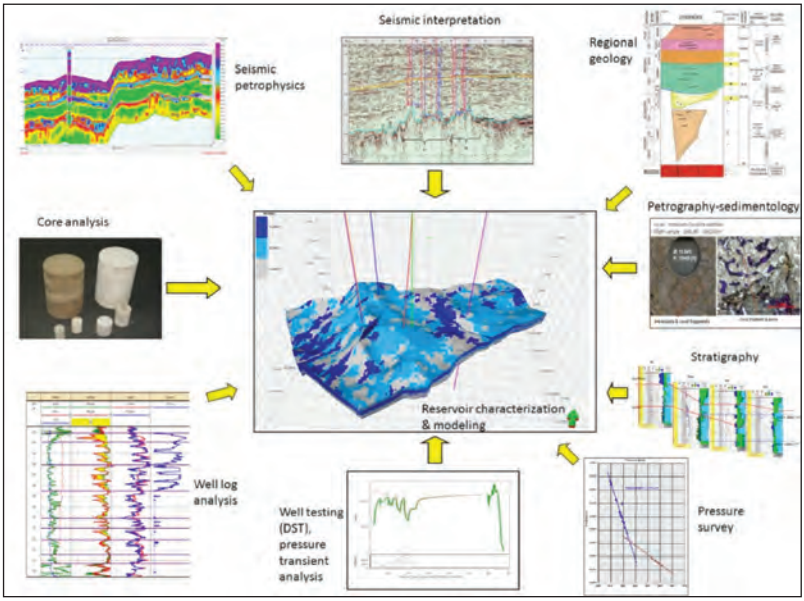

Source: Widarsono's documentation

Figure 1.1 The schematic diagram shows sources of data needed for reservoir characterization leading to geological reservoir modeling. The direct measurement method of core analysis and indirect methods of well-log analysis, well testing and seismic petrophysics contribute to providing petrophysical properties. Core analysis results are—through various means—used to validate results to be produced by the indirect methods.

In petrophysical analysis for reservoir characterization, a range of activities is carried out. The activities include:

1) **Determination of lithology and depositional facies**; through combining information obtained from drill cutting, log char-

acteristics, and is supported by petrographic and mineralogical determinations laboratory. Rock types, clay types, and mineral composition are determined and used as reference in calculation of porosity and water saturation. Anomalous minerals, such as heavy and conductive minerals, have to be noted. The depositional facies is also used as a source of comparison in grouping petrophysical properties and to the establishment of hydraulic facies.

2) **Determination of porosity**; through well log analysis and is validated using porosity derived from core analysis. Various log analysis models and techniques are available depending on log data reliability and availability. Porosity values and profiles from core laboratory testing under overburden pressure are used as a reference for validity. Lithology, mineral composition, and clay fraction play an important role in determining rock matrix properties needed by the porosity models. Potential bias due to presence of minor minerals must be compensated. Porosity trends and characteristics could be different from one region to another, depending on factors such as burial history, tectonics, thermal gradient, and source rocks. Porosity estimates derived from seismic velocity impedance benefit for their validity through the use of averaged log porosity and/or regional vertical porosity trends.

3) **Determination of permeability**; traditionally performed through the use of other petrophysical properties such as porosity and irreducible water saturation (S_{wirr}). Porosity-permeability transform is normally developed using data from core analysis and permeability is determined through its application on porosity from porosity logs. Various empirical models can also be used with S_{wirr} as additional required variable. Similar to poros-

ity, permeability values and profile from core analysis (under overburden pressure) are also used as calibrator and reference for validity. Another traditional means of determining permeability is through well test analysis. Along with determination of information regarding reservoir pressure, formation damage, radius of investigation, and location of permeability barrier permeability are determined using specific model and completion schemes. Permeability validity is also achieved through the use of averaged core permeability. Like porosity, permeability is then put into both vertical and horizontal variograms for geo-statistical reservoir modeling. Permeability anisotropy (K_v/K_h) from this data is also required for reservoir simulation modeling.

4) **Determination of water saturation**; is normally made through log analysis and utilization of core derived capillary pressure data. For open-hole logs, resistivity log data is used as the main input to the most appropriate water saturation (S_w) models, while for cased wellbore logs, such as carbon/oxygen (C/O) and nuclear magnetic resonance (NMR) are used. This means of S_w determination is often combined with S_w determination using core-derived drainage capillary pressure data especially for heterogeneous reservoirs with wide and varied transition zone. Validated capillary pressure curves are normalized and converted to saturation-height function(s) that are then put into reservoir model grids following facies classification and distribution in reservoir. Validity of S_w estimates is checked using combined core (e.g. core displacement test, fractional flow) and well testing (e.g. DST and MDT) data. Recent developments in seismic petrophysics have been attempting to develop techniques to derive S_w from seismic attributes.

5) **Determination of cut-off values**; is made in order to distinguish between pay and non-pay parts of reservoir. Standard cut-off parameters used in petrophysical analysis are porosity/permeability, shale contents, and water saturation. These parameters are estimated as core analysis data (e.g. 'flow' or 'no-flow' permeability), well log output, and well testing data. Then they are cross-examined. Through applying these parameters in well log interpretation reservoir net pay thickness, data is obtained.

6) **Special petrophysical properties**; are measured in special core analysis laboratory (SCAL). These properties encompass all core properties other than the basic rock petrophysical properties such as porosity, permeability, and bulk density. Relative permeability and capillary pressure, with regard to fluid types and displacement schemes, are the principle measured properties. Through selection and normalization, the properties help in governing connate or irreducible water saturation (S_{wirr}) distribution and flow performance in the geological and simulation models. Rock wettability plays a crucial role in which it influence shapes of data curves considerably. Rock pore volume compressibility is another important property that reflects additional driving mechanism in reservoir, from which representative curves have to be chosen and incorporated into simulation model.

As in the case of acquisition techniques with their respective scopes of investigation, reservoir characterization also encompasses different scales. This is related closely to what reservoir characterization is for. In general, there are two scale-related utilizations of reservoir characterizations. First, well-scale utilization which includes well-based applications such as well stimulation (e.g. acidizing and hydraulic fracturing), production optimization, well completion, and support in studying inter-well connectivity. Second, field-scale

applications through development of static and dynamic reservoir models for estimation of original oil/gas in place, production forecast, production strategy, and related activities such as design of field facilities and economics evaluation (Figure 1.2).

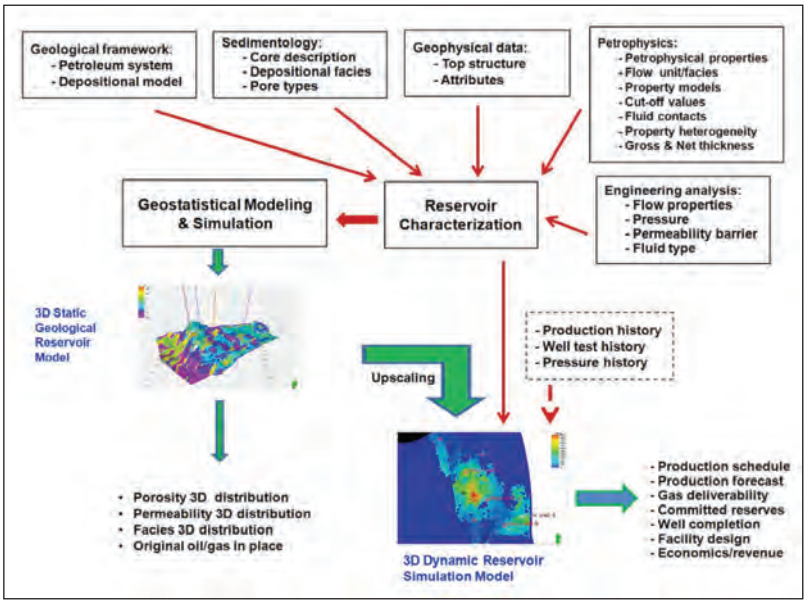

Source: Widarsono's documentation

Figure 1.2 Workflow of activities from reservoir characterization to static geological and reservoir simulation modeling. Note that data of production, testing, and pressure history is used in the case of fields having production life.

C. Data Origin

In the studies forming the five main chapters of this book, data from thousands of core samples were involved. These samples were essentially tested in LEMIGAS core laboratory—since the laboratory's establishment in mid 1970s—under both research-related and commercial purposes. Some samples are still available physically and the rest of the samples were stored in the form of images, descriptions, and reports in LEMIGAS' archive. Observations and review over both physical samples and reports have revealed the wide range of variety in reservoir rock types and origins. This part of this introductory chapter presents brief overview over the twelve main productive sedimentary basins (Figure 1.3) from which the core samples used in the studies were derived from. The objective of presenting the brief overview is not as means for giving full understanding of the basins' regional setting, but instead is to give brief general review over the basins' stratigraphic aspects, productive formations, and their oil and gas reservoirs. The twelve sedimentary basins are North Sumatra, Central Sumatra, South Sumatra, West Natuna, Sunda-Asri, Northwest Java, Northeast Java, Barito, Kutai, Tarakan, Bone, Banggai, Salawati, and Bintuni. Most of the overview are based on information presented in LEMIGAS (2006) and Inameta (2006).

1) **North Sumatra Basin**. The North Sumatra Basin is an asymmetrical basin located in the northeast part of Sumatra island with roughly 10,500 km^2 of land area. The basin is geologicaly surounded by Andaman Islands to the north, Malacca Platform to the East, Asahan Arch to the south, and Barisan Mountain to the west. Stratigraphically, the basin is regarded as underlain by pre-Tertiary 'economic basement' that consists of dense and fractured sandstones and carbonates. On top of the basement is a subsided deposition of sediments of up to 5,500

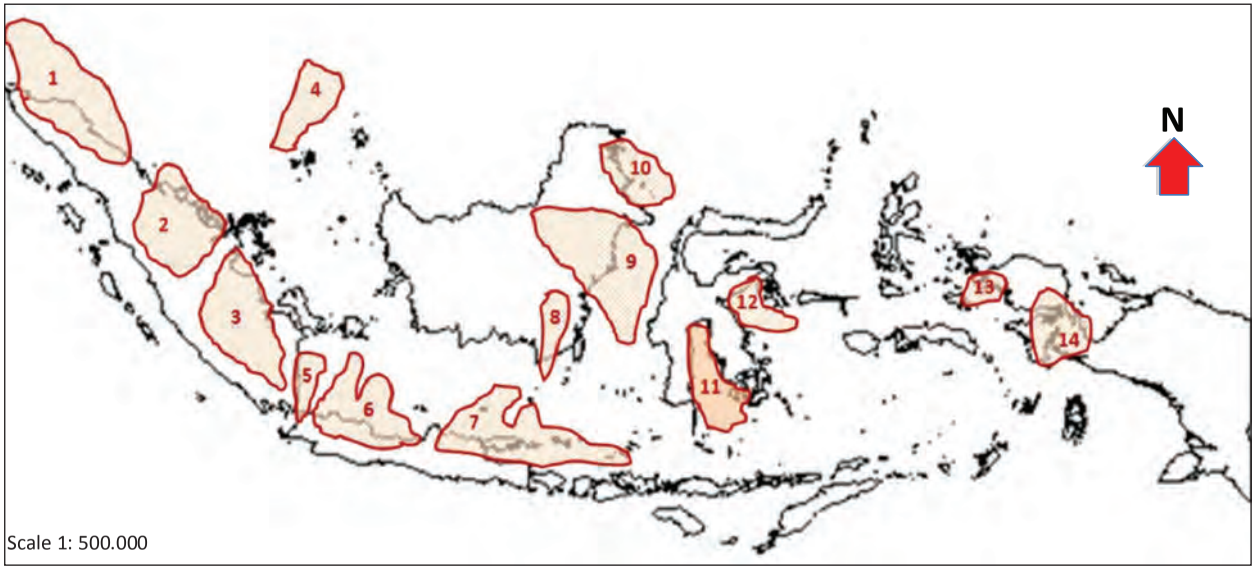

Figure 1.3 Productive sedimentary basins in Indonesia, with their approximate size and shape, from which core samples for the studies are taken. The basins are: 1) North Sumatra, 2) Central Sumatra, 3) South Sumatra, 4) West Natuna, 5) Sunda-Asri, 6) Northwest Java, 7) Northeast Java, 8) Barito, 9) Kutai, 10) Tarakan, 11) Bone, 12) Banggai, 13) Salawati, and 14) Bintuni.

meter thick at the center of the basin. The sediment column is made of Tampur Formation, Bruksah and Bampo Formations that were formed during early syn-rift phase, Belumai and Peutu Formations formed during late syn-rift to transitional phase, Baong Formation as a result of a major transgression, Keutapang Formation that was formed during syn-inversion regime, and younger formations of Seurula and Julurayeu. The two main source rock formations are the Miocene (Figure 1.4) neritic-bathyal Baong and the Oligocene-Early Miocene shallow marine Bampo Formations. Main reservoirs in the North Sumatra Basin are the Belumai's sandstones (porosity = 15–20%, permeability = 5–500 mD) and localized limestones. Other important reservoirs are the Peutu's Arun limestones and Malacca carbonates (porosity = 2–20%), while some light oils are trapped in the deltaic lobes and estuarine Keutapang sandstones (average porosity = 20%). Minor reservoirs are also found in the middle Baong turbidite sands (average porosity = 25%) and the porous intra-rift Bruksah Formation.

2) **Central Sumatra Basin**. The Central Sumatra Basin (Area= +119,000 km^2) was formed during the Eocene-Oligocene in form of half grabens and horst blocks. A column of sediments was deposited on the pre-Tertiary Basement of slate, phyllite, meta-arcose, and argillite. The Basement is overlain by Oligocene Kelesa-Pematang Formation, Upper Oligocene-Early Miocene Lakat (Menggala-Bangko) Formation, Early Miocene Tualang (Bangko-Bekasap-Duri) Formation, Early-Middle Miocene Telisa Formation, Middle Miocene Petani Formation, and Late Miocene Korinci-Minas Formation. The main source rocks in the basin is the lacustrine brown shales of the Pematang/Kelesa Formation, with the richest parts confined in a series of grabens trending north-south. The reservoirs in

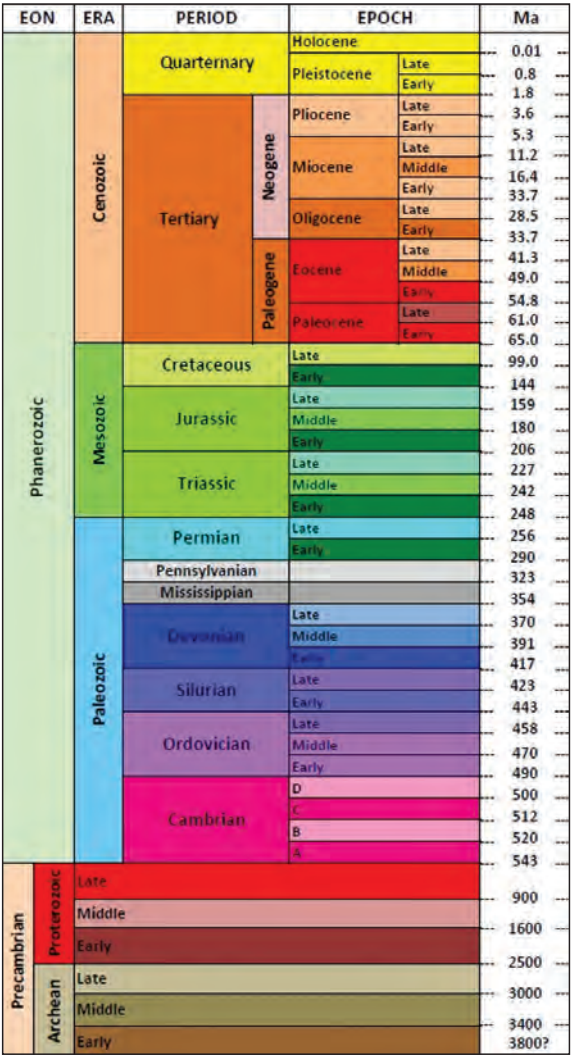

Source: U. S Geological Survey (2007)

Figure 1.4 Basic/General Geological Time

this basin occur in the Sihapas Group (Menggala, Bangko, Bekasap, Duri, and Telisa Formations), Pematang Formation, and Petani/Minas Formation. Main reservoirs of the Sihapas Group are situated in the lower part of it, which in general are thick, clean, and quartzose sandstones with minor glauconites, detrital clays, feldspars, and rock fragments. Sihapas Group's thickness varies within 230–260 m, and porosity in general is good with intergranular primary porosity as the predominant feature (porosity = 16–28%, permeability = 575–2,400 mD). The open shallow marine sandstone reservoirs in Telisa, despite lower quality, are also important with thickness varies within 115–210 m with average porosity of 15%. For Pematang Formation, on the other hand, thick coarse-grained and conglomeratic sandstones serve as the main reservoirs. Other reservoirs are the shaly sandstone reservoirs of the Petani Formation and the conglomeratic sandstone of Minas Formation.

3) **South Sumatra Basin**. The South Sumatra Basin (Area = ±85,000 km^2) was formed in the latest pre-Tertiary time (Upper Cretaceous) to the beginning of Tertiary time. The basin is confined by the Barisan Mountains to the southwest and the pre-Tertiary Sunda Shelf to the northeast, and contains two sub-basins of Jambi (in the northern quarter of the basin) and Palembang. The Cretaceous Formations can at least be grouped into two Formations of the volcanoclastic Saling and Linsing, while the Tertiary part of the basin contains Lahat, Pre-Baturaja Clastics (Lemat in some parts), Baturaja, Telisa/Gumai, and Palembang (Air Benakat, Muara Enim, and Kasai) Formations. The main source rocks are black shales in the Late Eocene-Lower Oligocene Lahat and mudstones in the Upper Oligocene-Early Miocene Talang Akar and the Early-Middle Miocene Gumai Formations. Sandstone reservoirs are

found in Talang Akar and Air Benakat Formations, whereas carbonate reservoirs are contained in the Baturaja Formation. The Talang Akar Sandstones consists of quartz sandstones and the carbonates are grouped into two of lagoon facies with wackestone texture and reefal facies consisting of coral, red algae, and molluscs with wackestone/packstone texture. In Jambi sub-basin, the largest production comes from the Air Benakat's deltaic-shallow marine sandstone reservoirs (porosity = 10–27%) and the Talang Akar's conglomeratic sandstones (max porosity = 30%, permeability = 12–180 mD). In this sub-basin reservoirs, the Baturaja Formation (max porosity = 19%) contributes to a minor production in southeastern of the sub-basin. In the Palembang sub-Basin, Talang Akar (porosity = 15–28%) and Baturaja Reservoirs are the major oil and gas producers, whilst reservoirs in Air Benakat and Muara Enim Formations come in second place. Some sandstone reservoirs in Gumai Formation also produce oil and gas.

4) **West Natuna Basin**. The West Natuna Basin (Area = ±90,000 km^2) is situated in the South China Sea. Geologically, the basin is confined by Khorat Platform to the north, Natuna Arch to the east, and Sunda Shelf to the south. In the west, the basin is directly connected to Malaya Basin since the West Natuna Basin is actually the eastern part of Malaya Basin. The West Natuna Basin is a Tertiary sedimentary basin that predominantly produces gas. The Tertiary sedimentary Formations that were deposited over the Pre-Tertiary Basement are the Lower Oligocene Gabus (up to 2,000 m in thickness), the Early Miocene Barat, and the Early-Late Miocene Arang Formations (up to 1,500 m in thickness). Over the three main Formations, Muda Formation was deposited in the form of shales and sandstones during Late Miocene-Pleistocene (thickness = 600–800

m). The main source rocks are the lacustrine shales of Barat Formation and the siltstones of the Lower Gabus Formation. Main sandstone reservoirs are contained in Gabus Formation with average porosity of 22%.

5) **Sunda-Asri Basin**. The Sunda-Asri Basin (Area = ±20,000 km^2) is located in the north of Sunda Strait. Geologically, the basin is formed of a series of grabens (Asri, Nunung, and Kitty-Nora grabens) and its roughly triangular shape is confined by the Sundari Platform to the north, the Seribu Platform to the east-south, and the Lampung High to the west-south. The stratigraphic setting of the Sunda-Asri Basin is similar to the South Sumatra Basin. Some similarities in formations also occur with some formations in Northwest Java Basin, in the form of presence of the Cisubuh and Parigi Formations. Deposition in the basin was initiated by the formation of the deltaic-lacustrine-fluvial Banuwati Formation during the first half of Paleogene. Further deposition occured and formed the Lower Oligocene-Early Miocene Talang Akar Formation, the Early Miocene marine Baturaja Formation, the Early Miocene near-bathyal Gumai, the Early-Middle Miocene littoral to shallow marine Air Benakat Formation with Parigi unit at its base, and the Late Miocene-Upper Pliocene Formation. The main source rocks are the Banuwati shale that acts as source rocks to some oil reservoirs in the basin. Better source rocks are considered to be the mudstone and siltstone of the Talang Akar Formation. These organic rich sediments are widely deposited adjacent to the reservoirs in the same formation. Reservoirs in the Sunda-Asri Basin are the alluvial fans sandstones and conglomerates in Banuwati Formation (porosity = 5–15%), the fluviatile channel quartz sandstones in Talang Akar Formation (porosity = 20–33%, permeability of up to several Darcies),

and the really extensive and often thick carbonates in Baturaja Formation. Other potential reservoirs are the Krisna sandstone, member of the Gumai seal Formation. However, although the sandstones are often thick (up to 60 m), the argillaceous and calcite cemented sandstones are of poor quality in general.

6) **Nortwest Java Basin**. The Northwest Java Basin (Area = ±61,000 km^2) is geologically located between Sunda Microplate and Indo-Australia Plate. The N-S normal faulting controlled formation of grabens and horst and therefore helping the sedimentation pattern in the basin. The Northwest Java Basin contains several sub-basins of Ciputat, Arjuna, Pasir Putih, Vera, and Jatibarang. The oldest sedimentary deposit in the basin is the Middle Eocene-Lower Oligocene Jatibarang Formation, which uncomformably overlied the pre-Tertiary Basement. This thick swampy-marine volcanic clastic and basaltic Formation is overlain unconformably by the Upper Oligocene Talang Akar (Lower Cibulakan) Formation's shales, sandstones, siltstones, and coals. The Talang Akar is comformably overlain by the Early Miocene Baturaja (Middle Cibulakan) Formation, which was followed by the Middle Miocene Upper Cibulakan Formation, the Late Miocene Parigi limestone Formation, and the Late Miocene-Late Pliocene Cisubuh claystone-siltstone Formation. The main source rocks in the basin are believed to be the carbonaceous shales of the Talang Akar Formation and the lacustrine black shales of the Jatibarang Formation. The Baturaja Formation is also considered as potential source rocks due to its high organic contents, but with low hydrogen index. Reservoirs in this basin are mainly in the four Formations, with fractured volcanoclastics in the Jatibarang Formation, deltaic sandstones of the Talang Akar Formation (porosity = 23–35%, permeability = 150–2,500 mD), deltaic-shallow

marine sandstones of the Upper Cibulakan Formation (average porosity of 30%, permeability up to 500 mD), and reefal build-up carbonates in Parigi Formation. The upper part of the Parigi Formation is a widely distributed platform/bioherm unit (150–500 m in thickness) with good porosity vugular, moldic, and intergranular reservoirs. It contains and keeps producing huge amounts of gas.

7) **Northeast Java Basin**. The Northeast Java Basin (Area = ±54,000 km^2) is tectonically complex that is roughly confined by Barito Platform to the north and the west, Sibaru Platform to the east, and Kendeng zone to the south for the onshore part. There are several sub-basins including Masalembo, Sakala, Lombok, South Kangean, Madura Strait, Ngimbang, Tuban, and Porong. The pre-Tertiary Basement was overlain during Paleogene by Middle-Late Miocene Pre-CD, which consists of alluvial, fluvial, and lacustrine sediments of basal clastics and coaly shales. On top of the Pre-CD, the Late Miocene-Lower Oligocene CD limestone Formation was deposited. On the onshore area of the basin, the Ngimbang clastic Formation was deposited over the pre-Ngimbang Formation during Late Eocene-Lower Oligocene. Proportion of carbonates in the basin increases with the deposition of Kujung II limestones in open marine transgression and was followed by deposition of the wide Kujung I Platform during Upper Oligocene-Early Miocene. Over the Kujung, Tuban (onshore) and Rancak (offshore) Formations were deposited locally during Early Miocene, and both overlain unconformably by sands of Ngrayong Members during Middle Miocene. During the rest of the Miocene and Pliocene, Wonocolo and Kawengan Formations were deposited mostly in the onshore part of the basin, while Karen limestone Formation was a wide platform in the offshore part of the ba-

sin. The main source rocks in the basin are thought to be the lower parts of the Ngrayong and Kujung Formations. Coal layers within the CD and Kujung II Formations are also potential source rocks. Reservoirs are mostly in Kujung patch/pinnacle reef limestone reservoirs, mostly in Kujung I and Kujung II units, as well as in the lowest part of the Formation often named Kujung III. Some potential reefall limestone reservoirs of a good quality are also indicated in Rancak Formation. Sandstone reservoirs are found in CD and Ngimbang Formations as the deepest target, with main reservoirs found in the Ngrayong Formation. Most of the sandstone reservoirs are shallow and of good quality (porosity can be > 35%, permeability up to 10,000 mD). Some minor sandstone reservoirs are found in Kujung Formation too, and very shallow sandstone reservoirs are also found in the shallowest Pliocene Ledok Formation.

8) **Barito Basin**. The Barito Basin (Area = ±70,000 km^2) is located in South Kalimantan, and is geologically bordered by Adang Fault to the north, Meratus Mountains to the east, and the Sunda Shelf to the south and west. The Early Tertiary extensional deformations produced NW-SE trending rifts to accommodate the first deposition of the alluvial-lacustrine Lower Tanjung Formation during Upper Paleocene-Middle Eocene. Over the formation, a major transgression during Middle-Late Eocene resulted in a widespread deposition of marine shale of the Upper Tanjung Formation. The subsequent geological events deposited the marine Berai Formation during Lower Oligocene-Early Miocene, clastic deposition in the deltaic-shallow marine Warukin (Lower and Upper) Formation during Early-Late Miocene, and molassic-deltaic sediments deposition of Dahor Formation during Pliocene-Pleistocene. The main source rocks of the basin are shale and coals of the Tanjung

Formation, as well as claystone, shale, and coals of the lower Warukin Formation. Upper part of the Berai Formation, marl and shale, is also considered as potential source rock. Reservoirs in the basin are mainly the sandstones and conglomerates of the Lower Tanjung Formation (porosity = 15–26%), and sandstones of the Middle Warukin Formation. Other reservoirs are the barrier reef of the Upper Berai Formation and the fractured Cretaceous Basement's granite intrusive.

9) **Kutai Basin.** The Kutai Basin (Area = ±165,000 km^2) is located in the eastern part of Borneo island (Kalimantan Timur), and is confined geologically by Mangkalihat High to the north, Neogene spreading of North Makassar basin to the east, Adang Patenoster Fault to the south, and the extended part of Kuching High to the west. The overall basin is large with its depositional center in the Mahakam Depocenter (onshore and offshore), Santan basinal low right north to it, and also covers the wide North Makassar Basin. The offshore part of the basin is estimated to be filled with 9,000 m thick sediments, of which about 6,000 m of the upper part is of exploration interest. In the onshore part, several smaller basinal lows are also present. In Kutai Basin, the Cretaceous Metamorphic Basement was overlain by the first Tertiary fluvial to shallow marine—coarse to fine—sediments to form the Kiham Haloq Formation during Paleocene-Early Eocene. Subsequent regional geological events had led to the deposition of the Early Eocene-Lower Oligocene Atan Formation, the Upper Oligocene-Early Miocene black carbonaceous shale Pamaluan Formation in the eastern part of the basin, the Early-Late Miocene Bebulu and Pulau Balang Formations in the open marine region in the east, and the Middle-Late Miocene Balikpapan Formation in the deltaic region. As the eastern part of the basin became deltaic

during Late Miocene, the coarse clastic sediments of Kampung Baru Formation was deposited. The Balikpapan Formation is considered as the best source rocks in the basin, which is very rich in organic matters and has more than 3,000 m in thickness, and formed the hydrocarbon in the northern, southern, and eastern of the Mahakam Delta. Shales and claystones of the Pemaluan and Pulau Balang Formations are also considered as potential source rocks even though with more varied organic contents. Sandstones in Kiham Haloq, Atan, Pulau Balak, Balikpapan, and Kampung Baru fomations are potential reservoirs. The reservoirs in the Paleogene Formations are actually good in quality (porosity = 5–25%, permeability up to 450 mD), but the relatively younger deltaic sandstone reservoirs of the Early Miocene-Pliocene Balikpapan and Kampung Baru Formations (porosity = 20–35%, permeability = 100–10,000 mD) trap most of hydrocarbon in the basin. Some limestone reservoirs are also found in these formations.

10) **Tarakan Basin.** The Tarakan Basin (Area = ±68,000 km^2) is located in the northeastern part of Borneo island (Kalimantan Utara Province). The basin is limited by the Samporna High to the north, Sekak-Berau High to the west, Mangkalihat High to the south, and opens eastwards and southeastwards into the Makassar Strait. The basin opened up eastward, and sea transgression brought marine shale sediments into it to form the Sembakung Formation (equivalent to Sujau Formation in the northern part) over the basin's pre-Tertiary Basement during Early-Middle Eocene. Successive geological events brought Seilor limestone platform and Mangkabua (Misaloi in the north) shale Formation during Oligocene, Tabalar reefal limestone and Birang (Naintupo in the north) shale Formations during Early Miocene, the Early Miocene Latih (Meliat

in the north) clastic Formation, the Middle Miocene-Pliocene Menumbar-Domaring limestone Formations in the south, and the Middle-Miocene The Tabul – Santul – Tarakan – Bunyu sandstone Formations in the north. Tabul Formation is considered to be the most predominant source rocks due to its high organic contents and significant thickness of up to 1,700 m. However, the deeper Sembakung and Meliat Formations are also potential at lesser degree. Reservoirs in the basin are proved to be in the deltaic Meliat, Tabul, and Santul Formations in the north. The reservoirs consist of sandstone, shale, siltstones, and coal seams, among which sandstone intervals are 40-60 m thick with maximum thickness of 115 m. Other reservoirs are the fluvio-deltaic sandstones of the Tarakan Formation.

11) **Bone Basin**. The Bone basin is located in Bone Bay (Area = ±50,000 km^2) in the southern part of Celebes (Sulawesi) island. The basin is divided as well as confined by a series of sub N-S major fault zones and has five sub-basins of North Bone, South Bone, SW Bone, East Sengkang, and West Sengkang. The oldest sedimentary Formation in the basin is the pre-Tertiary Balangbaru. Following a series of tectonic events, the deltaic-shallow marine Toraja-Malawa Formation was formed during Eocene, the Late Eocene-Lower Oligocene volcanic Langi Formation in Bone sub-basins, the Late Eocene-Early Miocene Tonasa-Makale limestone Formation in Sengkang sub-basins, the Early-Middle Miocene Camba (volcanic-limestone Lower Member and volcanic-sandstone Upper Member) Formation, the Middle Miocene-Lower Pliocene Tacipi limestone Formation, and the unconformably overlying Late Miocene-Upper Pliocene Walanea mudstone Formation. Main source rocks are thought to be the shales in the Toraja-Malawa Formation. Sandstone reservoirs are found in the Toraja-Malawa Forma-

tion that could reach 20 m thick (average porosity of 20%) interbedded with–6 m coal seams. Potential limestone reservoirs are contained in the Tonasa-Makale and Tacipi Formations. Tonasa limestones vary from micritic limestone to packstone-grainstone with a poor quality in general (porosity around 6%, permeability < 1 mD). The younger Tacipi reefal limestone is predominantly made of algae, coral, foraminifera, and molusc wack-boundstone with their mouldic, vuggy, and intergranular pores. The Tacipi limestone is thicker (60 to 400 m) and in general of good quality (porosity = 15–39%, permeability = 1–3,200 mD).

12) **Banggai Basin.** The Banggai Basin (Area = ±18,000 km^2) is situated in the eastern part of Celebes Island (Central Sulawesi Province). The basin is believed to be situated in a fragment (Banggai-Sula microplate) of the Australia-New Guinea continent that moved towards the Asian continent leading to a series of events that filled the basin with sediments. The regional stratigraphy ranging with age with the pre-Jurassic Basement of granites and volcanic sediments at the bottom being overlain by the Jurassic-Cretaceous continental to shallow marine clastic sediments Kabauw and Bobong Formations, the Middle Jurassic-Lower Cretaceous limestone Buya Formation, and the unconformable Middle Jurassic carbonate-shale Tanamu Formation. Tertiary sediments overlaid the pre-Tertiary Formations are combinations of widespread shallow marine platforms and reefal carbonates, as well as local sandstones and conglomerates. The Tertiary intervals overlying the pre-Tertiary rocks are primarily the Early-Middle Miocene Tomori limestone Formation, the Middle Miocene clastic-coal Matindok Formation, the Middle-Late Miocene Minahaki limestone Formation, and the Pliocene-Holocene sandy shale-conglomerates Sulawesi Group.

Source rocks in the basin are probably the Jurassic-Lower Cretaceous shales in the Buya Formation and others, since no Cretaceous and Tertiary Formations are considered suitable due to absence of sufficient organic-carbon content. There are two groups of potential reservoirs in the basin, the Pre-Tertiary and Tertiary groups. The Pre-Tertiary group covers the Jurassic clastic reservoirs (porosity = 2–22%) and the Cretaceous massive chalky carbonates of the Tanamu Formation (porosity = 4–26%), and are considered as the secondary target for this basin. The primary targets are reservoirs of the Tertiary group, which mainly come from the widely deposited carbonate platform with reefal limestones of the Minahaki Formation. This platform can be as thick as 500 m and contains both tight and highly porous intervals including excellent intergranular rocks and foraminifer packstones (overall porosity = 0.5–34%). Sandstones in lower part of the Tomori Formation are also potential reservoirs.

13) **Salawati Basin.** The Salawati Basin is located in the Bird's Head region in the New Guinea island, in Indonesia's West Papua (Papua Barat) Province. Geologically, the basin is marginalized in the north and the west by the Sorong Fault Zone, separated by Bintuni Basin in the east by the Ayamaru High, and limited to the south by the Misool-Onin anticline. Stratigraphically, the Pre-Carboniferous Basement (Kemum Formation) is overlain by the Permo-Carboniferous clastic sediments Alfam Group, the Jurassic-Cretaceous Kembelangan Group sediments, and the Tertiary Group. The Tertiary Group overlying the pre-Tertiary Formations consists of the Lower Paleocene Waripi calcareous sandstone-dolomite Formation, the Paleocene-Lower Oligocene Faumai foraminifer limestone Formation, the Lower Oligocene Sirga mudstone-siltstone Formation (cap rock to the Faumai

limestones), the Upper Oligocene-Late Miocene Kais reefal limestone Formation, and the Late Miocene-Pliocene Klasafet and Klasaman mainly calcareous mudstone seal Formations, over which the Pleistocene Sele conglomerate Formation was deposited. Studied source rocks in the basin are shales of the Sirga, Klasafet, and Klasaman Formations that have rich organic matter and advanced maturity condition. Reservoirs in the basin are played by the Kais Formation's porous reefal traps, consisting of bioclastic packstones and wackestones (porosity = 18–27%), throughout the reef platform especially in the southern part of the basin.

14) **Bintuni Basin.** The Bintuni Basin (Area = ±39,000 km^2) is positioned in the southern part of the Bird's Head region of the New Guinea island, in Indonesia's West Papua (Papua Barat) Province. The basin is separated with the Salawati Basin by the Ayamaru Plateau and Kemum Block, limited in the east by the Arguni Thrust, bordered in the south by the Tarera-Aiduna fault, and cut to the west by the Skak Ridge and Faf-Fak-Kumawa structural high. During the pre-Carbonaferous, clastic (shale, greywackes, and coarse clastic) sedimentation prevailed and the Basement of Kemum Formation was established. Overlying the Basement sedimentation through various geological/tectonic events occurred resulting in the deposition of the Permian Aifam Group (Aimau, Aifat, and Ainim Formations), the Triassic-Early Jurassic Tipuma sandstone-shale Formation, the Upper Cretaceous Kembelangan Group's Jass marine sediment Formation, the Paleocene-Early Eocene Waripi clastic Formation, the Early Eocene-Late Miocene Faumai-Sago-Kais limestone Formations, and the Pliocene-Pleistocene Sele conglomeratic Formation. Main source rocks in the basin are interpreted as the old Ainim continental shales and coals Formation,

the Early Jurassic unit of Kembelangan shale-coal Formation, and the Waripi marine calcareous shale Formation. The main reservoirs in the basin are the Jurassic gas bearing sandstones of the Lower Kembelangan Group (porosity = 5–15%, permeability = 10–20 mD could be higher to 250 mD; Vera, 2009) interpreted to have been primarily deposited under distributary channel and point bars forms. Large gas reservoirs are found within this group hence providing the main gas producers in the basin. Coral limestones of the Kais Formation (porosity = 6–28%, permeability = 7–2,500 mD) are also found to trap some hydrocarbon and secondary sandstone reservoirs in the Tipuma and Ainim may serve as additional exploration targets.

D. Book Contents

This book, *Petrophysical Characteristics of Some Indonesian Reservoir Rocks*, presents several features regarding some Indonesian reservoir sandstone and limestone rocks. The contents consist of one introductory chapter and five main chapters. Among the five main chapters, Chapter 2 presents result of study of porosity trends shown by reservoirs in eight sedimentary basins in Indonesia. The study was carried out on data reported from laboratory tests on 4,654 sandstone core samples, which results is presented in Widarsono (2014b) and the published article is adopted for the main part of the chapter. Vertical porosity trends are observed for individual basin and comparisons are made with porosity-depth model previously proposed by past studies. Anomalous trends are also indicated and general trends that represent basinal trends are also presented.

Permeability is always considered as the most crucial petrophysical property in petroleum production. Permeability anisotropy—ratio between vertical and horizontal permeabilities (K_V/K_H)—is always needed in reservoir simulation modeling, and the most representative

values are always desired. A series of analyses on 7,489 sandstone and carbonate core samples taken from 12 sedimentary basins has been performed. Results are presented in Widarsono et al. (2006). Median and mode values are indicated for various categories including sedimentary basins, porosity and permeability values, and lithological types. Cases for extreme permeability anisotropy in different heterogenity—vertical and lateral—leves are also presented. The published article is taken as the bulk in Chapter 3 after some important corrections.

Chapter 4 contains discussions over rock wettability of Indonesia reservoir sandstones and limestones. This petrophysical property is known for its influence on capillary pressure and relative permeability, two rock properties that govern initial fluid distribution in reservoir and the way the fluids move in the reservoir body. The study presented by Widarsono (2010) and Widarsono (2011b) was made on data obtained from a total of 725 sandstone and limestone core samples derived from reservoirs in 11 sedimentary basins. Using four wettability indicators, classification is established and presented, and it is shown that core cleaning as part of core analysis tends to change wettability or at least reduces its strength. Facts about general wettability of sandstones and limestones, that are not neccessarily the same as common belief, is also exhibited. The two articles are combined in a chapter with some additional information.

Irreducible water saturation is strongly related to permeability and plays a significant role in the determination of original oil/gas in place (OGIP or OOIP). Chapter 5 contains the article presented in Widarsono (2011a) with some additional information. The study that was made on 760 sandstone core samples benefited for the data from special core analysis tests on the samples. The chapter exhibits the irreducible water saturation trends in its relation with permeability, as well as with geological units of basin, formation, and down to field

scales. Differences and similarities are presented. Correlations between irreducible water saturation and premeability are also exhibited for various wetness strength, as well as for individual sedimentary basin.

The final chapter, Chapter 6, presents work by Widarsono (2014a) that shows results of rock compressibility study on 86 limestone samples taken from 11 active fields in four sedimentary basins. Comparisons are shown between rock compressibility data with existing models depicting that not all models can suitably represent the data. Accordingly, a set of proposed models are presented. These correlations are hopefully useful for application cases in Indonesia. The chapter also presents differences and similarities between distant sedimentary basins in rock compressibility characteristics.

CHAPTER II
POROSITY–ITS CHARACTERISTICS IN RELATION WITH DEPTH

A. General

As put in the previous chapter, in reservoir characterization and formation evaluation, determination of petrophysical properties is one of the most important parts. One of those petrophysical properties is porosity. Porosity is known as the most important reservoir rock property in, among others, the determination of original hydrocarbon in place (OHIP) and its corresponding reserves. Magnitudes, types, and distribution of porosity directly affect reserves and the strategy or scenario required for exploiting them.

Indonesia and its complex geological setting are without doubt to be associated with significant levels of rock heterogeneity in its hydrocarbon reservoirs. The higher the heterogeneity level, the more complex porosity distribution both laterally and vertically. In order to understand this heterogeneity in porosity, distribution knowledge over local trends is always desired, obtaining which may ease the efforts to model porosity distribution both in regional and local/reservoir levels. For producing and non-producing reservoirs in mature Indonesia's sedimentary basins, this will enhance knowledge over the porosity distribution through various aspects—e.g. judgment on level of porosity

heterogeneity and the most likely average porosity values—while, on the other hand, may help in the evaluation of speculative hydrocarbon resources in exploration areas or in the less mature basins.

In reservoir characterization and formation evaluation, it is generally accepted that porosity decreases variably with depth. This presumption is, to some degree, used as a guideline in related activities such as well log analysis. Local knowledge over porosity distribution with depth is often used as a comparison in judging sensibility of resulting porosity values. This comparison is therefore an indicator whether or not a re-analysis is needed and in case of porosity anomalies are indeed in existence, what factors that have possibly caused them.

In Indonesia, local knowledge over porosity versus depth is certainly posessed by any local field operators, but it is usually at structure or field levels and for ones that have reached advanced stages of their production life. For fields that are still at their appraisal stages, external sources that can provide this knowledge is definitely important. This information can be established through data gathering from any available sources at regional or basin scale. This chapter is to present results of such study previously presented by Widarsono (2014b) through the use of data from thousands of reservoir core samples taken from hundreds of structures/reservoirs in Western Indonesia's eight productive sedimentary basins. It is hoped that this information can be of any use for supporting sub-surface studies performed at any stages of a field's development.

B. Relation of Porosity versus Depth

Sand grains that have just settled and been buried in relatively short geological time form sandstones that are very porous with porosity above 40%. With the progress of burial and its subsequent physical and chemical processes, the sandstones become more compacted and

less in porosity values. Basically, porosity is reduced by two independent factors; compaction and cementation. Compaction is marked by decrease in both pore and bulk volumes, while cementation is also associated to decrease in pore volume but with constant bulk volume. With some exceptions, compaction is regarded as the predominant factor during early stages of burial whereas cementation becomes more important with the increase of depth and burial time.

Characteristics of porosity versus depth can be different from one region to another depending on the different parameters that may affect the two factors. Various parameters have been suggested as the results of various studies. Among others are pre-burrial mineralogical composition and rock texture (e.g. Pittman & Larese, 1991; Ramm & Bjorlykke, 1994), pressure and temperature gradients (e.g. Gautier & Schmoker, 1989; Bjorkum et al., 1998; and Bloch et al., 2002), geological age (e.g Ehrenberg et al., 2009), timing of petroleum emplacement in reservoir (e.g Bjorkum & Nadeau, 1998; Worden et al., 1998; Barclay & Worden, 2000; Marchand et al., 2001; Bukar, 2013), porosity rearrangement (e.g Giles & de Boer, 1990), fluid-related porosity enhancement (e.g. Ehrenberg & Jakobsen, 2001; and Sattler et al., 2004 (carbonates), and tectonic lifting (e.g. Ehrenberg & Nadeau, 2005). Variations in the parameters may be different for different regions due to differences in local geological setting. Regional tectonics events, depositional environments, thickness of sediments, nature of petroleum systems, and presence of magmatic intrusions are among the geological features that may produce the differences.

As has previously been stated, porosity tends to decrease with depth. However, it is a norm rather than an exception that porosity values are not always in line with trends, usually in the forms of data scatter and values considerably greater than the trends suggest. Porosity preservation for anomalously high porosity values and excessive cementation for anomalously low porosity values are thought to be

the causes. Excessive cementation may be caused by various factors. Loucks et al. (1977) suggested some mechanisms such as massive quartz overgrowth and development of sparry pore-fill calcite cement. Creep process due to high clay—or other ductile materials—contents may also result in excessive porosity reduction (e.g. Beard and Weyl, 1973; Renard et al., 2000; Gratier et al., 2013). On the other hand, porosity preservation at great depths may be caused by various occurrences. Among others are influence of grain size and grain sorting (e.g. Nagtegaal, 1978), early presence of hydrocarbon prior to cementation (e.g. Marchand et al., 2001; Wilkinson et al., 2006; Wilkinson & Haszeldine, 2011; Bukar, 2013), quartz cement growth inhibition through dissolution of sponge spicules (Osborne & Swarbrick, 1999), continuous subsurface leaching of some particular minerals (Loucks et al., 1977), and grain-coating by micro-quartz cement (Aase et al., 1996), and overpressure that reduces effective stress (e.g. Bloch et al., 2002).

Relative domination between the two porosity modification factors varies from one place to another. For instance, cementation levels may vary significantly for sandstones in the same formation, depths, and geographical locations. For example, Ramm et al. (1997) showed a case in Central Graben (North Sea), in which some Upper Jurassic sandstones from similar depths (±4,000 m) exhibit considerable porosity variation.

Variation in the domination between the two factors can also be seen from its potential in generating scatter in the porosity-depth relation. For a particular rock group in a particular geographical location, it can be said that compaction factor plays the main role in porosity reduction (primary reduction) and cementation reduces the porosity further (secondary reduction). This suggests that for a particular depth level, the highest porosity is associated with the least cemented. As Ehrenberg & Nadeau (2005) put, this is often

associated with lithologies that can preserve original porosity (e.g. clean sandstone). On the contrary, the lowest porosity in the group indicates the highest level of cementation. Through these assumptions, the degree of scatter in porosity values can therefore be regarded as reflecting variations in the intensity of cementation.

Efforts to understand relation between porosity and depth have been spent for long time. As put by Gluyas & Cade (1997), two approaches are usually taken, through laboratory experiments and through the use of field data. As early as in 1968, Vesic and Clough published their results of laboratory compression tests on some sandstone samples and concluded that relation between porosity and stress is by nature linear. This conclusion was later supported by Atkinson & Bransby (1978), who stated that this linear porosity – stress relation is indeed true as long as there is no presence of over-pressured intervals. A similar laboratory study on deep sea sediments using porosity rebound concept also managed to construct porosity-depth profiles (Hamilton, 1976). Later laboratory studies, such as one by Scherer (1987) managed to model porosity versus depth with taking into equation parameters of grain sorting, percentage of quartz grain, and geologic age. Nevertheless, availability of data for the supporting parameters may impose problem for any practical use.

By using data published by Vesic & Clough (1968) and Atkinson & Bransby (1978), Gluyas & Cade (1997) has drawn a mathematical correlation between porosity (ϕ) and depth (D) of

$$\phi = 50 \exp\left(\frac{-10^{-3} D}{2{,}4 + 5 \times 10^{-4} D} \right) \qquad (2\text{-}1)$$

with porosity in percent and depth in meter.

Graphically, the curve on Figure 2.2 depicts the porosity-depth expression in Equation 2-1 with porosity data, mostly obtained from North Sea reservoir rocks, that in general represents sandstones with

moderate degree of cementation. The model represents behavior of this type of sandstones under compaction, which tend to show non-linear porosity-depth trend under lower overburden stress at depths closer to the surface and become more linear at greater depths due to compaction under larger loads. This model represents a burying process that involves limited mechanisms other than compaction under overburden load.

The search for establishing porosity-depth relation has also been performed using field data (e.g. log analysis data). In the same study, Gluyas & Cade (1997) observed porosity values greater than the values predicted by the correlation, and they stated that this is caused by overpressure. In the cases of overpressure, compaction process is hindered by higher than normal pressure (i.e. hydrostatic pressure) resulting in lower effective overburden and tectonic loading.

Sandstones that undergo overpressure bear the same effective stress to other sandstones having subjected to hydrostatic pressure only but at shallower depths. The difference in depths—between the effective and the true depths—is proportional to the magnitude of overpressure. This can somehow be used as indicator of severity of the overpressure. Gluyas & Cade (1997) put that effective depth for a sandstone that is subjected to overpressure can be estimated using

$$D' = D - \left(\frac{u}{(\rho_r - \rho_w) g (1 - \phi)} \right) \tag{2-2}$$

with D' = effective depth, ρ_r = density of rock column (kg/m^3, normally 2,650–2,700), ρ_w = formation water density (kg/m^3, 1,050 for brine), g = gravity force (m/s^2, 9,8), f = porosity (fraction), and u = overpressure (MPa). They also noted that Equation 2-2 works well with using average porosity of 0.2 for depths of 2,000–4,000 m with clay contents of 15–25%. For shallower depths and unusually higher

clay contents in reservoirs, more representative average porosity values have to be determined.

In a similar manner earlier, but with using field data as support, Ramm & Byorlykke (1994) studied porosity-depth trends in Viking Grabben and Haltenbanken areas in offshore Norway using porosity data from 110 wells, supported with mineralogical and log data as well as well test-derived pressure data. For the first estimation, they suggest to use the linear equation of

$$\phi = 42.7 - 6.9 \ ^*Z \qquad (2\text{-}3)$$

with ϕ in percent and Z in km. This linear equation applies only for compaction factor only, and after which the resulting porosity values have to be analysed with taking into considerations factors such as pore pressure, hydrocarbon saturation, and mineralogical compositions. Through analyzing the influence of these factors, deviations from Equation 2-2 can be estimated.

Despite the great volume of works throughout the world that have been spent into studying the characteristics of porosity trends with depth, not much studies—in the form of published articles—have been devoted to this issue for Indonesian cases. A study of Ehrenberg et al. (2009) utilized a huge amount of data including average porosity values of more than 36,000 producing reservoirs throughout the world encompassing from Precambrian-Silurian to Pliocene-Pleistocene Ages. The basic data is a combined core and log analysis data sampled for average values (i.e. P50 values) at every 0.5 km of depth intervals. The study produced global porosity-depth depth trends of the various geological ages, including data from Tertiary reservoirs, mostly in western Indonesia. However, since data from Indonesian reservoirs constituted only a minor part to the total volume of data, no relevant information can be obtained from the results. Similar information for Indonesian cases is required.

C. Data Inventory

In the study presented in Widarsono (2014b), data from 4.654 core samples was used. The core samples are made of 1.773 core plugs taken from full-diameter whole cores (termed FD-plugs) and 2881 percussion sidewall cores (termed SWC). All data was obtained from LEMIGAS archieve (oldest report used is dated December 1972 and the newest is dated September 2013). The core samples were taken from 222 fields (including exploration areas) through 549 wells located in eight main producing sedimentary basins in Indonesia; North Sumatra, Central Sumatra, South Sumatra, West Natuna, West Sunda-Asri, Nortwest Java, Northeast Java, and Kutai. Figure 1.3 shows locations and approximate coverage of the eight basins, while Tables 2.1 through 2.8 present background details regarding the data including formations, fields, number of wells, depth ranges, number of samples and their types, and number of vertically averaged data number used for deriving porosity-depth models.

Table 2.1 Data and Its Field of Origin, North Sumatra Basin

Basin	Field/structure (*) (no. of wells)	Depth range (m, ssl)	No. of core samples	No. of average data values (**)
North Sumatra Main formation(s): Seurulla, Keutapang, Belumai	Onshore: Basilam (2), Batumandi (1), Gedondong (1), Gurame (1), Kuala Simpang Barat (1), P Tabuhan Barat (1), Paluh Sipat (1), PRP (4), P Tabuhan Timur (1), Rantau (7), Lhok Sukon (2), Serang (1) Total wells = 23	271.0 – 2996.0	105 Full-diameter core (horiz. plug) = 90 Sidewall core = 15	30

(*) Including exploration area(s)
(**) Data median (average, P50) in intervals of 50 – 100 m depth

Table 2.2 Data and Its Field of Origin, Central Sumatra Basin

Basin	Field/structure (*) (no. of wells)	Depth range (m, ssl)	No. of core samples	No. of average data values (**)
Central Sumatra Main formation(s): Pertama, Kedua, Duri, Bekasap, Bangko, Telisa, Petani	Onshore: Balam South (3), Bangko (4), Bekasap (5), Beruk (4), Binanga (1), Duri (5), Jorang (3), Kopar (3), Kotabatak (9), Kulin (2), Libo (1), Libo SE (3), Minas (4), Pager (1), Pedada (2), Pematang (1), Petani (6), Petapahan (2), Pinang (1), Pudu (2), Puncak (1), Pungut (3), Pusaka (1), Rantau Bais (4), Selat Panjang (1), Talang South (1), Tambusai (1), Tanjung Tiga (1), Telinga (1), Zamrud (5) Total wells = 82	94.8 – 3907.0	420 Full-diameter core (horiz. plug) = 409 Sidewall core = 11	51

(*) Including exploration area(s)
(**) Data median (average, P50) in intervals of 50 – 100 m depth

Table 2.3 Data and Its Field of Origin, South Sumatra Basin

Basin	Field/structure (*) (no. of wells)	Depth range (m, ssl)	No. of core samples	No. of average data values (**)
South Sumatra Main formation(s): Gumai, Talang Akar, Air Benakat, Muara Enim,	Onshore: Abab (1), Bajubang (3), Benakat (1), Beringin (3), BRC (1), Budi (1), E Benakat (1), E Kayuara (1), E Karangagung (1), Ganesha (1), Gemuruh (1), Ginaya (1), Gunung Kemala (2), Jirak (3), Kalalili (1), Karangagung (1), Karangdewa (1), Kenali Asam (4), Kerumutan (1), Ketaling Barat (2), Leko (1), Lembak (1), Limbur (1), Lirik (1), Lupak (1), Manduru (1), Mentawak (1), Merbau (3), Meruap (1), Molek (1), Ogan (1), Panerokan (3), Pinang (1), Raja (1), Ramba (4), Sekamis (1), SWA (1), Tabuan (1), Talang Akar (1), Talang Jimar (5), Tanjung Tiga (2), Tanjung Tiga Timur (1), Tapus (3), Tempino (2), Tanjung Miring Timur (1), Tuba Obi East (1), W Air Komering (1) Total wells = 74	23.7 – 2796.0	586 Full-diameter core (horiz. plug) = 438 Sidewall core = 148	53

(*) Including exploration area(s)
(**) Data median (average, P50) in intervals of 50 – 100 m depth

Table 2.4 Data and Its Field of Origin, West Natuna Basin

Basin	Field/structure (*) (no. of wells)	Depth range (m, ssl)	No. of core samples	No. of average data values (**)
West Natuna Main formation(s): Lower Gabus, Upper Gabus, Arang,	Offshore: 'A' structures (4), Anoa (1), Bandeng (1), Belanak (4), Belut (3), Binturong (1), Hiu (1), Kakap (1), Kerang (1), Krapu (2), Kuda Nil (1), Porel (1), SAL (1), Sembilang (1), Sepat (1), Tembang (2), Tenggiri (1), Teri (1), Terubuk (1), Tiram (1), Todak (8), Udang (8) Total wells = 39	108.0 – 5852.0	306 Full-diameter core (horiz. plug) = 173 Sidewall core = 133	67

(*) Including exploration area(s)
(**) Data median (average, P50) in intervals of 50 – 100 m depth

Table 2.5 Data and Its Field of Origin, West Sunda Basin

Basin	Field/structure (*) (no. of wells)	Depth range (m, ssl)	No. of core samples	No. of average data values (**)
West Sunda Main formation(s): Gumai, Talang Akar	Offshore: Cinta (7), Farida (7), Gina (1), Gita (1), Karmila (3), Kartini (2), Krisna (9), Lastri (1), Lucia (1), Maya (1), Nani (1), Rama (4), Rena (1), Selatan (2), Sundari (4), Titi (5), Veritas, (1), Wanda (7), Yani (1), Yvonne (2), Zelda (9) Total wells = 77	826.9 – 3256.8	464 Full-diameter core (horiz. plug) = 73 Sidewall core = 391	46

(*) Including exploration area(s)
(**) Data median (average, P50) in intervals of 50 – 100 m depth

Table 2.6 Data and Its Field of Origin, Northwest Java (NW Java) Basin

Basin	Field/structure (*) (no. of wells)	Depth range (m, ssl)	No. of core samples	No. of average data values (**)
Northwest Java (NW Java) Main formation(s): Talang Akar, Cibulakan	Onshore: Akasia Bagus (1), Bojong Raong (1), Cemara Barat (4), Cemara Selatan (1), Cemara Timur (4), Haurgeulis (1), Jati Keling (1), Jatinegara (1), Karang Degan 91), Karang Luhur (1), KRG (1), Melandong (2), MLP (1), Pondok Tengah Raya (1), Pegaden (1), Pondok Makmur (2), Pondok Tengah (3) Offshore: Arimbi (13), Arjuna (61), Bima (9), NW Corner (6) Total all wells = 118	156.0 – 3134.0	1293 Full-diameter core (horiz. plug) = 205 Sidewall core = 1088	59

(*) Including exploration area(s)
(**) Data median (average, P50) in intervals of 50 – 100 m depth

Table 2.7 Data and Its Field of Origin, Northeast Java (NE Java) Basin

Basin	Field/structure (*) (no. of wells)	Depth range (m, ssl)	No. of core samples	No. of average data values (**)
Northeast Java (NE Java) Main formation(s): Ngrayong, Ledok	Onshore: Arusbaya (1), Banyu Urip (1), Cendana (2), Kawengan (1), Ledok (1), Lengowangi (1), Nglobo (5), Semanggi (1) Offshore: Kepodang (1), Poleng (1) Total all wells = 18	33.8 – 2824.9	86 Full-diameter core (horiz. plug) = 36 Sidewall core = 50	28

(*) Including exploration area(s)
(**) Data median (average, P50) in intervals of 50 – 100 m depth

Table 2.8 Data and Its Field of Origin, Kutai Basin

Basin	Field/structure (*) (no. of wells)	Depth range (m, ssl)	No. of core samples	No. of average data values (**)
Kutai Main formation(s): Balikpapan, Kampung Baru,	Onshore: Badak (17), Blambangan (1), Belonak (1), Bongkaran (2), Buat (1), Dondang (1), E Manpatau (1), Kejumat (1), Kemang (1), Kembang (2), Keruing (1), Lamaru (1), Lampake (1), Mengatal (1), Mentawir (1), Meranti (1), Mutiara (6), N Mumus (1), Nenang (1), Nilam (9), N Kutei Lama (1), Pamaguan (10), Parangat (2), Penajam (2), Prangat (1), Punjung (1), Riko (1), Runtu (1), Samboja (2), Sanga-sanga (16), SBT (1), Sebulu (1), Semberah (6), Separi (1), Seturian (1), Tambora (9), Tembesi Bay (1), Terap (1), Tutung (1), UKM (1), W Nilam (2), W Santan (1), Wailawi (1) Offshore: Attaka (13), Bekapai (2), Handil (6), Kerindingan (1), Merah Besar (1), N Handil (1), Nubi (3), NW Peciko (2), Peciko (3), Sisi (2), Tunu (21), W Nubi (1), W Sisi (1), Yakin (1) Total all wells = 118	32.0 – 4561.0	1394 Full-diameter core (horiz. plug) = 349 Sidewall core = 1045	90

(*) Including exploration area(s)
(**) Data median (average, P50) in intervals of 50 – 100 m depth

Considering their different natures of coring, different approaches were adopted for selection of FD-plugs and SWC data. For FD-plugs, due to their limited coverages, the approach of selection was through emphasizing samples that reflect the reservoir rocks' heterogeneity. Therefore, for the usually limited vertical interval covered, the data must represent maximum variety in porosity values. On the other hand, for the vertically far more extensive SWC, the focus in data selection was through data picking for roughly every 25 m interval whenever possible. This is to avoid unneccessary data redundancy and statistical bias due to huge data number of similar porosity values. Furthermore, due to the nature of the percussion SWC, special caution was also made to avoid as much as possible SWC data taken from

samples with possible occurrence and defects such as sample insufficiency, mud contamination, and fracture creation during testing. Since not all data includes measurement under overburden pressure, only porosity without overburden pressure was used.

As part of Routine Core Analysis, porosity data was obtained through helium porosity measurement following American Petroleum Institute (API) Recommended Practice No. 40. The second edition of the guideline is the API (1998). Descriptively, following the recommended practice, samples used in the laboratory measurements were cleaned using solvents in order to both extract hydrocarbon and leach all salts contained by the core samples. The cleaned samples were then dried carefully controlled by oven. For SWC samples, some irregularity in shape was solved through the use of sample mounting. The dried samples were then tested, which porosity was obtained using Boyle's law as the guiding principle.

D. Porosity versus Depth

Upon observing porosity versus depth trends, despite the scatters, plot of all FD-plugs and SWC porosity values exhibit that in general porosity decreases with depth (Figure 2.2). Both FD-plugs and SWC data sets show the same trend, and since the two groups overlap to each other, there is seemingly no significant disparity between magnitudes of the two groups in general. However, comparison between the two may differ when made at lower levels, e.g. at basin level or even at field level.

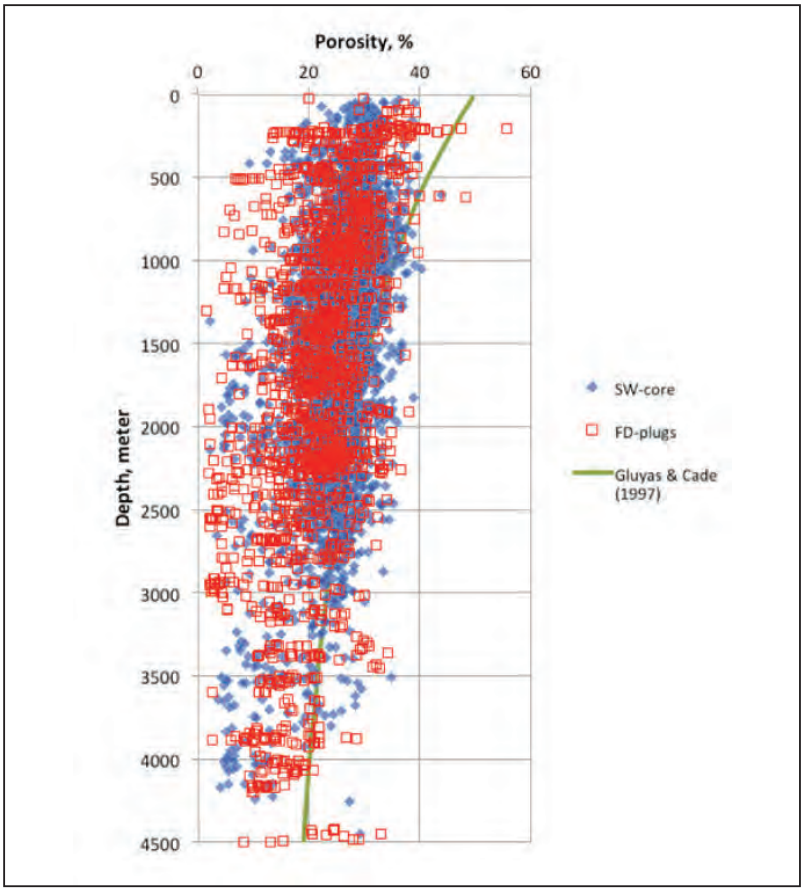

Source: Widarsono (2014b)

Figure 2.1 Porosity Versus Depth for All Porosity Data

Another occurrence that may easily be observed on Figure 2.2 is a fact that the Gluyas & Cade (1997) porosity-depth model deviates significantly from the general trend of the porosity cluster. Considering the nature of the deviation, it is obvious that same occurrence is likely to take place when compared to porosity-depth data at lower levels. This prompts to the need to see the data at lower level and models that fit them.

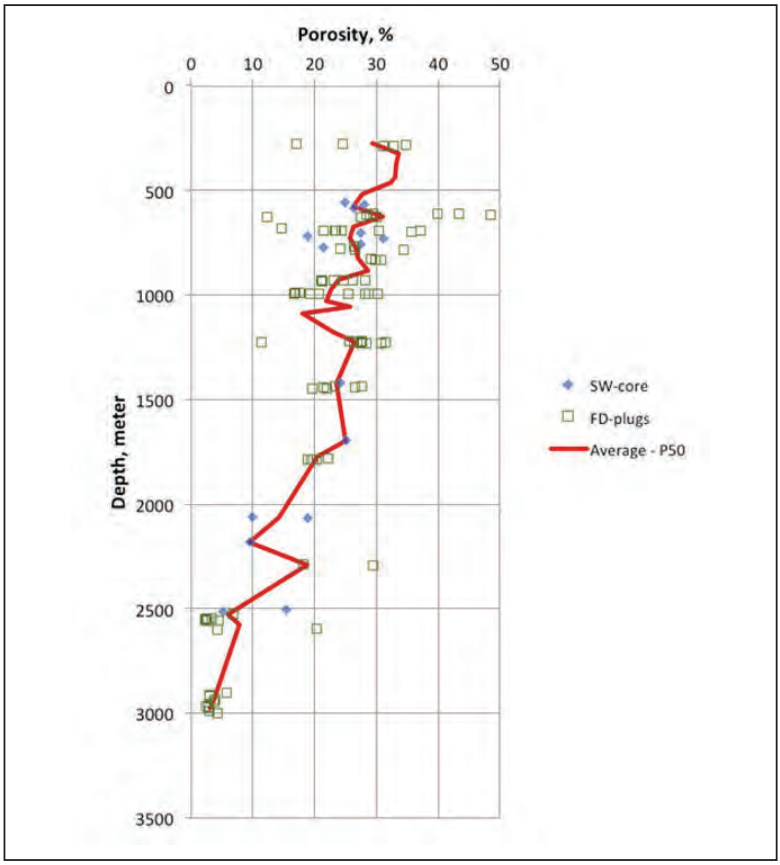

Source: Widarsono (2014b)

Figure 2.2 Porosity Versus Depth for Data from North Sumatra Basin (90 FD-plugs and 15 SW-cores), Including the Curve Representing Average Values

Porosity-depth relation at lower (i.e. sedimentary basin) level appears to have similarity in general to the one shown on Figure 2.2. Figure 2.3 through 2.10 exhibits the porosity-depth data plot for sandstones in the eight sedimentary basins in western Indonesia. In a manner similar to the general trend shown by the all data plot (Figure 2.3), the tendencies exhibited by porosity data in the individual basin are, despite the scatter, apparently to decrease with depth.

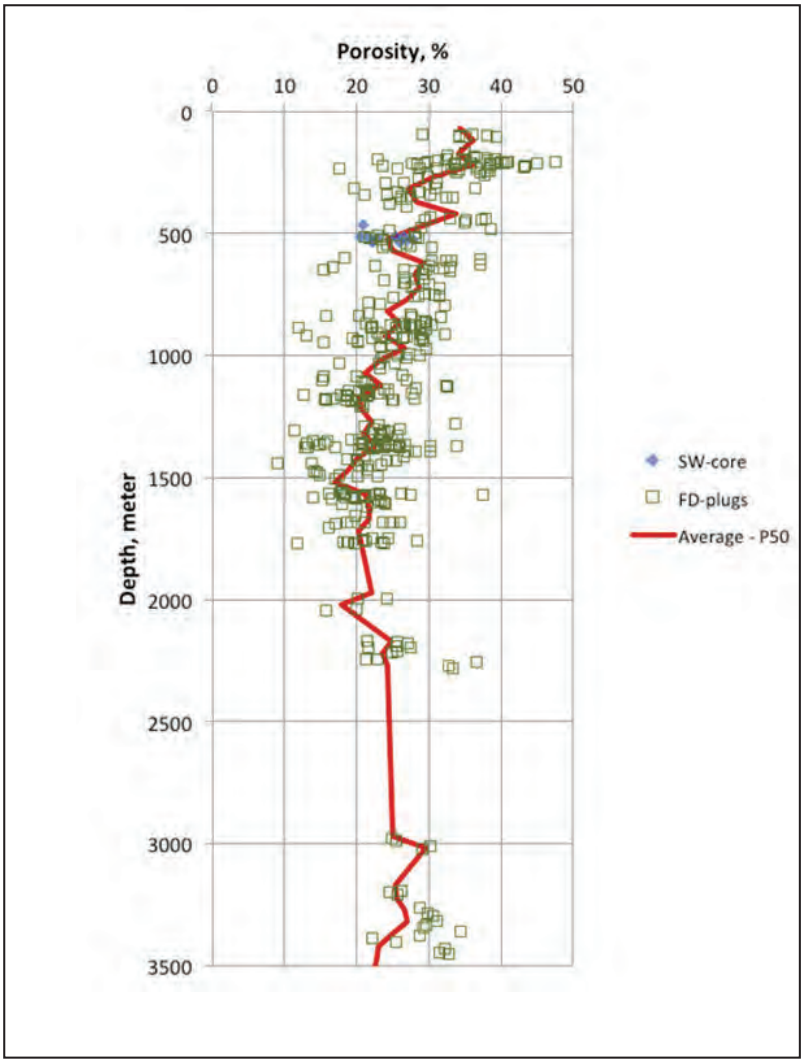

Source: Widarsono (2014b)

Figure 2.3 Porosity versus depth for data from Central Sumatra Basin (409 FD-plugs and 11 SW-cores), including the curve representing average values. Notice the relatively high porosity values at great depths probably due to porosity preservation effects.

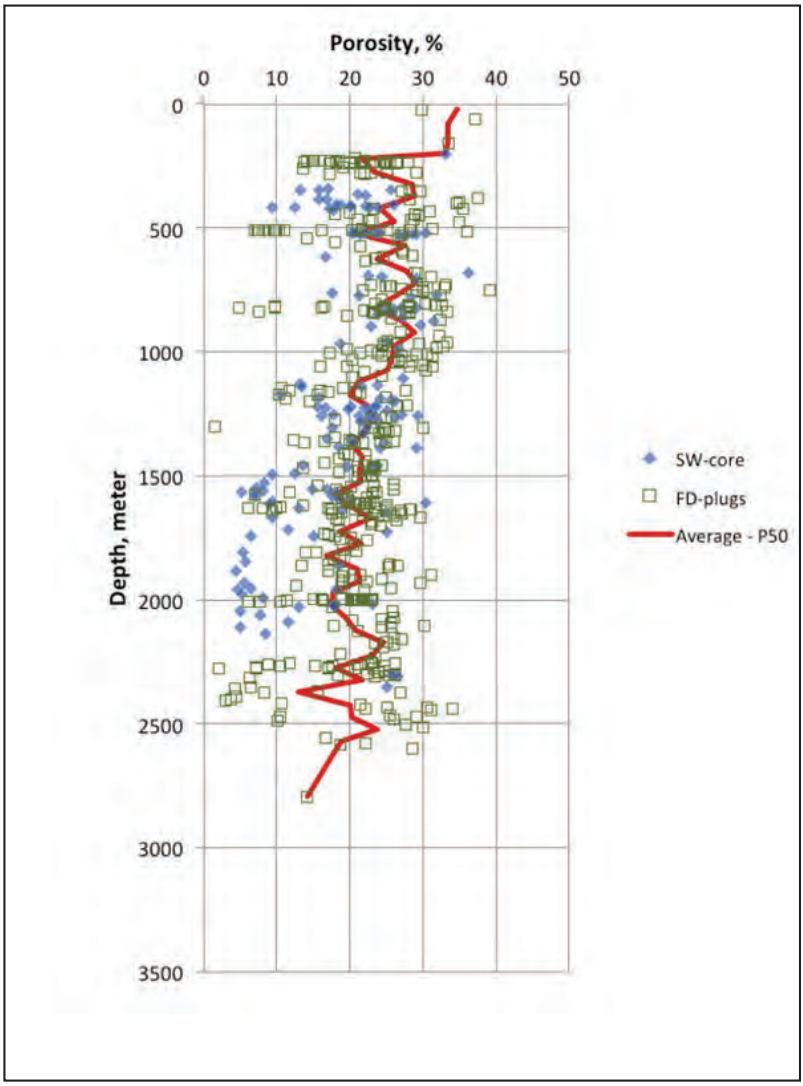

Source: Widarsono (2014b)

Figure 2.4 Porosity Versus Depth for Data from South Sumatra Basin (438 FD-Plugs and 148 SW-Cores), Including the Curve Representing Average Values

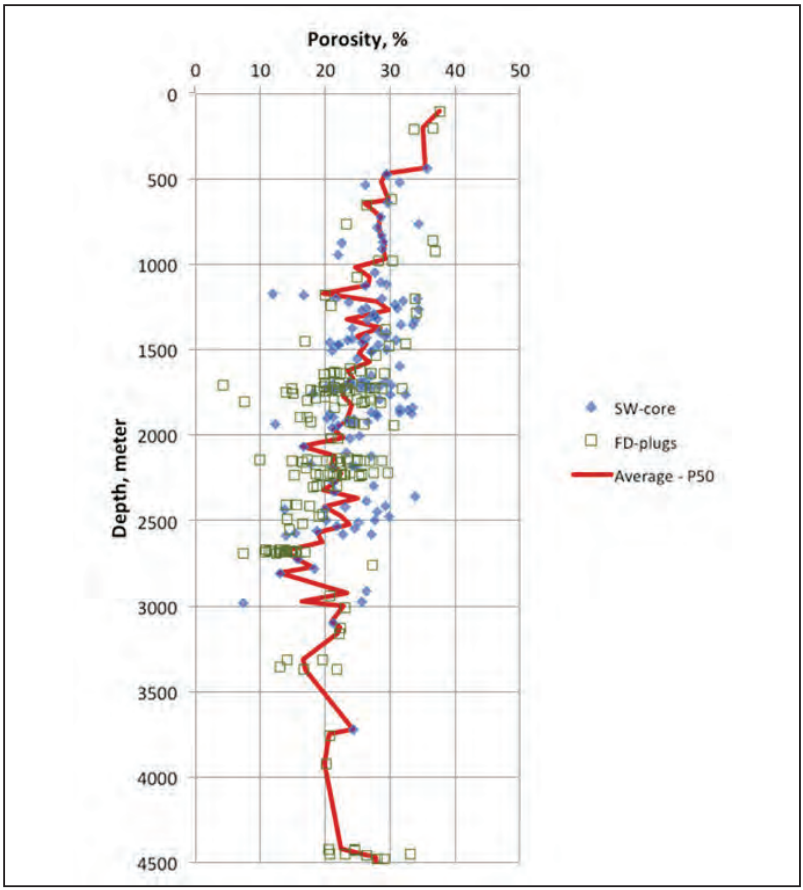

Source: Widarsono (2014b)

Figure 2.5 Porosity versus depth for data from West Natuna Basin (173 FD-plugs and 133 SW-cores), including the curve representing average values. The bottom part of the data exhibits relatively high porosity values indicating porosity preservation effects.

In order to obtain a more obvious picture over the porosity-depth trends, representative porosity values were established for depths ranging from the shallowest data point to the deepest. In Ehrenberg et al. (2009), averaging was made on log analysis data at every 0.5 km interval for data throughout the world. Following

the same approach ('P50 points' for the averaged porosity values in accordance to Ehrenberg et al., 2009) averaging in study presented in Widarsono (2014b) was also performed at smaller intervals of 50 m to 100 m depending on core data availability. For depth intervals with plenty data points averaging was made at 50 m intervals, and averaging was made at greater intervals of up to 100 m for intervals with scarcer data points. For 'no data' intervals of greater than 100 m, no porosity avaraging was made, and the corresponding trend line sections were made straight through connecting one averaged data to the nearest ones. The resulting trend lines are also depicted on Figure 2.3 through 2.10.

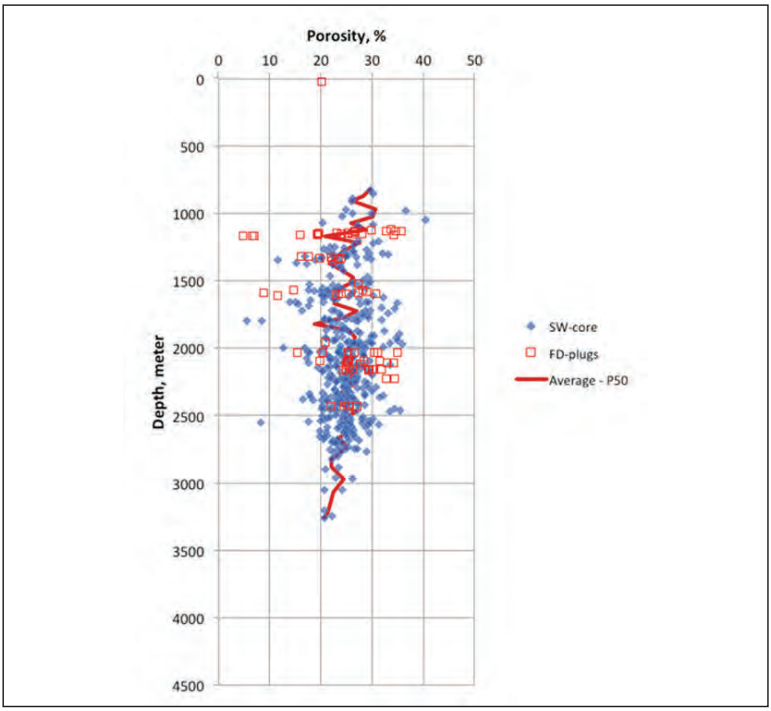

Source: Widarsono (2014b)

Figure 2.6 Porosity Versus Depth for Data from West Sunda Basin (73 FD-plugs and 391 SW-cores), Including the Curve Representing Average Values

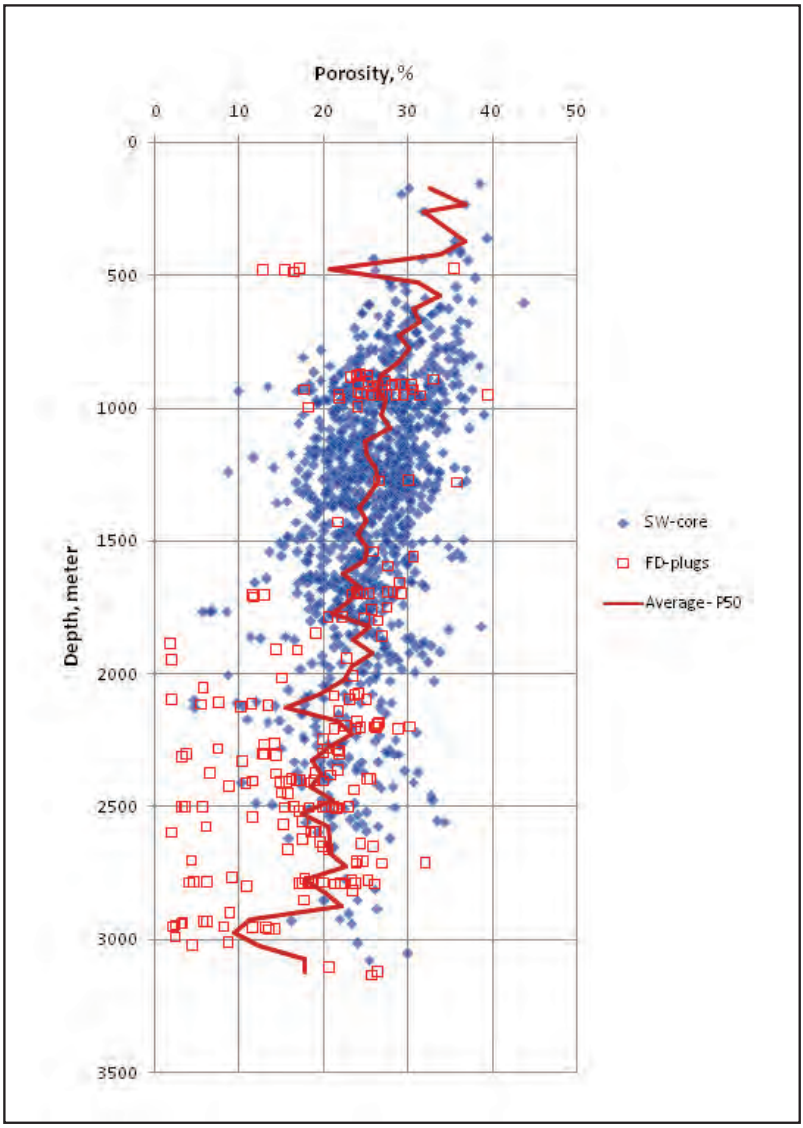

Source: Widarsono (2014b)

Figure 2.7 Porosity Versus Depth for Data from Northwest Java Basin (205 FD-plugs and 1088 SW-cores), Including the Curve Representing Average Values

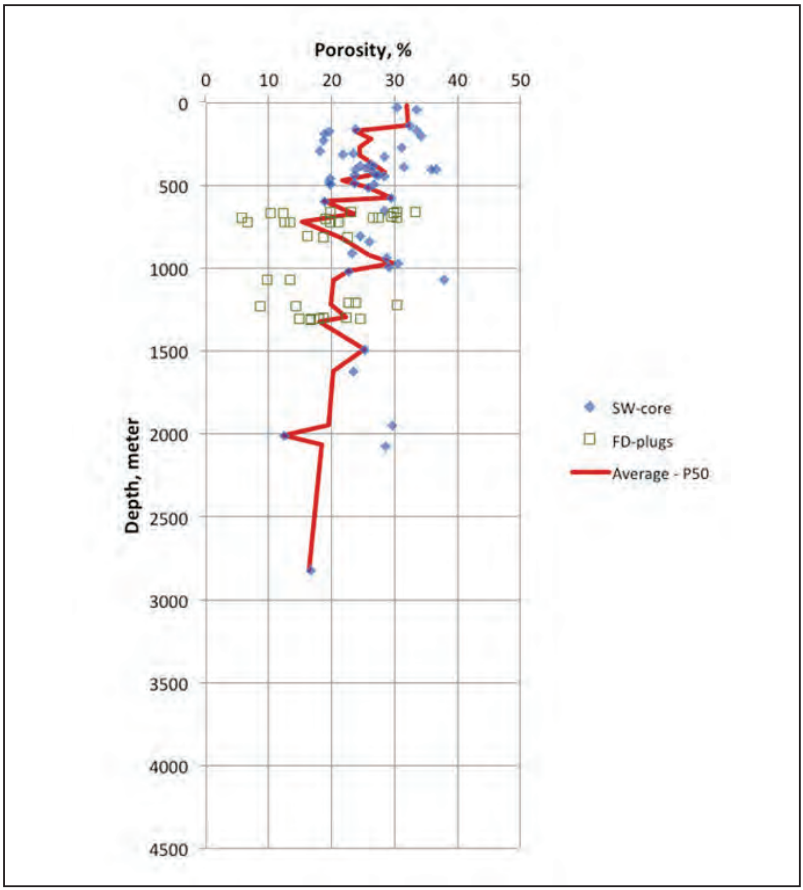

Source: Widarsono (2014b)

Figure 2.8 Porosity Versus Depth for Data from Northeast Java Basin (36 FD-Plugs and 50 SW-Cores), Including the Curve Representing Average Values

From the trend lines shown on Figure 2.3 through 2.10, the tendencies are clearer in showing the decrease in porosity with depth, with some deviations at a great depth. For the purpose of providing some practical use to the porosity-depth trend lines, empirical mathematical models have been establihed. Through modifying the Gluyas & Cade (1997) model, the model is transformed into the form of

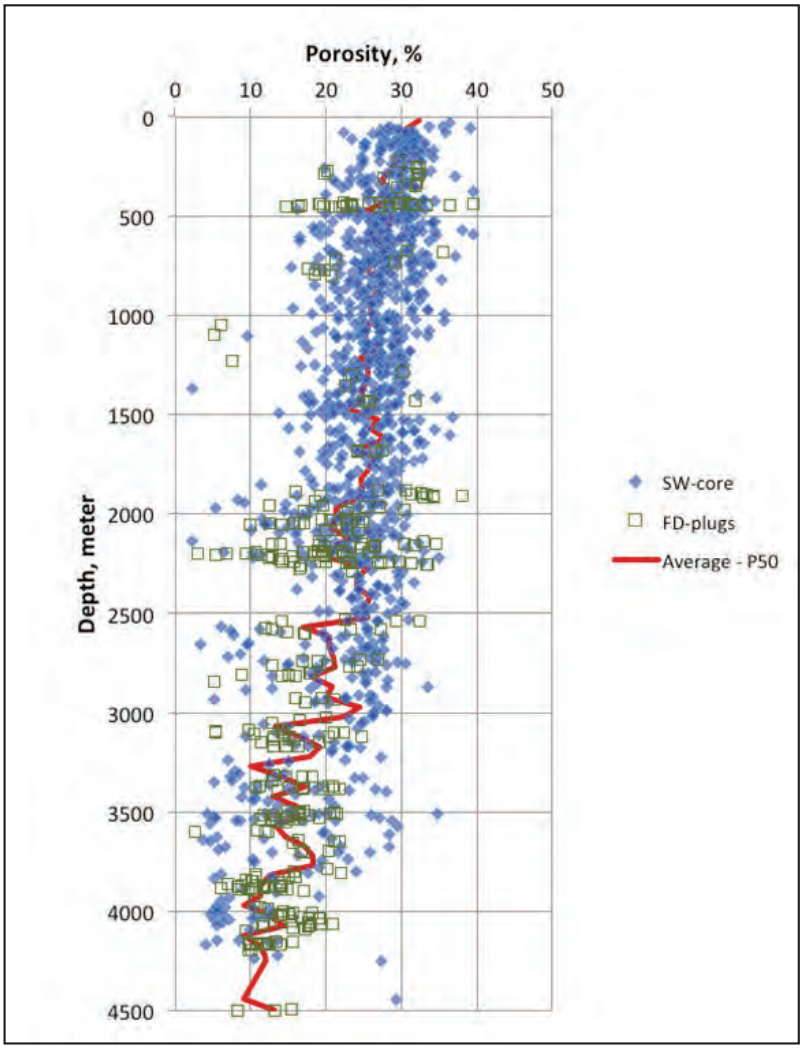

Source: Widarsono (2014b)

Figure 2.9 Porosity versus depth for data from Kutai Basin (349 FD-plugs and 1045 SW-cores), including the curve representing average values. The lower part of the trend (P50) curve (depth > 2500 m ss) shows gentler slope indicating presence of compaction.

$$\phi = ae \times p\left(\frac{bD}{c + dD}\right) \tag{2-4}$$

with *a*, *b*, *c*, and *d* are constants specific to different data sets belonging to the porosity-depth data of the eight sedimentary basins (Widarsono, 2014b). Summary of the constants for the modified Gluyas & Cade (1997) model is presented in Table 2.9. Comparisons between that porosity-depth P50 trends and the respective porosity-depth models are presented on Figure 2.11 through 2.18.

Table 2.9 Summary of Alternative Constants to the Coefficients in the Gluyas & Cade (1997) Model for the Eight Sedimentary Basins in Western Indonesia

Basin	*a*	*b*	*c*	*d*
North Sumatra	36	-10^{-3}	2.4	1.5×10^{-4}
Central Sumatra	35	-10^{-3}	2.1	5×10^{-4}
South Sumatra	32	-10^{-3}	3.4	5×10^{-4}
West Natuna	39	-10^{-3}	2.6	5×10^{-4}
West Sunda/Asri	32	-10^{-3}	5.9	7×10^{-4}
Northwest Java	37	-10^{-3}	2.9	5×10^{-4}
Northeast Java	29	-10^{-3}	3.9	5×10^{-4}
Kutai (upper part)	36	-10^{-3}	6.4	1×10^{-4}
Kutai (lower part)	32	-10^{-3}	7.4	-8×10^{-4}

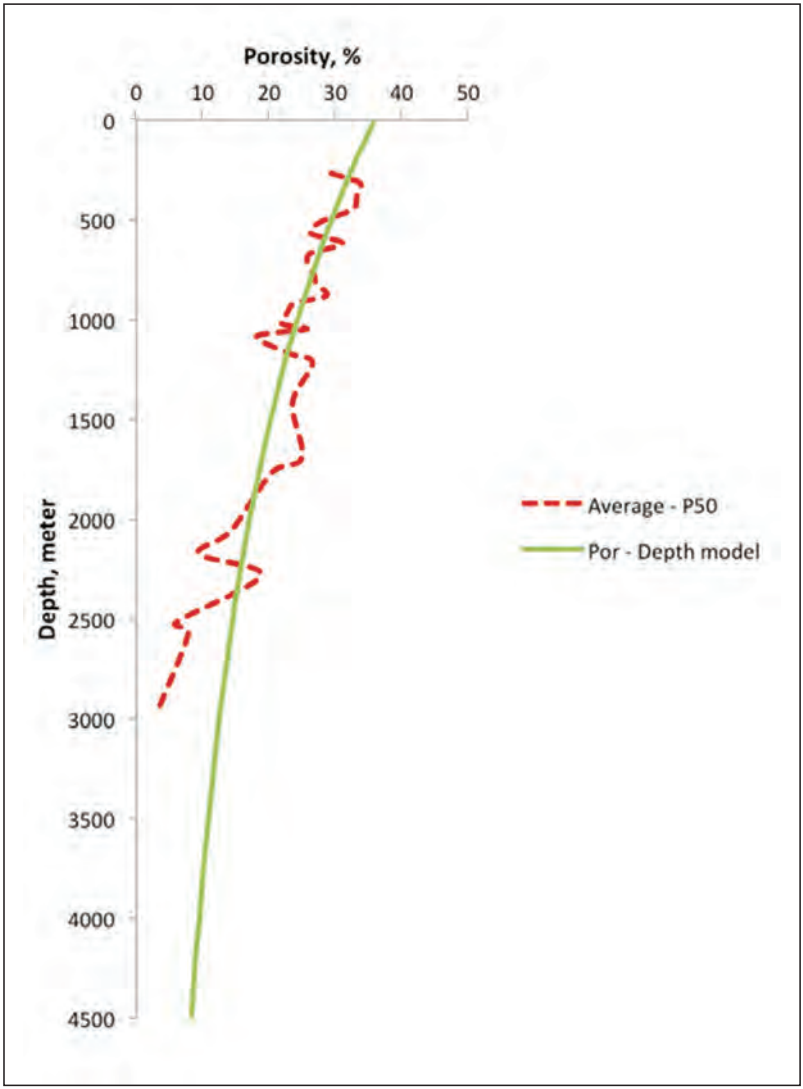

Source: Widarsono (2014b)

Figure 2.10 Porosity-Depth Model Fitting on Averaged P50 Porosity Data (P50 Point Number = 30) for North Sumatra Basin Data

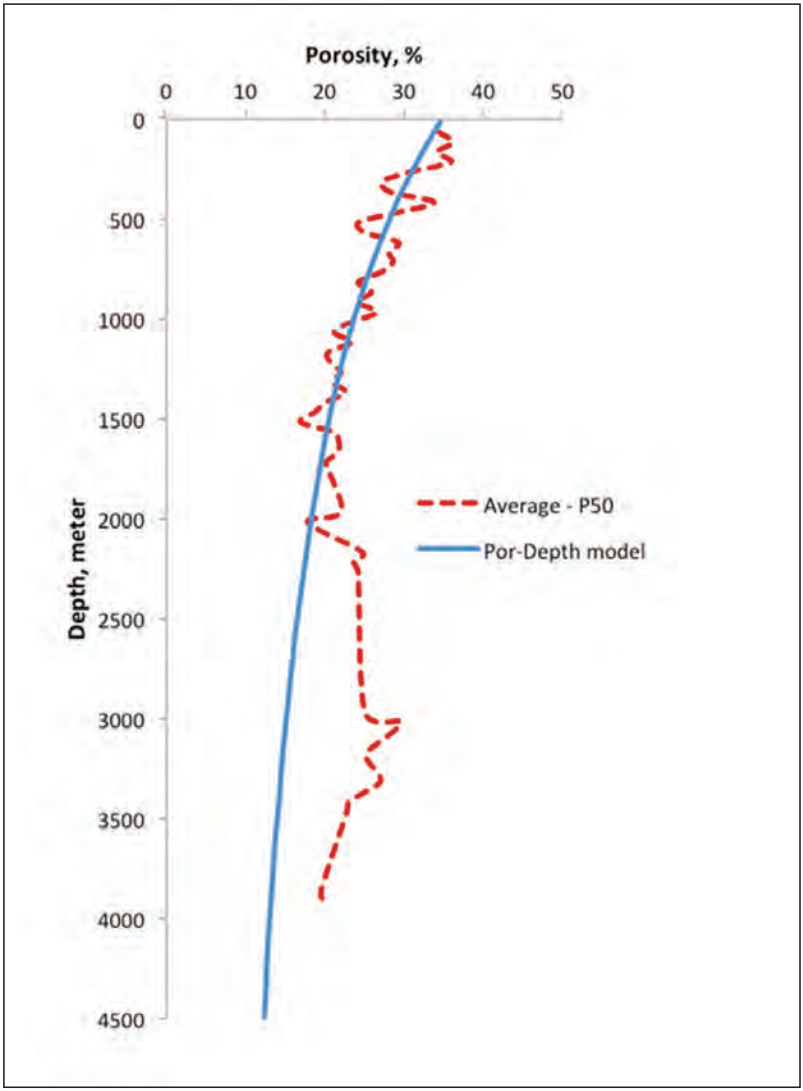

Source: Widarsono (2014b)

Figure 2.11 Porosity-depth model fitting on averaged P50 porosity data (P50 point number = 51) for Central Sumatra Basin data. Notice evidence of the pressumably porosity preservation at the lower part of the P50 curve.

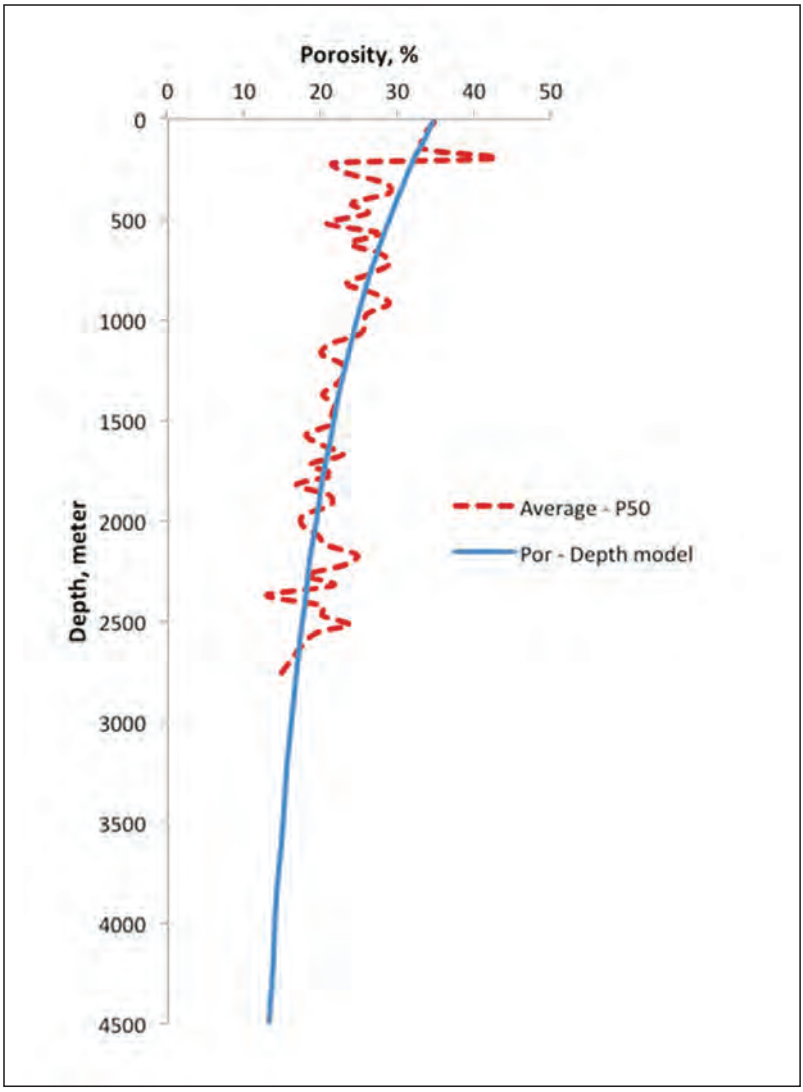

Source: Widarsono (2014b)

Figure 2.12 Porosity-Depth Model Fitting on Averaged P50 Porosity Data (P50 point number = 53) for South Sumatra Basin Data

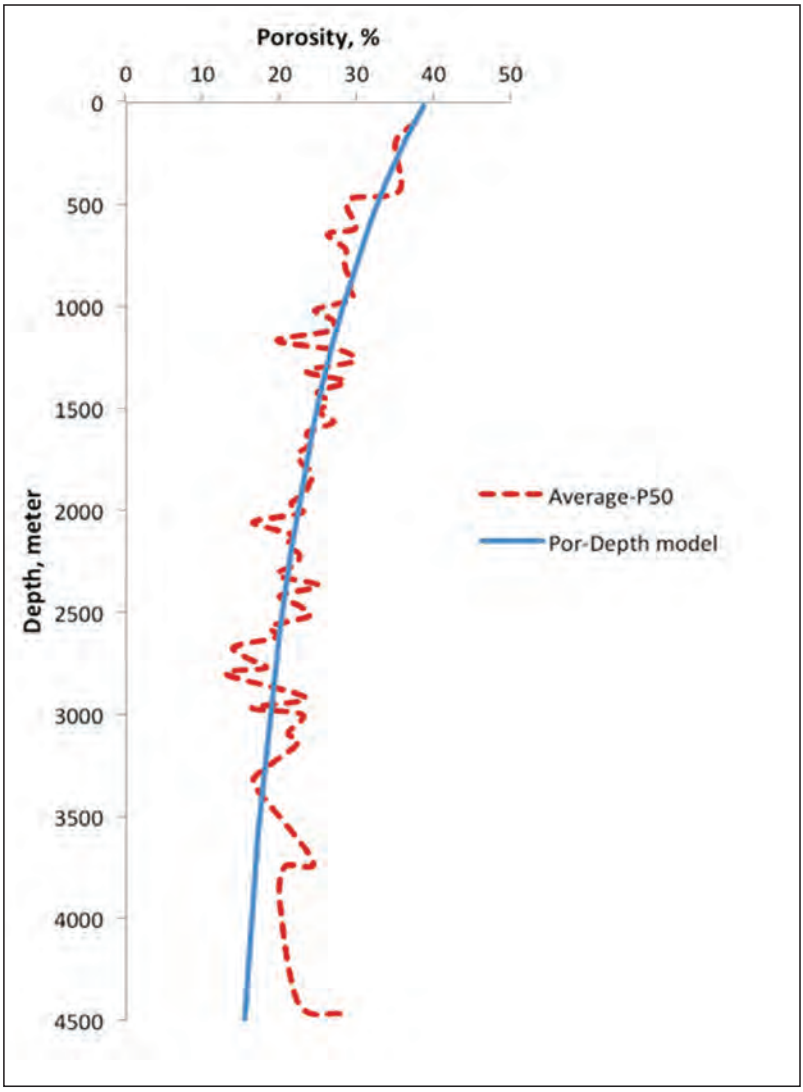

Source: Widarsono (2014b)

Figure 2.13 Porosity-depth model fitting on averaged P50 porosity data (P50 point number = 67) for West Natuna Basin data. Sign of porosity preservation at great depths are also visible.

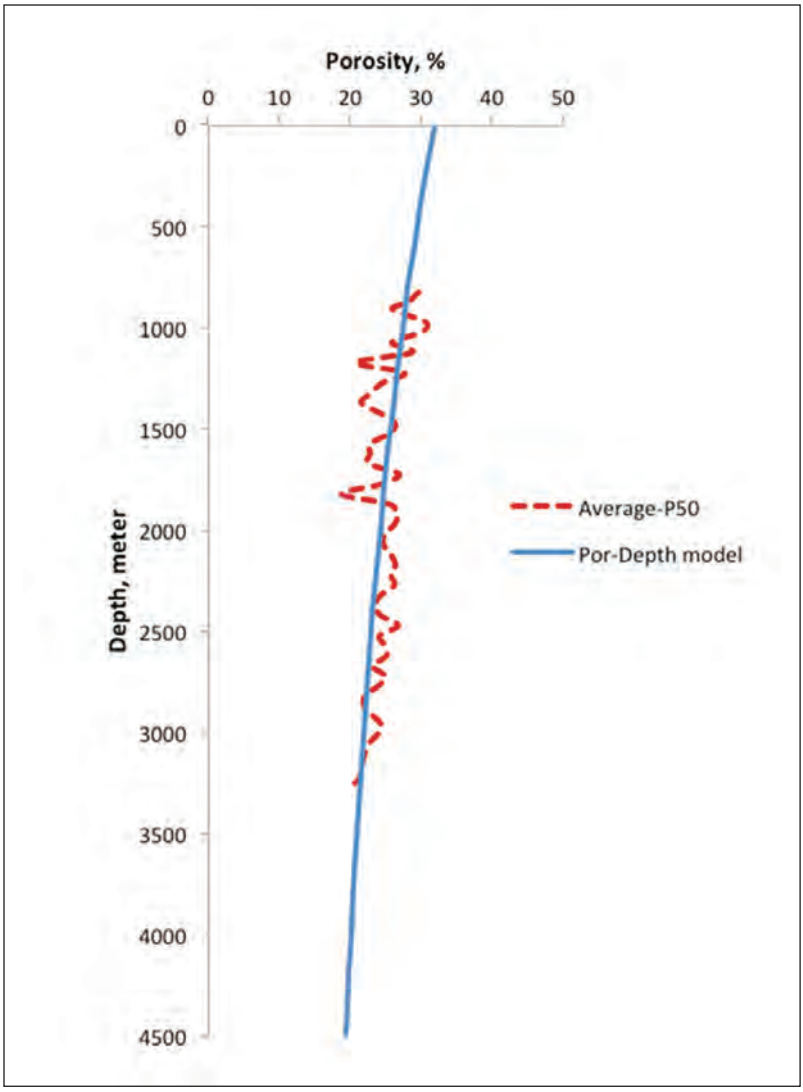

Source: Widarsono (2014b)

Figure 2.14 Porosity-Depth Model Fitting on Averaged P50 Porosity Data (P50 point number = 46) for West Sunda/Asri Basin Data

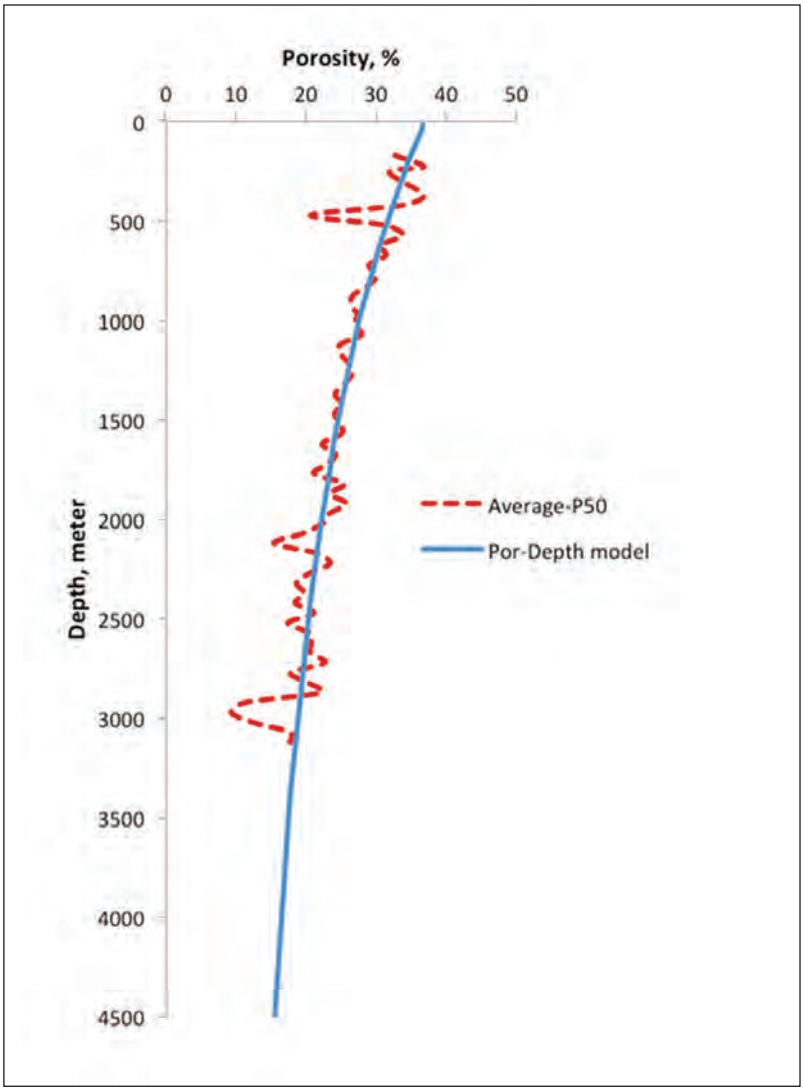

Source: Widarsono (2014b)

Figure 2.15 Porosity-Depth Model Fitting on Averaged P50 Porosity Data (P50 point number = 59) for Northwest Java Basin Data

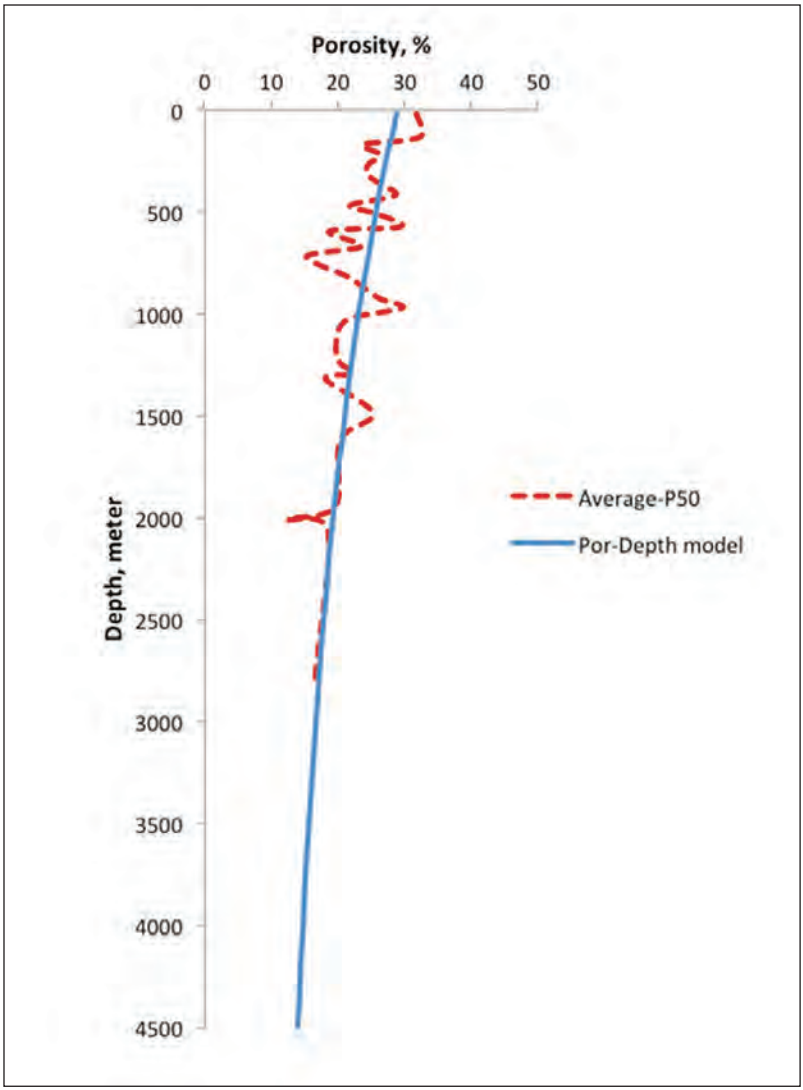

Source: Widarsono (2014b)

Figure 2.16 Porosity-Depth Model Fitting on Averaged P50 Porosity Data (P50 point number = 28) for Northeast Java Basin Data

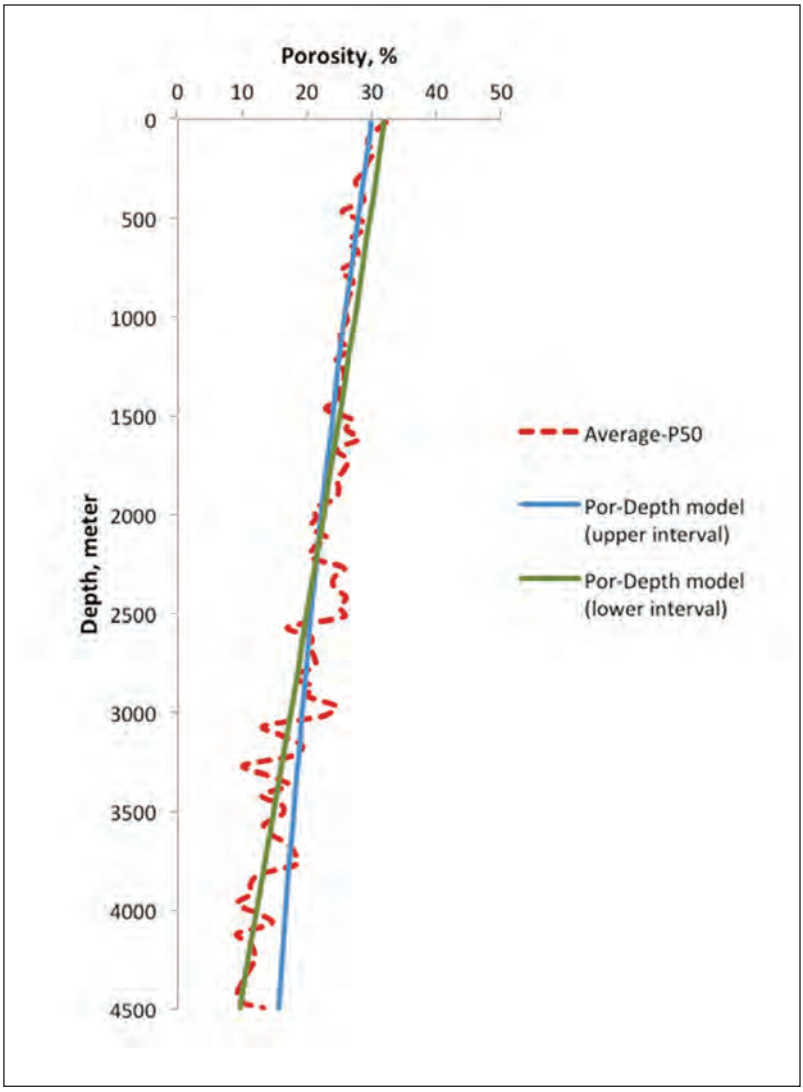

Source: Widarsono (2014b)

Figure 2.17 Porosity-depth model fitting on averaged P50 porosity data (P50 point number = 90) for the Kutai basin data. Signs of compaction at lower part of the porosity-depth column leads to a separate porosity-depth model.

E. Full-diameter versus Sidewall Core Porosities

In petrophysics, porosity values derived from FD-plug is in general regarded as more reliable than porosity values obtained from measurements on sidewall core (SWC) samples, especially the percussion (SWC) samples. This pressumption is indeed justified considering the method in which the percussion SWC samples are retrieved in the wellbore. Craft and Keelan (1985), in their study using large number of comparisons from Gulf Coast formations, revealed that FD-plug and SWC samples tend to show similarity in values for rocks with moderate porosity values (porosity of 27–33%). For rocks with porosity higher than 33% (i.e. soft rocks), the SWC-derived porosity tends to show lower values than FD-plug values due to impact of compaction on the relatively soft. On the other hand, rocks with SWC-derived porosity lower than 27% the reverse is true due to possible cracking on the retrieved samples (i.e. shattering effect). Measures normally taken (i.e. sample mounting and wrapping) are usually considered as inadequate to preserve the original porosity.

As shown on Figure 2.2, however, FD-plug and SWC derived porosity values has shown similarity in general. Clusters of the porosity values of the two groups appear to overlap to each others. Observation over plots at lower level (i.e. at sedimentary basin) shows the same occurence except for data from NW Java Basin (Figure 2.8) and NE Java (Figure 2.9), eventhough for NE Java Basin the number of data may be considered as to small. The sufficiently large number of NW Java appears to confirm the finding presented by Craft & Keelan (1985), eventhough in Widarsono (2014b) cautions were made to avoid data representing fractured or insufficient samples. In general, therefore, the study has shown that there is no much differences between the

two sources of porosity data. This fact is important for validity of the overall porosity data used for generating the porosity-depth models.

F. Porosity-depth Regional Trends

Comparisons between porosity-depth trend for all data and the trends for data at basin level appear to exhibit similar occurrences. The porosity tends to decrease with the increase of depth. No firm suggestions indicate that the main mechanism affecting the porosity decrease with depth is caused solely by overburden (i.e. burial) effect. Further investigation at lower levels than basin level—field level or lower—may suggest differently, in which non-burial mechanisms such as cementation and porosity preservation prevail. Nevertheless, noticeable occurences are observed for Central Sumatra and West Natuna data (Figures 2.4 and 2.6 or Figures 2.12 and 2.14, respectively). In these two cases, porosity tends to deviate and be higher than the overall trends indicating porosity preservation as suggested by, for instance, Ehrenberg & Nadeau (2005). On the other hand, signs of porosity reduction at great depths are shown by Kutai Basin data (Figures 2.10 and 2.18). At depths deeper than 2,500 m, sandstone porosity decreases at a tendency stronger than the original trend as, for instance, suggested by Gratier et al. (2013). These two occurrences have shown that all mechanisms are apparently at work in the eight sedimentary basins.

All models for the eight sedimentary basins (Figure 2.19) show variety of trends in porosity decrease with depth. They are similar like in the case of South Sumatra and Central Sumatra data, whereas others are sufficiently different when North Sumatra and West Natuna gradients are put into comparison. This indicates that each sedimentary basin may have followed similar process in the burial but may have also been differentiated by various mechanisms depending on

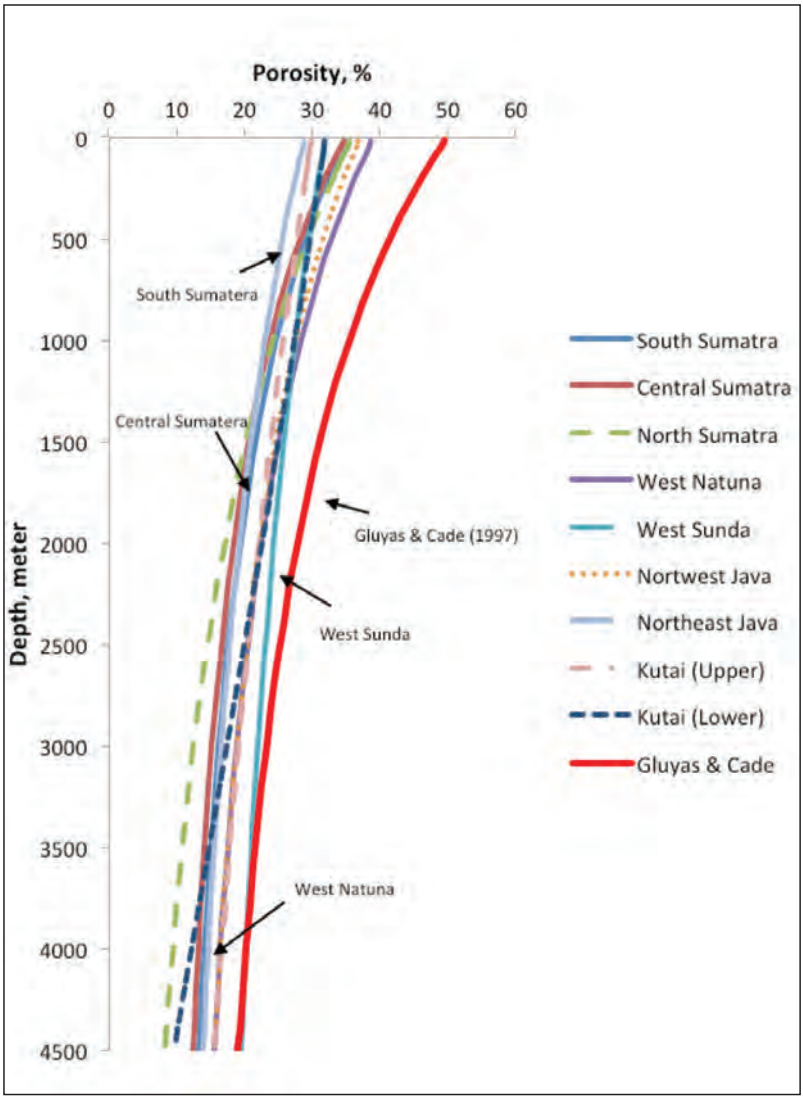

Source: Widarsono (2014b)

Figure 2.18 Porosity-depth models of the Eight Sedimentary Basin in Western Indonesia. The significant difference shown by Gluyas & Cade (1997) model leads to a conclusion that the model is not valid for the eight basins.

intrinsical factors within individual basin. Mineral compositions, hydrocarbon entry, levels of quartz cementation, temperature gradients, tectonic activity, and other factors can both be similar and different for the basins. Nonetheless, a significant difference is exhibited by the Gluyas & Cade (1997) model both in magnitudes and trends. The model represents higher overall porosity values and steeper porosity reduction with depth compared to the western Indonesian models. Differences in geological setting and ages for the two world regions are likely to enhance the differences in the above factors.

G. Validity of Information

The porosity values used in the study were measured without overburden loading. This may lead to a consideration over the validity of the porosity-depth models for any practical uses. However, as Widarsono (2014b) put, there is no intention whatsoever to regard the eight models as the true representative of the porosity variation with depth *in situ*. The models may have been better regarded as general indicators in judgements over the likely average porosity at field levels and potential anomalies that may be encountered. Therefore, since the differences between overburdened and non-overburdened porosity values are likely to be small (i.e. maximum difference of just one-twentieth of the non-overburdened porosity values), and certainly far smaller than data scatters, the issue of model practicability should not be overemphasized.

Another fact shows that distribution of data quantity among the eight sedimentary basins is uneven. For instance, the Kutai Basin is represented by 1,394 samples (Table 2.8) while the Northeast Java Basin has only 86 samples considered suitable or fit to the purpose (Table 2.7). For basins with limited samples available like Northeast Java (86 samples) and North Sumatra (105) (Table 2.1), this condition

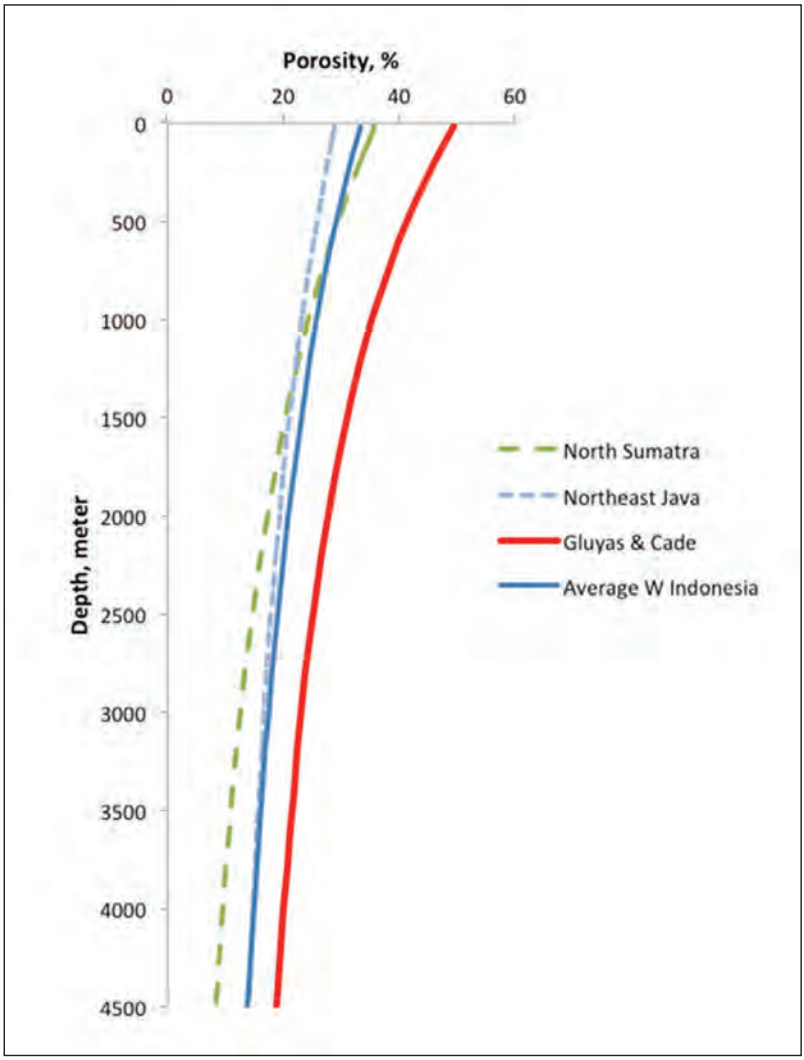

Source: Widarsono (2014b)

Figure 2.19 Comparison between North Sumatra/Northeast Java Models and Average Western Indonesia Model (average values). The two models appear to be more in agreement with the average model than with Gluyas & Cade (1997) model indicating some extent of validity for the two models.

may lead to a question over the validity of the models representing them. However, when a comparison is made between the models representing the two basins and an average model representing all eight basins, the comparison shows more agreement to the average model than to the Gluyas & Cade (1997) model. This indicates that, despite the data limitation, the models of North Sumatra and Northeast Java Basins have at least some extent of validity due to its resemblance to the all other basins represented by the average model. The two models can therefore still be regarded as representative at large for the two basins.

CHAPTER III
PERMEABILITY–VERTICAL ANISOTROPY

A. General

Permeability estimation and variation of values always draw the-attention of any engineer and geoscientist whenever they come to the task of characterizing and producing reservoirs as good and efficient as they can. In homogeneous reservoirs, permeability is considered the same in all directions. On the contrary, in heterogeneous reservoirs, permeability tends to differ with direction. The more heterogeneous a reservoir, the higher variation in directional permeability it tends to show. In this case, permeability may be different in all directions, making it difficult to obtain the overall picture of permeability distribution in a reservoir. In lesser degree of heterogeneity, the permeability in vertical direction is still considerably different than the permeability in horizontal direction but with similar permeability in all horizontal directions (transversely isotropic). Nevertheless, the net impact of such changing permeability in different directions is especially marked on all aspects that involve flows of reservoir fluids such as natural recovery efficiency, enhanced oil recovery, well testing, and completion scheme.

In reservoir modeling and simulation for determining field development and natural recovery efficiency, permeability anisotropy

levels of concerning reservoir rocks play a very important role. Various related studies that involve permeability anisotropy have been performed. For instance, Yetkin et al. (2009) studied and introduced a method for representing permeability anisotropy in reservoir numerical modeling, while Paul et al. (2011) studied the effect of permeability anisotropy caused by fault damage zone on reservoir simulation hence improving history matching quality. Other applications using reservoir modeling have also taken permeability anisotropy into consideration (e.g. Heinemann et al., 1991; Duquerroix et al., 1993; Dicksen et al., 2002; Wu et al., 2004). Effects of permeability anisotropy on well productivity/performance (e.g. Economides et al., 1996; Al-Hadrami and Teufel, 2000; Furui et al., 2003), well stimulation/hydraulic fracturing (e.g. Gatens et al., 1991, Aghighi & Rahman, 2010), and well completion (e.g. Odeh & Babu, 1990; Ansah et al., 2002; East et al., 2004) schemes are also recognized. The importance of permeability anisotropy extends even further to areas that are not directly related to conventional oil and gas production such as coal bed methane (CBM) (e.g. Gu & Chalaturnyk, 2010; Pan & Connell, 2012), carbon capture and storage (CCS) (e.g. Ennis-King & Paterson, 2002), and hydrology (e.g. Marechal et al., 2004).

Some methods are known to be available for determining permeability anisotropy. Among others are through direct measurement (i.e. core measurement or permeability probe measurement) (e.g. Meyer & Krause, 2006), indirect measurements such as well testing (e.g. Angeles et al., 2005) and geophysical (e.g. Shapiro et al., 1999; Rasolofasaon & Zinsner, 2002), and combined between direct and indirect approaches (e.g. Morton et al., 2002). This chapter is dedicated to presenting permeability anisotropy features of some Indonesian reservoir rocks. The chapter essentially adopts the work presented in Widarsono et al. (2006) and Widarsono et al. (2007) with some corrections and additional information.

B. Permeability Anisotropy

Many studies have been devoted to understand the effect of permeability anisotropy in reservoir. McGuire & Sikora (1960), for example, studied the effect of high vertical permeability caused by fractures on well productivity. They concluded that the presence of anisotropy changes the flow pattern significantly, hence modifying well productivity previously estimated under assumption of both radial and linear flow patterns. Landrum and Crawford (1960) also studied the effect of anisotropic horizontal permeability on sweep efficiency in waterflooding, whereas more recently Datta Gupta et al. (1986) conducted simulation modeling to study the effect of permeability contrast between layers (i.e. transversely isotropic condition) on recovery factor of polymer flooding, from which they concluded that less contrast tends to show higher recovery factor. A similar study on foam flooding has also been reported by Dicksen et al. (2002).

In areas more related to field operational level, Tariq et al. (1989) studied the effect of anisotropy on perforation and fluid flow near wellbore using finite element method and found that high shot density is required in anisotropic/laminated formation, while Smith et al. (1981), Gatens et al. (1991), and Aghighi & Rahman (2010) studied effect of horizontal permeability anisotropy on hydraulic fracturing and witnessed its significant effects on generated fracture dimension and production gain brought by the fractures. Furthermore, a simulation study carried out by Besson (1990) suggested that slanted wells show better production performance than horizontal wells in anisotropic medium. Odeh & Babu (1990), Ansah et al. (2002), and East et al. (2004) carried out modeling studies for well completion optimization. All these studies underline the significance of recognizing the presence and degree of permeability anisotropy in formations.

Permeability anisotropy is often used to express the degree of heterogeneity in the formation. Vertical permeability (K_V) is usually different from horizontal permeability (K_H), even for homogeneous rocks. Such vertical anisotropy effects are generally the result of depositional environment and post-depositional compaction history of the rock. For sandstones and other clastic sedimentary rocks, shale contents and types, grain size, grain shape, and particle orientation are the most important factors in K_V–K_H relationship. However, permeability anisotropy is also likely to be influenced by the scales of heterogeneity. As often presented in studies (e.g. Tiab and Donaldson, 2004), as a part of evaluation on heterogeneity, scales of heterogeneity may be classified into a set of levels: microscopic (core scale), macroscopic (well scale), mesoscopic (inter-well scale), megascopic (field scale), and gigascopic (formation or basin scales). This implies that heterogeneity and permeability anisotropy should be viewed as dependent on size and scale of the rock mass. Therefore, permeability anisotropy in formation has ideally to be viewed through its relevant scale of heterogeneity.

By observing this principle of scale-related permeability anisotropy, it is implied that considered reservoirs are normally engineered and managed at macroscopic (log) and mesoscopic (inter-well) scales, then information regarding the anisotropy should also be derived at these scales. Many investigators have spent efforts to derive vertical permeability at its most appropriate scale. For instance, Nisle (1958) and Brons & Marting (1961) studied the effect of well's partial penetration on pressure drop around wellbore and suggested that the smaller the degree of vertical permeability anisotropy, the larger the pressure drop expected to occur, and Renard & Dupuy (1991) put that magnitude of vertical permeability relative to horizontal permeability may magnify the effect of damage zone around wellbore. Later, other studies suggested analysis of pressure transient test data as

a source of determining vertical permeability. Moncada (2003), who showed how to derive vertical permeabilty from pressure derivative type-curve-matching, is one example.

Despite its importance, measurement of permeability anisotropy at appropriate scale cannot always be conducted for various practical reasons. Instead, most field operators still rely on the traditional way of obtaining the information: direct core analysis at smaller levels of macroscopic scale. In core-derived permeability anisotropy, K_V and K_H are determined on regular basis of common depths. When core samples are of full-diameter type, the K_V and K_H are simply measured on the same sample, whereas for plug samples, K_V and K_H are measured on a pair of vertical and horizontal plug-samples taken from a common depth point. Many studies based on core measurements have been devoted on different lithology; sandstones (e.g. Meyer, 2002; Benson et al., 2005; Meyer & Krause, 2006), carbonates (e.g. Sahin et al., 2007; Saleh et al., 2009), shale/clays (e.g. Clennen et al., 1999; Burton & Wood, 2013), and mudstone (e.g. Yang & Aplin, 1998; Mondol et al., 2010). Using core-derived information, some investigators have gone further to provide means of determining K_V through empirical K_V–$(K_H/\phi)^{0.5}$ relationships (e.g. Peffer & O'Callagan, 1997; Manseur et al., 2002; & Zahaf & Tiab, 2002).

Permeability anisotropy in Indonesia, with its complex geological setting, can always be regarded as an ever-factual issue in reservoir fluid flow-related matters. In Indonesia's case, the common practice of picking a single representative K_V/K_H ratios through assumption could be misleading since the ratios may differ from one reservoir to another and even to one location within a reservoir to another. In essence, there may not be a single representative K_V/K_H ratio at all for a reservoir of concerned. Based on writing in Widarsono et al. (2006), this chapter is providing a general view over permeability vertical

anisotropy in Indonesian reservoirs so that engineers and geoscientists operating in Indonesia can have a useful source of relevant information in their day to day professional activities.

C. Data Inventory

In the study presented in Widarsono et al. (2006), a large amount of core analysis data has been used. Since its first involvement in mid 1970s, LEMIGAS Core Laboratory has been conducting tens of thousands of measurements on core samples for their permeability data, as well as porosity and other basic petrophysical data. For the study, a data inventory has been set up involving vertical and horizontal permeability values of both full-diameter and pairs of plug samples. In selecting the data, careful measures were made to underline that: 1) Permeability data is a combined air and liquid permeability data, and not all air permeability values are corrected for slippage effects; 2) Vertical and horizontal plugs were taken from common depth points; 3) From a range of minimum to maximum horizontal permeability measured on full-diameter core samples, a mid-value is taken as the representative value to form K_V/K_H ratio with the corresponding K_V value.

A total of 7,489 K_V/K_H ratio data was collected, of which 6,441 (4,312 sandstones and 2,129 carbonates) are pairs of vertical and horizontal plug samples and 1,048 (336 sandstone and 712 carbonates) are full-diameter (FD) core samples. They were taken from 251 wells representing 129 oil and gas fields in 12 Indonesia's productive sedimentary basins (Figure 3.1 and Tables 3.1 through 3.4). The sandstone samples covered in the study represent a wide range of types, from clean sand, laminated shaly sand, argillaceous sand, conglomeratic sand, to sand containing special minerals such as micaceous, glauconitic, and carbonaceous sands, whereas the carbonates samples covered limestone, dolomite, and other carbonate rocks.

Table 3.1 Kv/KH Data for Plug and Full-Diameter (FD) Cores and Its Field of Origin: North Sumatra, Central Sumatra, and South Sumatra Basins

Basin	Field/structure (no. of wells)	Number of K_v/K_h data points			
		Sandstones		Limestones	
		FD	Plug	FD	Plug
North Sumatra Main formation(s): Seurulla, Keutapang, Belumai	Arun (7), Basilam (1), Batumandi (1), Keureutu (1), NSB (1), NSO (3), Lhok Sukhon (1), Perapen (2), Peutow (1), Rantau (1), Rayeu (1), S. Lhok Sukon (7), STB (1) Total wells = 28	120	98	426	482
Central Sumatra Main formation(s): Pertama, Kedua, Duri, Bekasap, Bangko, Telisa, Petani	Ampuh (1), Duri (3), Bekasap (3), Hiu (1), Kasikan (1), Kotabatak (1), Kulin (3), Libo SE (1), Minas (2), MS.DZ (1), Pedada (3), Pukat (1), Sabak (1), Sintong (1), S. Pulai (1), Telinga (1), Ubi (1) Total wells = 24	22	1340	-	-
SouthSumatra Main formation(s): Gumai, Talang Akar, Air Benakat, Muara Enim, Baruraja Lm	Bajubang (5), Bentayan (2), Betung (1), Jirak (3), Karang Agung (1), Kenali Asam (2), Leko (1), Limau (3), Lubuk (1), Meruo Senami (1), Musi (1), N. Kluang (1), Sungai Gelam (1), Supat (1),Talang Jimar (1), Talang Jimar Selatan (1), Tapus (3), Tempino (1) Total wells = 29	15	688	51	267

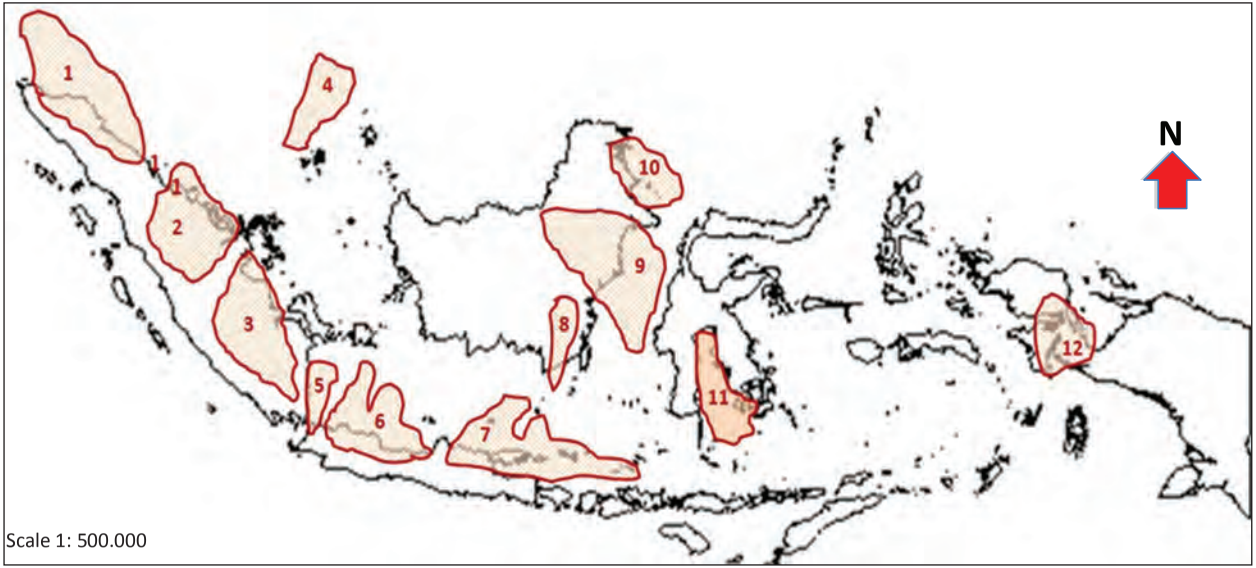

Figure 3.1 The 12 Productive Sedimentary Basins of 1) North Sumatra, 2) Central Sumatra, 3) South Sumatra, 4) West Nauna, 5) West Sunda, 6) Northwest Java, 7) Northeast Java, 8) Barito, 9) Kutai, 10) Tarakan, 11) Bone, and 12) Bintuni, from which the Core Samples Were Derived

Table 3.2 Kv/KH data for Plug and Full-Diameter (FD) Cores and Its Field of Origin: West Natuna, Northwest Java and Northeast Java Basins

Basin	Field/structure (no. of wells)	Number of K_v/K_h data points			
		Sandstones		Limestones	
		FD	Plug	FD	Plug
West Natuna Main formation(s): Lower Gabus, Upper Gabus, Arang,	Alu-alu (1). Forel (1), Kepiting (1), Kodok (1), S. China Block (4), Tembang (1), Terubuk (1), Todak (1), Udang (2) Total wells = 13	37	528	-	-
Northwest Java Main formation(s): Baturaja Lm, Talang Akar, Cibulakan	Cicauh (1), Cemara Barat (2), Cemara Selatan (2), Cemara Timur (2), Cilamaya Selatan (1), Cilamaya Utara (1), Jatinegara (2), Kandanghaur Barat (1), Kandanghaur Timur (2), Melandong (1), ONWJ (11), Pamanukan (1), Pegaden (2), Rengasdengklok (6), Serang (1), Subang (4), Tambun (10), Tugu Barat (4) Total wells = 54	29	91	30	433
Northeast Java Main formation(s): Ngrayong, Ledok, Kujung	Bawean (1), Jatirogo (1), Kawengan (2), KE (3), Kepodang (1), Ledok (1), Mangkang Kulon (1), Nglobo (1), Poleng (2), Purwodadi (1) Total wells = 14	-	120	40	141

Table 3.3 Kv/KH Data for Plug and Full-Diameter (FD) Cores and Its Field of Origin: Barito, Kutai, Tarakan, and Sengkang Basins

Basin	Field/structure (no. of wells)	Number of K_v/K_h data points			
		Sandstones		Limestones	
		FD	Plug	FD	Plug
Barito Main formation(s): Tanjung, montalat, Warukin	Berimbun-A (1), Pulau Laut (1), Tanjung (3) Total wells = 5	26	143	-	84
Kutai Main formation(s): Balikpapan, Kampung Baru	Badak (3), E. Manpatu (1), Handil (3),Kerbau (1), Mutiara (4), Nilam (4), Nubi (3), NW Apar (1), NW Peciko (1), Parangat (2), Sangatta (4), Semberah (3), Sisi (1), Tambora (7), Tunu (14), Tutung (1), UKM (1) Total wells = 54	12	1212	-	84
Tarakan Main formation(s): Bunyu, Tabul	Bunyu (3), Bunyu Barat (1), P. Tibi (1) Total wells = 5	61	32	-	-
Sengkang Main formation(s): Tonasa-Makale, Tacipi, Toraja-Malawa	Kampung Baru (2), Sampi-sampi (1), Tironge (1), Walanga (1) Total wells = 5	-	-	121	95

Table 3.4 Kv/KH Data for Plug and Full-Diameter (FD) Cores and Its Field of Origin: West Sunda and Bintuni Basins

Basin	Field/structure (no. of wells)	Number of K_v/K_h data points			
		Sandstones		Limestones	
		FD	Plug	FD	Plug
West Sunda Main formation(s): Talang Akar, Baturaja	Karmila (1), Krisna (3), Nurbani (1), Rama (3), Titi (1), Yanti (1), Yuli (1) Total wells = 11	14	56	22	361
Bintuni Main formation(s): Kembelangan, Kais	NW Mogoi (1), Rawarra (1), Tanemot (1), Wasian (2), Wiriagar (1), West Wiriagar (1) Total wells = 7	-	-	22	182

D. Sandstones Anisotropy

In analysing the K_V/K_H ratio, Widarsono et al. (2006) carried out groupings, classification, and comparisons. Groupings were made based on some aspects such as sedimentary basins, porosity ranges, horizontal permeability ranges, sandstone types, individual well vertical variation, and field lateral variation. For sandstones, data is presented in both histogram and Cartesian plots with K_V/K_H intervals of 0.1. All values less than 0.1 and greater than 1.5 are included in categories of < 0.1 and > 1.5, respectively. For carbonates, due to their wider range of data, data is also presented in both histogram and Cartesian plots but with K_V/K_H intervals of 0.3. All values less than 0.3 and greater than 4.2 are included in categories of < 0.3 and > 4.2, respectively. Exact values equal to the range limiting values are treated as to belong to the lower range. It is also worth noting that even though, for a practical reason, all the K_V/K_H values greater than 1.5

and 4.2 are included into one class (K_V/K_H > 1.5 and > 4.2), they will not make a misinformation problem since in total they numerically are usually lower than 10% of the total population.

1. Trends for Different Sedimentary Basins

Following the number of productive sedimentary basins in Indonesia, the first grouping is based on sedimentary basin of origin (Figure 3.1). All data roughly falls below K_V/K_H = 1.2. The value of the underlined idea of having the data based on these sedimentary basins is the possibility of different heterogeneity pattern at gigascopic scale between one basins to another. For instance, Figures 3.2 through 3.5 and Figures 3.6 through 3.9 present example K_V/K_H populations of sedimentary basins for and plug and FD samples, respectively. The plots based on this basin grouping have shown that distribution for core plug samples (with large population) is relatively even for the four basins presented, with mode within the range of 0–0.1. However, the small proportion that represents this mode (mostly between 13–17% of population, except for South Sumatra Basin with its 26% of population) can be regarded as preventing the mode as the most representative values.

In general, the distribution pattern shown by FD sample population is different compared to the pattern shown by core plug sample population. Distributions shown by the four basins in Figures 3.6 through 3.9 follow different patterns. This difference is likely caused by two factors: size difference (i.e. rock heterogenity) and number of population.

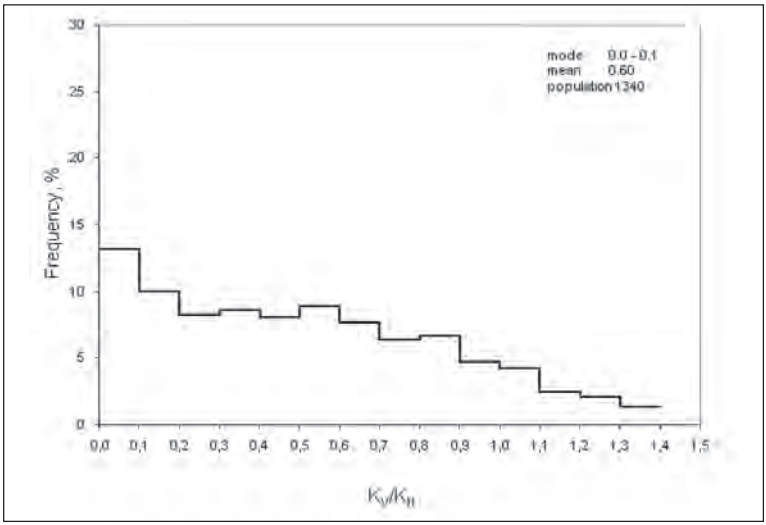

Source: Widarsono et al. (2006)

Figure 3.2 Anisotropy Distribution of Sandstone Core Plugs from Central Sumatra Basin

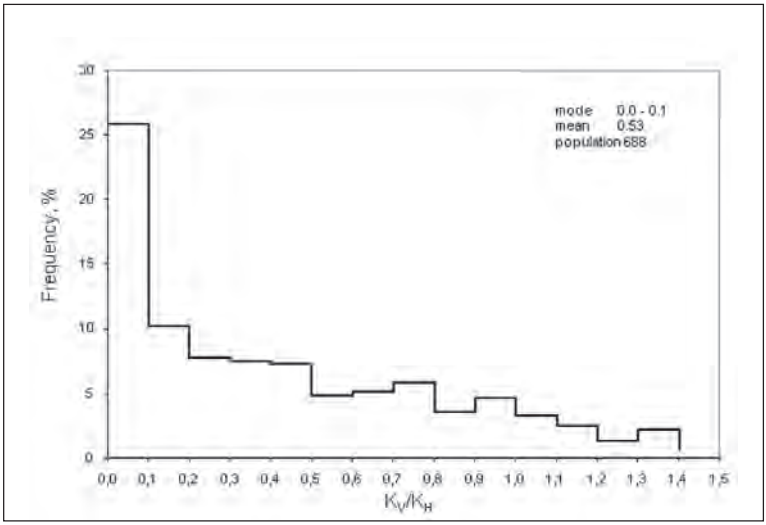

Source: Widarsono et al. (2006)

Figure 3.3 Anisotropy Distribution of Sandstone Core Plugs from South Sumatra Basin

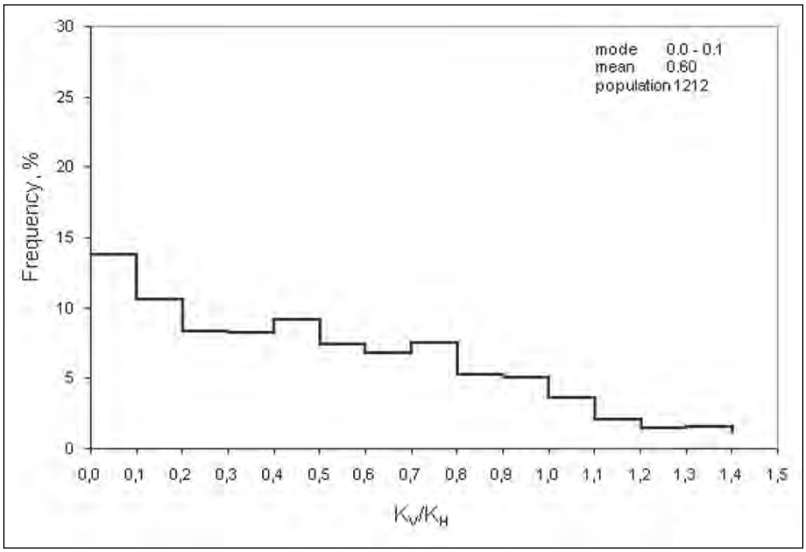

Source: Widarsono et al. (2006)

Figure 3.4 Anisotropy Distribution of Sandstone Core Plugs from Kutai Basin

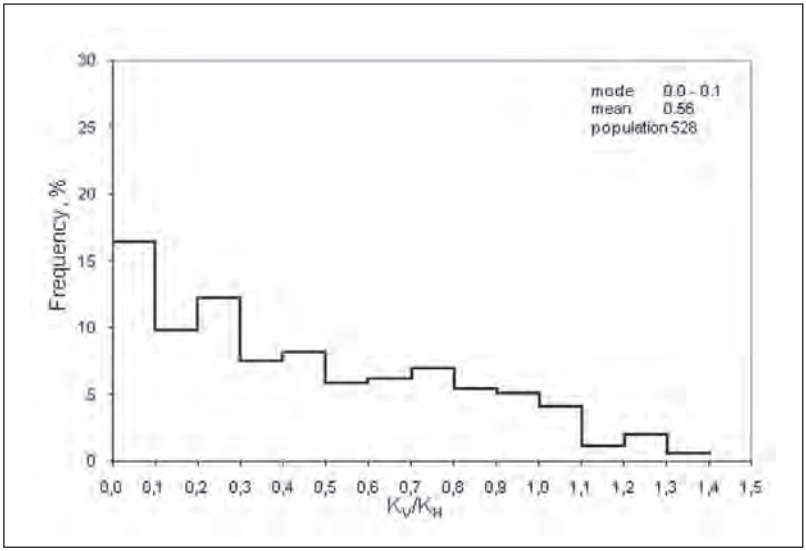

Source: Widarsono et al. (2006)

Figure 3.5 Anisotropy Distribution of Sandstone Core Plugs from West Natuna Basin

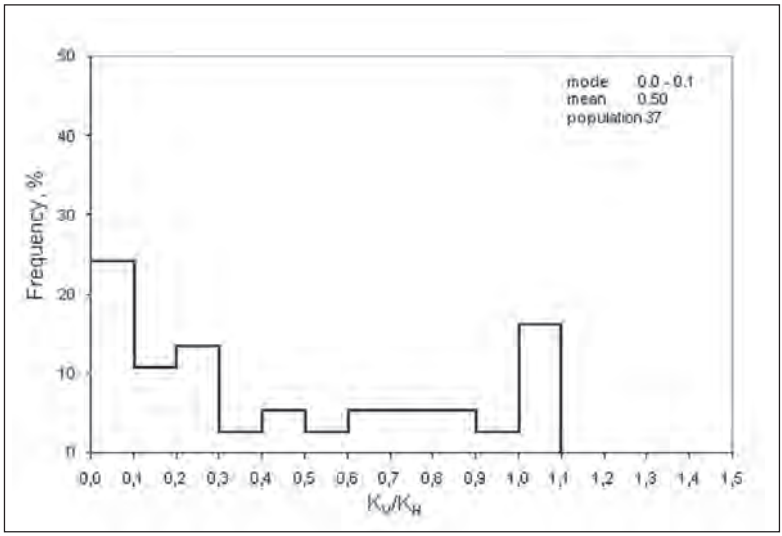

Source: Widarsono et al. (2006)

Figure 3.6 Anisotropy Distribution of Sandstone Full-Diameter (FD) Cores from West Natuna Basin

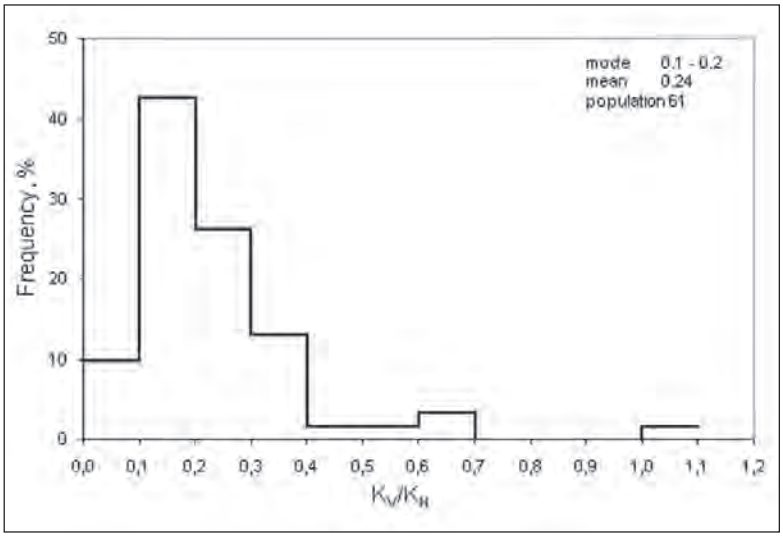

Source: Widarsono et al. (2006)

Figure 3.7 Anisotropy Distribution of Sandstone Full-Diameter (FD) Cores from Tarakan Basin

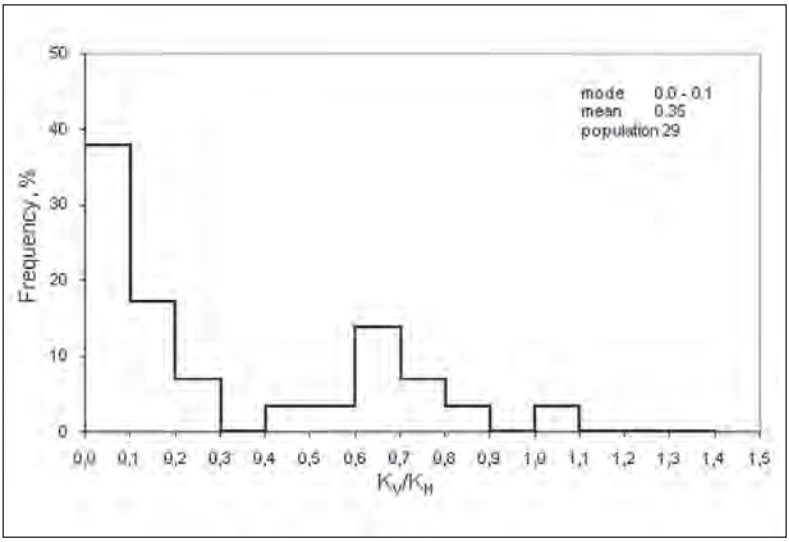

Source: Widarsono et al. (2006)

Figure 3.8 Anisotropy Distribution of Sandstone Full-Diameter (FD) Cores from Northwest Java Basin

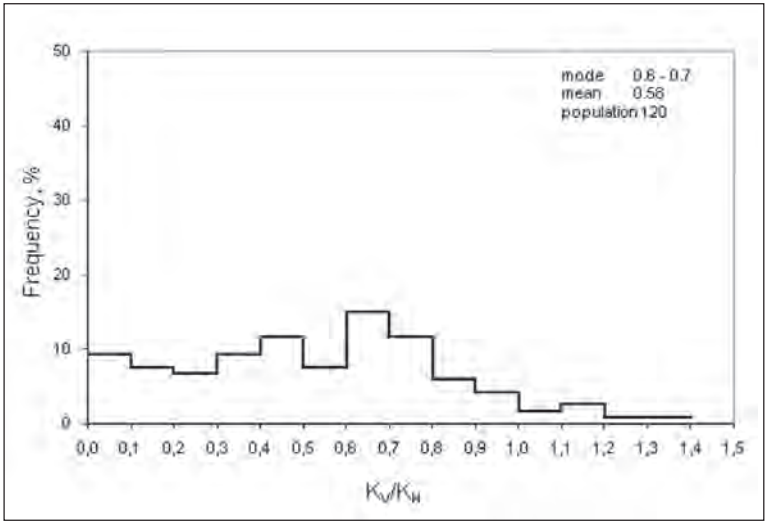

Source: Widarsono et al. (2006)

Figure 3.9 Anisotropy Distribution of Sandstone Full-Diameter (FD) Cores from North Sumatra Basin

2. Trends with Porosity Ranges

It is commonly acknowledged that actually there is no direct relationship between porosity and permeability, since magnitudes of permeability are rather directly determined by size and distribution of pore throat within the rock pore system. However, common practices in petrophysical analysis often link the two parameters from some practical reasons, and for some cases the relationships are proven useful. Therefore, the study also considers possible influence of differences in porosity on the K_V/K_H anisotropy. Porosity is divided into three classes: low (< 15%), medium (15–25%), and high (> 25%). Figures 3.10 through 3.12 present the K_V/K_H population for plug samples whereas Figures 3.13 through 3.15 present the same population for FD samples.

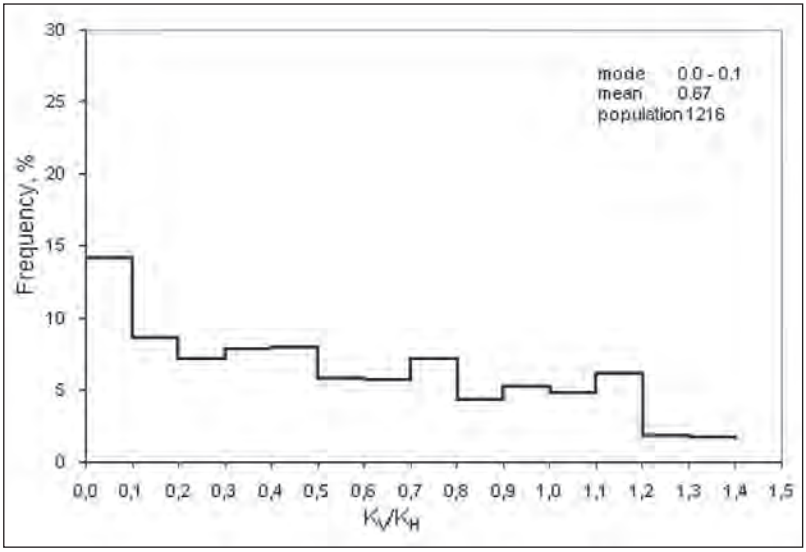

Source: Widarsono et al. (2006)

Figure 3.10 Anisotropy Distribution of Sandstone Full-Diameter (FD) Cores from Tarakan Basin

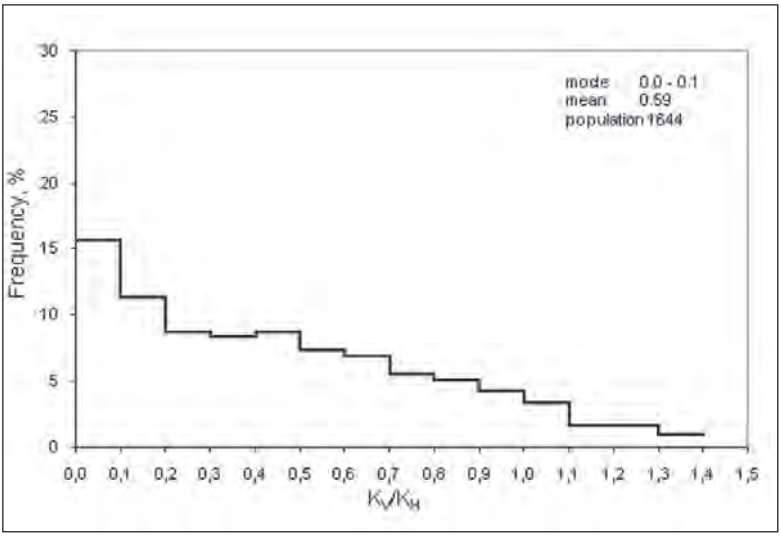

Source: Widarsono et al. (2006)

Figure 3.11 Anisotropy Distribution of Sandstone Core Plugs Classified As of Medium Porosity (ϕ = 15–25%)

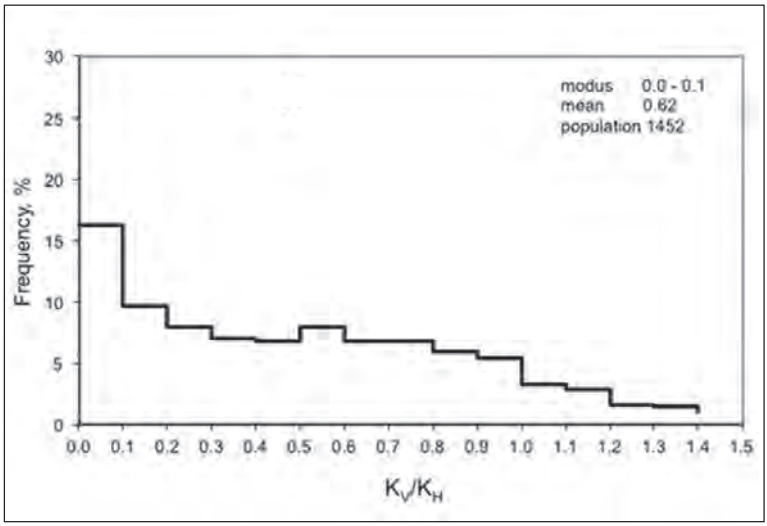

Source: Widarsono et al. (2006)

Figure 3.12 Anisotropy Distribution of Sandstone Core Plugs Classified As of High Porosity (ϕ > 25%)

The plots for the core plug samples exhibit similarity to the observation on the sedimentary basin grouping, which also show larger proportion for lower K_V/K_H ranges and mode value within 0–0.1 range but at an unrepresentatively low number proportionally to total population. The plots in general show that the population is relative uniformly distributed among the K_V/K_H ranges indicating no unique single representative K_V/K_H value. All data falls roughly below $K_V/K_H = 1.2$.

A special observation found in the effect over different porosity ranges is the similarity in distribution patterns of the whole core samples (Figures 3.13 through 3.15) to the core plug patterns. Obvious similarities are visible when whole core samples patterns are compared to the core plug patterns for their corresponding porosity ranges (e.g. Figure 3.10 with Figure 3.13 for low porosity range). Indeed, 'local' differences are also obvious, but semblances of similarity are also too clear to be omitted. This can be taken as an indication that, despite low in number of population, the K_V/K_H ratio measured at whole core size is also influenced by the same causes (e.g. pore configuration) as in the case of core plug samples.

From the overall picture obtained from observing permeability anisotropy versus porosity, it is almost clear that porosity has little influence on K_V/K_H distribution. This is indicated by similarity in the distributions for all porosity ranges, especially for the core plug samples (i.e. large sample number). This is very logical since permeability is actually not directly influenced by porosity.

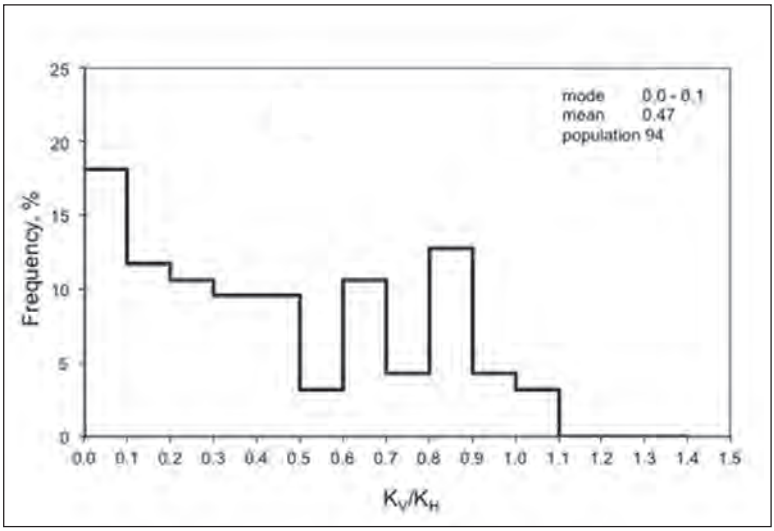

Source: Widarsono et al. (2006)

Figure 3.13 Anisotropy Distribution of Sandstone Full-Diameter (FD) Cores Classified As of Low Porosity (ϕ < 15%)

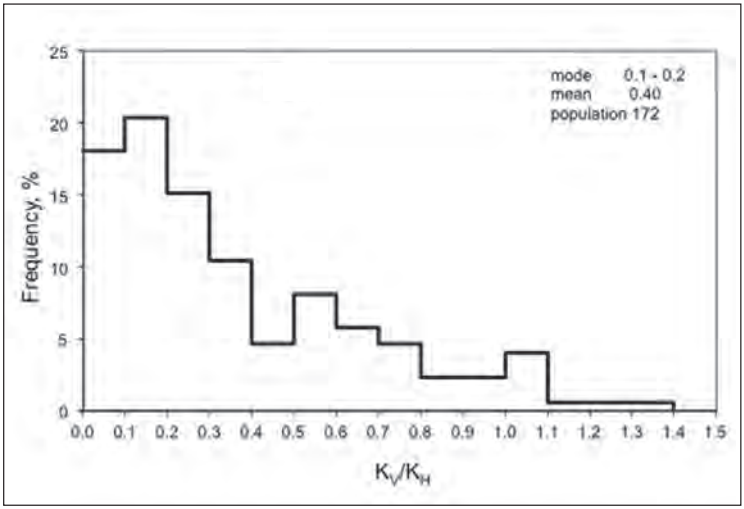

Source: Widarsono et al. (2006)

Figure 3.14 Anisotropy Distribution of Sandstone Full-Diameter (FD) Cores Classified As of Medium Porosity (ϕ = 15–25%)

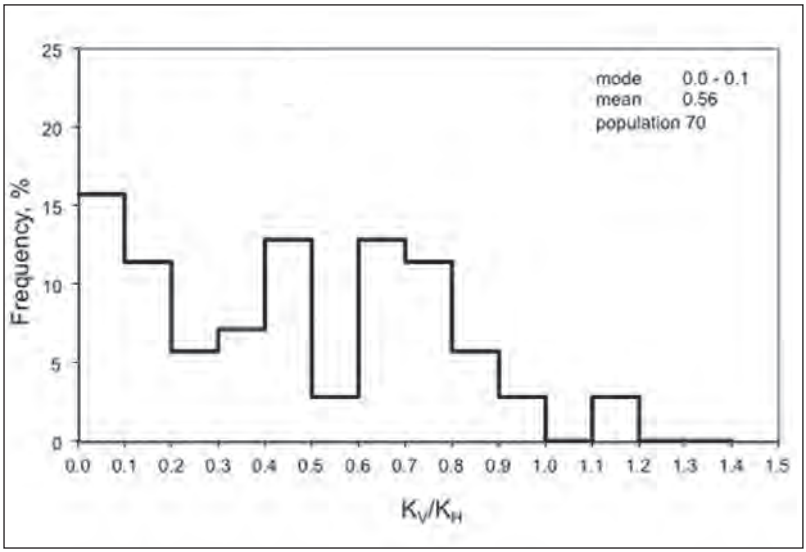

Source: Widarsono et al. (2006)

Figure 3.15 Anisotropy Distribution of Sandstone Full-Diameter (FD) Cores Classified As of High Porosity (ϕ > 25%)

3. Anisotropy with Horizontal Permeability Ranges

Since the magnitude of vertical permeability is always expressed in a form relative to horizontal permeability, it is therefore neccessary to observe the K_V/K_H tendencies with variations in horizontal permeability values. Theoretically, there is no direct influence that might be exerted by horizontal permeability towards vertical permeability, and the relationship between the two permeabilities is likely to be more influenced by rock's pore types. However, any evidence from analysis on the influence of horizontal permeability variations on K_V/K_H can still be regarded as useful. Permeability is divided into four classes: low (< 10 mD), medium (10–200 mD), high (200–800 mD), and very high (> 800 mD). Figures 3.16 through 3.19 and Figures 3.20 through 3.23 present K_V/K_H populations for plug and FD samples, respectively.

In a manner similar to effect of porosity, there are also similarities in the population distribution for the four horizontal permeability ranges, even though a relatively high K_V/K_H (frequency = 24%) is observed for medium permeability range. This can probably be interpreted as there is no direct influence exerted by horizontal permeability on vertical permeability. In other words, vertical permeability tends to be independent from horizontal permeability.

Also similar to results of permeability anisotropy trend versus porosity, there are semblances of similarity between core plug and FD sample distributions, despite the presence of 'local' differences. These differences are likely to be caused by the limited FD core sample population.

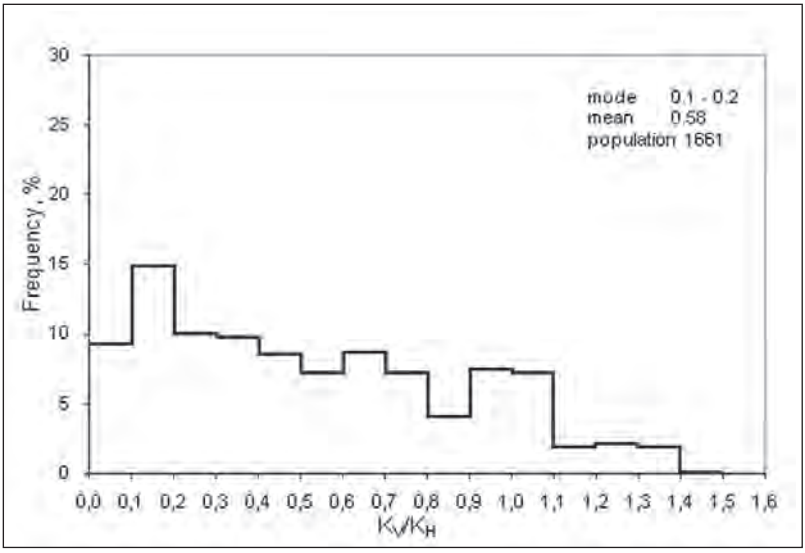

Source: Widarsono et al. (2006)

Figure 3.16 Anisotropy Distribution of Sandstone Core Plugs Classified As of Low Permeability (K < 10 mD)

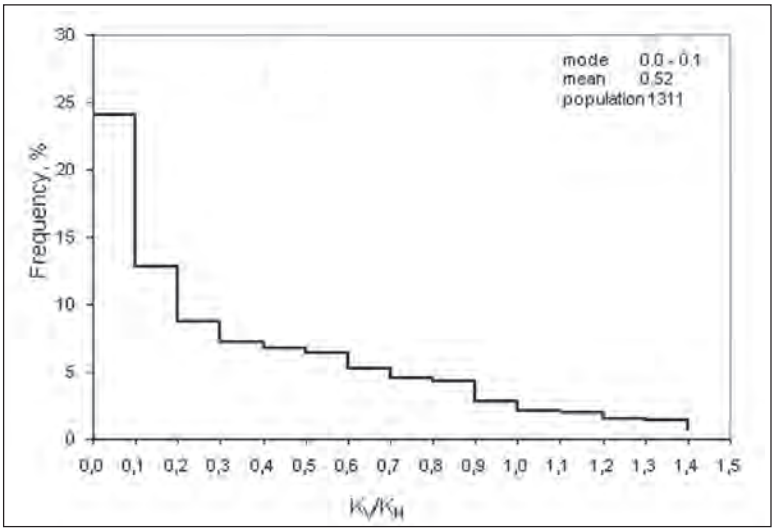

Source: Widarsono et al. (2006)

Figure 3.17 Anisotropy Distribution of Sandstone Core Plugs Classified As of Medium Permeability (K = 10–200 mD)

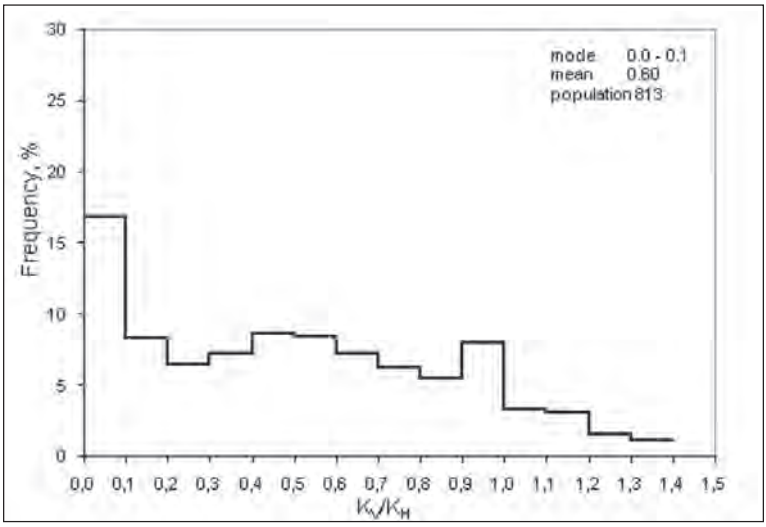

Source: Widarsono et al. (2006)

Figure 3.18 Anisotropy Distribution of Sandstone Core Plugs Classified As of High Permeability (200 mD < K < 800 mD)

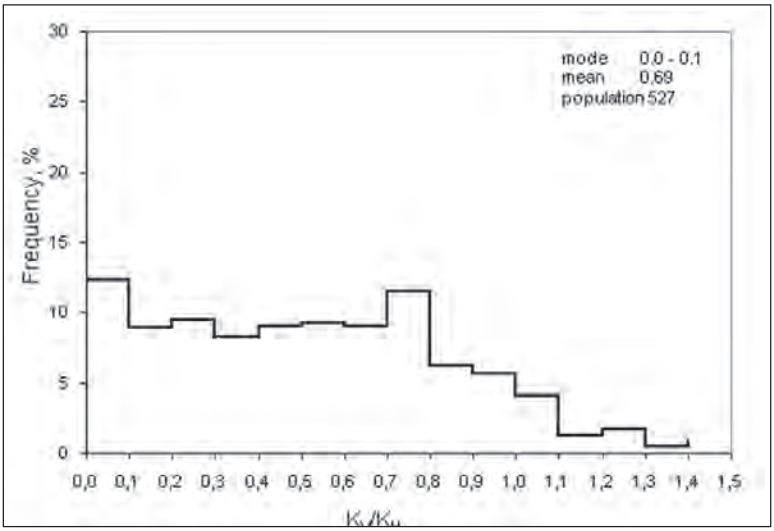

Source: Widarsono et al. (2006)

Figure 3.19 Anisotropy Distribution of Sandstone Core Plugs Classified As of Very High Permeability (K > 800 mD)

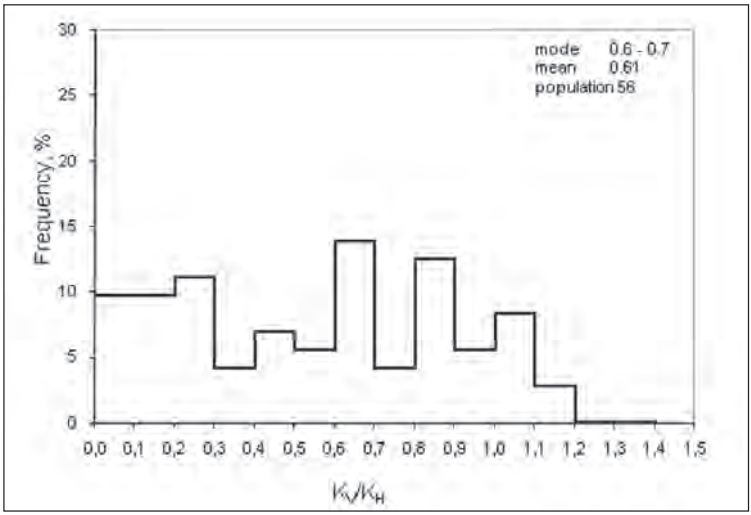

Source: Widarsono et al. (2006)

Figure 3.20 Anisotropy Distribution of Sandstone Full-Diameter (FD) Cores Classified As of Low Permeability (K < 10 mD)

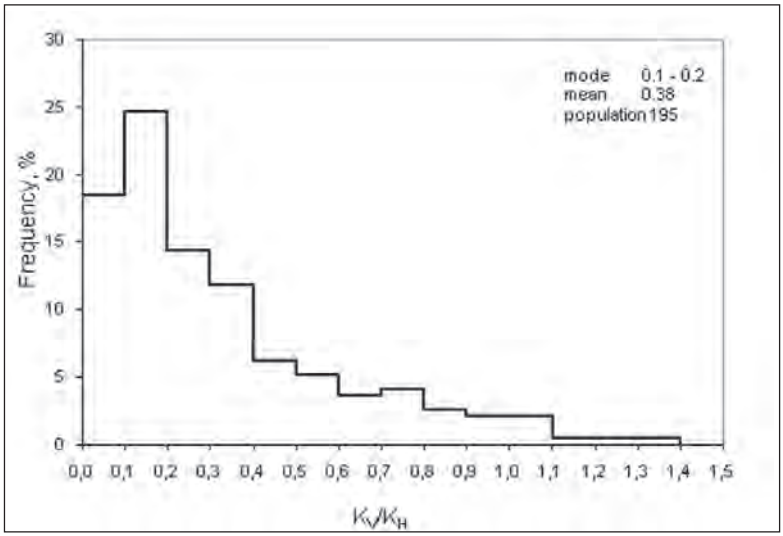

Source: Widarsono et al. (2006)

Figure 3.21 Anisotropy Distribution of Sandstone Full-Diameter (FD) Cores Classified As of Medium Permeability (10 mD ≤ K < 200 mD)

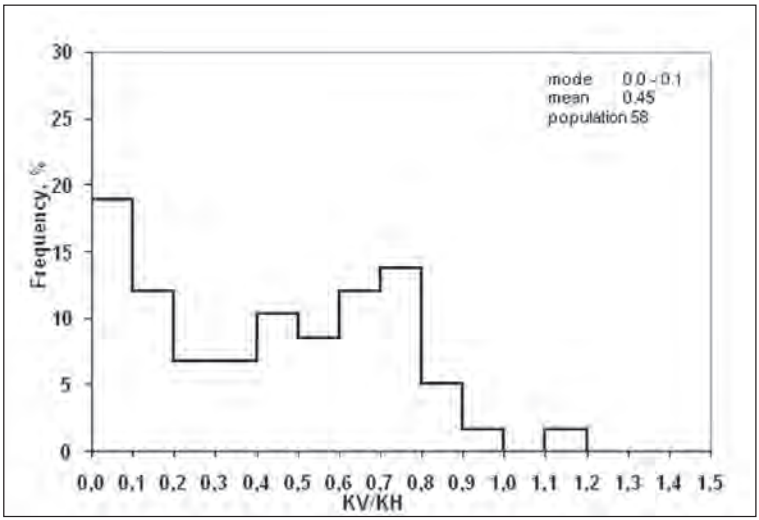

Source: Widarsono et al. (2006)

Figure 3.22 Anisotropy Distribution of Sandstone Full-Diameter (FD) Cores Classified As of High Permeability (200 mD ≤ K < 800 mD)

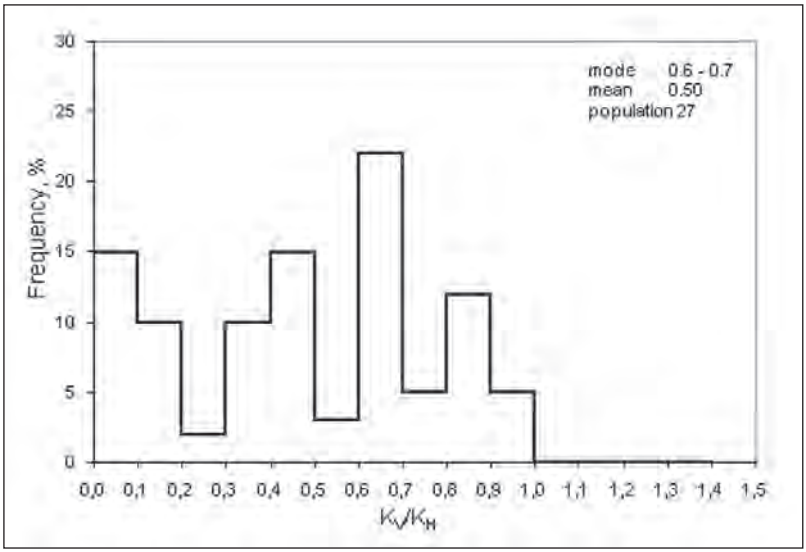

Source: Widarsono et al. (2006)

Figure 3.23 Anisotropy Distribution of Sandstone Full-Diameter (FD) Cores Classified As of Very High Permeability ($K \geq 800$ mD)

4. Anisotropy Characteristics Based on Lithology

The 4,648 sandstone plug and FD samples used by the study consist essentially of various types of sandstones based on rock fabric, clay/shale structure, and presence of special mineral(s). Five sandstone types have been used for exemplary grouping: conglomeratic, glauconitic, argilaceous, micaceous, and laminated shaly sandstones. Not all samples were used, only plug samples were taken into analysis, and only samples with distinct descriptions that belong to the specified sandstone types were taken into use. Figures 3.24 through 3.28 present the K_V/K_H population for plug samples. Due to limited quantity, no analysis was made for FD samples.

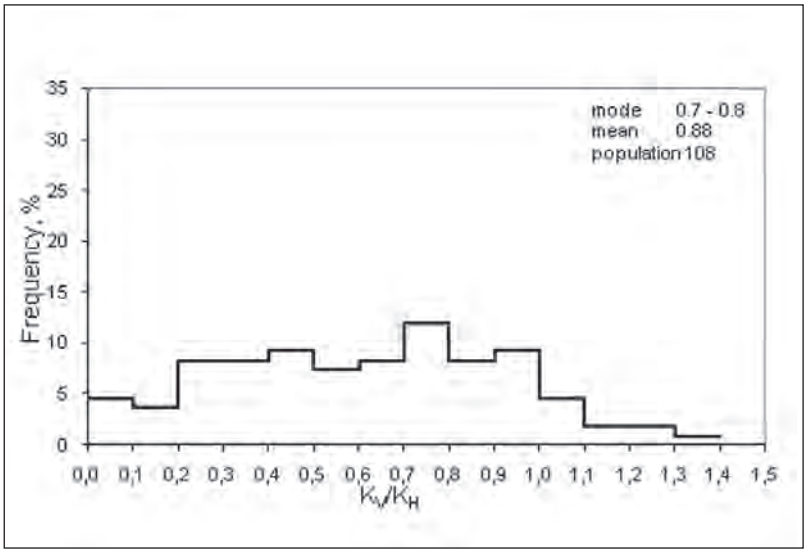

Source: Widarsono et al. (2006)

Figure 3.24 Anisotropy Distribution of Core Plugs for Conglomeratic Sandstones

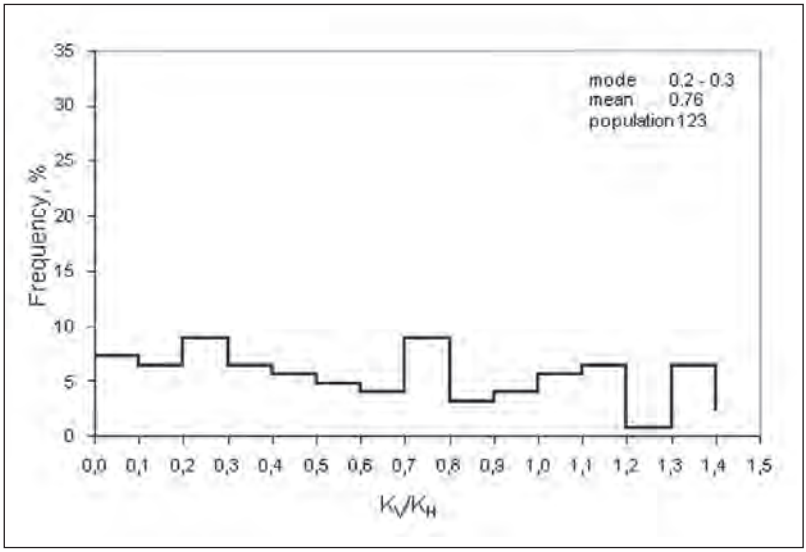

Source: Widarsono et al. (2006)

Figure 3.25 Anisotropy Distribution of Core Plugs for Glauconitic Sandstones

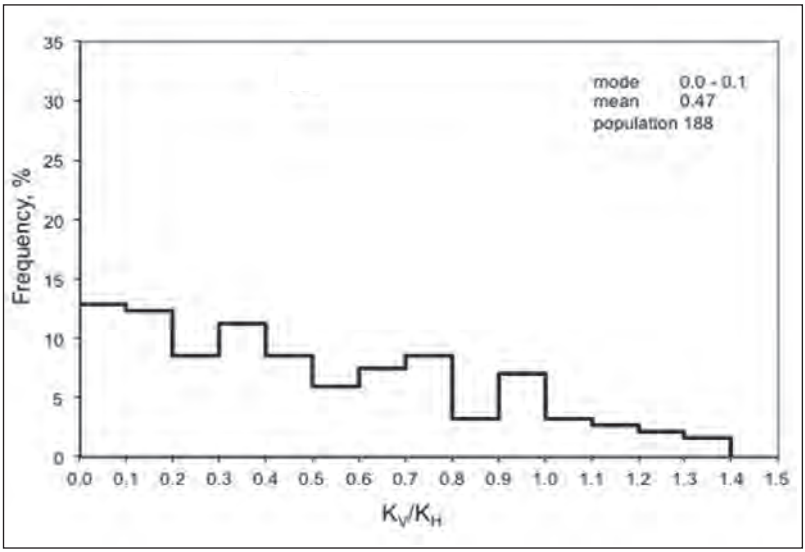

Source: Widarsono et al. (2006)

Figure 3.26 Anisotropy Distribution of Core Plugs for Argilaceous Sandstones

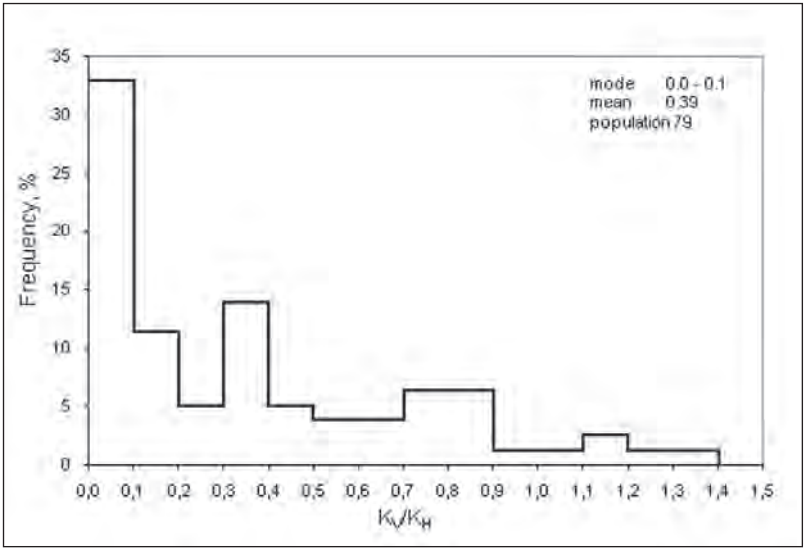

Source: Widarsono et al. (2006)

Figure 3.27 Anisotropy Distribution of Core Plugs for Micaceous Sandstones

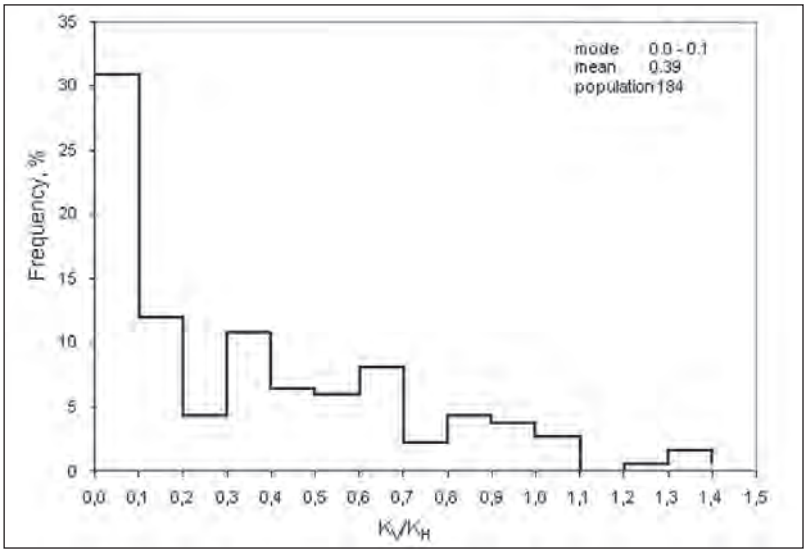

Source: Widarsono et al. (2006)

Figure 3.28 Anisotropy Distribution of Core Plugs for Laminated Shaly Sandstones

The plots in the figures show clearly the effect of sandstone types (i.e. pore system types). Conglomeratic and glauconitic sandstones show strong non-preference K_V/K_H distribution implying their irregular and heterogeneous pore network, whereas the argillaceous sandstone show slight preference towards smaller K_V/K_H ranges indicating the probable influence of fine and very fine grains present in the pore network on the rock. Strong preferences towards low K_V/K_H are shown by the micaceous and laminated shaly sandstones. For the two sandstone types, more than 30% of the population are characterized by K_V/K_H values within the range of 0–0.1. This occurrence is very logical considering the platty nature of the mica and laminated clay that are present in the rocks.

Observing the anisotropy tendency upon variation in sandstone lithology, it is reasonable to put that low K_V/K_H values to be used in any relevant reservoir studies for cases where micaceous or laminated shaly sandstones are the reservoir forming rocks. For other sandstone lithological types, more careful analysis using relevant core samples have to be performed.

5. Vertical variation of K_V/K_H ratio

Most wells from which the K_V/K_H data were taken have sufficient samples that enable one to observe degree of K_V/K_H variations in vertical direction. From all wells contributing to sandstone samples directory, approximately 90% of them (120 wells) exhibit high degree of K_V/K_H vertical variation (i.e. high variance). This is indicated by their degree of variance, which is greater than 0.6 (this value is taken arbitrarily to distinguish between low and high degree of variance). For some extreme cases, the degree of variation is as high as 1.6. Figures 3.29 and 3.30 show plots in two wells with lowest and highest K_V/K_H vertical variations, respectively.

Vertical variations of K_V/K_H are actually strongly linked to sandstones lithological types, of which it can be seen that vertical variation is largely influenced by rock structure. Reservoir rocks with low K_V/K_H variation tend to be associated with groups of micaceous and laminated shally sandstones. On the other hand, the reverse is true for other types of sandstone. In general, however, the significant majority shown by the wells with high variance K_V/K_H data underlines the neccessity of not neglecting facts about vertical K_V/K_H variations in any relevant reservoir studies.

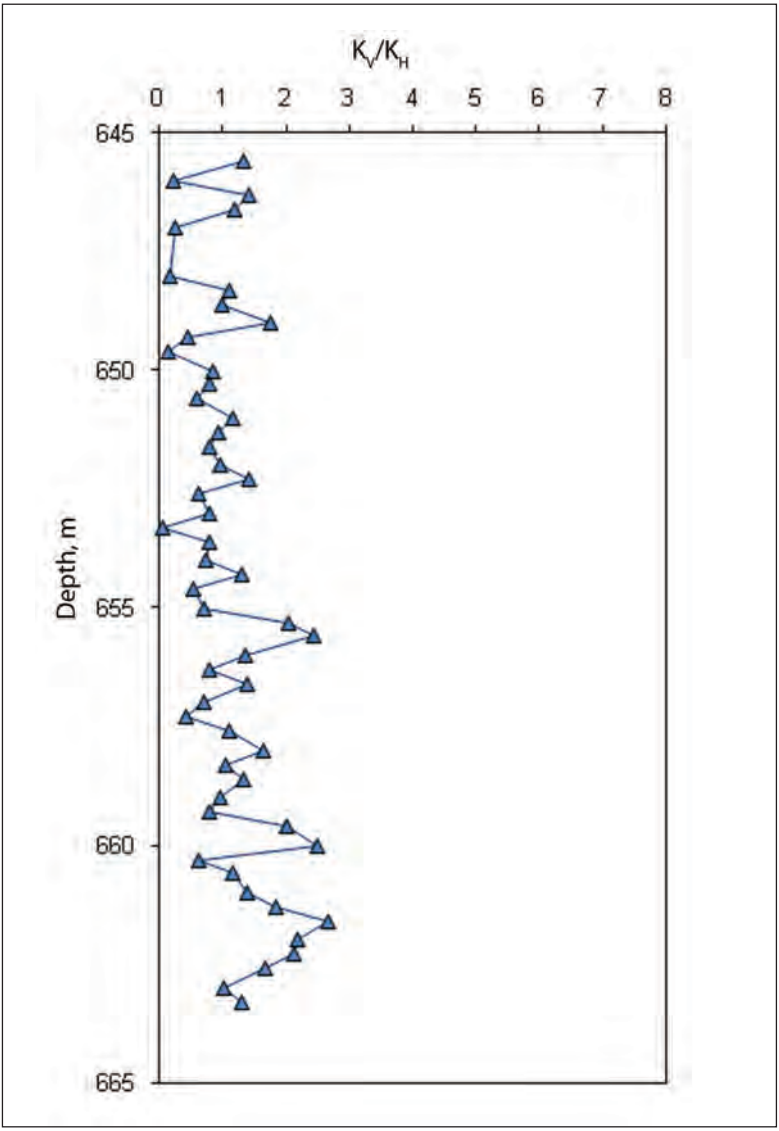

Source: Widarsono et al. (2006)

Figure 3.29 Low Vertical K_V/K_H Variation Observed in a Well in Bekasap Field, Central Sumatra Basin

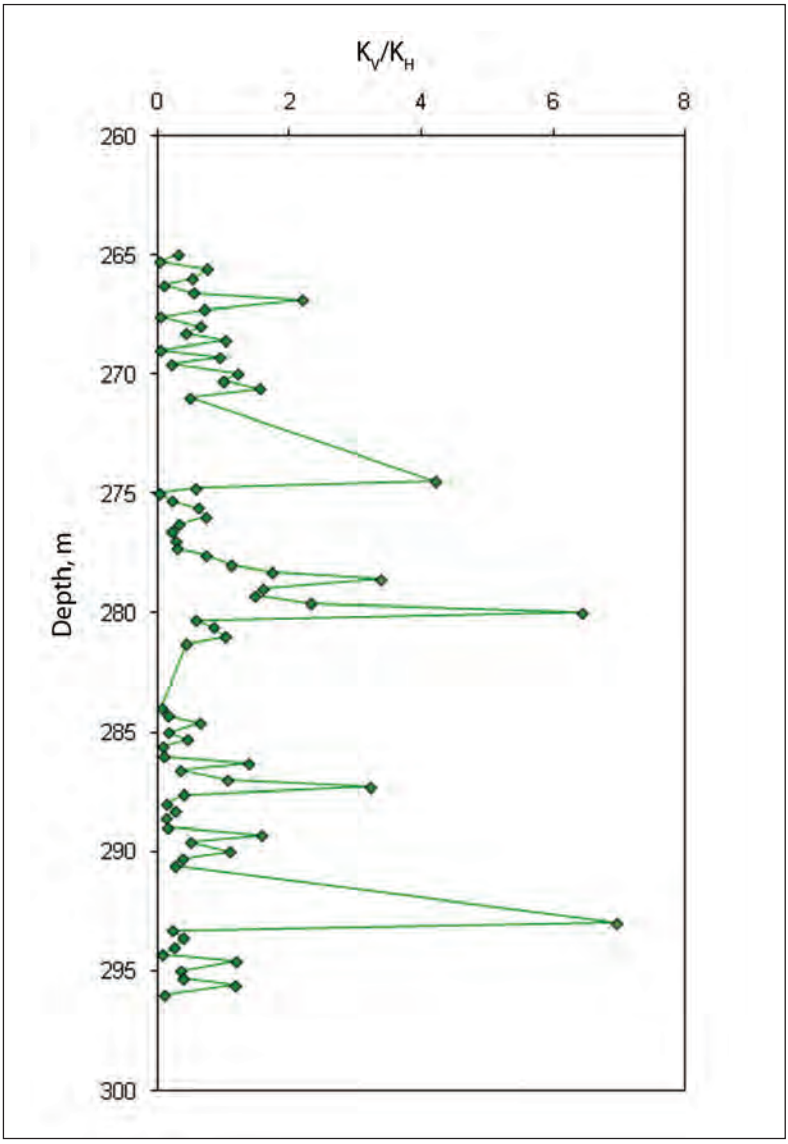

Source: Widarsono et al. (2006)

Figure 3.30 High Vertical K_V/K_H Variation Observed in a Well in Rantau Field, North Sumatra Basin

6. Lateral Variation of K_V/K_H Ratio

Nature of sandstones during their sedimentation and depotitional process suggests, depending on various factors, variations in rock quality in lateral directions. Sandstones with different depositional environments are likely to show different lateral variations. The observation was essentially made by comparing K_V/K_H mode and mean values of wells penetrating same reservoirs or sands.

Of all wells available to the study, as many as 24 reservoirs (or sand units) were found to have 2 or more wells with K_V/K_H data. The data in general also shows that maximum number of wells having K_V/K_H data for a single reservoir or sand unit is 4, except one field in Kutai Basin that was found to have 12 wells with K_V/K_H data (study in Widarsono (2006) stated that there are many reservoirs or sand units having many wells with core analysis data but rarely with K_V/K_H data).

Analysis on mode and mean K_V/K_H values has shown that K_V/K_H varies laterally in significant manner. Figures 3.31 and 3.32 present mode and mean K_V/K_H values for two examplary cases, Tanjung (Barito Basin) and Bekasap (Central Sumatra Basin) fields with each represented by three wells, respectively. The plots show that for the two fields, regardless distances between the wells, both K_V/K_H mode and mean values vary laterally. This is consistently shown by mode K_V/K_H values of the Tanjung and, at a lesser degree, Bekasap fields. Similar occurrences also prevail in the case of other fields. This evidence proves that K_V/K_H values may also differ laterally.

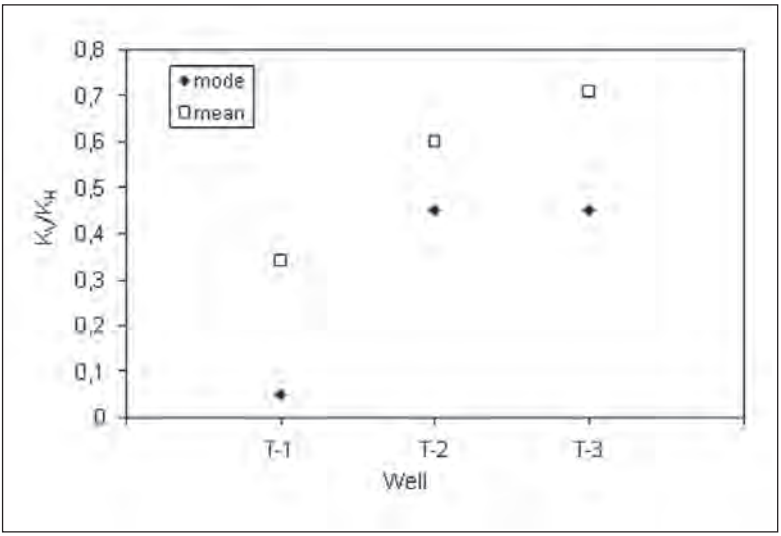

Source: Widarsono et al. (2006)

Figure 3.31 Lateral K_V/K_H Variation Observed in Tanjung Field, Barito Basin (the well codes do not represent the real well identification)

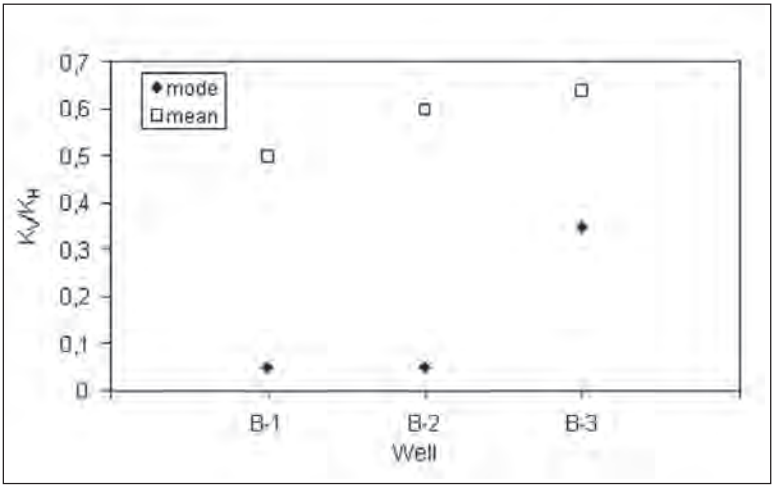

Source: Widarsono et al. (2006)

Figure 3.32 Lateral K_V/K_H Variation Observed in Bekasap field, Central Sumatra Basin (the well codes do not represent the real well identification)

E. Carbonate Rocks Anisotropy

1. Anisotropy in Different Sedimentary Basins

For carbonate rocks, Widarsono et al. (2006) presented that the K_V/K_H grouping based on sedimentary basin was made in the manner similar to the one for sandstones. Figures 3.33 through 3.35 and Figures 3.36 through 3.38 present K_V/K_H populations for plug and FD samples, respectively, representing three sedimentary basins with large sample number: Northwest Java, South Sumatra, and North Sumatra. All other basins representing very limited data did not enough to yield any reliable information.

The most obvious occurrence of the plotted data from the three basins, both core plugs and FD cores, is that most data fall in the range of $K_V/K_H < 1.2$ even though their distribution patterns are not

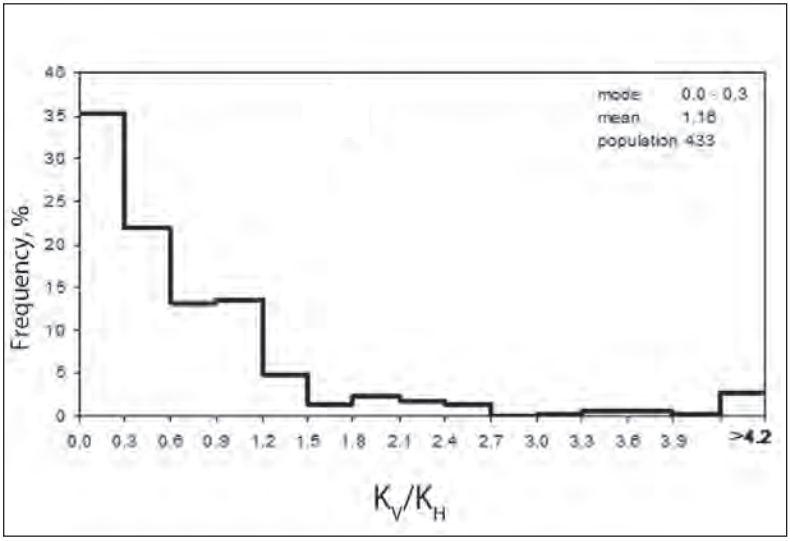

Source: Widarsono et al. (2006)

Figure 3.33 Anisotropy Distribution of Carbonate Core Plugs from Northwest Java Basin

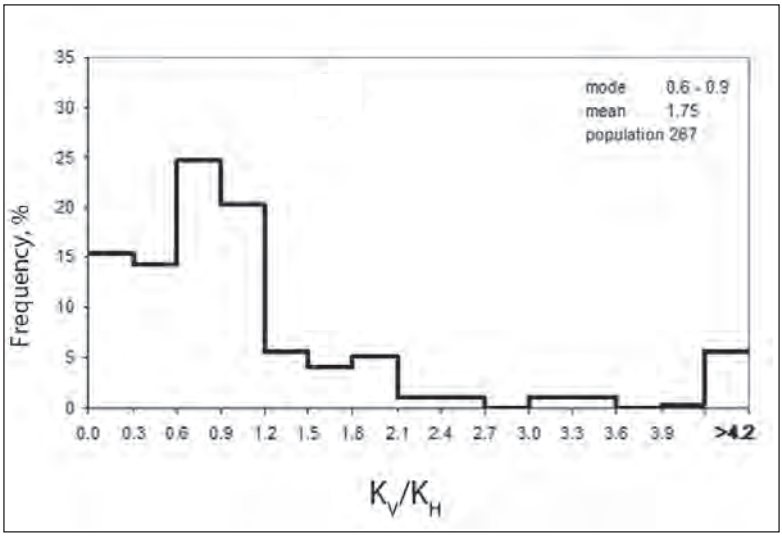

Source: Widarsono et al. (2006)

Figure 3.34 Anisotropy Distribution of Carbonate Core Plugs from South Sumatra Basin

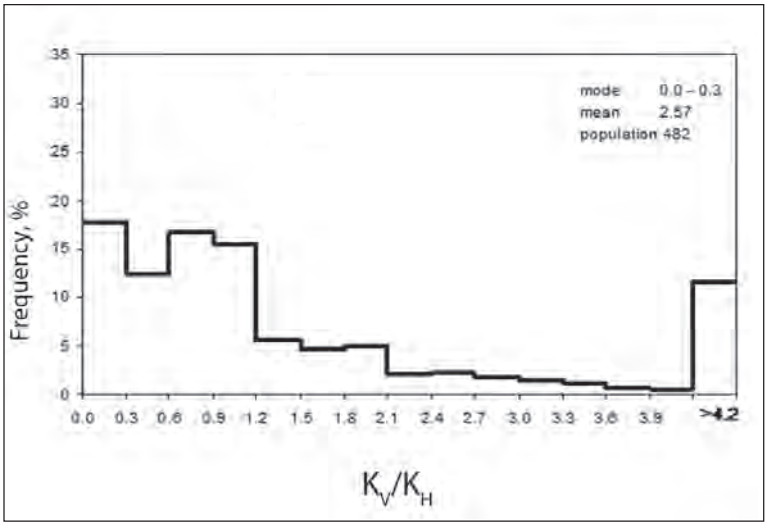

Source: Widarsono et al. (2006)

Figure 3.35 Anisotropy Distribution of Carbonate Core Plugs from North Sumatra Basin

necessarily the same. For instance, Northwest Java Basin's core plugs show large proportion of K_V/K_H data within the range of 0–0.3, while the mode for South Sumatra Basin is in the range of 0.6–0.9. This may reflects carbonate rocks usual high degree of heterogeneity. There are also obvious differences shown when comparisons are made by the patterns of core plugs and FD cores. While core plugs from Northwest Java and South Sumatra basins show different modes, whole cores from the two basins show similarity in patterns indicated by their considerably similar modes of 0–0.3. However, similarity between FD cores and core plugs data for Northwest Java Basin and difference between the two sets of data for South Sumatra Basin can be taken as evidence that the two basins have different patterns of vertical anisotropy. Vertical anisotropy in North West Java Basin probably occurs at scale greater than FD core size, while anisotropy in South Sumatra Basin occurs at scales between the size of plug and

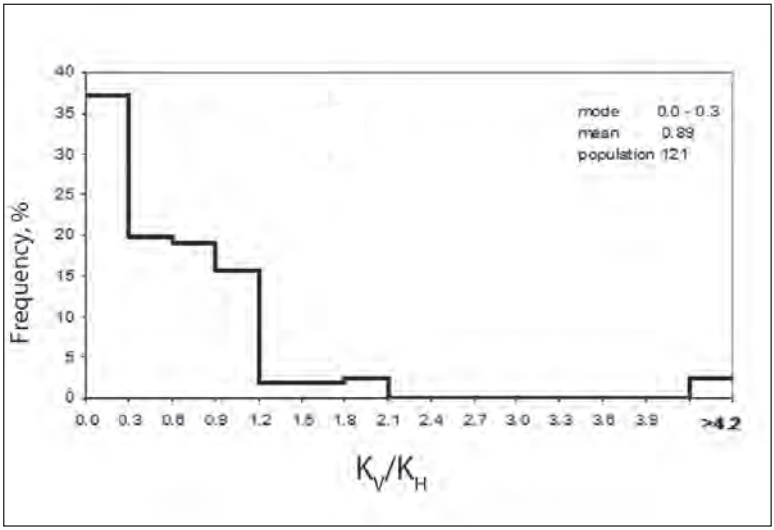

Source: Widarsono et al. (2006)

Figure 3.36 Anisotropy Distribution of Carbonate Full-Diameter (FD) Core Samples from Bone (Sengkang) Basin

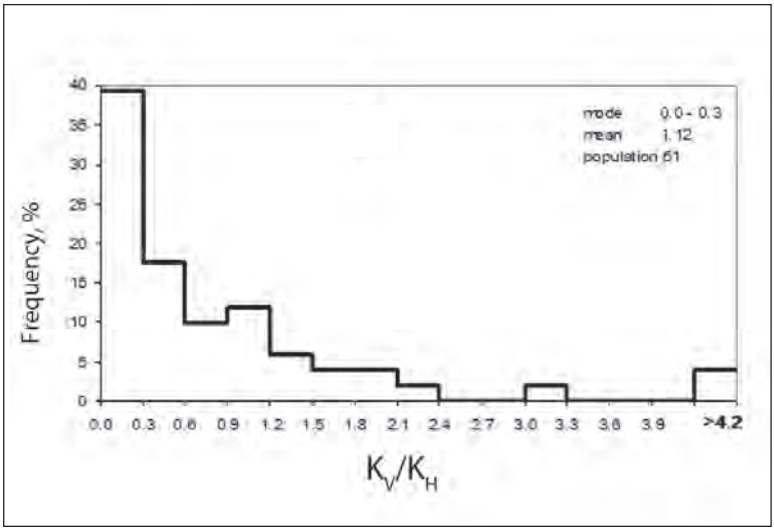

Source: Widarsono et al. (2006)

Figure 3.37 Anisotropy Distribution of Carbonate Full-Diameter (FD) Core Samples from South Sumatra Basin

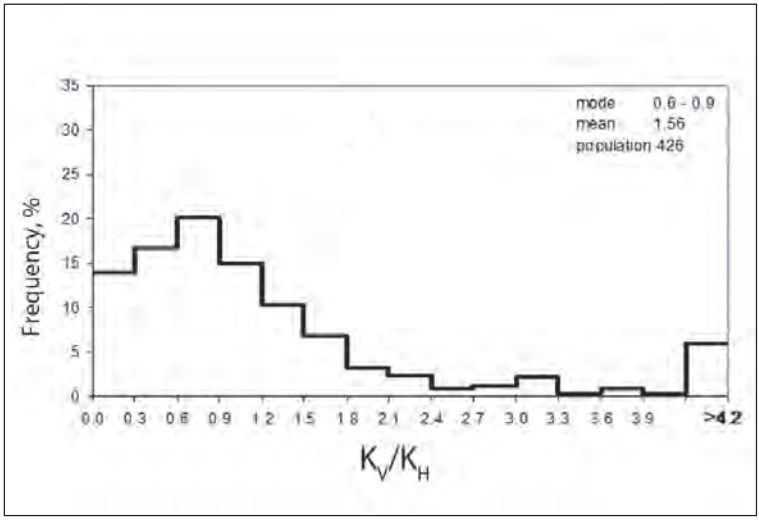

Source: Widarsono et al. (2006)

Figure 3.38 Anisotropy Distribution of Carbonate Full-Diameter (FD) Core Samples from North Sumatra Basin

FD core. Other basins may probably show different scale of vertical anisotropy, but their modes may still fall between 0 and 1.2.

Other important information that is drawn from the observation is the significant presence of K_V/K_H data larger than 4.2, indicating signicantly larger vertical permeability than its corresponding horizontal permeabily. Analysis on core visual description indicate that core samples with very large K_V/K_H values are usually associated with presence of cracks or fissures, their planes most probably lies paralel to vertical or sub-vertical directions. This K_V/K_H of 4.2 can favourably be used as a clue for minimum K_V/K_H value for fractured tight limestone reservoirs.

2. Porosity-related K_V/K_H Variation

Using the same porosity ranges, Figures 3.39 through 3.41 and Figures 3.42 through 3.44 show present K_V/K_H population for plug and FD core samples, respectively, representing three porosity ranges: low (0–15%), medium (15–25%), and high (> 25%).

All six data distributions show similar distribution patterns, which are strikingly characterized by most of the K_V/K_H data to fall bellow 1.2. This may in general be interpreted that porosity does not affect K_V/K_H significantly. In a manner similar to sandstone data, similarity in patterns between core plugs and FD core data also indicate that porosity does not affect K_V/K_H at any scales. Therefore, it can be said that despite differences in ranges and patterns between sandstones and carbonate rocks, porosity is not a major governing factor to the K_V/K_H.

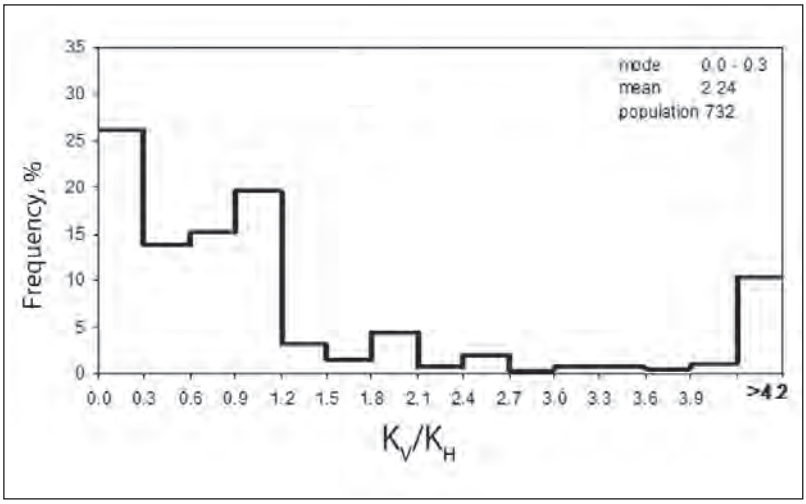

Source: Widarsono et al. (2006)

Figure 3.39 Anisotropy Distribution of Carbonate Core Plugs Classified As of Low Porosity (ϕ < 15%)

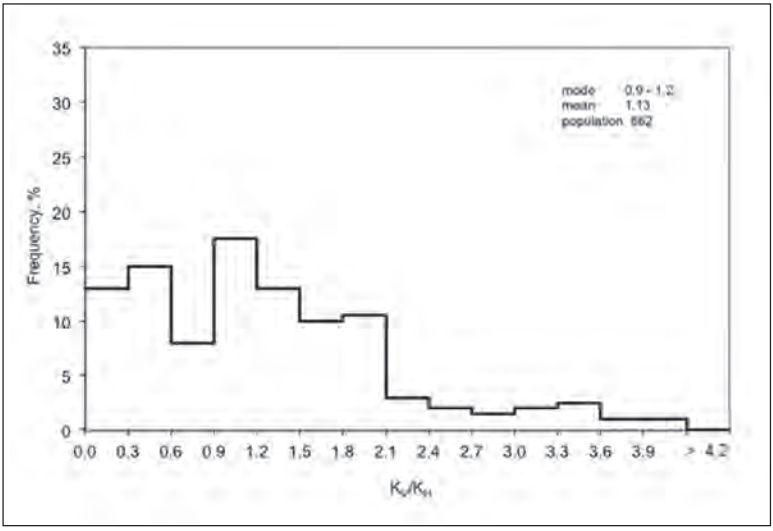

Source: Widarsono et al. (2006)

Figure 3.40 Anisotropy Distribution of Carbonate Core Plugs Classified As of Medium Porosity (ϕ = 15–25%)

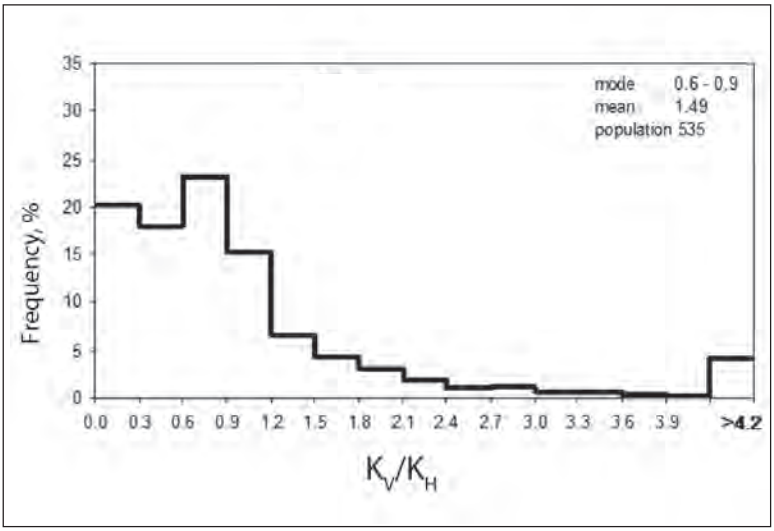

Source: Widarsono et al. (2006)

Figure 3.41 Anisotropy Distribution of Carbonate Core Plugs Classified As of High Porosity (ϕ > 25%)

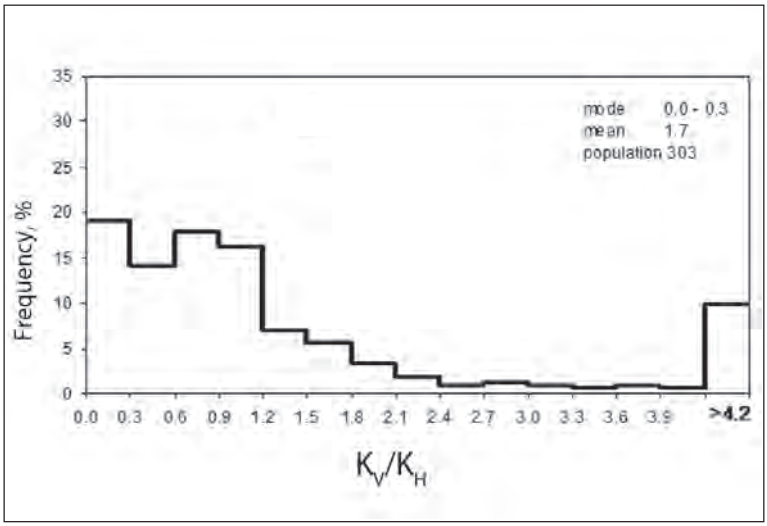

Source: Widarsono et al. (2006)

Figure 3.42 Anisotropy Distribution of Carbonate Full-Diameter (FD) Core Samples Classified As of High Porosity (ϕ < 15%)

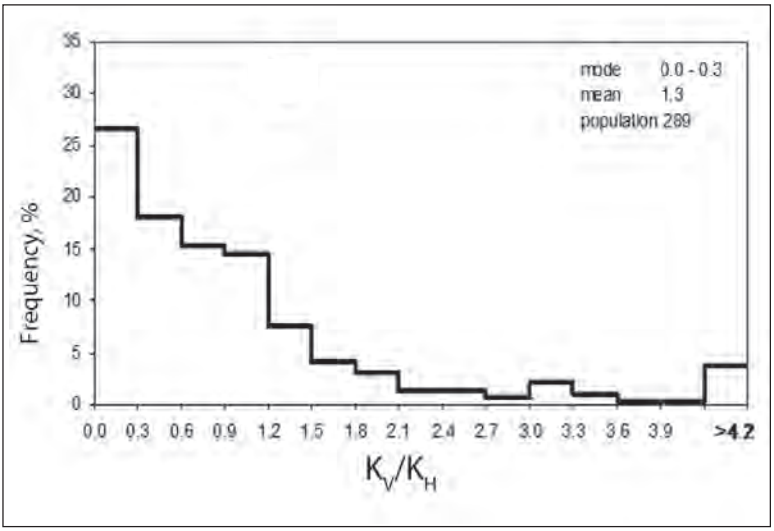

Source: Widarsono et al. (2006)

Figure 3.43 Anisotropy Distribution of Carbonate Full-Diameter (FD) Core Samples Classified As of Medium Porosity (ϕ = 15–25%)

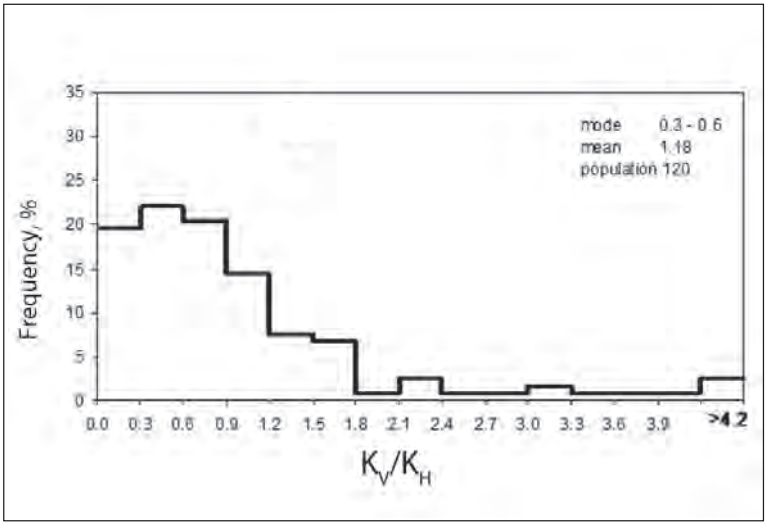

Source: Widarsono et al. (2006)

Figure 3.44 Anisotropy Distribution of Carbonate Full-Diameter (FD) Core Samples Classified As of High Porosity (ϕ > 25%)

3. K_V/K_H Anisotropy and Horizontal Permeability

Similar permeability ranges as ones used on sandstone data were operated in the observation for carbonate rocks. Figures 3.45 through 3.48 and Figures 3.49 through 3.52 show present K_V/K_H population for plug and FD core samples, respectively, representing four permeability ranges: low (0–10 mD), medium (10–200 mD), high (200–800 mD), and very high (> 800 mD).

Like in the case of other observations, the classification into ranges of permeability showed similar trends in which the bulk majority of K_V/K_H data fall below the number of 1.2, both for plug and whole core samples. However, a rather obvious difference is observed in the form of larger population with $K_V/K_H < 0.3$ for plug samples compared to for FD samples. Permeability ranges for plug samples with large

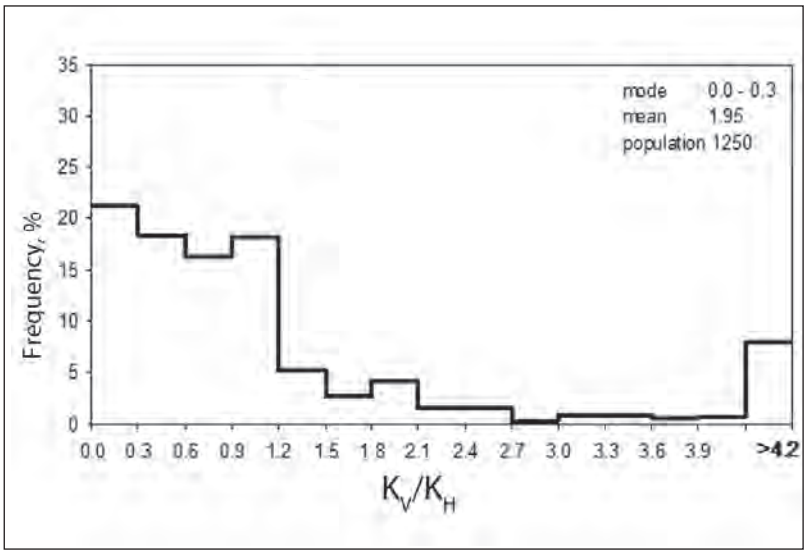

Source: Widarsono et al. (2006)

Figure 3.45 Anisotropy Distribution of Carbonate Core Plugs Classified As of Low Permeability (K < 10 mD)

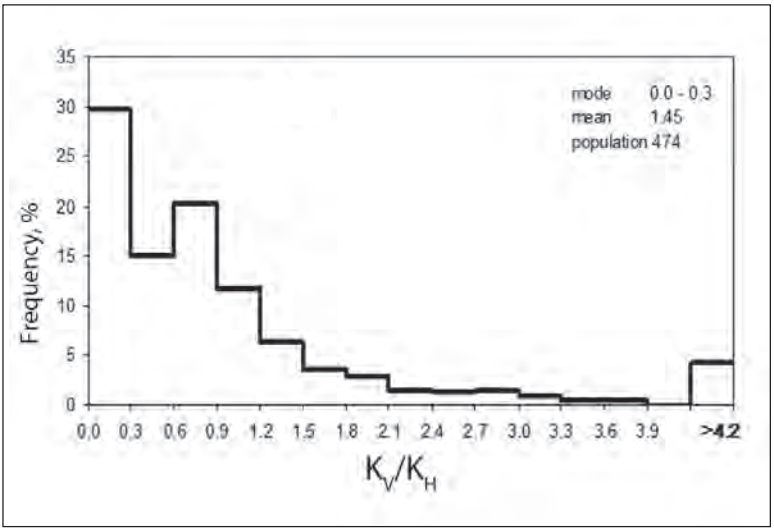

Source: Widarsono et al. (2006)

Figure 3.46 Anisotropy Distribution of Carbonate Core Plugs Classified As of Medium Permeability (K = 10–200 mD)

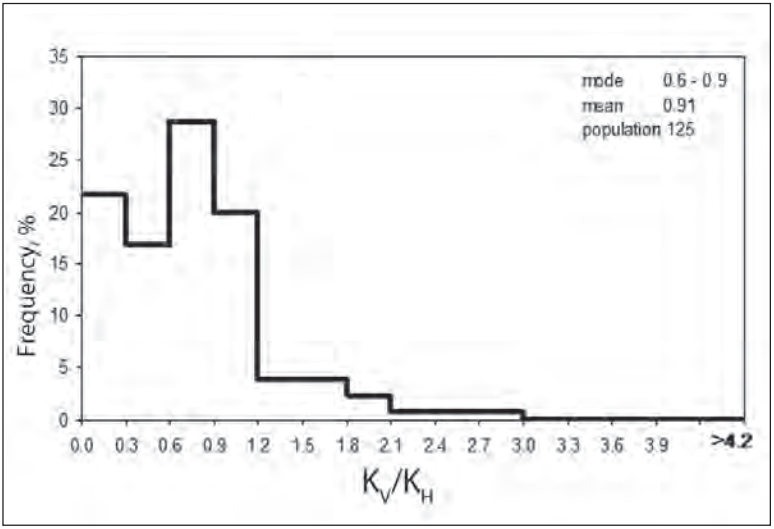

Source: Widarsono et al. (2006)

Figure 3.47 Anisotropy Distribution of Carbonate Core Plugs Classified As of High Permeability (200 mD < K < 800 mD)

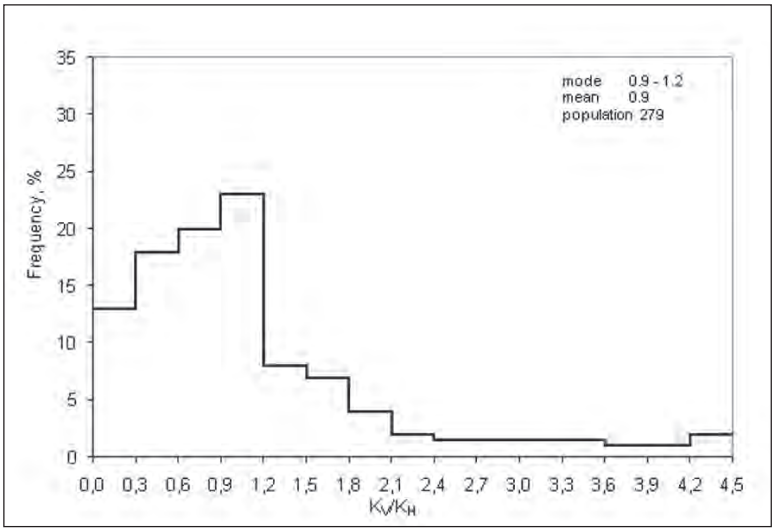

Source: Widarsono et al. (2006)

Figure 3.48 Anisotropy Distribution of Carbonate Core Plugs Classified As of Very High Permeability (K > 800 mD)

population, e.g 'low' and 'medium' ranges (Figures 3.45 and 3.46), tend to show larger proportion of K_V/K_H values < 0.3 whereas 'high' permeability range with its smaller population (Figure 3.47) shows much lower K_V/K_H values < 0.3. On the other hand, 'low' permeability range for FD core samples, wich is the largest population for FD core samples, shows much lower proportion of K_V/K_H values < 0.3. The differences in trends between plug and whole core data population can definitely be taken as evidence that high level of heterogenity is shown by the carbonate rocks.

Despite differences shown by both plug and FD core samples, it is still obvious that the similarity in general trend of having most of K_V/K_H values lower than 1.2 can be taken as an indication that the K_V/K_H values are not governed by the horizontal permeability. In other words, the magnitudes of vertical permeability are independent of horizontal permeability.

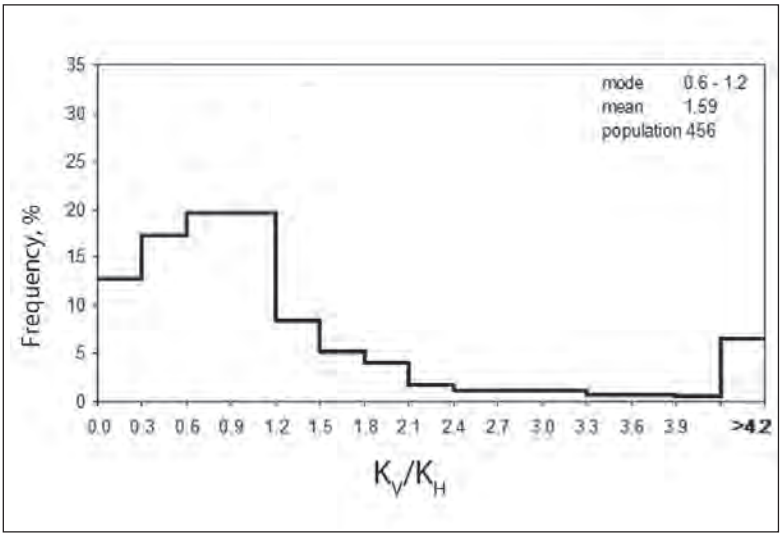

Source: Widarsono et al. (2006)

Figure 3.49 Anisotropy Distribution of Carbonate Full-Diameter (FD) Cores Classified As of Low Permeability (K < 10 mD)

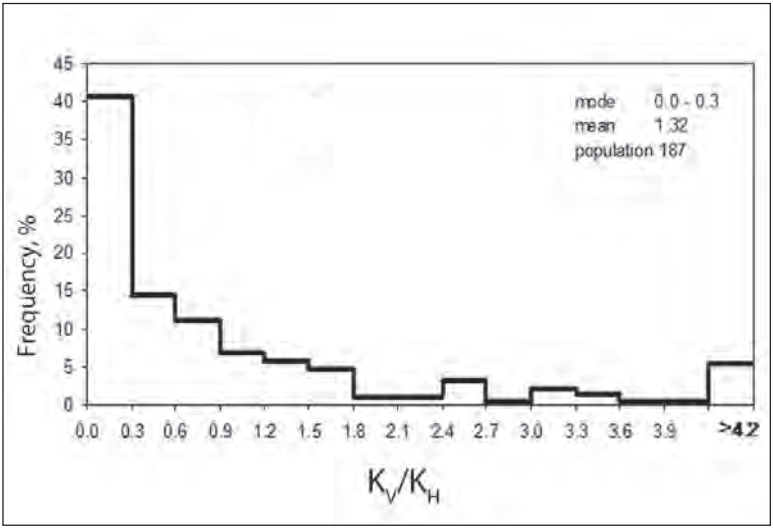

Source: Widarsono et al. (2006)

Figure 3.50 Anisotropy Distribution of Carbonate Full-Diameter (FD) Cores Classified As of Medium Permeability (10 mD < K < 200 mD)

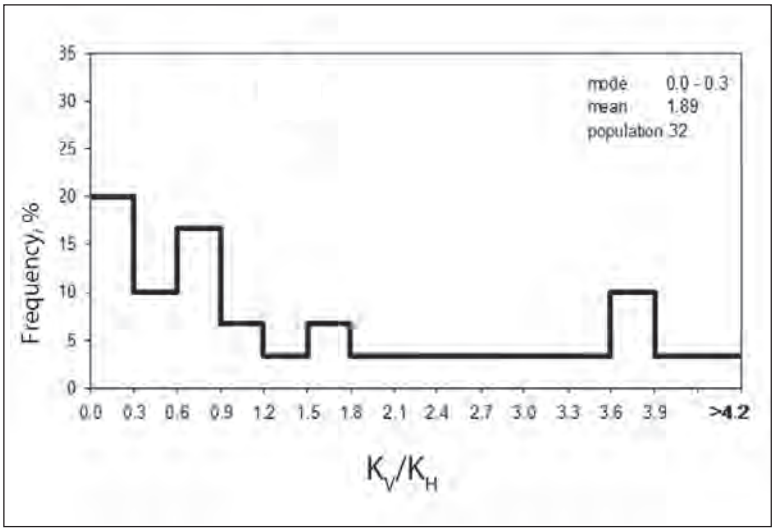

Source: Widarsono et al. (2006)

Figure 3.51 Anisotropy Distribution of Carbonate Full-Diameter (FD) Cores Classified As of High Permeability (200 mD < K < 800 mD)

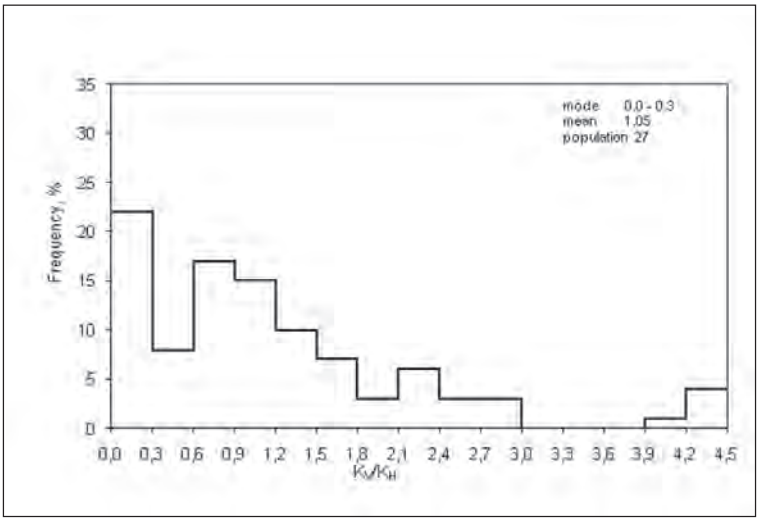

Source: Widarsono et al. (2006)

Figure 3.52 Anisotropy Distribution of Carbonate Full-Diameter (FD) Cores Classified As of Very High Permeability (K > 800 mD)

4. Anisotropy for Different Carbonate Rock Types

The carbonate rocks used in the study presented by Widarsono et al. (2006) covered various limestones (roughly 80% of total) and dolomitic rocks (roughly 20% of total). No anhydrites and evaporites were available to the study. This is understandable since presence of the two carbonates in Indonesian reservoirs is almost none. However, for simplicity, the classification in the observation followed Dunham classification (Dunham, 1962): mudstone, wackestone, packstone, grainstone, boundstone, and crystalline. For simplification, the classification was simplified further by combining mudstone and packstone into one class, and grainstone and boundstone into another. Therefore, the carbonate rock type classification is: mudstone-wackestone, packstone, grainstone-bounstone, and crystalline. This simplified Dunham classification was considered more suitable for the study, shown by the fact that all data that are represented by other types of classifications were all converted into the simplified classification. Figures 3.53 through 3.56 and Figures 3.57 through 3.60 show present K_V/K_H population for plug and FD core samples, respectively, representing four rock types: mudstone-wackestone, packstone, grainstone-boundstone, and crystalline.

As in other observations, similar patterns were also observed. Considering its nature, the Dunham classification is essentially a way of classifying quality of carbonate rocks in term of petrophysical properties. This directly relates to rock permeability. What can obviously be observed is that there is no significant difference in pattern among the four rock quality classes. In a manner similar to the other observations, all classes show that most K_V/K_H data falls below the value of 1.2 and a portion of total population in each class fall above K_V/K_H = 4.2. Differences in rock texture do not seem to yield much different correlation between vertical and horizontal permeabilities.

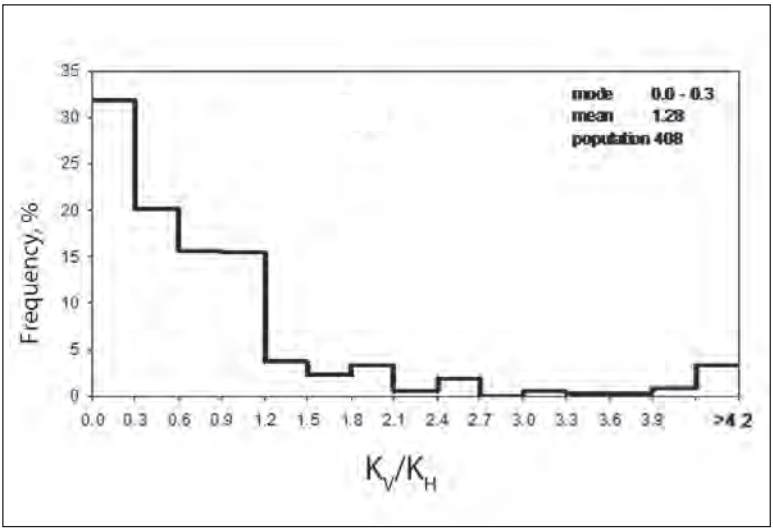

Source: Widarsono et al. (2006)

Figure 3.53 Anisotropy Distribution of Carbonate Core Plugs Classified As of Mudstone–Wackestone Type

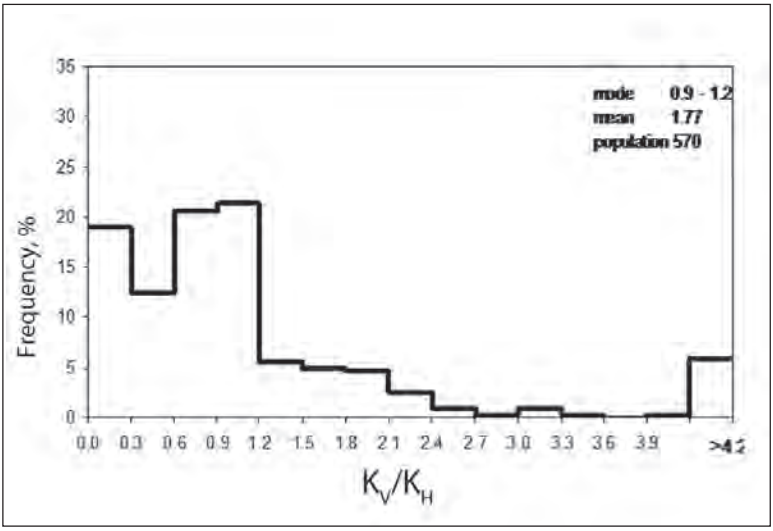

Source: Widarsono et al. (2006)

Figure 3.54 Anisotropy Distribution of Carbonate Core Plugs Classified As of Packstone Type

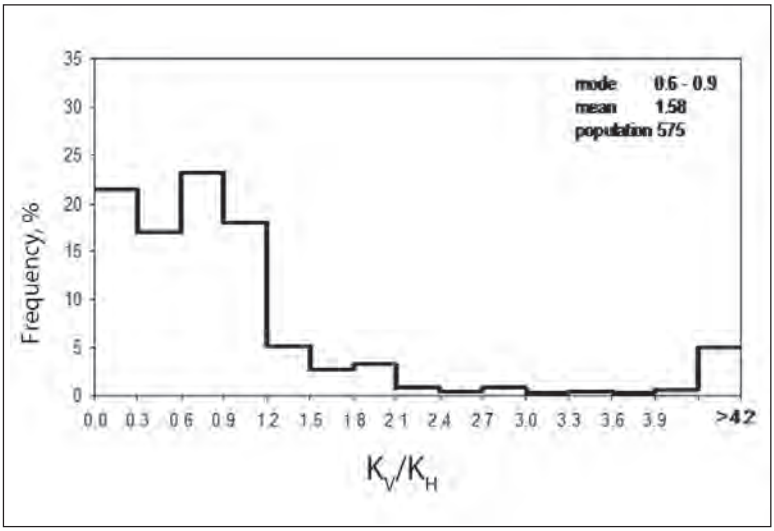

Source: Widarsono et al. (2006)

Figure 3.55 Anisotropy Distribution of Carbonate Core Plugs Classified As of Grainstone-Boundstone Type

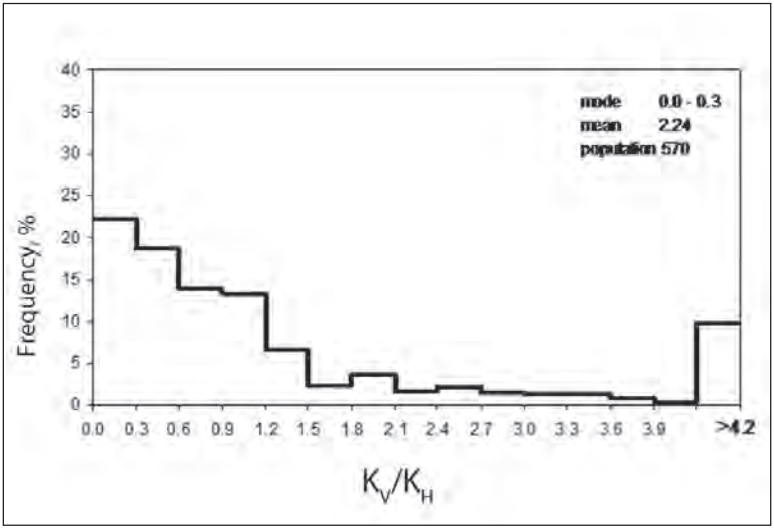

Source: Widarsono et al. (2006)

Figure 3.56 Anisotropy Distribution of Carbonate Core Plugs Classified As of Crystalline Type

It is also obvious that improvements in horizontal permeability due to presence of better rock texture and pore configuration are always somewhat acompanied by improvements in vertical permeability.

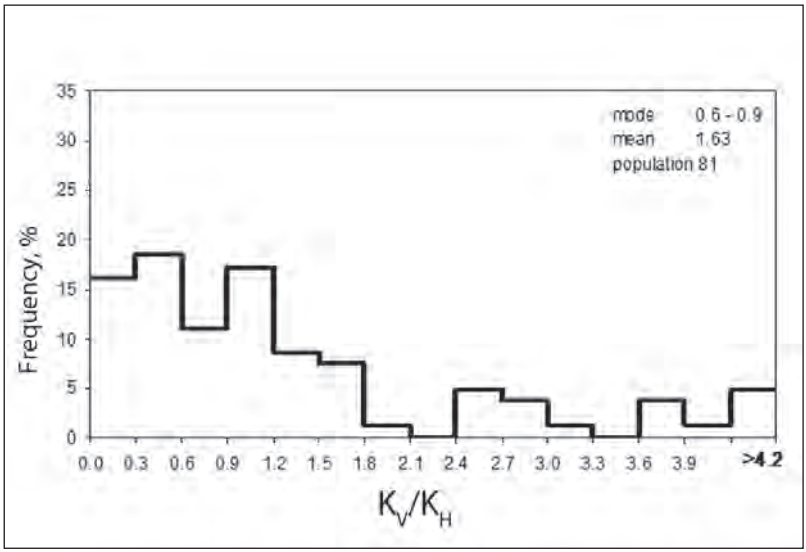

Source: Widarsono et al. (2006)

Figure 3.57 Anisotropy Distribution of Carbonate FD Core Samples Classified As of Mudstone–Wackestone Type

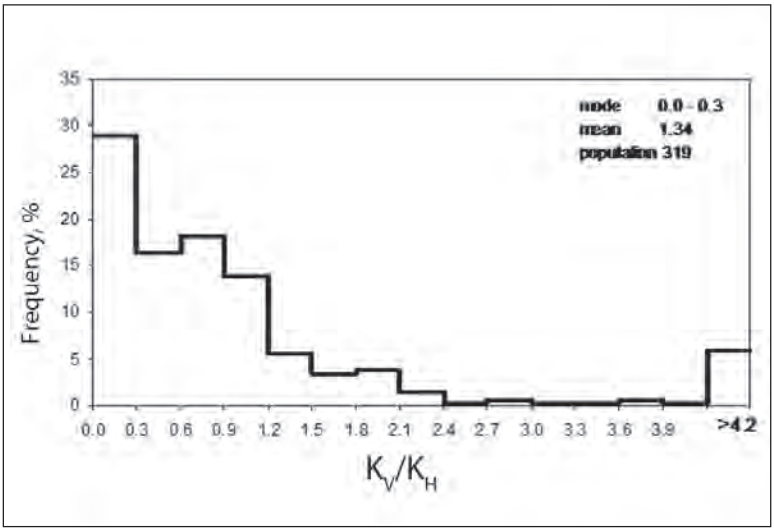

Source: Widarsono et al. (2006)

Figure 3.58 Anisotropy Distribution of Carbonate FD Core Sampless Classified As of Packstone Type

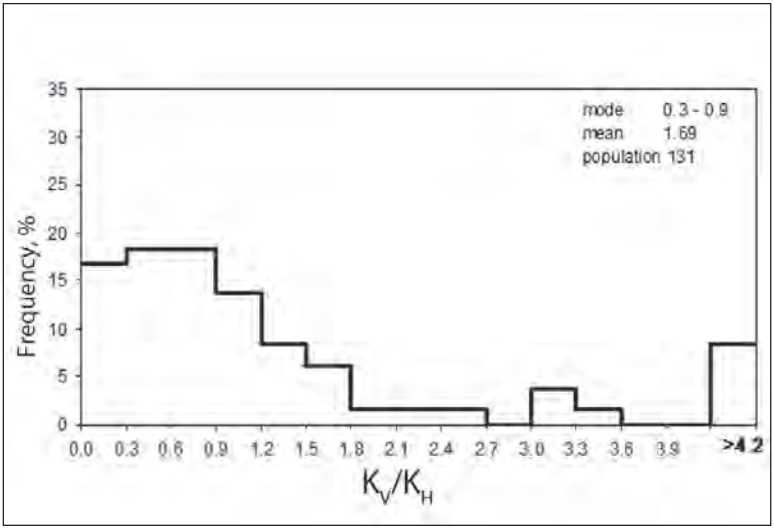

Source: Widarsono et al. (2006)

Figure 3.59 Anisotropy Distribution of Carbonate FD Core Samples Classified As of Grainstone-Boundstone Type

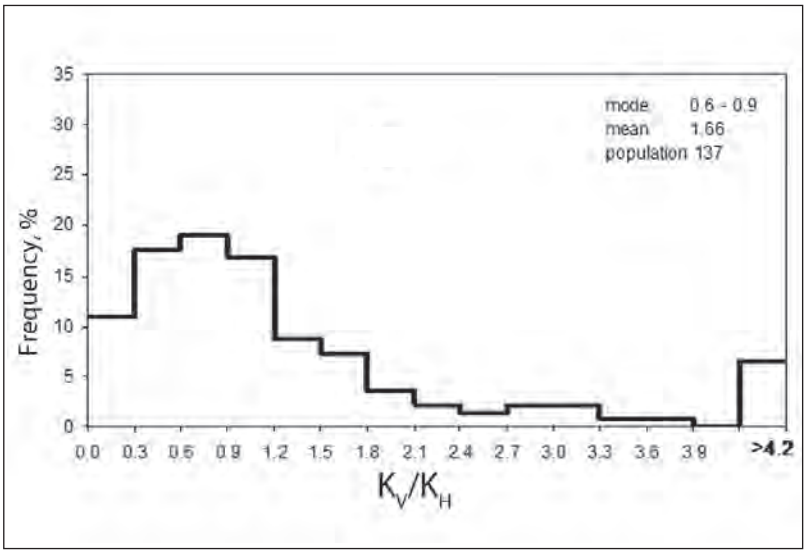

Source: Widarsono et al. (2006)

Figure 3.60 Anisotropy Distribution of Carbonate FD Core Samples Classified As of Crystalline Type

5. Anisotropy and Vertical Variation

Similar to sandstone's case, observation on vertical variation was made through searching for core samples with the lowest degree of vertical K_V/K_H variation (close to isotropic) and core samples with the highest degree of K_V/K_H variation (.). Figures 3.61 and 3.62 show low vertical variation (Figure 3.61) and high vertical variation, respectively. This comparison of two extremes was made in the way similar to those sandstone sample populations (Figures 3.29 and 3.30).

As in the case of sandstone, carbonate's vertical K_V/K_H variation also shows moderate case. Figure 3.61 depicts data for an examplary well with the least variation profile could be found among the data. By comparing it to its corresponding counterpart in sandstone population (Figure 3.29), it is obvious that the K_V/K_H vertical variation in

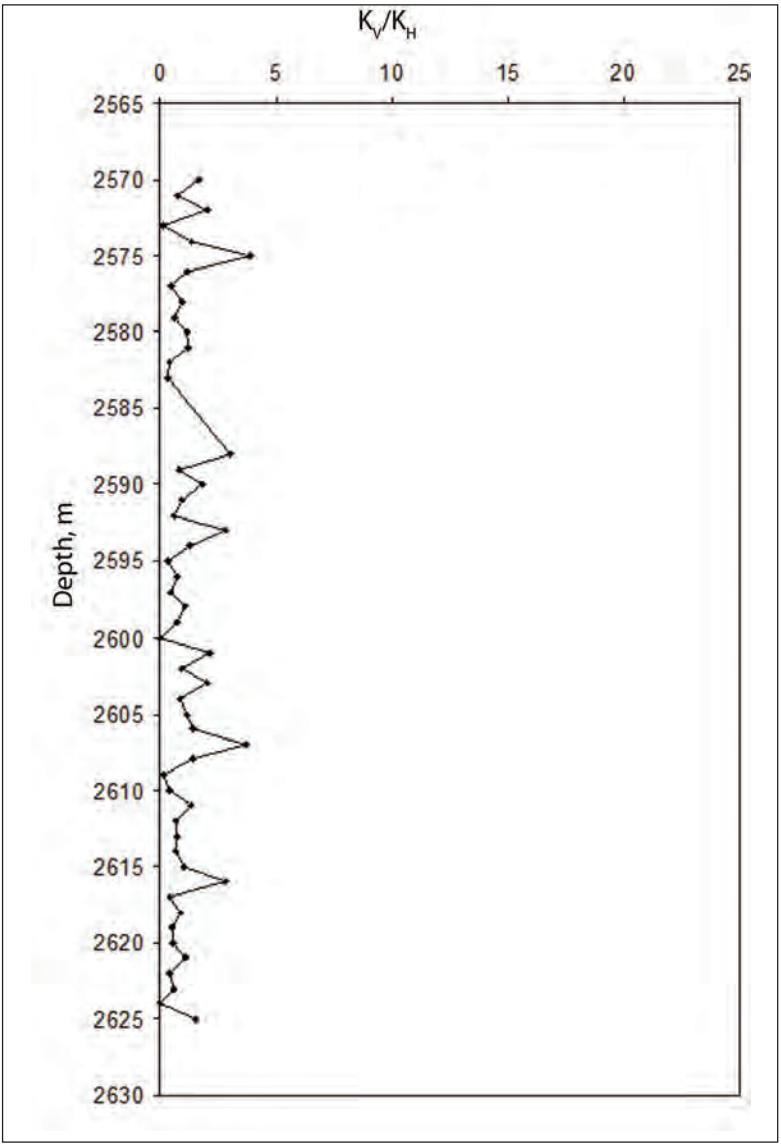

Source: Widarsono et al. (2006)

Figure 3.61 Low Vertical K_V/K_H Variation of Carbonate Sample Observed in An Examplary Well of KE Field (Northeast Java Basin)

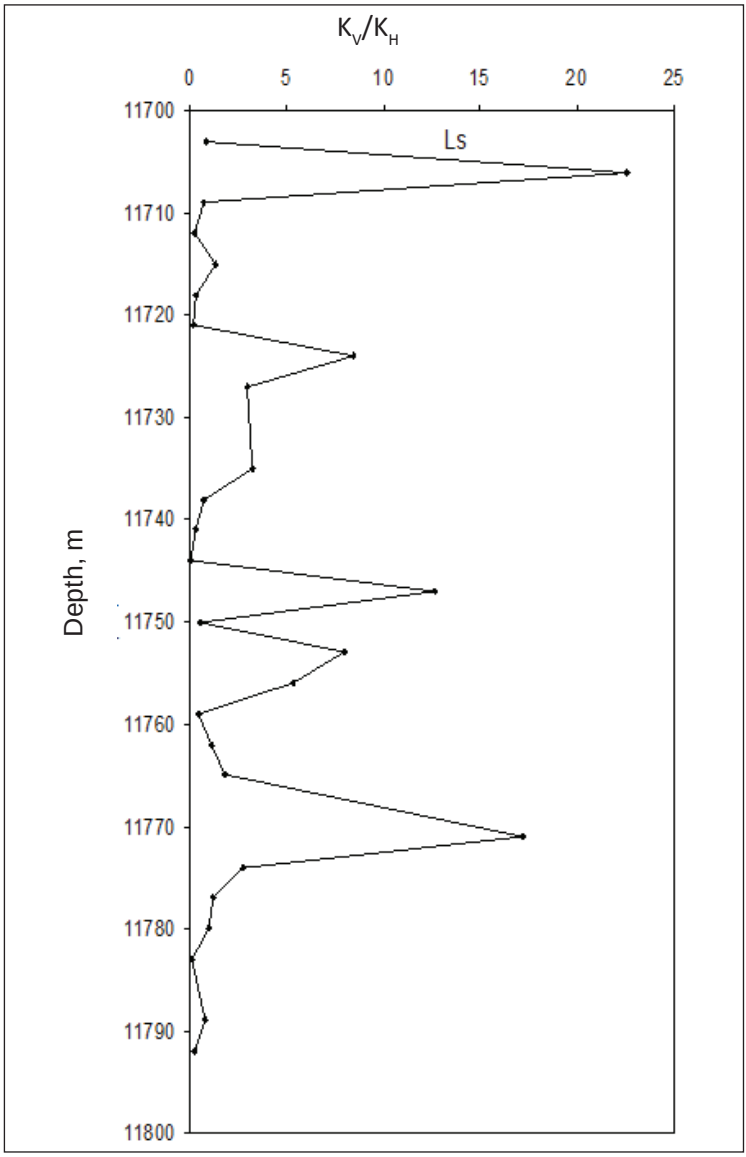

Source: Widarsono et al. (2006)

Figure 3.62 High Vertical K_V/K_H Variation of Carbonate Samples Observed in An Examplary Well of Arun Field (North Sumatra Basin)

carbonates, even at its lowest variation, is still more significant than in sandstone (on Figure 3.29, the highest K_V/K_H value for sandstone is around unity, whereas even the average K_V/K_H value for the carbonate on Figure 3.61 is around 2).

The other extreme case, the maximum variation, also shows significant degree of difference. The average K_V/K_H value for the carbonates presented on Figure 3.62, around 4 to 5, is still comparable to the K_V/K_H maximum values of around 6 shown by the sandstones presented on Figure 3.30. Although the comparison also suggests that in some cases there is a possibility that sandstone's K_V/K_H vertical variation may be more significant that carbonate rock's K_V/K_H vertical variation, but in many cases it is no doubt that K_V/K_H vertical variation in carbonate rocks tend to have more problems than in the case of sandstones.

F. Sandstone versus Carbonate Anisotropy

Observations on both sandstone and carbonate rocks have revealed the similarity in distribution between the two rock groups. Both populations, using all kinds of classifications and observations, behave similarly in the form of most data falls roughly below $K_V/K_H = 1.2$, except that carbonate rocks tend to have larger proportions of K_V/K_H values greater than 1.2 (even greater than 4.2). Both rock groups do not show specific tendency in their most representative figures of K_V/K_H. Some classifications show modes of $K_V/K_H = 0.1$, but others show different preference. The similarity in pattern between the two groups is somewhat unexpected since it is commonly acknowledged that the two rock groups are often characterized by different rock textures and pore configuration. This can be taken as evidence that there is a kind of uniformity in the nature despite differences in many of its physical aspects.

Investigating deeper, from the six observations over the sandstone's K_V/K_H data, Widarsono et al. (2006) put that there is no single value that can be regarded as the sole representative value for all sandstones, even though 0–0.1 often appears as the mode of K_V/K_H range. Indeed, by definition, 'mode' represents values or range of values that appear most frequently, but the data in general show that the mode values rarely represent a significant portion of data population at any grouping scenario. Exceptions are observed for specific grouping of sandstone types, from which micaceous and laminated shale sandstones show K_V/K_H mode values of 0–0.1 at around 30% of population. The remaining population exhibits no strong preference to any particular K_V/K_H values.

This non-preference tendency is clearly shown by core plug population for individual sedimentary basin, from which all basins (particularly basins with large sample population, say larger than 500) exhibit similar general distribution of K_V/K_H population. Similar distribution is also shown by core plug population for groupings based on porosity and horizontal permeability ranges except for medium permeability range, which shows larger proportion for K_V/K_H = 0–0.1. Non-preference tendencies are also found in population based on lithology except for the micaceous and laminated shale sandstones.

For carbonate rocks, some observations have shown that the K_V/K_H range of 0–0.3 appears to be the most important range. This may falsely be taken as the most representative K_V/K_H range, since this range is often represented by observation range that is made by small population only (e.g. Figures 3.48 and 3.52). What is clearly shown by the carbonate rocks is that a considerable majority of their K_V/K_H values are lower than 1.2, even though the observations also show that some data also fall in the region of $K_V/K_H > 4.2$. This value of 1.2 can therefore be safely taken as the most likely maximum K_V/K_H value for carbonates in Indonesia.

G. Permeability Anisotropy and Concept of Representative Elementary Volume

For sandstone samples, comparisons between core plug and FD core sample populations have shown differences in their respective general patterns. The general patterns that characterize most core plug sample populations show 'smooth' and more even distributions among K_V/K_H ranges compared to the patterns shown by the FD core populations. In order to investigate the cause, Widarsono et al. (2006) presented a separate observation on size effect on permeability, by comparing permeabilities of FD core and plug samples at same depths (data for plug samples were chosen from the same depth belonging to FD core samples' depth, or at least directly adjacent to them). The log-log plots for K_V and K_H (Figures 3.63 and 3.64, respectively) show that there are some degree of difference between the FD core and plug samples permeabilities indicated by the scatter shown, even though in general the data fall roughly around the 45° equality line. This implies that in general, the 'representative elementary volume' (REV), as borrowed from the definition presented by various publications (e.g. Hudson & Cooling, 1988) for rock mechanical properties, of sandstones is probably still larger than the size of whole core samples. Volumes smaller than REV are likely to show significantly different permeability values, while volumes of much larger tend to exhibit similar permeability values. In other words, rock properties measured at scales of plug and FD core samples are still heavily influenced by rock heterogeneity. With this in consideration, it is therefore likely that the difference in patterns shown by the plug and FD core samples are likely caused by not only the smaller sizes of the FD core samples population (total number = 336) relative to the plug sample population (total number = 4,312), but also to the intense heterogeneity that characterize the core samples.

This 'difference' between plug-size and FD core-size is even greater for the more complicated carbonate rocks. Data shown on Figures 3.65 and 3.66 have shown even higher degree of scatter indicating the more obvious absence of 'agreement' between plug-size and FD core-size, both vertical and horizontal permeability. It was even further shown that permeabilities measured at FD core-size, both vertical and horizontal, are always greater than values measured at plug-size scale. When REV concept is applied to the carbonate rocks, it is obviously considered that FD core-size samples are more representative to the reservoir in general. However, the similarity in patterns between two sizes, as well as the inconsistencies of the patterns when number of population is put into concern (e.g. large plug sample population may have similar pattern to small FD core sample population, and vice versa) are likely to be an indication that the true REV may be obtained at scales larger than both plug and FD core sizes.

In general, it is also understood that different reservoir may have different REV, but from comparisons between sedimentary basins

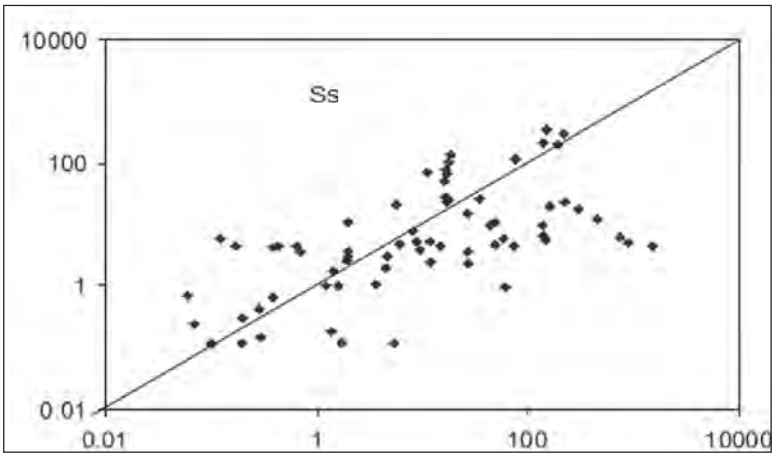

Source: Widarsono et al. (2006)

Figure 3.63 Comparison between Sandstone Core Plug and FD Core Vertical Permeability

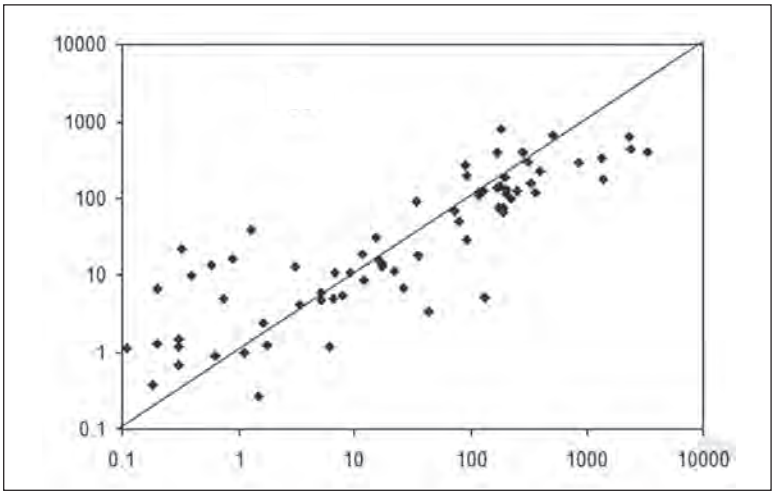

Source: Widarsono et al. (2006)

Figure 3.64 Comparison between Sandstone Core Plug and FD Core Horizontal Permeability

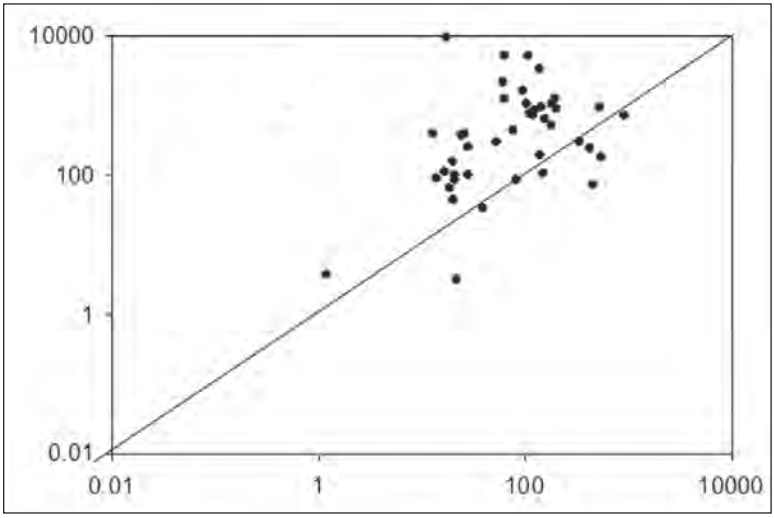

Source: Widarsono et al. (2006)

Figure 3.65 Comparison between Carbonate Core Plug and FD Core Vertical Permeability

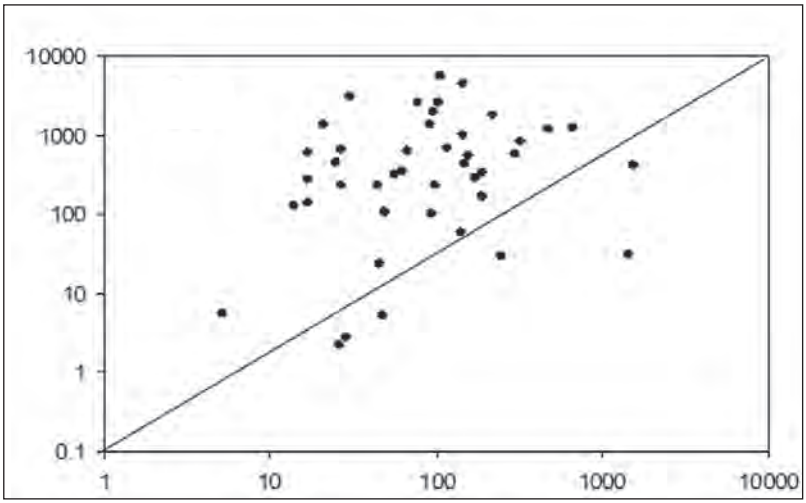

Source: Widarsono et al. (2006)

Figure 3.66 Comparison between Carbonate Core Plug and FD Core Horizontal Permeability

with large population, it can also be shown that heterogeneity has its effect at scales smaller than basin size or more precisely at field or reservoir scales. This is in line with evidence for sandstones showing K_V/K_H variations in vertical and lateral directions and for carbonates showing K_V/K_H variations in vertical direction. When put into the concept of REV, which previously states that it may probably occur at sizes as small as core plug samples, the K_V/K_H vertical and lateral variations taking place at volumes larger than the REV appear inconsistent since at volumes larger than REV K_V/K_H should remain the same. However, this can be understood when it is assumed that the previously stated REV is taken as 'apparent REV' for a specific sandstone or lithology. The 'true REV' for a field or reservoir must be in place at scales larger than both plug and FD core volumes. At volumes larger than this 'true REV' and smaller than basin-size or reservoir-size, then K_V/K_H would not vary much anymore.

CHAPTER IV
WETTABILITY–STATE AND ITS ALTERATION ON SOME SANDSTONES AND LIMESTONES

A. General

Another important physical properties of reservoir rocks is wettability. Wettability is basically an inclination of reservoir rocks to be wetted by certain fluids, either oil or water, due to which other rock physical properties, such as capillary pressure and relative permeability, are influenced. Reservoir rocks that tend to be water-wet respond differently to oil flow compared to what is shown by oil-wet ones, which in turn control capillary pressure and relative permeability behavior, hence govern hydrocarbon displacement and ultimate hydrocarbon recovery. Behavior of capillary pressure and relative permeability in turn influence reserves and production performance, as well as other aspects of petroleum production. Various works have been devoted in investigating this matter.

Early in 1958, Bobek & Mattax had recognized the importance of reservoir rock wettability to recovery factor during primary production. Later and more advanced studies also investigated the effect of wettability—as well as other factors such as temperature, combined ions, brine salinity, oil composition—on oil recovery (e.g. Zhang & Austad, 2006; Zhang & Morrow, 2006). Investigations were also

done for imperative issues, such as improved oil recovery (IOR) in the fields of waterflooding (e.g. Jadhunandan & Morrow, 1995; Zhou et al., 2000; Jackson et al., 2003; Austad et al., 2010; Austad et al., 2011; Alotaibi et al., 2011; Qiao et al., 2014), IOR/EOR-surfactant (e.g. Morvan et al., 2011), IOR/EOR thermal (e.g. Rao, 1999), and wettability alteration (e.g. Buckley et al., 1998; Austad & Standnes, 2003; Qiao et al., 2014). Works and discussions were also dedicated to study links between rock wettability and less direct influencing factors to production performance such as rock electrical properties (e.g. Anderson, 1986a, b) and *in situ* reservoir quartz cementation inhibition/permeability preservation (e.g. Barclays & Worden, 2000).

In oil saturated water-wet rocks, the oil rests on thin film of water spread over the rock's interior surface area. When the rock is in contact with water, the water imbibes and displaces the oil out. Water tends to fill all pores including the smallest ones. On the contrary, in oil saturated oil-wet rocks, the oil tends to act as water in a water-wet system. The oil displaces water and enters into the finest pores. The two different tendencies shown by the two different preferences to wettability certainly have different consequences on any attempt to produce the oil out from the rocks.

The fact stated above has been long studied by engineers and earth scientists. It is widely seen that sandstones tends to exhibit neutral to water-wet characteristics (e.g. Block & Simms, 1967) due to the acidic nature of the rock's surface that repels most crude oil behaving as weak acid. This wettability characteristic of sandstones is also stated in various sources (e.g. Archer & Wall, 1986) and is widely presumed in day-to-day related activities.

On the other hand, we still can find easily engineers and geo-scientists who assume that limestones are always oil-wet in nature. This presumption is not unfounded since results of past laboratory studies, such as Treiber et al. (1972) and Chillingarian & Yen (1983),

had revealed such conclusion. Nevertheless, some sources (e.g. Amyx et al., 1960; Sayyouh et al., 1990; Sayyouh et al., 1991; Hoeiland et al., 2001; Shedid & Ghannam, 2004) put and presented that rocks can have both wettability characteristics depending on their mineral/lithological composition, as well as oil characteristics.

Apart from the importance of original wettability, alteration of original wettability—a situation in which a rock sample (or a part of reservoir body) is no longer representing the reservoir's original wettability—is also considered important. Various causes are understood to potentially cause wettability alteration, such as presence of combined oil asphalthene contents and temperature (e.g. Al-Aulaqi et al., 1991), clay stabilization and contact with CO_2 (e. g. Wolcott et al., 1993), and contact with acid additives (Saneifer et al., 2011). One of the most frequent causes of wettability alteration, however, is core cleaning prior to laboratory testing. As stated in various sources (e.g. Timmerman, 1982), laboratory core extraction using hot solvent and the subsequent drying process may lead to changes in rock-wetting characteristics. Along with original wettability, wettability alteration presented in Widarsono (2010) and Widarsono (2011b) makes up the biggest part of this chapter. Through contents of this chapter, it is hoped that better understanding over wettability characteristics of some Indonesia's reservoir rocks can be attained including of how extensive the core preparation-related wettability alteration may have occurred among the reported laboratory testing results.

B. Wettability: A Brief Introduction

In a porous rock, wettability characteristic is essentially resulted from interactions between active surface forces, not only between two immiscible liquid phases but also between liquid and the rock's solid surfaces. The interactions produce forces including adhesive tension

that determines what liquids would wet the rock surfaces. Figure 4.1 exhibits a simple illustration of a condition in which a droplet of water sticking to a solid surface and is surrounded by oil. For determining the degree of wetness raised by two liquids, by convention, contact angle (q) is measured referring to the heavier among the two (in reservoir rocks water is usually taken) within a range of 0° to 180°. In a simple manner, the adhesive tension can be presented by (Amyx et al., 1960):

$$AT = \sigma_{SO} - \sigma_{SW} = \sigma_{wo} \cos\theta_{wo} \tag{4-1}$$

where AT, σso, σsw, and σwo are adhesive tension, interfacial tension between solid and the lighter liquid (usually oil), interfacial tension between solid and the heavier liquid (usually water), and interfacial tension between the two liquids, respectively (Amyx et al., 1960). By arranging Equation 4.1, and in accordance with illustration in Figure 4.1, contact angle can be expressed as

$$\cos\theta = \frac{\sigma_{SO} - \sigma_{SW}}{\sigma_{wo}} \tag{4-2}$$

Positive adhesive tension indicates that the heavier liquid tends to wet the solid's surface, while zero adhesive tension is resulted from a condition showing the two liquids as having similar affinity towards the solid's surface. The larger adhesive tension (i.e. the smaller contact angle), the easier for the wetting phase to stick and spread on the solid's surface. On the contrary, smaller adhesive tensions (i.e. larger contact angles) require external energy to force the wetting phase to spread on the same surface. By convention, it can be taken that if the contact angles are less than 90°, then the heavier liquid phase acts as wetting phase, and at contact angle of 90°, the wetting characteristic is considered as neutral with equal wetting tendencies for both liquids. As a guiding criterion, Treiber et al. (1972) established that for

water-oil system: contact angle of 0–75° is for water-wet, 75–105° for neutral, and 105–180° for oil-wet.

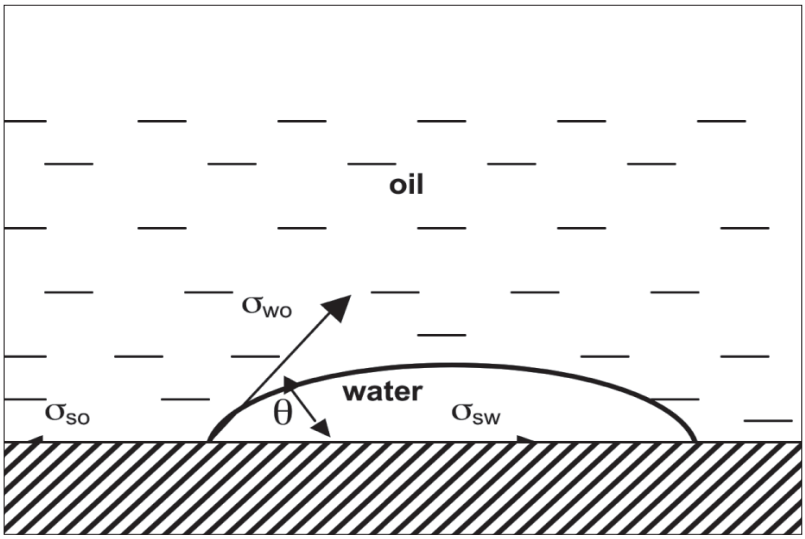

Figure 4.1 Equilibrium of Interfacial Forces in Water–Oil–Solid System

In sandstones, the rock's solid surface usually tends to be acidic, hence inclined to react easily with basic substances. The reverse is true when the solid is exposed to acidic liquid substance. The main organic component in most crude oil usually tends to behave like weak acids leading to be expelled by the rock's acidic silica and forming water-wetting tendency. In their experiments, Block & Simms (1967) showed that the basic octa-decylamine organic substance was easily absorbed by glass surfaces, while the also used stearic acid was not absorbed at all.

As stated above, even though most crude oil has weak acid components, some types of oil can be of either basic or acidic in nature, especially with those containing resins and asphaltenes (e.g. Denekas

et al., 1959). With presence of these components, sandstones can actually behave both in water-wet and oil-wet manners, even though the degree of strength is very much governed by the quantity of the two components. Wettability of limestone is as varied as in the case of sandstone, even though it is often perceived that limestone is in general more inclined towards oil wettability than sandstone.

This common perception is certainly not unfounded since some studies regarding the issue have been performed in the past. For instance, Treiber et al. (1972) conducted a series of wettability tests on 30 sandstone and 25 limestone samples and found that 88% of the limestone samples are oil wet by nature, with the remaining comprised of 4% neutral and 8% water-wet. In a similar but more recent study, Morrow (1976) using same quantity of samples found limestones with neutral wetness tendency (64%) and sandstones with slightly inclined on water-wetness (40%). Later, Chilingarian & Yen (1983) found on their study using 160 limestone samples of 80% oil-wet, 12% neutral, and 8% water-wet (Table 4.1). In a manner differently, the sandstone samples in Treiber et al. (1972) tend to show same inclination towards the two wetness characteristics.

Table 4.1 Relative Wetting Tendencies in Sandstones (Ss) and Limestones (Ls) from Past Studies

Wettability	Treiber et al. (1972)		Morrow (1976)		Chilingarian and Yen (1983)
	Ss, %	Ls, %	Ss, %	Ls, %	Ls, %
Water wet	43	8	40	8	8
Neutral	7	4	33	64	12
Oil wet	50	88	27	28	80

The brief discussion and past laboratory studies presented above imply that wettability is strongly related to rocks' and fluids chemical compositions and the resulted relative pH. Differences in chemical compositions are also likely to respond differently to external factors

such as pressure and heat. The process itself is very complex. Various investigators have, however, put some factors considered responsible for forming wettability, such as mineral composition (e.g. Anderson, 1986a, b), clay contents (e.g. Sayyouh et al., 1990), rock pore structure (e.g. Hirasaki, 1991), rock surface electrical charge (e.g. Buckley et al., 1989), polar compound of crude oil (e.g. Sayyouh et al., 1991), crude oil acid fraction (e.g. Hoeiland et al., 2001), brine composition (e.g. Zhang & Morrow, 2006), water droplet volume (e.g. Shedid and Ghannam, 2004), and pressure-temperature (e.g. Rajayi & Kantzas, 2011). Nevertheless, all petroleum reservoir rocks are believed to have inclination towards water-wetness originally (Tiab and Donaldson, 2004), but it is most probably due to these different responses that changes in wettability had occurred and eventually produced the rock wettability in this study encountered today.

C. Indicators of Wettability

Considering the importance of wettability, this rock property is among the most important properties, information regarding them is compulsory for acquisition. In very careful experiments, direct measurements can basically be made to obtain contact angle data in water-oil system with Sessile Drop (e.g. Treiber et al., 1972) and Wilhelmy Plate (e.g. Mennella et al., 1995) measurements. Afterwards, Rao & Girard (1996) established a Dual Drop Dual Crystal alternative technique for measuring contact angle. These techniques can certainly provide the needed information, but are often considered as too meticulous in preparation, and their need for homogeneously smooth solid surface implies that test results may not represent the commonly multi-mineral reservoir rocks.

In addition to the direct measurement methods mentioned above, there are several laboratory indirect techniques such as Amott

Wettability Index, one suggested by the United States Bureau of Mines (USBM), and Direct Imbibition (DI). There are also some other 'non-standard' techniques that had been established later such as Dubey & Doe (1993) and Wu et al. (2008), out of which Mwangi et al. (2013) singled out Dubey and Doe technique as the more consistent. Apart from the three 'standard' direct indicators, there is an indirect indicator that plays a very important role in the study, water-oil relative permeability curves. The four methods are briefly described as follows:

1) **Amott Wettability Index.** This technique was suggested by Amott (1959) and is essentially based on spontaneous imbibition and forced displacement of oil and water out of tested core plugs. Through spontaneous imbibition two indexes are made, the oil index (I_O) and water index (I_W). The oil index is a ratio between volumes of water in a water-saturated core sample displaced by oil, if any, in an imbibition (immersion in oil) process and volumes of all remaining water displaced through forced displacement by oil until irreducible water saturation (S_{wirr}) is reached. The volume of displaced water resulted from slow imbibition process is denoted by V_{wi}, whereas V_{wd} symbolizes the water volume yielded through the forced displacement by oil (includes V_{wi}) following the completion of imbibition process. The process for producing water index follows, in which the already oil-saturated sample (at S_{wirr}) is imbibed with water (immersion in water) leading to some displaced oil, if any, (V_{oi}) and—in the same manner with oil forced displacement—is followed by water forced displacement to yield total produced oil volume of V_{od} (includes V_{oi}). Mathematically, the two indexes are expressed as:

$$I_O = \frac{V_{Wi}}{V_{Wd}} \tag{4-3}$$

and

$$I_W = \frac{V_{Oi}}{V_{Od}} \tag{4-4}$$

Forced displacement is usually performed using centrifuge or core flow apparatus, while imbibition process is suggested to take at least 20 hours (Amott, 1959) or much longer for rocks with neutral wettability (Anderson, 1986a).

Interpretation using the two indexes is somewhat relative in nature and there is no guideline for definitive judgment. Amott (1959) put 1.0 as strong wettability, while a value of zero indicates neutral wettability, and values approaching zero are indication of preferential wettability. Inclination towards either wettability is judged from relative comparisons between the two indexes. When wettability is put as I_w-I_o, the Amott wettability index would vary from +1 for absolute water wet to -1 for absolute oil wet with zero indicating neutral wettability.

For the purpose of clear classification and comparison with other wettability indicator techniques, wettability in this study is divided into 'strong oil wet', 'oil wet', 'preferential oil wet', 'neutral', 'preferential water wet', 'water wet', and 'strong water wet'. Table 4.2 presents value ranges for the wettability categories. The established value ranges are indeed subjective in nature, but their assignments are considered appropriate to accommodate reasonable discretization on gradation in the wettability strength.

Table 4.2 Categorization Criteria Used in the Study

Wettability class	Amott	USBM	Imbibition	Relative permeability
	$\Delta I = I_W - I_O$	I	$\Delta V = V_w - V_o$	$S_w \text{ at } K_{ro} = K_{rw}$
Strong water-wet	$0.8 < \Delta I \leq 1$	$1 < I \leq +\infty$	$50 < \Delta V \leq 100$	$0.85 < S_w \leq 1$
Medium water-wet	$0.5 < \Delta I \leq 0.8$	$0.25 < I \leq 1$	$15 < \Delta V \leq 50$	$0.65 < S_w \leq 0.85$
Weak water-wet	$0.1 < \Delta I \leq 0.5$	$0.1 < I \leq 0.25$	$5 < \Delta V \leq 15$	$0.55 < S_w \leq 0.65$
Neutral/mix	$-0.1 \leq \Delta I \leq 0.1$	$-0.1 \leq I \leq 0.1$	$-5 \leq \Delta V \leq 5$	$0.45 < S_w \leq 0.55$
Weak oil-wet	$-0.5 \leq \Delta I < -0.1$	$-0.25 \leq I < -0.1$	$-15 \leq \Delta V < -5$	$0.35 < S_w \leq 0.45$
Medium oil-wet	$-0.8 \leq \Delta I < -0.5$	$-1 \leq I \leq -0.25$	$-50 \leq \Delta V \leq -15$	$0.15 < S_w \leq 0.35$
Strong oil wet	$-1 \leq \Delta I < -0.8$	$-\infty \leq I \leq -1$	$-100 \leq \Delta V \leq -50$	$0 \leq S_w \leq 0.15$

Source: Widarsono et al. (2010)

2) **USBM Wettability Index.** The technique basically uses capillary curves obtained through displacing oil and water using centrifuge equipment (Donaldson et al., 1969). The displacement is peformed alternately in a way similar to forced displacement process in the Amott technique, in which a water-saturated sample is spun under various rotational speeds, while immersed in oil to reach S_{wirr}. The process is repeated by spinning the now oil-saturated sample in water immersion. Capillary pressures are calculated based on the known rotational speeds.

The fundamental principle of the method is that displacement of a non-wetting phase by a wetting phase requires less force than the reverse. This results in different capillary pressure curves with the case of non-wetting phase displacing wetting phase having higher and steeper curve. This means that the areas under the two curves between S_{wirr} and water saturation at residual oil saturation (S_{wor}) are different, and the ratio between the two is an indicator of the rock's wettability. Figure 4.2 shows the hysteresis in capillary curves as the results of

the alternately forced displacements. Donaldson et al. (1969) then put

$$I_W = \log\left(\frac{A_1}{A_2}\right) \tag{4-5}$$

as the wettability index, with A_1 and A_2 are respectively area under curve of oil displacing water (from S_{wor} to S_{wirr}) and area under curve of water displacing oil (from S_{wirr} to S_{wor}).

The index presented in Equation 4-5 shows that wettability index values could range from + ∞ (complete water wet) to – ∞ (complete oil wet) with zero for neutral wettability. There is no guideline in regard to classification of wettability. Therefore, in the same fashion used for Amott wettability index, the USBM index is also divided using the same categorization into the same seven wettability types. Table 4.2 presents the value ranges in the categorization.

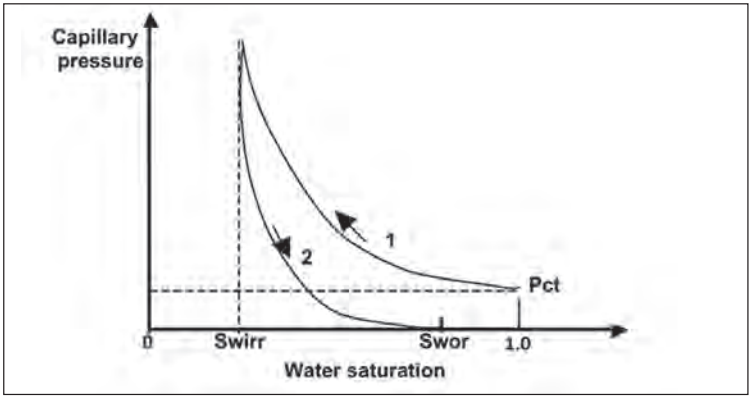

Figure 4.2 Oil displacing water curve (1) and water displacing oil curve (2) for a water wet system. S_{wirr} is irreducible water saturation, whereas S_{wor} is water saturation at residual oil saturation. Note the threshold capilary pressure (Pct) that is needed by the oil to displace water as wetting phase.

3) **Direct Imbibition.** The technique is based on recognition that spontaneous imbibition on porous rocks leads to volume and rate of imbibition that relate directly to the rocks general wettability. Unlike Amott and USBM techniques, Direct Imbibition technique relies solely on liquid imbibition process despite the knowledge that imbibition rate is also influenced by other factors such as imbibing liquid viscosity, permeability, porosity, artificial tension, and sample's edge condition (Tiab & Donaldson, 2004). Acknowledging these factors, Ma et al. (1999) used scaling correlation for evaluating imbibition-driven oil recovery in fractured water-drive reservoir introduced by Mattax & Kyte (1962) for evaluating wettability in this Direct Imbibition method. Nevertheless, the most common judgment for establishing wettability type is through relative comparison between imbibition rates of water and oil, and the reported conclusion for the two sandstone samples is used without any further review. Deeper description is not spent and index categorization is not established for this technique.

4) **Water-oil relative permeability curves.** As wettability tendencies affect capillary pressure curves in the form of hysteresis, the tendencies also affect water-oil relative permeability curves. Basically, a core flow test designed to obtain relative permeability curves is meant to observe on how a particular rock sample pore system influences the multi-phase flow behavior. With presence of different wetting inclination shown by different reservoir fluids, however, this porous medium–fluid interaction is biased. Different degrees of wettability lead to different fluid saturating characteristics within the rock, hence changing the effective permeability of the fluids present.

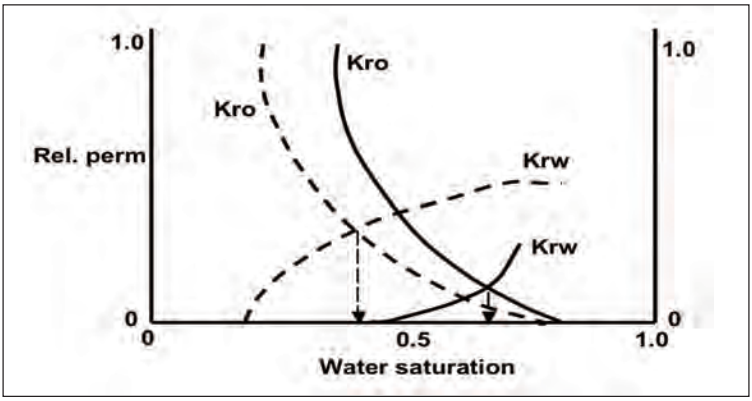

Figure 4.3 Shift in permeability curves intersects due to change in wettability system. Relative permeability of an oil-wet system (dashed curves) tend to show higher water effective permeability leading curve intersect at lower water saturations. On the contrary, higher oil effective permeability in water-wet system (solid curves) tends to yield intersects at higher water saturations.

Figure 4.3 illustrates changes in relative permeability due to different wettability. In comparison, water-wet system and oil-wet system become different even though the shape of curves remains the same. At condition of oil-wet system, the flow tends to be of earlier water breakthrough due to easier movements of water compared to oil. In this condition, the point of Kro = Krw occurs at lower values of water saturation with higher values of Krw and lower Kro values at most values of water saturation. Change in wettability towards more water wettability shifts the Kro = Krw point to higher water saturation points due to the fact that the water tends to lose mobility, hence requiring higher water saturation to enable it to move under the same pressure difference (Amyx et al., 1960; Craig, 1971; Archer and Wall, 1986). Anderson (1986c) and Anderson (1987) discussed further in more depth the influence of wettability on relative permeability curves.

Wettability is indeed not the sole factor that can influence water-oil relative permeability curves. In their report on a series of experimental works, Geffen et al. (1951) put that variation in overburden pressures and the resulting changes in pore size distribution may provide blocking effect to the two liquid phases' movements and shifts the relative permeability curves. Increases in temperature also change wettability towards a more water-wet tendency. These all imply that any test for relative permeability has to be performed under reservoir condition (i.e. overburden pressure, pore pressure, and temperature). However, common industrial practices in this regard rarely meet this ideal condition for various reasons, including equipment limitation and simplicity. All relative permeability data used in this study was obtained under atmospheric temperature. This is also the case for measurements on wettability, for which both imbibition and forced displacement processes were carried out under atmospheric temperature. Therefore, similarity in testing condition for the three wettability indicators suggests that wettability remains the sole predominant factor in the shift of relative permeability intersects (i.e. Kro = Krw).

Through the use of this later conclusion, shift in intersect between the two curves can, therefore, be used as indicator for rock's wettability. Water-wet rocks tend to have curves' intersect to be at water saturation values lower than 50%, and the reverse is true for oil-wet system. No clear guideline has been given by past studies regarding values or value ranges that represent certain degrees of wettability (need further explanation and/or references). It is logical, however, that neutral wettability systems would have curve intersect at around 50% water saturation, and strong wetting tendencies at water saturation values approaching S_{wirr} and residual oil saturation (S_{or}) for water-wet and oil-wet systems, respectively. Gradual degrees in wetting tendencies

for both wettability systems naturally fall between neutral and the two strong wetting.

In order to make this indirect wettability indicator comparable to the other two standard techniques discussed earlier, a clear guideline is needed. Similarly, the seven-class wettability division used for the other two techniques is also used here, with water saturation ranges represent the permeability curves' intersects as reference. Table 4.2 presents the water saturation ranges assigned to serve the purpose.

Nonetheless, in establishing the ranges in Table 4.2, Widarsono (2011b) stated that the criteria set presented in Table 4.2 should not be taken as a rigid and absolute reference since it is merely a tool for analysis. Moreover, the term 'mix-wettability' is taken as equal neutral wettability, in an understanding that if neutral wettability is attributed to rocks that do not absorb neither water nor oil, then the mix-wettability represent rocks that tend to attract the two liquids in roughly similar quantity/portion. The commonly used term of 'preferential wettability'—such as ones shown in laboratory reports of Tables 4.6 through 4.9—for rocks that draw more of one liquid than the other one is not in use. This term in this book is instead replaced by either water-wet or oil-wet with different strength levels.

D. Data Inventory

Widarsono (2010) and Widarsono (2011b), in performing the studies, used data from 363 sandstone and 362 limestone core samples, taken from 45 oil and gas fields in Indonesia (Figure 4.4). Tables 4.3 through 4.5 present lists of data covering sample origins and their type of wettability indicators. Amott technique appears to make the bulk of wettability test results (221 samples) among the three wettability test methods, while relative permeability, as a non-wettability test technique, is also available in even larger number (447 samples).

Amott test results are presented in tabular form, whereas the USBM and relative permeability data are in both tabular and graphical forms. Table 4.6 depicts an exemplary Amott test data (BK-232 well, Central Sumatra Basin) from which overall preferential to water wetness is concluded. Table 4.7 and Figure 4.5 present example (T-105 well, Barito Basin) for USBM technique, the resulting values indicate sufficiently strong inclination to be oil-wet. For Direct Imbibition test, Table 4.8 presents an example (RD-1 well, Northwest Java Basin), which shows a preference towards water-wetness. All wettability tests were performed using native cores—i.e. uncleansed—leading to results representing their unaltered wettability.

For relative permeability data, most data available to the study has complete curves to enable observation on the curves' intersects. Nevertheless, in some cases (less than 3% of overall data) with incomplete data, extrapolations were made so that the desired information is obtained. Figure 4.6 exhibits three examples with three different wetness tendencies and Table 4.9 shows a summary of examples obtained from limestone samples of TB-24 well, Northwest Java Basin. In accordance to the procedure, all samples were cleansed using solvent prior to relative permeability tests, meaning that the resulting data is likely to represent 'unrestored' or 'altered' wettability condition.

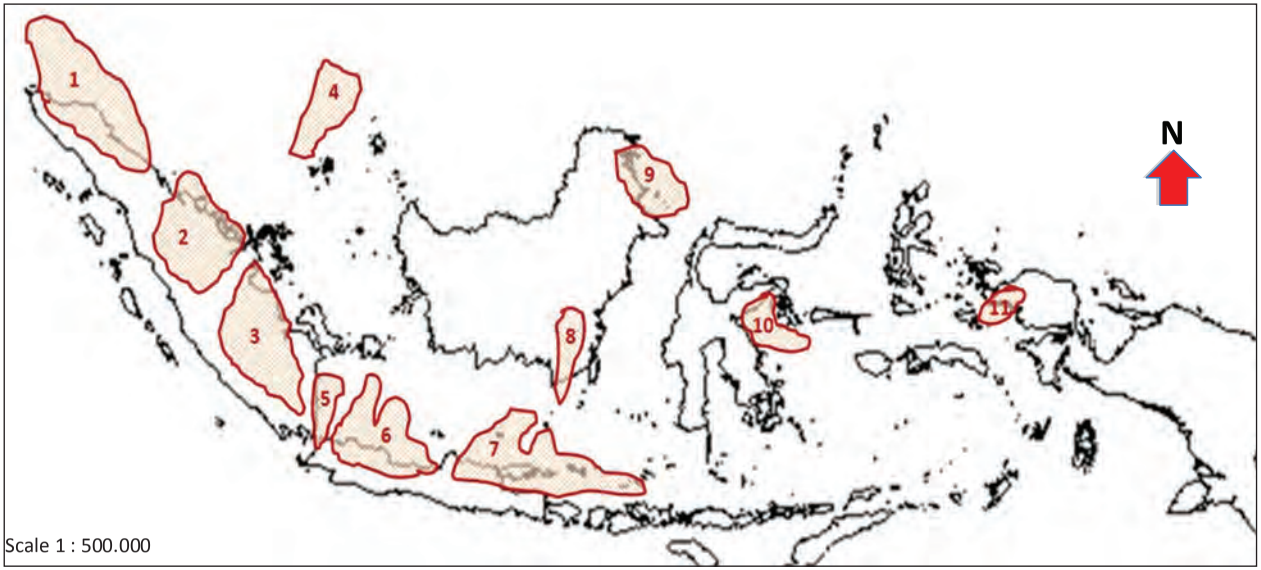

Figure 4.4 Western Indonesia's Sedimentary Basins, the Place of Origin of the Sandstone and Limestone Core Samples Used in the Study: (1) North Sumatra Basin, (2) Central Sumatra Basin, (3) South Sumatra Basin, (4) West Natuna Basin, (5) West Sunda/Asri Basin, (6) Northwest Java Basin, (7) Northeast Java Basin, (8) Barito Basin, 9) Tarakan Basin, 10) Banggai Basin, and 11) Salawati Basin.

Table 4.3 Number of Sandstone Core Samples per Wettability Indicator (Amott, USBM, Imbibition, and Relative Permeability) and Its Field of Origin, North Sumatra, Central Sumatra, South Sumatra, and Northwest Java Basins

Basin	Field/structure (no. of wells)	Number of samples			
		Amott	USBM	Imbibition	Rel. perm
		$\Delta I=I_w-I_o$	I	$\Delta V=V_w-V_o$	$S_w@K_{ro}=K_{rw}$
North Sumatra Main formation(s): Seurulla, Keutapang, Belumai	Gebang (1), Kuala Simpang Barat (2), Paluh Tabuhan Timur (2), Rantau (2), Tabuhan Barat (1) Total wells = 8	18	8	-	31
Central Sumatra Main formation(s): Pertama, Kedua, Duri, Bekasap, Bangko, Telisa, Petani	Bangko (2), Kopar (2), Libo (1), Petani (4) Total wells = 9	20	-	-	38
SouthSumatra Main formation(s): Gumai, Talang Akar, Air Benakat, Muara Enim,	Bajubang (1), Bentayan (1), BNG (1), Jirak (2), Karang Agung (1), Kenali Asam (1), Ketaling Timur (1), Lubuk (1), Lirik (1), Tanjung Tiga Timur (1), Tapus (1) Total wells = 12	38	10	-	65
Northwest Java Main formation(s): Talang Akar	Cemara Barat (2), Cemara Timur (4), Melandong (1) Total wells = 7	23	2	-	47

Table 4.4 Number of Sandstone Core Samples per Wettability Indicator (Amott, USBM, Imbibition, and Relative Permeability) and Its Field of Origin, West Natuna, Northeast Java, Barito, and Tarakan Basins

Basin	Field/structure (no. of wells)	Number of samples			
		Amott	USBM	Imbibition	Rel. perm
		$\Delta I=I_w-I_o$	I	$\Delta V=V_w-V_o$	$S_w@K_{ro}=K_{rw}$
West natuna Main formation(s): Upper Gabus, Lower Gabus, Arang	Kakap (1) Total well = 1	5	-	-	15
Northeast Java Main formation(s): Ngrayong, Ledok	Nglobo (1), Semanggi (1) Total wells = 2	4	-	-	6
Barito Main formation(s): Tanjung, Montalat, Warukin	Tanjung (1) Total well = 1	-	4	2	14
Tarakan Main formation(s): Bunyu, Tabul	Sembakung (1) Total well = 1	5	-	-	8

Table 4.5 Number of Limetone Core Samples per Wettability Indicator (Amott, USBM, Imbibition, and Relative Permeability) and Its Field of Origin, South Sumatra, Sunda-Asri, Banggai, and Salawati Basins

Basin	Field/structure (no. of wells)	Number of samples			
		Amott	USBM	Imbibition	Rel. perm
		$\Delta I=I_w-I_o$	I	$\Delta V=V_w-V_o$	$S_w@K_{ro}=K_{rw}$
South Sumatra Main formation(s): Baturaja	ASDJ (1), Kaji (2), Karangdewa (1), Musi (3), Pagardewa Selatan (1), Semoga (1), Sopa (2), Suban Barat (1), Tanjung Laban (1) Total wells = 13	23	-	5	53
Sunda-Asri Main formation(s): Baturaja	Kitty (1), Krisna (3), Nora (1), Nurbani (1), Rama (1) Total wells = 7	8	4	2	25
Northwest Java Main formation(s): Baturaja		72	-	20	138
Banggai Main formation(s): Minahaki	Donggi (1), Senoro (2) Total well = 3	5	-	-	5
Salawati Main formation(s): Kais	Kasim (1) Total well = 1	-	-	-	2

Table 4.6 Result example of wettability test using amott technique. The generally preferential water-wet rocks are from BK-232 well, Central Sumatra Basin.

Sample number	Perme-ability (mD)	Porosity (%)	Wettability Index			Inter-pretation
			W-wet	O-wet	ΔI	
1	23	25.4	0.4167	0.0000	0.4167	preferential water-wet
10	3251	32.5	0.4355	0.1719	0.2636	preferential water-wet
13	772	31.4	0.3352	0.0789	0.2563	preferential water-wet
19	22	22.6	0.4800	0.0000	0.4800	preferential water-wet
20	9	25.5	0.4857	0.4113	0.0744	Neutral

Source: Widarsono et al. (2010)

Table 4.7 Result example of wettability test using USBM technique. The generally oil-wet rocks are from T-105 well, Barito Basin.

Sample No.	Permeability (mD)	Porosity (%)	$I = \log\left(\frac{A_1}{A_2}\right)$	Interpretation
276	147	24.7	-0.336	oil wet
265B	47	21.8	0.106	preferential water wet
217a	29	23.6	-0.346	oil wet
216	34	24.6	-0.392	oil wet
119B	844	28.1	-0.199	preferential oil wet
105	62	27.5	-0.140	preferential oil wet

Source: Widarsono et al. (2010)

Table 4.8 Example of wettability test data obtained through the use of direct imbibition technique. The Baturaja limestones derived from RD-1 well, Northwest Java Basin, are generally water-wet.

Sample number	Permeability (mD)	Porosity (%)	Imbibed fluid (%PV)			Interpretation
			Water	Oil	ΔV	
6	1.4	22	40.3	ND	40.3	medium water-wet
11	0.6	14	65.7	ND	65.7	strong water-wet
39	3.2	16	43.4	ND	43.4	medium water-wet
41	12	21	27.6	ND	27.6	medium water-wet

ND: not detected

Source: Widarsono et al. (2010)

Table 4.9 Example of wettability indication from water-oil relative permeability data. The data set is from T-24 well, Northwest Java Basin.

Sample No.	Permeability (mD)	Porosity (%)	Sw @ Krw= Kro, (%)	Interpretation
1	457	23.2	38	weak oil-wet
9A	47	14	44	weak oil-wet
16A	226	24.3	40	weak oil-wet
19	6.3	12.6	50	neutral/mix

Source: Widarsono et al. (2010)

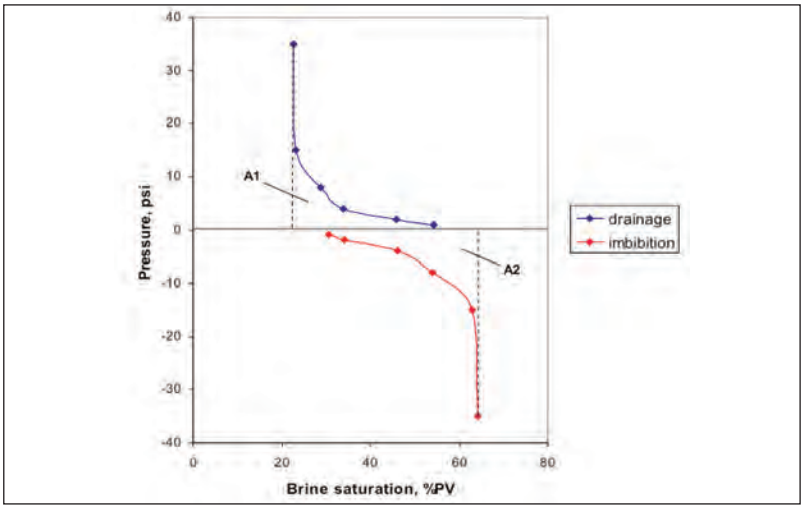

Figure 4.5 Example of USBM wettability test graphical result for a core sample taken from T-105 well, Barito Basin. The test yields $I = \log(A_1 / A_2)$ value of -0.140 indicating preferential tendency towards oil wetness (preferential oil-wet).

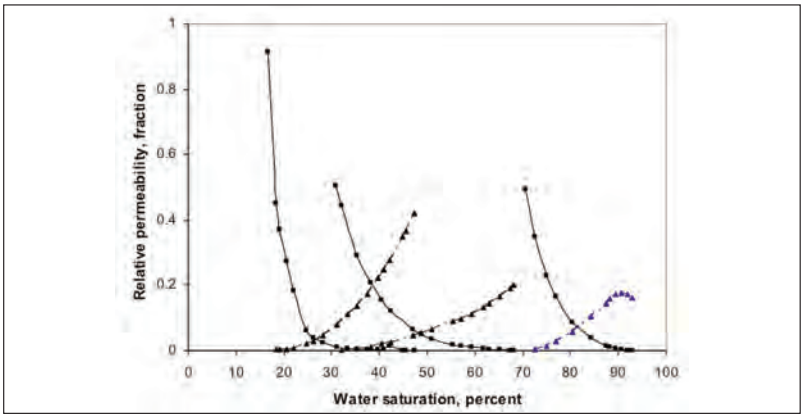

Figure 4.6 Three pairs of relative permeability curves (solid and dashed ones for Kro and Krw, respectively) taken from; a) PP-CC5 well (Sumatra Basin), b) KW P6 well (NE Java Basin), and FW-2 well (NW Java Basin). In accordance with the criteria established in this study, the three exemplary data sets tend to exhibit wettability tendencies of oil-wet, neutral, and strong water-wet, respectively.

E. Wettability of Sandstones

In analyzing the data, observations in Widarsono (2010) were performed on two issue: original wettability as indicated by wettability tests and wettability alteration due to core cleansing.

1. Original wettability

In general, results from three wettability indicating techniques have exhibited no strong preference towards specific wettability types. As depicted in Figure 4.7, 'preferential water-wet', 'water-wet', and 'strong water-wet' are respectively represented by 39, 21, and 3 samples. A combination of these figures, making 48.2% of all samples, is grouped into water-wetness tendency. On the other hand, a combination of 'preferential oil-wet' and 'oil-wet– 32 and 10 samples, respectively– tendencies establishes a corresponding figure of 30.2% for oil-wetness tendency. No 'strong oil-wet' result has been observed.

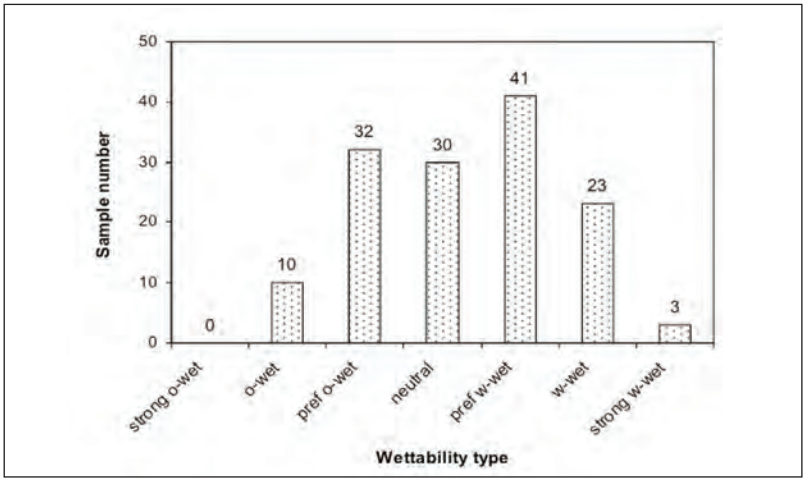

Source: Widarsono et al. (2010)

Figure 4.7 Wettability composition of the sandstone samples, which wettability test results are used in this study. Water-, neutral-, and oil-wet groups make 48.2%, 21.6%, and 30.2% of the total core samples, respectively.

These 'oil-wet' and 'water-wet' composition,– along with 21.6% of 'neutral' wettability, – have shown that Indonesian reservoir sandstones are not different from other sandstones from other places in the world. As put earlier, even though Block & Simms (1967) showed that silicate glass tends to show strong water-wetness, but combined presence of rock mineral impurities and oil pH preference– as proved by Treiber et al. (1972, tends to exhibit even tendencies toward oil- and water-wetness (Table 4.1). Comparing these results and those shown in Figure 4.8 comparable compositions are obvious with strong similarity in water-wetness. Larger amount of samples on both sides may probably lead to more similar compositions.

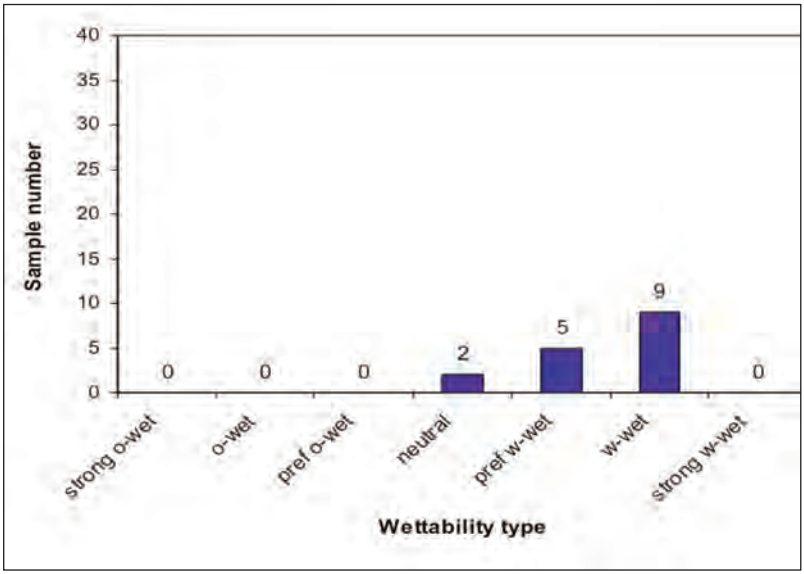

Source: Widarsono et al. (2010)

Figure 4.8 Wettability composition of sandstone samples that originally belonged to 'strong water-wet' class. Although most samples still retain water-wetness inclination, some have lost their preference to water-wetness.

2. Wettability alteration

As put earlier, core plugs are usually cleansed and extracted of all salts normally present in native cores prior to measurement for rock basic properties. This is often, and indeed has become a recommended practice (API, 1960 or its 1998 version), for both practical and objective reasons (e.g. air permeability and helium porosity are measured on cleansed core plugs). Therefore, it is expected that wettability alteration has occurred.

In analyzing the alteration, assumptions were taken as follows. 1) For original wettability from wettability tests, overall wettability of one sample set (i.e. from a well) is adopted based on majority in wettability type shown by the tested samples. This is due to the fact that samples used in wettability tests were not of same samples used in relative permeability test, even though they belonged to the same sample set. This 'overall wettability' was then compared with relative permeability curves intersects from individual samples in order to observe changes in wettability. 2) Relative permeability curves' intersect (@ Kro = Krw) can be used as wettability indicator based on recognition that the pair of curves shift along water saturation axis with changes in rock sample's wettability type. 3) The established index categorization for wettability classification serve well for the three wettability indicators (minus the Direct Imbibition technique) to justify comparison among results of all the four techniques. Figures 4.8 through 4.13 present the change of samples originally belonging to each wettability class.

From the originally described as belonging to a strong water-wet sample set– as indicated by the wettability test– one of the 16 samples tested for water-oil relative permeability data indicates strong water drive class of wettability (Kro = Krw @ $S_w > 0.8$) (Figure 4.8). The changes in wettability, some samples still retain water-wetness at lesser

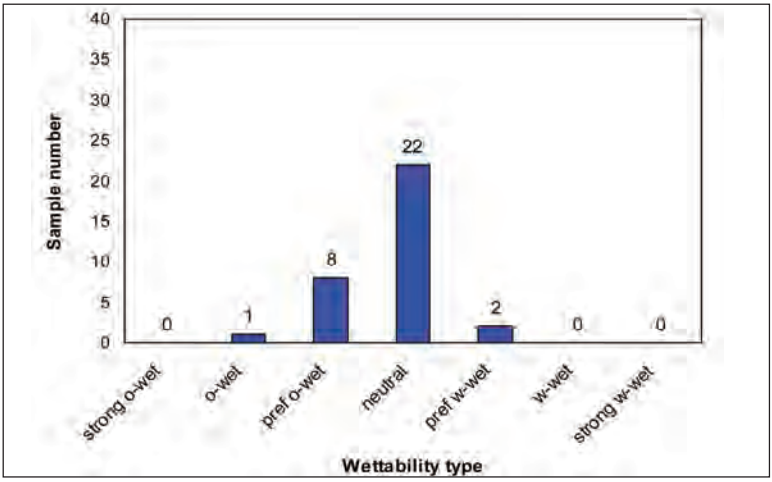

Source: Widarsono et al. (2010)

Figure 4.9 Wettability composition of sandstone samples that originally belonged to 'water-wet' class. Most sample have become 'neutral', but oddly enough some of them 'switch side' into 'oil-wet' group.

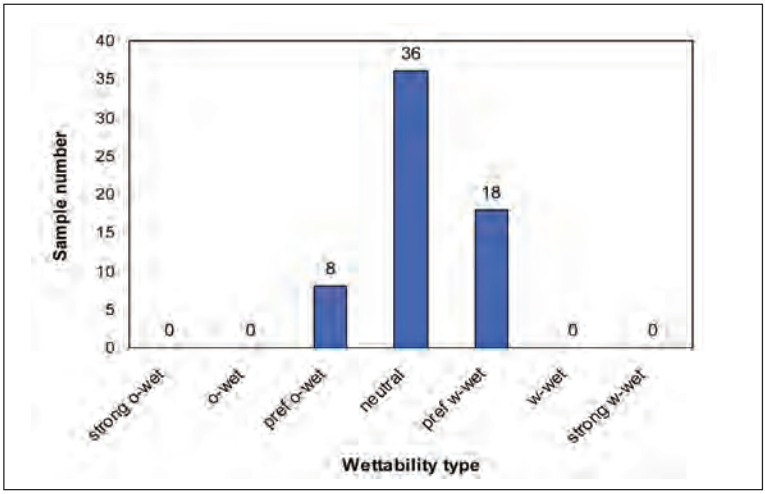

Source: Widarsono et al. (2010)

Figure 4.10 Wettability composition of sandstone samples that originally belonged to 'preferentially water-wet' class. Some samples retain their original wettability, but most samples have become 'neutral'. Small portion of samples also become 'preferentially oil-wet'.

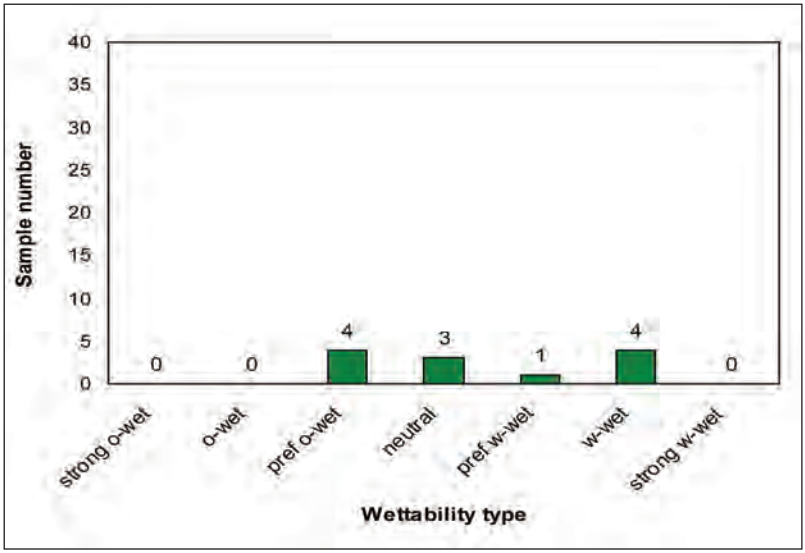

Source: Widarsono et al. (2010)

Figure 4.11 Wettability composition of sandstone samples that originally belonged to 'oil-wet' class. None of the samples retain their original wettability and most samples have degraded into 'softer' wettability, and some even become inclined into the 'water-wet' group.

degrees, even extend to 'neutral' (Kro = Krw @ $S_w \cong 0.5$) meaning that the samples of concern have lost affinity tendency towards water (and also oil).

Similar to the case of 'strong water-wet', all samples that originally belonged to 'water wet' category have degraded in wettability strength against water (Figure 4.9) and most of the samples have become 'neutral' and even 'switch side' into the oil-wet group. The case is not entirely the same for 'preferentially water-wet' class, out of which some still retains their original wettability (18 samples) even though most of the samples have become 'neutral'. Similar to the case of 'water-wet' class, some of the originally 'preferentially water-wet' samples have become 'preferentially oil-wet'. The degradation in water-wetness

due to core cleansing is understandable, but change into oil-wetness indeed requires more thorough explanation.

In the oil-wet group, no originally strong oil-wet samples are at disposal, which means only two classes available: 'oil-wet' and 'preferentially oil-wet'. In a manner similar to the cases in the 'water-wet' class, the samples belonging to 'oil-wet' samples have degraded into 'preferentially oil-wet' and 'neutral' classes with some even switched wettability into more oil-wet orientation (Figure 4.11). A resemblance in behavior to 'preferentially water-wet' class samples is also shown by its counterpart in the 'preferentially oil-wet' class. Many of the originally preferentially oil-wet samples retain their wettability, while most have become 'neutral' with the remaining few jump onto the other side of the wettability spectrum (Figure 4.12). Although this

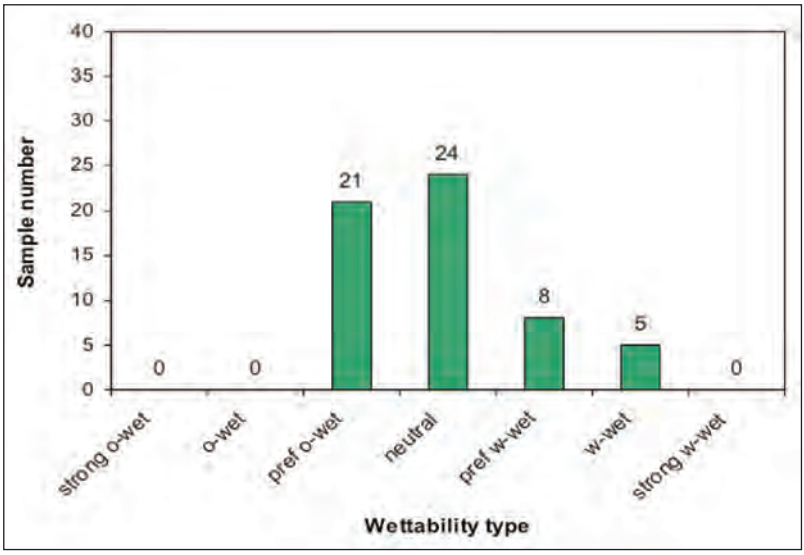

Source: Widarsono et al. (2010)

Figure 4.12 Wettability composition of sandstone samples that originally belonged to 'preferentially oil-wet' class. Similar to the case of 'preferentially water-wet' class, many of the samples retain their original wettability and most became 'neutral'. Some few samples have gone to oil-wet tendency, however.

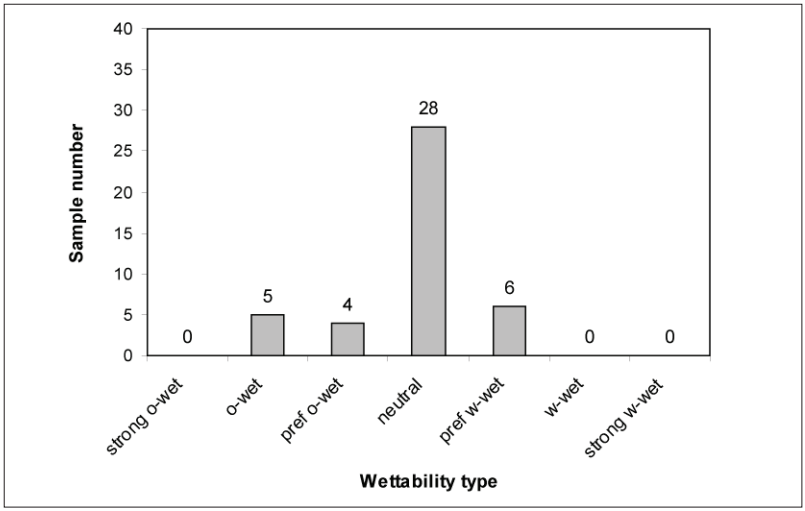

Source: Widarsono et al. (2010)

Figure 4.13 Wettability composition of sandstone samples that originally belonged to 'neutral' class. Majority of samples remain 'neutral', and if samples of the two preferential wetness classes are included on the ground of classification uncertainty, this portion is even higher to reach 88.4% of total samples.

wettability switch occurred only on few samples (22% of total in the class), this phenomenon requires attention.

For 'neutral' class (Figure 4.13), the samples' wettability behavior differs significantly from the tendencies shown by the wettability groups on the two sides of the spectrum. This case is characterized by the retaining of wettability by the bulk of the samples (65% of total), and if samples of the two preferential wetness are included– on the ground of uncertainty in boundaries between classe– the portion is even higher (88.4%). This fact, combined with wettability degradation in strength after core cleansing, has led into a thought that rock wettability tends to move towards neutrality if the causes of the original wettability have removed from the rock's surfaces.

From individual analysis based on individual wettability class (Figures 4.8 through 4.13), overall figures have shown that out of 299 water-oil relative permeability samples, only 67 (29.9%) retain their original wettability. If this group is expanded to include samples that remain in their wettability group (e.g. a water-wet sample that was originally strong water-wet), the overall number becomes 80 (35.7%) only. These figures correspond to the total figure of samples that remain or become 'neutral'–after core cleansing– of 110 or 49.1% of total samples. This further underlines the fact that cleansed core samples tend to move towards neutrality in wetness tendency, along with all validity consequences on the data measured afterward.

F. Wettability of Limestones

In carrying out the study, Widarsono (2011a, b) compiled data from 362 core samples comprising 350 from Baturaja Formation in South Sumatra, Sunda-Asri, and Northwest Java Basins, and 12 from Banggai (Minahaki Formation) and Salawati (Kais Formation) Basins (Table 4.5). Widarsono (2011a, b) presented results of analysis made on Baturaja limestone samples. In the time of the analysis, it was also proved that inclusion of the 12 non-Baturaja samples did not make any difference in the general wetness characteristics. The results presented in Widarsono (2011a, b) are therefore fully adopted for this chapter.

1. Original Wettability

The data provided by the three wettability tests have shown that the limestone samples do not preferentially inclined onto a specific wettability type. Results from the three wettability tests have revealed a composition of 41.8% water-wet, 40.3% oil-wet, and 17.9% neutral/mix wettability. These percentages represent 56 water-wet, 54 oil-

wet, and 24 neutral neutral/mix wettability samples of the total 134 samples. Figure 1 presents the wettability composition in general.

Figure 4.15 depicts a more detailed wettability grouping in accordance with the categorization criteria presented in Table 4.2. The histogram in Figure 4.15 promptly shows that the even wettability tendency as exhibited on Figure 4.14 is not exactly the case. Although it appears that 'weak water-wet' group comes out as the group with the largest number (42 samples), the oil-wet group is more evenly distributed with 'medium oil-wet' and 'strong oil-wet' groups having more significant weight than their counterparts in the water-wet group. This creates 'weak oil-wet' group that sizes only about a half of its water-wet counterpart. This skewed composition towards oil wettability can be interpreted as a proof that the limestone samples are evenly distributed quantitatively, but more oil-wet qualitatively.

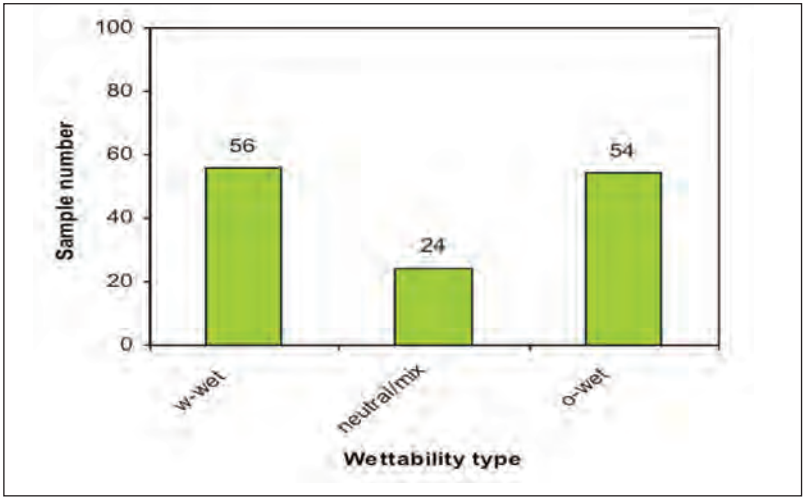

Source: Widarsono et al. (2010)

Figure 4.14 Wettability composition of limestone samples, in which wettability test results are used in this study. Water-, neutral-, and oil-wettability make 41.8%, 17.9%, and 40.3% of the total core samples, respectively.

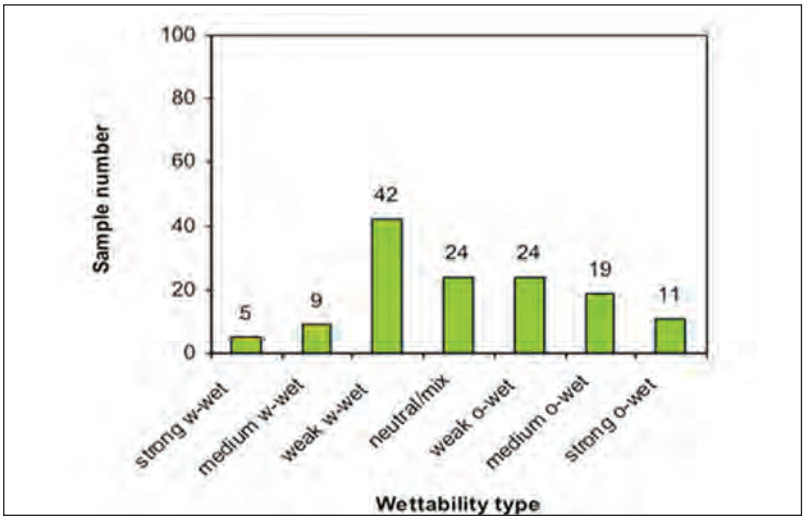

Source: Widarsono et al. (2010)

Figure 4.15 A More detailed wettability composition of the limestone samples. Although weak water-wettability is the largest single group, the composition exhibits stronger oil wettability tendency shown by the significant presence of 'medium oil-wet' and 'strong oil-wet' samples.

As described in Chapter 1, the Baturaja Formation is an extensive rock Formation existing in an area that spans from eastern part of West Java to the southern part of Central Sumatra, although the rocks of concern are mostly reef limestone in nature, differences may exist. Figures 4.16 to 4.18 show the wettability distribution for the limestone from the three sedimentary basins. Histogram on Figure 3 shows that the limestones from the Northwest Java Basin (92 samples) have 44.5% water-wet, 37% oil-wet, and 18.5% neutral/mix wettability. The corresponding respective figures are 35.7%, 46.4%, 17.9% for limestones in South Sumatra Basin (28 samples) and 35.7%, 50%, 14.3% for the Sunda-Asri Basin's limestones (14 samples).

From the wettability compositions shown on Figures 4.16 to 4.18, one may promptly concludes that limestones from the North-

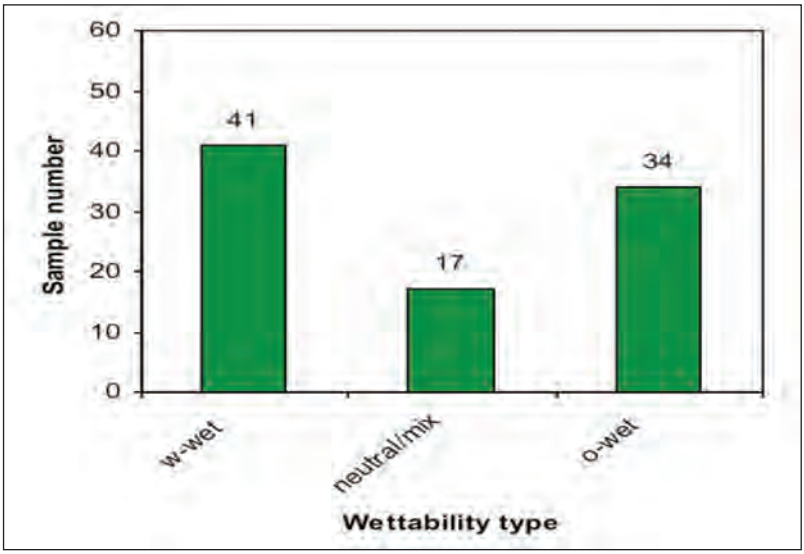

Source: Widarsono et al. (2010)

Figure 4.16 Wettability composition of limestones taken from Northwest Java Basin (92 samples). Water-wet samples appear to be of majority (44.5%), but the oil-wet group trails closely behind (37%). Like the picture in general, the neutral/mix wettability samples are the smallest in proportion (18.5%).

west Java Basin tends to be more water-wet, while the reverse is true for limestone from the two other sedimentary basins. This may be true quantitatively, but considering the stark similarity shown by the three sample populations—large but more or less even for water-wet and oil-wet and small for neutral/mix wettability—a more general conclusion should prevail. This consideration may channel the analysis into a more general conclusion that, despite differences that may exist due to local factors, the limestone from the three sedimentary basins show similar wettability compositions. Detailed compositions for the three sets of samples are also similar to the general composition shown on Figure 4.15.

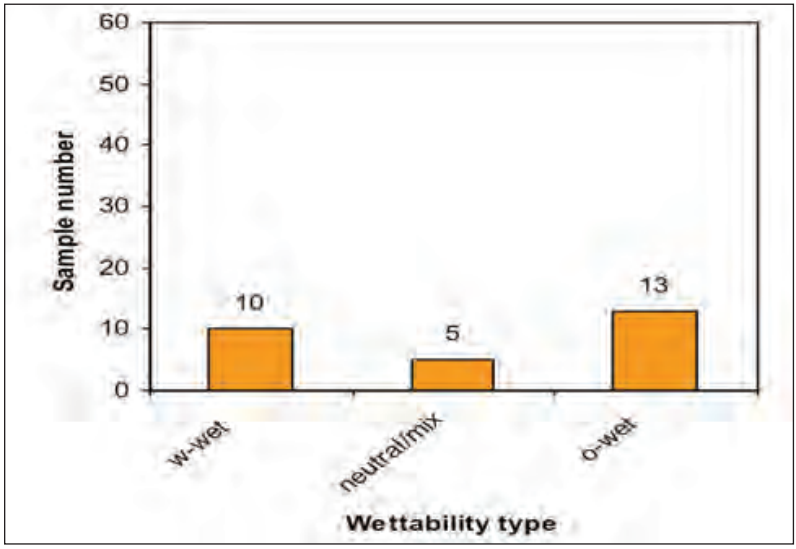

Source: Widarsono et al. (2010)

Figure 4.17 Wettability composition of limestones taken from South Sumatra Basin (28 samples). Water-wet samples are apparently not as numerous as the oil-wet samples (35.75% and 46.5%, respectively), and the neutral/mix wettability samples are typically the smallest in proportion with 17.9%.

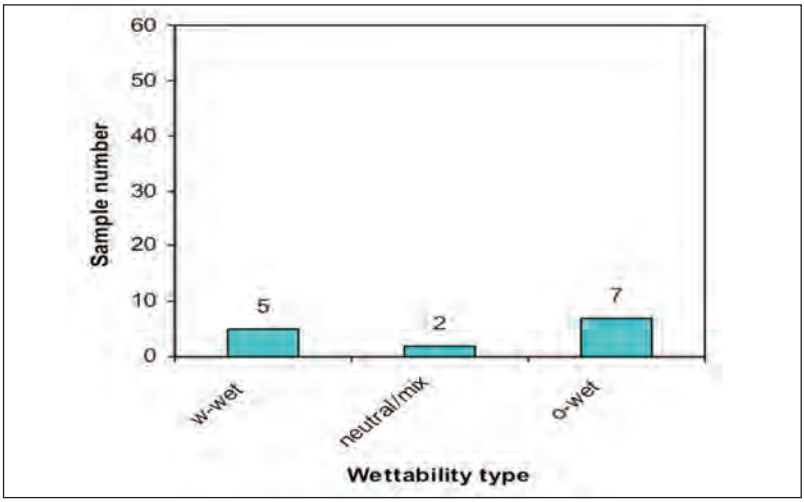

Source: Widarsono et al. (2010)

Figure 4.18 Wettability composition of limestones taken from Sunda Basin (14 samples). Similar to the case of South Sumatra samples, the limestones from the Sunda Basin—despite small in number—tend to have more oil-wet samples (50%) than water-wet (35.7%) and neutral/mix wettability (14.3%) samples.

2. Wettability Alteration

The influence of hot cleaning of core samples prior to water-oil relative permeability tests are obviously shown by the relative permeability-derived wettability (Figure 4.19). Out of the total samples of 216, 54.6% (118 samples) are of neutral/mix wettability group. Although the samples used in relative permeability tests are not the same as the ones for wettability tests, samples assigned for wettability tests are usually taken at points a few centimeters away from the samples assigned for relative permeability tests, and the data can still speak of wettability alteration. A more detailed view is provided on Figure 4.20 in which all seven wettability classes are exhibited. Out of the neutral/mix wettability group, the rest of the data appears to belong to 'weak' wettability groups both oil (46 samples) and water (33 samples). The two, combined with the neutral/mix wettability group

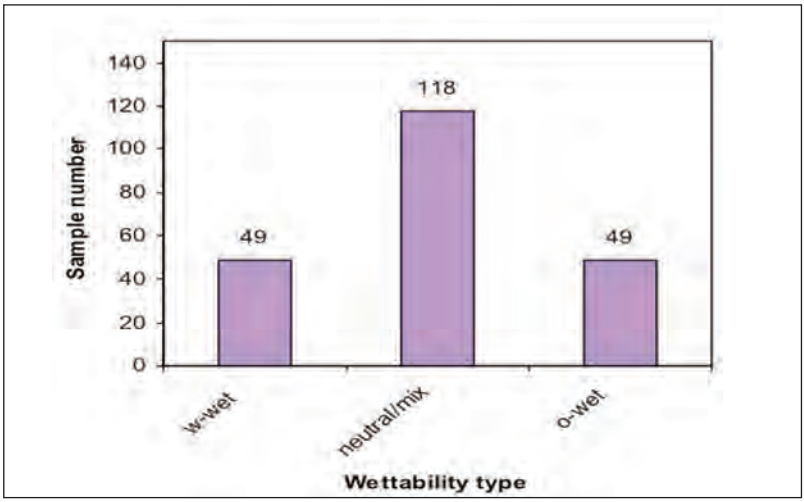

Source: Widarsono et al. (2010)

Figure 4.19 Composition of relative permeability-derived wettability for all limestones used in the study (216 samples). The data shows clear majority for neutral/mix wettability group (54.6%) compared to 22.7% each for the water-wet and oil-wet groups.

make up 91.2% of total samples. When compared to the original wettability depicted on Figure 4.15, a weakening in wettability strength is apparent.

A further analysis made to observe this wettability alteration effect on the samples from the three sedimentary basins tends to show shifts toward neutral/mix wetness. Figure 4.21 to 4.23 present the information. There are differences in wettability compositions for the three data sets, but similar trends are existent, all of which show that neutral/mix wettability group makes up the bulk of the data. A more detailed analysis involving all wettability classes also exhibit similar compositions to the one shown on Figure 4.20.

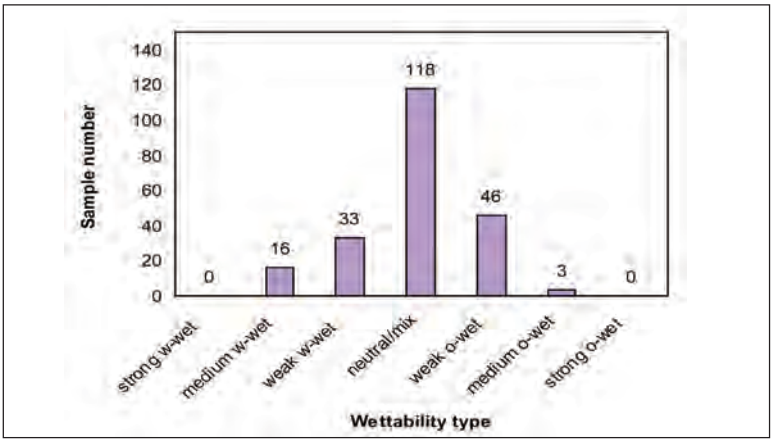

Source: Widarsono et al. (2010)

Figure 4.20 The fully detailed composition of the relative permeability-derived wettability of limestone samples (216 samples). When the two groups of weak water-wet and weak oil-wet are combined with the neutral/mix wettability group, they make up 91.2% of total. Notice the absence of strong wettability samples.

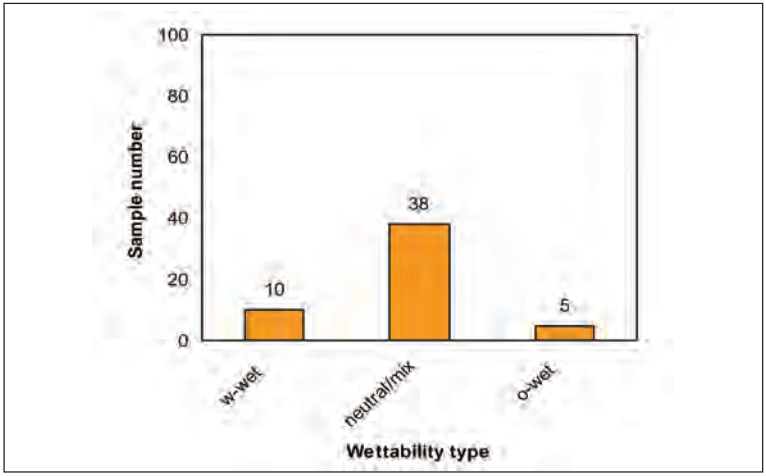

Source: Widarsono et al. (2010)

Figure 4.21 Relative permeability-derived wettability for limestone samples taken from South Sumatra Basin (53 samples). The neutral/mix wettability group makes 71.7% of total, leaving the water-wet and oil-wet groups with 18.9% and 9.4%, respectively.

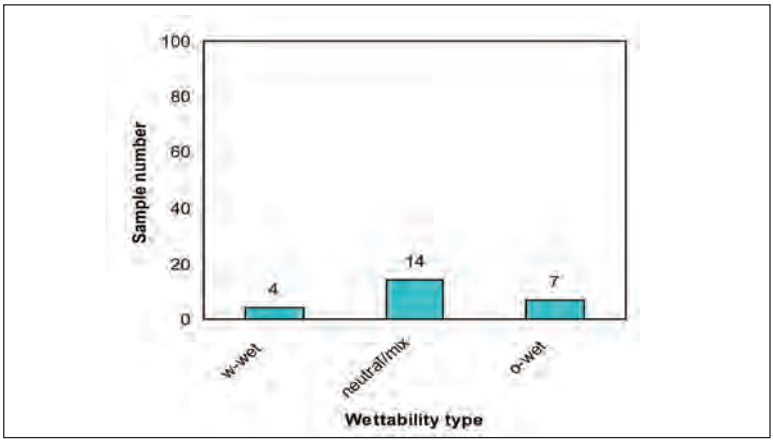

Source: Widarsono et al. (2010)

Figure 4.22 Relative permeability-derived wettability for limestone samples taken from Sunda Basin (25 samples). Despite the limited quantity, a similar composition to the general composition prevails in which 56% belongs to neutral/mix wettability group, 16% to water-wet group, and 28% to oil-wet group.

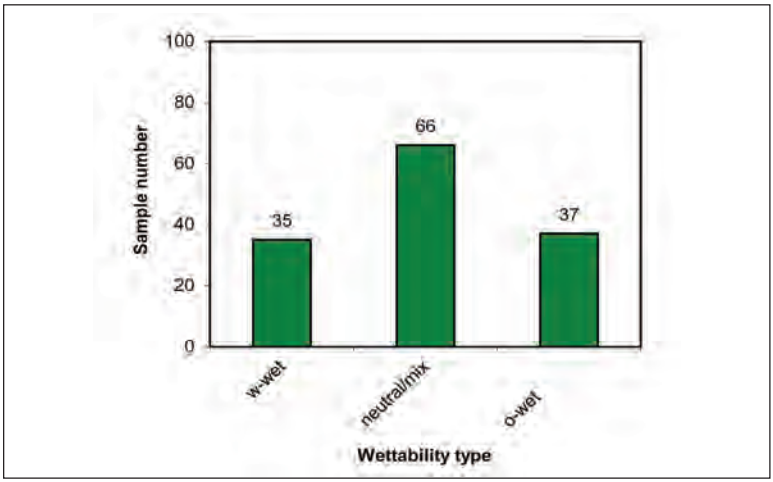

Source: Widarsono et al. (2010)

Figure 4.23 Relative permeability-derived wettability for limestone samples taken from Northwest Java Basin (138 samples). The large number of samples underlines further the tendency toward neutral/mix wetness (48%) after core cleaning. The remaining samples retain their relative oil wetness (27%) and water wetness (25%).

G. Change in Wettability and its Strength

Rock's surface mineral composition and polar organic components in crude oil, acting as either weak basic or weak acidic compound depending on the amount of resin and aspalthene contents, can react to each other to form a very thin layer of active compounds on the rock's solid surface. This thin layer of active compound affects wetting characteristics of the rock-fluid system. During core cleansing prior to many laboratory applications and tests, this thin layer is to be either completely or partially removed. The result is degradation in wettability strength, or a full shift to 'neutral' wettability if the thin layer is completely wiped out. This mechanism is likely to serve as an explanation over the wettability change commonly observed during the study.

One question related to wettability change remains. What actually causes the switch in wettability, from water-wetness to oil-wetness and vice versa? The only possible explanation at this stage is that hot solvent (usually toluent and methanol) used in the core sample cleansing has somehow chemically reformed the thin layer of wettability-affecting compound on the rock sample's surface to form an opposite wetting tendency. However, since this occurred on 50 samples only (22.3% of the total 224 samples), and is further reduced to 10 samples (4.5%) if 'preferentially oil-/water-wet' samples are excluded on classification uncertainty ground, this 'switch' is likely to be caused by other factor than reform of the 'thin layer compound' by hot solvent. Generalization of original wettability on heterogeneous rocks and the fact that samples used in wettability tests are usually different from the ones used in water-oil relative permeability test, even though belonging to the same rock formation, are probably the factors causing this apparent wettability switch. Speculatively, therefore, the

process of core cleansing using hot solvent causes degradation in wettability down to the point of neutral wetness tendency at most.

Regardless the real cause of change and switch in rock wettability, this occurrence may affect validity of the ensuing tests performed after the core cleansing. As previously discussed, changes in wettability affect relative permeability curves with all of its consequences. Furthermore, Widarsono (2008a, b) pointed out in length the effect of wettability alteration on rock electrical properties, which in turn through well log analysis may affect severely any estimation of water saturation. In the article, he also underlined the need to either restore rock's wettability through core-ageing or use cold core cleansing technique that utilizes cold solvent flow in order to dissolve oil and salts within samples. Through these methods, invalidity of laboratory test results caused by wettability alteration can hopefully be minimized.

H. Wetness Characteristics of Baturaja Limestones

From the results of wettability tests, study results presented in Widarsono (2011) had shown that the Baturaja limestones are characterized with equally strong wetting tendencies between water wettability and oil wettability with each having around forty percent in proportion. This fact is certainly different from what is commonly believed that carbonate rocks tend to be strongly inclined to oil wettability. As put previously, Treiber et al. (1972) and Chillingarian & Yen (1986) found 80% or higher of carbonate samples they studied as being oil-wet. The Baturaja limestones certainly behave differently in a sense that a significant portion of them tend to be water-wet, and when combined with some of the neutral or mixed in wettability, the oil-wet limestone in the formation are obviously not the majority (40.3%, Figure 4.4). However, when the water-wet and oil-wet tendencies are of concern,

detailed classification presented on Figure 4.15 obviously shows that, qualitatively, the Baturaja limestone is still inclined towards oil wettability rather than water wettability. For the oil-wet group, 55.6% belongs to medium oil-wet and strong oil-wet groups, whereas only 25% belonging to the corresponding groups in the water-wet group. This cannot, nevertheless, be taken as a strong preference towards oil wettability.

Widarsono (2010) reported that from the 139 sandstone samples obtained from various fields in western Indonesia indicated that 48.2% are water-wet, 30.2% oil-wet, and 21.6% neutral. This was also reported as in common with results from past reported studies on sandstones from other parts of the world. Nonetheless, when this finding is compared to the results for Baturaja limestone, a semblance of similarity in composition is observed. It is not yet obvious that other limestones from other rock formations (e.g. the Minahaki and Kais formations from the Banggai and Salawati Basins, respectively) will behave likewise, but this evidence has shown that wetting tendencies of both limestone and sandstone may behave similarly. As put by Tiab & Donaldson (2004), all petroleum reservoirs are thought of having water-wet tendency originally, but different processes and interactions along their existence had resulted in the present-day rock wettability.

CHAPTER V
IRREDUCIBLE WATER SATURATION – CHARACTERISTICS OF WESTERN INDONESIA'S RESERVOIR SANDSTONES

A. General

Irreducible water saturation is loosely defined as the minimum level of water saturation, for a certain type of reservoir rock with its intrinsic properties, that can be established using mechanically forced fluid displacement. Irreducible water saturation, often interchanged with connate water saturation or interstitial water saturation, plays a significant role in the determination of hydrocarbon in place and reserves. No known hydrocarbon-bearing reservoir rocks are in existence without presence of water, be it deposited either during diagenesis process or later. This is also the case even for very high permeability reservoirs such as reservoirs with natural fractures.

In the estimation of underground hydrocarbon volume, accurate and reliable unrepresentative S_{wirr} values certainly result in misleading oil or gas original in place (OOIP/OGIP) with all of its consequences. Widarsono (2008) in his studied over the error of connate water saturation estimation on OGIP put that an error by merely ten water saturation unit (i.e. percent of pore space) may result in approximately 20% error in OGIP estimation—for relatively small

reservoir bulk volumes (< 5 million reservoir barrel)—and gets even more pronounced for larger reservoirs.

Irreducible water saturation is also proved to have effects on reservoir production performance. For instance, connate water saturation tends to reduce effective gas permeability in gas condensate reservoirs. As early as Calhoun (1953) in a series of laboratory investigations—as quoted in Amyx (1960)—showed that higher S_{wirr} values reduce ratio of gas-to-oil permeability (K_g/K_o) significantly, from a maximum value of 60 at S_{wirr} = 20% to 1.5 at S_{wirr} = 40%. This reduction in gas effective permeability has the potential to provide a set back for any recovery scenarios from a gas field. Information regarding irreducible water saturation is therefore crucial.

At lower scale, knowledge over irreducible water saturation is also important for standard log interpretation for petrophysical properties, reservoir contents, and reservoir productivity (e.g. Crowell et al., 1995; Heidari et al., 2011; Ogbe et al., 2013). Validity over water saturation estimates are often judged from consistency between permeability, porosity, water cut from well-fluid sampling, and known representative S_{wirr} values usually obtained from core analysis. Needs for reservoir rocks' permeability led to development of empirical equations relating permeability with irreducible water saturation (e.g. Tixier, 1949; Wyllie & Rose, 1950; Timur, 1968; Coates & Dumanoir, 1974, and were later improved further or applied for specific cases by workers such as Torskaya et al., 2007; Permadi et al., 2011; and Alavi et al., 2014). Other examples of applications that require irreducible water saturation data are rock typing, estimation of movable water, and reservoir simulation modeling. Recent research results presented by, for example, Al-Omair & Garrouch (2010), Taktak et al. (2011), Xu and Torres-Verdin (2012), and Xu et al. (2013) showed the use of irreducible water saturation profiles in reservoir rock typing. For water saturation, Harris (1992) showed a relationship to estimate water

saturation from irreducible water saturation data, and vice versa, hence enabling the estimation of water cut. In reservoir modeling, Wang et al. (2006) and Masalmeh et al. (2007), for instance, have shown the importance of capillary pressure and irreducible data for model initialization and estimation of production performance. Nonetheless, the vital role of information regarding irreducible water saturation in the determination of water saturation will in turn influence the reliability of OOIP/OGIP and reserves estimates (also discussed in Harrison & Jing, 2001).

The most reliable and representative S_{wirr} for an oil or gas field is best established through direct sampling or measurements made in the field of concern. However, not all fields or reservoirs have such data, even in the mature western Indonesia's sedimentary basins. Moreover, understanding characteristics of S_{wirr} in the region's sandstone reservoirs is imperative and is certainly needed to be enhanced further through any existing data for better reservoir characterization and modeling in the future. The understanding over the region's S_{wirr} characteristics—the objective of the study—was made through investigating the S_{wirr} variation in relation to other rock properties such as permeability and wettability, as well as to geographical aspects such as different fields, rock formations, and sedimentary basins.

There are at least four methods known for obtaining irreducible water saturation: open-hole well log interpretation (e.g. Uguru et al., 2010), advanced log measurements (e.g. Straley et al., 1994; Xiao et al., 2012), fluid saturation measurement on core samples drilled using oil-base mud (e.g. Ringen et al., 2001 for dean stark application), and capillary pressure data (SCAL-based method, e.g. Harrison and Jing, 2001 for utilization). Well log interpretation has limitation in that the estimated water saturation may not necessarily $S_{wirr,}$ while the use of oil-base mud is not much and is increasingly limited. On the contrary, due to its nature as part of special core analysis laboratory

(SCAL) tests, capillary pressure data is usually readily available in sufficient quantity.

Taking advantage of the irreducible water saturation data availability, a study over its trends and characteristics for Indonesian reservoir sandstones had been performed and the results were presented in Widarsono (2011a). The article that makes the bulk of this chapter presented characteristics of irreducible water saturation for different aspects; i.e. individual sedimentary basin, field and formation, as well as its variation in regard to other petrophysical properties. It is hoped that the understanding over the characteristics will enrich further our understanding upon the implication of its influence towards reserves and production in the regions.

B. Irreducible Water Saturation: A Brief Review

After formation, hydrocarbons were compacted, concentrated, and squeezed out of its source rocks, from which it then migrated upward following buoyancy and hydrodynamic flow mechanisms (Tissot and Welte, 1978; Chapman, 1986). In their path, following continuous phase in long filaments, the hydrocarbons encountered various pore and pore-throat sizes, permeability, rock-forming minerals, and formation water with their different affinity tendencies toward the migrating fluids. As the hydrocarbon reached suitable rock structural and/or stratigraphic traps, they finally rested after displacing as much as possible the pre-existing formation water—depending on capillary forces and pressure gradient—with leaving specific levels of irreducible water saturation (S_{wirr}) within the traps. Provided that later geological events permitted these hydrocarbons to migrate further to find more suitable traps, which we find today.

Irreducible water saturation is normally defined as water saturation representing a remaining volume of water within reservoir rock's pore space that cannot be displaced by any further mechanical means at work within the pore system. This water saturation is usually regarded as the remaining interstitial water that is trapped within the pore structures in a drainage process taking place during hydrocarbon inward migration into the trap. Calculations of initial oil/gas in place use this water saturation. However, this is not to be misunderstood as trapped water saturation, or even connate water saturation, in general sense. Irreducible water saturation is much influenced by permeability and capillary pressure, while trapped water saturation could be formed by various other means. Zhou et al. (2000) put that there are four different forms of trapped water: 1) hydration water attached to clay surface area, 2) 'pendular rings' due to irregular pore geometry, 3) water trapped in dead ends of pore network, and 4) water by-passed in pores due to two-phase flow processes in reservoir. This can easily be comprehended that trapped water saturation could either of the same value or greater than the irreducible water saturation.

Irreducible water saturation has causative inter-relations with at least two other very well-acknowledged petrophysical properties; permeability and capillary pressure. Intrinsic rock permeability (K) is very dependent on the complexity of the rock's pore structure and pore-throat size distributions. Higher complexity usually means lower rock permeability. This higher complexity also means higher capillary force. Capillary force (P_c) is easilly represented with the basic equation of

$$P_c = \frac{\sigma \cos\theta}{r} \tag{5-1}$$

with *s, q,* and *r* are interfacial tension between wetting and non-wetting phases, contact angle between wetting phase and rock surface, and rock average pore radius, respectively. Higher rock pore complex-

ity effectively reduces *r* resulting in higher P_c. This P_c is heightened further when interfacial tension (*s*) between the pre-existing formation water and the migrating hydrocarbons is high and the rock tends to be water-wet (i.e. low *q* values).

The migration of hydrocarbons as droplets in water-saturated rocks, during migration or within final traps, was opposed by the capillary forces. This implies that rocks, under the same wettability tendency, tend to increase in S_{wirr} with decrease in permeability, and vice versa. On the other hand, rocks with similar permeability tend to have higher S_{wirr} for those with water-wettability than ones with more oil-wetness tendencies. In the both cases mentioned above, higher P_c values conceptually have led to higher capillary-bound water hence higher S_{wirr}.

Experimentally, the K – S_{wirr} relationship had been reported as early as in 1947 by Welge and Bruce (as quoted in Amyx et al., 1960). They showed that all of the tested 13 sandstone types tended to have their connate water saturation increases with decrease in permeability. They also showed that there is not a single general trend exhibited by the tested samples. Instead, individual sandstone type shows distinctive K – S_{wirr} trend even though some of them show similarities. No mentions, however, had been presented with regard to any possible relation between the trends and the samples' wettability.

The causative or mutual interaction between S_{wirr}, K, and P_c are further exhibited by the reverse relationship, in which levels of S_{wirr} influence effective permeability of hydrocarbons moves through them. Upon realizing this relationship, several investigators had studied the phenomenon and produced some empirical models. For instance, Wyllie and Rose (1950) proposed

$$K = \left(\frac{C\phi^3}{S_{wirr}} \right)^2 , \text{mD} \qquad (5\text{-}2)$$

with C is a constant that depends on hydrocarbon density (e.g. C = 250 for medium gravity oil and C = 79 for dry gas) and f is porosity (in fraction). Note that S_{wirr} is also in fraction. Later, Timur (1968) proposed a more general—i.e. independent of hydrocarbon types—form of

$$K = 0.136 \frac{\phi^{4.4}}{S_{wirr}^{\ 2}}, \text{ mD} \qquad (5\text{-}3)$$

with f and S_{wirr} are both in percentages. Later investigators, such as Torskaya et al. (2007), took the advantage of computer-generated synthetic rocks, taking into account pore-scale aspects like structure and wettability, to develop further the permeability–porosity–S_{wirr} correlation. Efforts have also been dedicated to develop similar correlations for local reservoir rocks (e.g. Alavi et al., 2014; on carbonate rocks). Similarly, Buckley (1965) developed a correlation between porosity and S_{wirr}, and later researchers like Holmes et al. (2009) improved further through linearization of the correlation.

Equations 5-2 and 5-3 show that with increase in S_{wirr}, the permeability decreases. Physically, this is understood as reduction in flow path cross-sectional radius as S_{wirr} increases hence reducing effective permeability to hydrocarbon moving through it. Being empirical in nature, as well as directly related to porosity and irreducible water saturation, these two equations are often used for estimating absolute permeability from standard open-hole log analysis.

C. Data Inventory

For the study presented in Widarsono (2011a, b), data from 760 sandstone core samples taken from 78 oil and gas fields situated in 10 sedimentary basins in western Indonesia were used (Figure 5.1). In addition, water-oil relative permeability from 574 sandstone core

samples from the same fields was also used as auxiliary data (Tables 5.1 through 5.3). Capillary pressure data used in the study were derived following drainage process (i.e. non-wetting phase displacing wetting phase) of which about 81% (615 samples) was obtained using porous plate semi-permeable technique. The technique is primarily performed through placing brine-saturated samples on a porous disk itself which is also saturated with brine. The semi-permeable disk is much less permeable than the samples to prevent the displacing fluid to penetrate the disk before the water saturation in the samples has reached its irreducible level. Irreducible water saturation (S_{wirr}) data from core laboratory testing are usually regarded as representing reservoir condition since it is obtained from infinite capillary pressure ($P_c = \infty$) condition, and in such condition theoretically there are no changes in rock's interfacial tension (i.e. $\sigma \cos\theta$)—whether they are H–T related or not—that may affect the rock's intrinsic S_{wirr}.

The displacing fluid, could be either air or oil with special disk arrangement, is pressurized in a series of fine increments to allow very slow displacement process. In this near static displacement condition, the displaced brine is recorded upon reaching static equilibrium. The assigned capillary pressure levels are then plotted with the recorded water saturation values (initial pore volume minus the displaced brine recorded upon reaching equilibrium at each displacement pressure). Figure 5.2 illustrates a couple of capillary pressure curves obtained from two samples with different permeability values. The irreducible water saturation is represented by water saturation levels through which vertical lines (dotted lines) meet asymptotically with the capillary pressure curves.

The drainage approach, under very small pressure increments, is designed and recorded in order to simulate the process of hydrocarbon displacement as it enters its trap. The length of equilibrium time needed after each pressure increment is very much dependent on

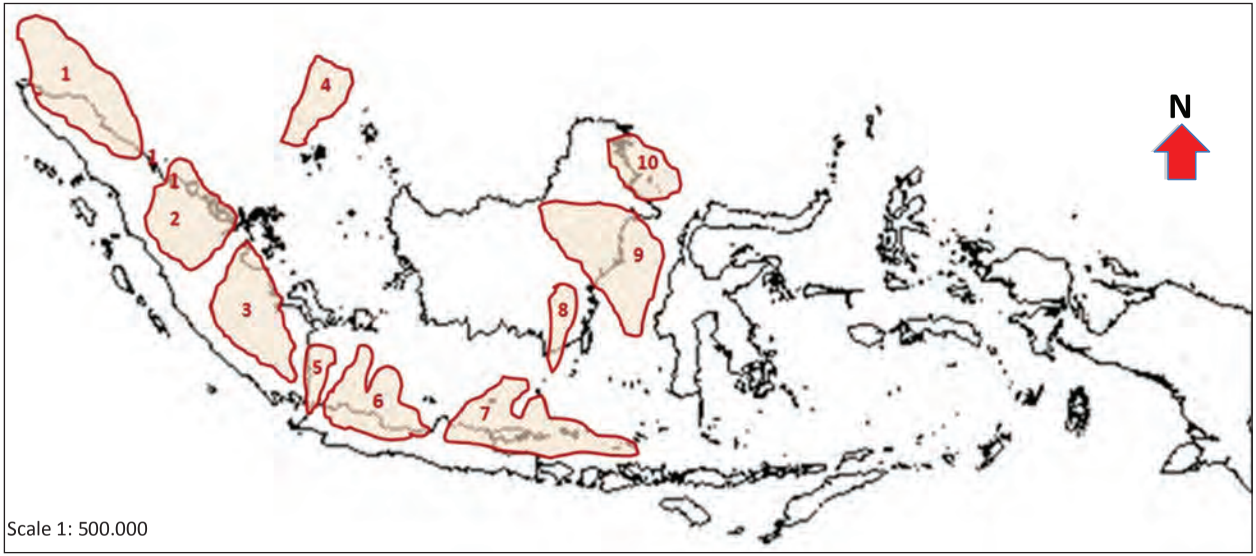

Figure 5.1 Sedimentary Basins, the Place of Origin of the Sandstone Core Samples Used in the Study on Irreducible Water Saturation: (1) North Sumatra Basin, (2) Central Sumatra Basin, (3) South Sumatra Basin, (4) West Natuna Basin, (5) West Sunda-Asri Basin, (6) Northwest Java Basin, (7) Northeast Java Basin, (8) Barito Basin, (9) Kutai Basin, and (10) Tarakan Basin

Table 5.1 Data Quantity from Core Plugs and Its Field of Origin, North Sumatra, Central Sumatra, and South Sumatra Basins

Basin	Field/structure (no. of wells)	Data		
		Capillary Press (*)	W-O relative permeability	Porosity - permeability
North Sumatra Main formation(s): Seurulla, Keutapang, Belumai	Gebang (1), Kualasimpang Barat (1),Paluh Tabuhan Timur (1), Rantau (3), Tabuhan Barat (1) Total wells = 7	48	31	79
Central Sumatra Main formation(s): Pertama, Kedua, Duri, Bekasap, Bangko, Telisa, Petani	Balam South (2), Bangko (4), Duri (1), Gemuruh (1), Jorang (3), Kopar (3), Kotabatak (2), Kulin (2), Libo (1), Merbau (2), Molek (1), Pager (1), Pinang (1), Pematang (1), Petani (4), Pudu (2), Rantau Bais (2), SE Libo (2), Tabuan (3), Telinga (1), Ubi (1) Total wells = 40	181	164	345
SouthSumatra Main formation(s): Gumai, Talang Akar, Air Benakat, Muara Enim,	Abab (1),Bajubang (2), Bentayan (2), BNG (1), BRC (1), E Benakat (1), E Kayuara (1), Jirak (3), Karang Agung (1), Kenali Asam (1), Ketaling Timur (1), Kerumutan (1), Lubuk (1), Lirik (1), N Merbau (1), Supat (1), Talang Jimar (1), Tanjung Laban (1), Tanjung Tiga (4), Tanjung Tiga timur (1), Tapus (3), Total wells = 30	161	160	321

(*) from porous plate (static) technique

Table 5.2 Data Quantity from Core Plugs and Its Field of Origin, Northwest Java, Kutai, Sunda-Asri (West Sunda), and West Natuna Basins

Basin	Field/structure (no. of wells)	Data		
		Capillary Press (*)	W-O relative permeability	Porosity - permeability
Northwest Java Main formation(s): Talang Akar	Bojongraong (1), Cemara Barat (2), Cemara Timur (5), Melandong (1), ONWJ (3) Total wells = 12	86	51	137
Kutai Main formation(s): Balikpapan, Kampung Baru	Attaka (1), Badak (6), Bekapai (1), Handil (4),Mutiara (1), Nilam (1), Semberah (1) Total wells = 15	130	70	200
Sunda-Asri (West Sunda) Main formation(s): Talang Akar	BTS (1), Cinta (2),Farida (1), Gita (1), Sundari (2), Titi (1), Yvonne (1), Zelda (2) Total wells = 11	63	46	109
West Natuna Main formation(s): Lower Gabus, Upper Gabus, Arang	Binturong (1), Kakap (1), Kuda Nil (1), Porel (1), Udang (1) Total wells = 5	68	29	97

(*) from porous plate (static) technique

Table 5.3 Data Quantity from Core Plugs and Its Field of Origin, Tarakan, Barito, and Northeast Java Basins

Basin	Field/structure (no. of wells)	Data		
		Capillary Press (*)	W-O relative permeability	Porosity - permeability
Tarakan Main formation(s): Bunyu, Tabul	Sembakung (1), UKM (1) Total wells = 2	10	10	20
Barito Main formation(s): Talang Akar	Tanjung (2) Total wells = 2	9	7	16
Northeast Java Main formation(s): Ngrayong, Ledok	Kawengan (1), Nglobo (1), Semangi (1) Total wells = 3	4	6	10

(*) from porous plate (static) technique

sample's permeability and may take very long for low permeability samples. For this reason, some of the samples—especially the low permeability samples—were tested using the dynamic centrifuge method. Through the exertion of centrifugal force, instead of relying on near pure capillary force, the drainage displacement process is forced and the desired equilibrium time is sped up. Around 19% of the data belongs to this technique. Readers can explore references such as Amyx et al. (1960) and Tiab and Donaldson (2004) for information regarding basic principle of centrifuge technique.

Apart from the 760 samples tested for their capillary pressure data, as many as 574 samples were also utilized for their water-oil relative permeability data. Both sample sets for water-oil relative permeability and capillary pressure tests were derived from the same depths in the same well. The primary purpose of this data is to provide indication over the wettability of the samples used in capillary pressure tests. As discussed in Widarsono (2010), interception between relative permeability to oil (Kro) and relative permeability to water (Krw) curves indicates the wettability of the tested sample. Figure 5.3 illustrates two conditions in which one of the Kro = Krw point (i.e. intercept) falls at a water saturation value of lower than 50% whereas the other falls at a value higher than 50%. The two examples indicate oil-wetting and water-wetting tendencies, respectively.

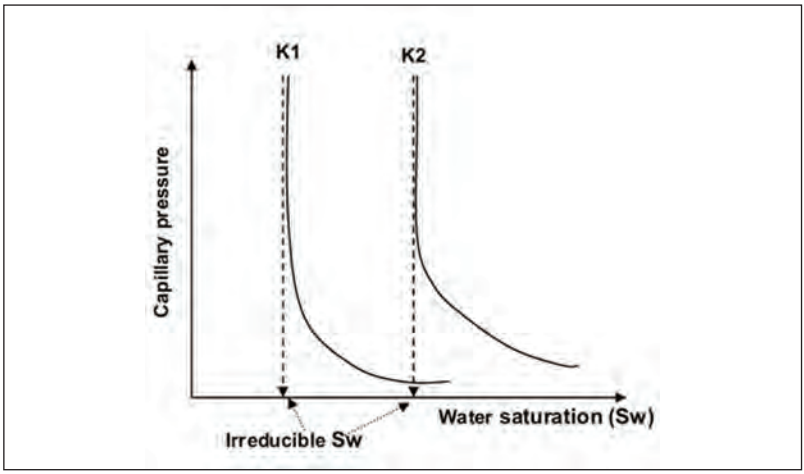

Figure 5.2 Irreducible water saturation (S_{wirr}) as indicated from capillary pressure curves. The two curves represent two rock samples with different permeability values (K1 > K2).

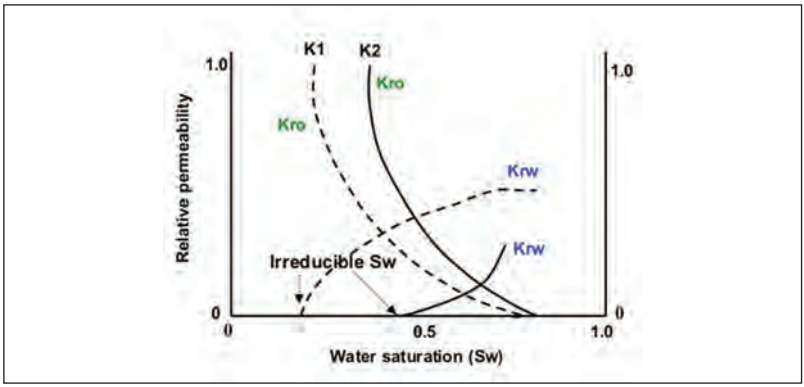

Figure 5.3 Wettability indication from water-oil relative permeability curves. When the Kro = Krw intersection falls at Sw < 0.5, the rock of concern tends to be oil-wet (dotted curves), while the reverse case indicates water-wettability (solid curves).

Another auxiliary data is porosity-permeability data from the combined capillary pressure and relative permeability of 1,334 samples. The use of the data is mainly to support in describing the nature of pore structure of the sample sets reflected in their porosity-permeability relationships.

D. Characteristics of Irreducible Water Saturation

In analyzing the data, Widarsono (2011a) established four groups. First group was designed to observe the influence of wettability, and permeability, on irreducible water saturation (S_{wirr}) characteristics. Second group was used to study what different sedimentary basins may tend to show their S_{wirr} characteristics. The consideration that underlines this group was that different sedimentary basins are likely to have differences in geological setting and other related aspects, hence influencing S_{wirr} characteristics. The remaining two groups analyzed on lower geological scales, individual field, and rock formations.

1. S_{wirr} variation with permeability and wettability

In this group, main indicator of wettability is the water-oil relative permeability data with wettability test data in auxiliary role only. The reason is that samples for both capillary pressure and water-oil relative permeability underwent core cleansing prior to test, in which alteration in wettability is most likely to occur, while wettability test always use native cores. However, as concluded in Widarsono (2010), hot core cleansing is not likely to change its wettability too considerably and is more likely to reduce the wetting tendency in strength. Therefore, any available wettability test data were used to support determination of general wettability of a core samples set whenever information from water-oil relative permeability tests is inconclusive.

In using the water-oil relative permeability data for wettability indicator, the criteria established for classification are: $S_w < 45\%$ for 'oil-wet', $45\% \leq S_w \leq 55\%$ for 'neutral', and $S_w > 55\%$ for 'water-wet' (Figure 5.3). These wettability criteria of the 760 core samples, from which the capillary pressure and S_{wirr} data were obtained, were determined. Out of the 760 samples, 298 are classified as water-wet, 291 as neutral, and 171 as oil-wet.

Figure 5.4 exhibits plot between permeability and S_{wirr} of all samples. In general, it is shown that S_{wirr} increases with decrease in permeability. This is in accordance with Equation 5-1 that implies lower permeability, i.e. smaller r , resulting in larger capillary pressure and therefore higher S_{wirr}. The large capillary force provides large opposition to the displacement of wetting phase (usually assumed as brine) by non-wetting phase (i.e. air or oil) in a drainage process resulting in high S_{wirr}. This explains that even though all three wetting tendencies exhibit similar $K - S_{wirr}$ characteristics samples with water-wettability tend to show stronger inclination towards higher S_{wirr}. The less definitive manner shown by neutral-wettability samples

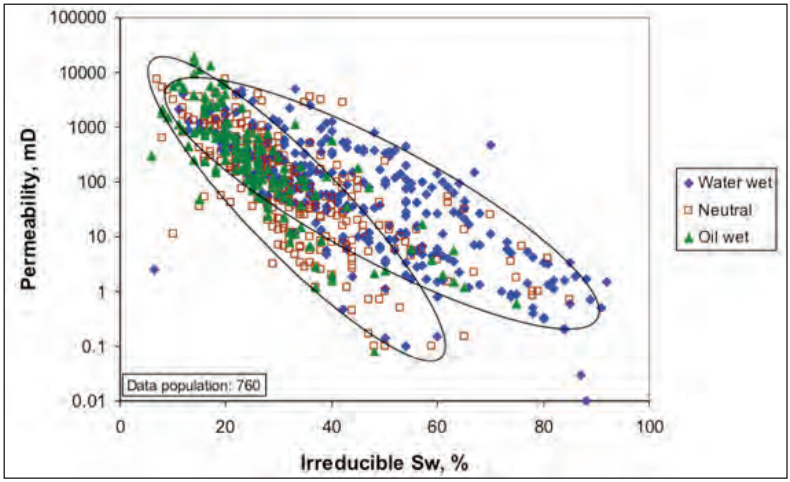

Source: Widarsono (2011a)

Figure 5.4 Plot showing increase in S_{wirr} with decrease in permeability. This trend is true for all sandstone samples with different wettability, but with water-wet samples exhibiting stronger tendency for higher S_{wirr}. Interestingly, samples with neutral wettability tend to be less definitive even though a larger portion of them is more aligned to oil-wettability.

is certainly caused by the very absence of the wetting tendency itself (i.e. neutral), leaving less direct and more complicated factors—e.g. pore size distribution and clay presence—to determine the S_{wirr} characteristics.

Deeper analysis on the effect of wettability on S_{wirr} was performed through observation on each wettabiliy group. Figure 5.5 shows the plot for water-wet group, cluster analysis on which indicates correlation of

$$\log K = 18683 e^{-0.125 * S_{wirr}} \tag{5-4}$$

with permeability (K) in mD and S_{wirr} in percent (%). Although the group appears to be represented by a single general correlation, the actual characteristics within the group are not necessarily uniform. As shown on Figure 5.5, significant difference is shown by strong

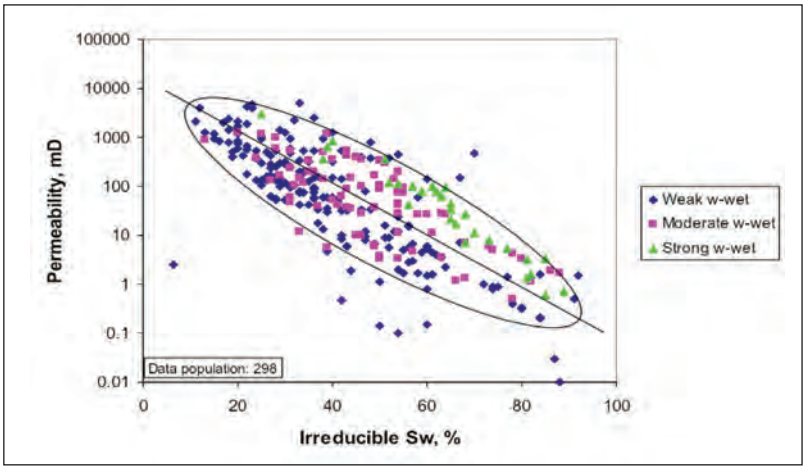

Source: Widarsono (2011a)

Figure 5.5 K - S_{wirr} plot for water-wet group samples. Despite overlapping separation between the three wettability sub-groups is obvious which indicates the strong influence of wettability strength on S_{wirr} characteristics.

water-wet and weak water-wet sub-groups, with the strong water-wet samples tend to have significantly higher S_{wirr} values. This can be logically explained using Equation 5-1, in which stronger water-wetness results in lower θ and higher P_c, hence higher S_{wirr}. It can therefore be conclusively observed that wetness strength plays a significant role in controlling S_{wirr} characteristics in water-wet sandstones.

Similarly, a more detailed observation was also made on the oil-wet group (Figure 5.6). The cluster enveloping of the data yields a general correlation of

$$\log K = 32952 e^{-0.196 * S_{wirr}} \tag{5-5}$$

In a manner different to the case of water-wet group, no significant division between different strength in oil-wetness is observed. Samples with weak, moderate, and strong oil-wetness behave inter-mingle and show similar K - S_{wirr} characteristics. Although data for the strong

oil-wet is very limited for a decisive conclusion, but a deviation from the weak and moderate oil-wettability is still noticeable. This can be taken as an indicator that the effect of oil-wettability on S_{wirr} is somewhat weaker than in the case of water-wettability.

More thorough examination on the wettability sub-groups within the water-wet and oil-wet groups result in a set of $K - S_{wirr}$ correlations. The correlations are

$$\log K = 15380 e^{-0.136 * S_{wirr}} \quad (5\text{-}6)$$

for weak water-wet sandstones,

$$\log K = 26250 e^{-0.134 * S_{wirr}} \quad (5\text{-}7)$$

for moderate water-wet sandstones,

$$\log K = 133795 e^{-0.137 * S_{wirr}} \quad (5\text{-}8)$$

for strong water-wet sandstones,

$$\log K = 33059 e^{-0.197 * S_{wirr}} \quad (5\text{-}9)$$

for weak oil-wet sandstones,

$$\log K = 32531 e^{-0.195 * S_{wirr}} \quad (5\text{-}10)$$

for moderate oil-wet sandstones, and

$$\log K = 11553 e^{-0.131 * S_{wirr}} \quad (5\text{-}11)$$

for strong oil-wet sandstones.

Validity of Equation 5-11 (strong oil-wet) is obviously questionable since the equation was derived using four data points only. The actual equation is likely to be not very different from Equations 5-2, 5-6, and 5-7, based on the presumption that oil-wetness strength influences S_{wir} characteristics in a manner weaker than water-wetness. This can also be considered as applicable to neutral wettability sandstones based on the observation that most of its data points fall in fine alignment with those belonging to oil-wet sandstones.

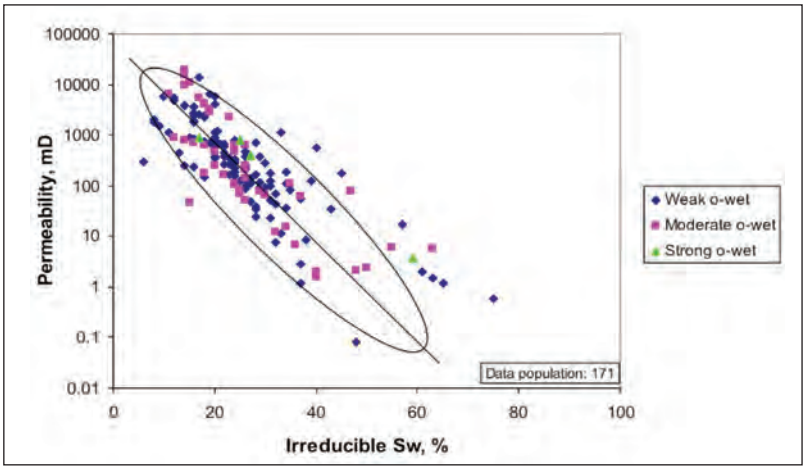

Source: Widarsono (2011a)

Figure 5.6 K - S_{wirr} plot for oil-wet group samples. No obvious separation is visible underlining the minimum influence of oil-wettability strength on S_{wirr} characteristics.

2. S_{wirr} characteristics for individual sedimentary basin

Sedimentary basins as the basic earth structure required for the formation of oil and gas reservoirs may be different in general characteristics depending on a long array of factors including mineral resources, physical and chemical interaction mechanisms, transportation and sedimentation system, depth and extent, and petroleum system. For instance, the Northwest Java Basin is described as having been filled with fluvial deposits along with shale and marl in its more restricted environments, such as Talang Akar Formation, from which most of the sandstone samples have been taken (Schlumberger, 1986). In comparison, the Tertiary sediments in the Kutai Basin are stratigraphically very complex with numerous facies changes and sedimentary strata that represent transgressive, regressive cycles in marine, deltaic environments. The transgressive sequence is mostly represented by coarse clastic and shales deposited in a paralic coastal plain to shallow

marine environments, while the regressive sequence mainly consists of thick deltaic to paralic clastics containing abundant coals and lignites (Schlumberger, 1986). These environmental differences in the sedimentary basin-related rock formations may have repercussion on the S_{wirr} characteristics.

In studying the effect of different sedimentary basins to S_{wirr} characteristics, data from seven main productive sedimentary basins are presented. Figure 5.7 presents the K - S_{wirr} plots for Central Sumatra, South Sumatra, and Northwest Java Basins, while Figure 5.8 depicts the corresponding data for North Sumatra, Kutai, Sunda-Asri, and West Natuna Basins. All seven sedimentary basins exhibit the same S_{wirr} behavior with regard to permeability, the lower the permeability the higher the S_{wirr} values. What differs one sedimentary basin to the others in this matter is the differences in the general K - S_{wirr} correlations even though some of them exhibit sufficient similarity.

Presented on Figure 5.7, samples from South Sumatra Basin exhibit higher S_{wirr} characteristics than ones from the other two basins for the same permeability levels. Similarly on Figure 5.8, deviation from the 'main stream' formed by samples from three sedimentary basins (Kutai, North Sumatra, and Sunda-Asri) is shown by samples from West Natuna Basin. Despite the differences in general, similarities are also visible in the S_{wirr} characteristics. The scatter shown by samples from North Sumatra leads to its inclusion in the cluster of data from the Sunda Basin (Figure 5.8). Similar S_{wirr} occurrence is also demonstrated by the Kutai data relative to the combined North Sumatra-Sunda Basins' data.

In general, K - S_{wirr} correlations for the seven main sedimentary basins are

$$\log K = 64606e^{-0.236*S_{wirr}} \qquad (5\text{-}12)$$

for Central Sumatra Basin (except for Pematang formation),

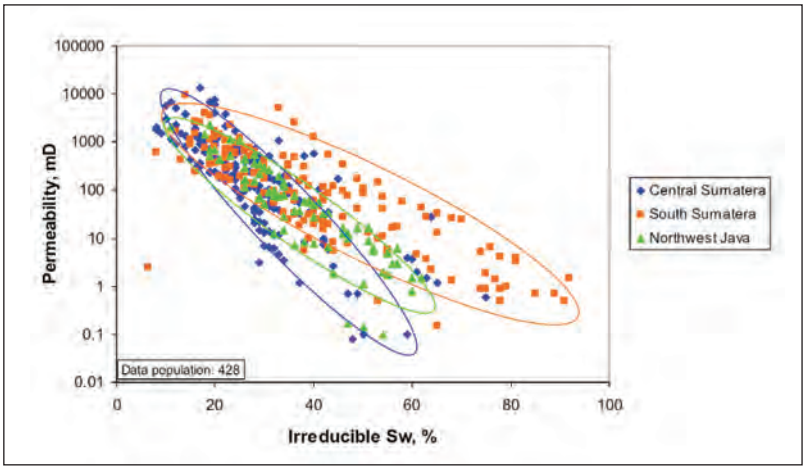

Source: Widarsono (2011a)

Figure 5.7 K - S_{wirr} plots for samples from Central Sumatra, South Sumatra, and Northwest Java Basins. The three show similar behavior, but in varried degrees towards variation in permeability.

$$\log K = 13429 e^{-0.124 * S_{wirr}} \quad (5\text{-}13)$$

for South Sumatra Basin,

$$\log K = 46913 e^{-0.191 * S_{wirr}} \quad (5\text{-}14)$$

for Northwest Java Basin,

$$\log K = 68500 e^{-0.245 * S_{wirr}} \quad (5\text{-}15)$$

for West Natuna Basin,

$$\log K = 19715 e^{-0.138 * S_{wirr}} \quad (5\text{-}16)$$

for Kutai Basin, and

$$\log K = 6815 e^{-0.104 * S_{wirr}} \quad (5\text{-}17)$$

for the combined North Sumatra-Sunda Basins.

Differences in S_{wirr} characteristics are undoubtedly caused by the specific characteristics of the rocks of concern. Although the empirical expressions of Equations 5.2 and 5.3 describe the correlation between permeability and irreducible water saturation, they do not accommodate its potential variations in the light of different rock characteristics. The expression can indeed be considered as inadequate since it has been previously discussed that S_{wirr} characteristics is not only influenced by rock's permeability (i.e. pore throat configuration) but also by wettability. This is best illustrated by the plots on Figures 5.4 to 5.8 showing that if the vertical variation in S_{wirr} is clearly caused by variation in permeability, then the horizontal S_{wirr} variation is therefore likely caused by the second factor – the rock wettability.

The effect of wettability is readily demonstrated when analysis is made on the wettability compositions of the samples plotted and presented on Figures 5.7 and 5.8. Histograms on Figures 5.9 and 5.10 depict wettability compositions of two clusters of samples with contrasting K - S_{wirr} trends as shown on Figures 5.7 and 5.8, respectively. Difference in K - S_{wirr} trends shown by Central Sumatra and South Sumatra samples (Figure 5.7) are accompanied by contrasting wettability compositions demonstrated by the two sets of samples (Figure 5.9). The lower S_{wirr} characteristics shown by the Central Sumatra samples are without a doubt connected to their predominantly oil-wet tendency, while the reverse is true for the South Sumatra samples' inclination towards more water-wettability.

Plots for the North Sumatra, Sunda-Asri, Kutai, and West Natuna Basins (Figure 5.8) provide another example, of which the West Natuna samples show low S_{wirr} characteristics while gentler K - S_{wirr} slope, i.e. higher S_{wirr} values, is exhibited by the combined North Sumatra/Sunda Basins' samples. Wettability composition presented on Figure 5.10 informs that both sets of samples have a leaning towards water-wetness indicated by the larger number of water-wet

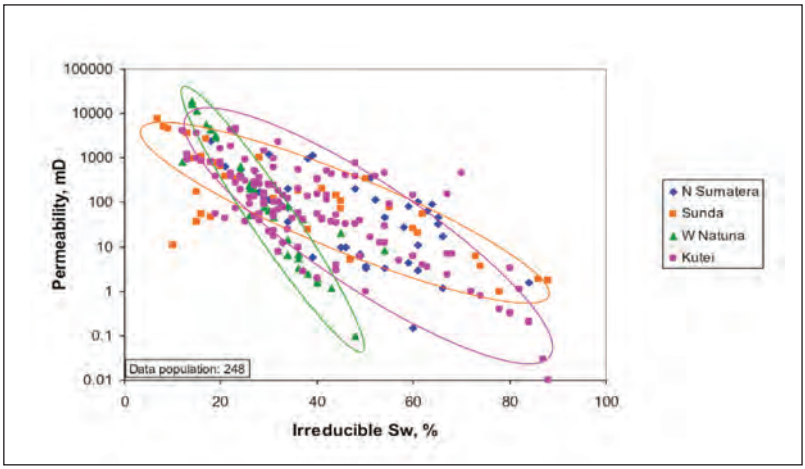

Source: Widarsono (2011a)

Figure 5.8 K - S_{wirr} plots for samples from North Sumatra, Sunda, West Natuna, and Kutai Basins. Different characteristics are visible except the scatter shown by North Sumatra data leaving it apparently included within the same cluster with data from Sunda Basin.

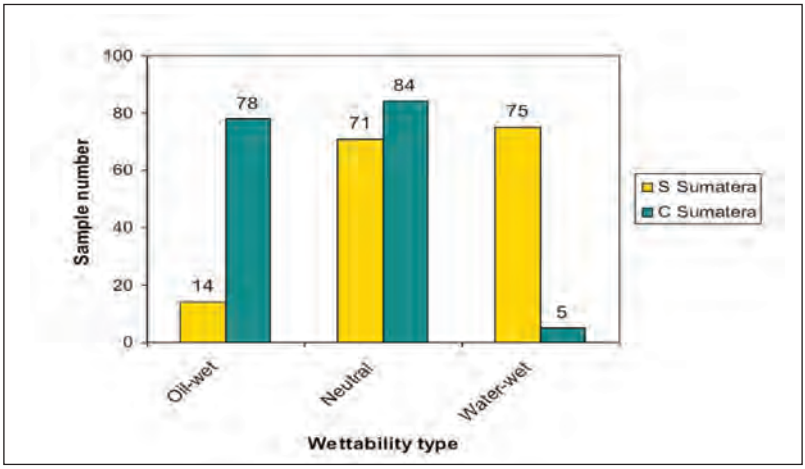

Source: Widarsono (2011a)

Figure 5.9 Wettabilitty composition of samples from South Sumatra and Central Sumatra Basins. The geographical proximity of the two sedimentary basins does not necessarily make them similar in wettability characteristics (note: numbers on top of histogram represent number of samples)

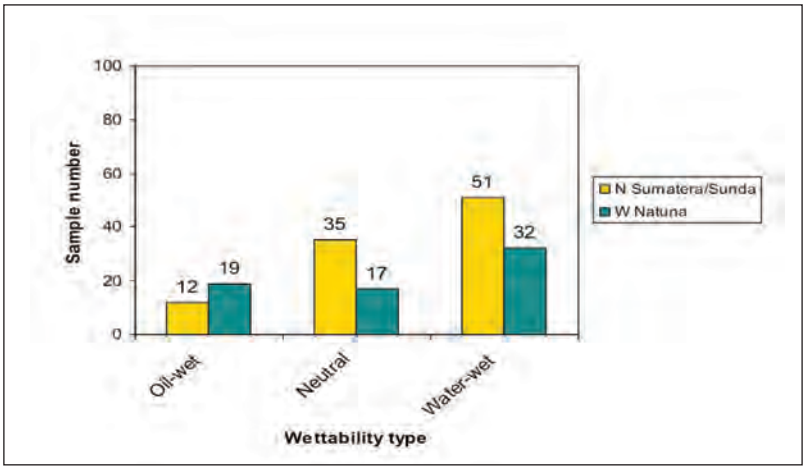

Source: Widarsono (2011a)

Figure 5.10 Wettabilitty composition of samples from West Natuna and combined North Sumatra-Sunda Basins. The three sedimentary basins tend to be predominantly water-wet but with different levels of strength and composition (note: numbers on top of histogram represent number of samples).

samples. The fact that the two sample sets are of preferentially water-wet suggests that the difference in the K - S_{wirr} slopes is most probably caused by different 'strength' in the water-wettability inclination. As clearly shown by the histogram on Figure 5.10, the North Sumatra/Sunda-Asri samples are 'stronger' in their water-wetness tendency when compared to the samples from the West Natuna Basin.

The conclusion drawn from Figures 5.7 to 5.10 is that S_{wirr} characteristics is much influenced by relative strength in water-wettability, while somewhat less effectively influenced by strength difference in oil-wettability. Evidence over the lower effectivity of oil-wettability, compared to water-wettability, to govern K - S_{wirr} characteristics is demonstrated by data plot on Figure 5.11, in which the largely oil-wet Central Sumatra samples fall amicably within the same cluster with the 'slightly' water-wet West Natuna samples. This reveals further that

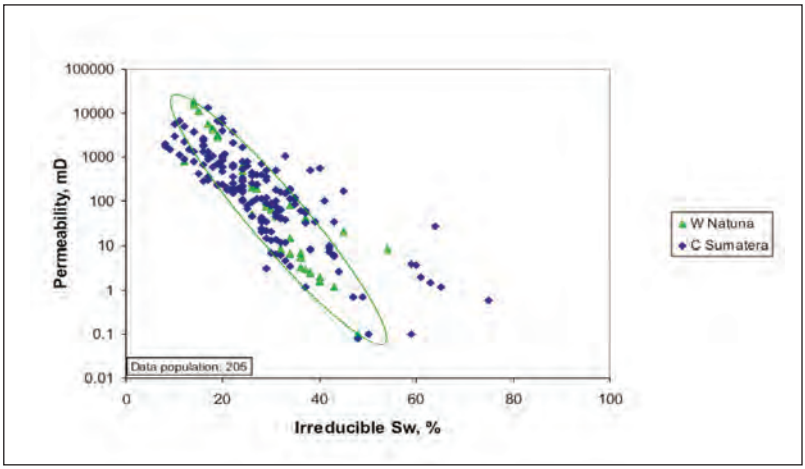

Source: Widarsono (2011a)

Figure 5.11 Comparison between the largely Oil-Wet Central Sumatra Samples and the 'Slightly' Water-Wet West Natuna samples. The similarity between the two sets may be taken as an evidence that oil-wettability hardly affect S_{wirr} characteristics

even though sedimentary basins are complex geologically and may differ from one to another, but wettability—as the manifestation of the complexity itself—plays an important factor in influencing S_{wirr} characteristics.

3. S_{wirr} in individual fields

It has been shown that specific complexity and characteristics of individual sedimentary basin may result in different S_{wirr} characteristics apparently due to, among others, differences in rock wettability. This tendency towards specific K - S_{wirr} characteristics for most of individual sedimentary basins, some show similarity however, do not actually mask the fact that the fields contained within the basins may also behave in a non-uniform manner. This is demonstrated by the following graphs.

Figures 5.12 to 5.14 present examples of K - S_{wirr} trends for some fields in Central Sumatra, South Sumatra, and Kutai Basins. The slopes were actually created without taking into consideration the possibility of multi-slope situation similar to the case of sedimentary basin at larger scale (mega scale). The single slope representation for individual field is aimed at investigating level of S_{wirr} heterogeneity within a single sedimentary basin.

In general, heterogeneity in K - S_{wirr} characteristics is clearly observed in any sedimentary basin among the three presented on Figures 5.12 to 5.14. For instance, although reservoir rocks in Central Sumatra fields are oil-wet in general, differences in the slopes are still palpably visible, with Bangko and Kulin samples apparently in the oddest deviation from the general trend (Figure 5.12). Despite the differences, similarity in slopes is also indicated by some fields with one representing Pematang, Ubi, and Pinang fields as an example. The variation in the K - S_{wirr} gradients for some fields and the uniform ones for other fields in spite of the fact that those fields are not necessarily located in geographical proximity shows that heterogeneity is certainly a norm in Central Sumatra Basin. Similar states of heterogeneity also occur in the other two cases (Figures 5.13 and 5.14).

Heterogeneity may affect any rock physical property, but in a way similar to what occurs at sedimentary basin scale, wettability can also play an important role in influencing the K - S_{wirr} characteristics at field scale within the basin. In order to observe the effect, comparisons in wettability composition have been made for each sedimentary basin between two of the most contrasting K - S_{wirr} gradients. For Central Sumatra samples, the SE Libo/Telinga and Jorang fields are taken while for South Sumatra and Kutai Basins, East Kayuara – Tapus and Attaka – Semberah comparisons were made, respectively. Figure 5.15 presents the wettability comparisons for the three cases.

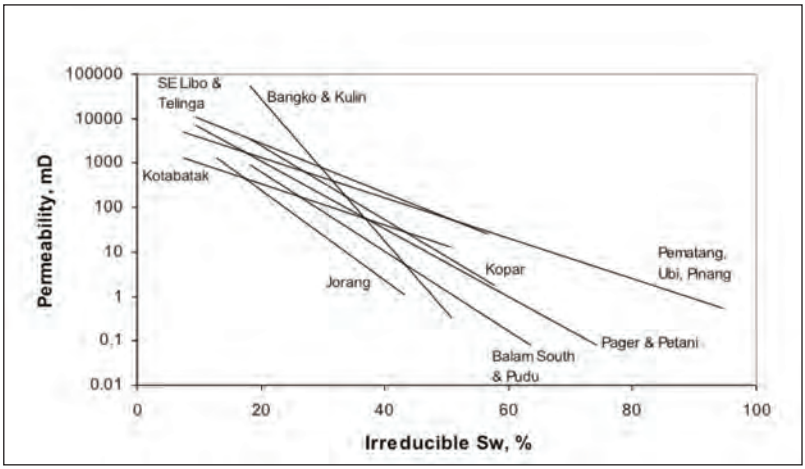

Source: Widarsono (2011a)

Figure 5.12 K - S_{wirr} Gradients for some fields in Central Sumatra Basin. Bangko and Kulin fields' samples appear to be more oil-wet than the others.

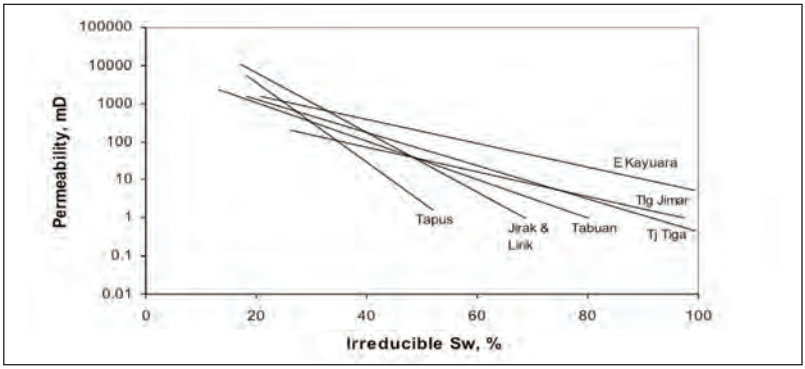

Source: Widarsono (2011a)

Figure 5.13 K - S_{wirr} Gradients for some fields in South Sumatra Basin. Samples from Tapus, Jirak, and Lirik fields appear to be weaker in water-wettability in a sedimentary basin that is largely water-wet in characteristics.

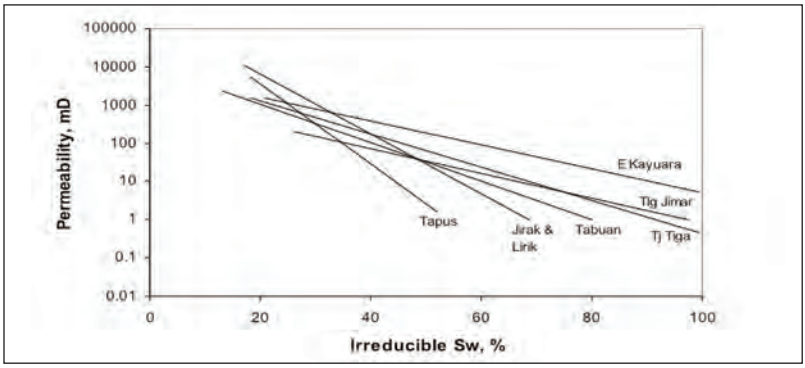

Source: Widarsono (2011a)

Figure 5.14 K - S_{wirr} Gradients for some fields in Kutai Basin. Note that the characteristics of Semberah field is markedly different from other fields that were also deposited under delta plain and delta front environments such as Handil, Badak, and Nilam fields, hence signifying complexities in sedimentary basin systems.

Wettability comparisons for the three cases demonstrate that wettability is indeed a significant factor in swaying K - S_{wirr} characteristics. For Central Sumatra's largely oil-wet samples, both sample sets that make SE Libo/Telinga and Jorang fields' K - S_{wirr} gradients are certainly oil-wet, yet different K - S_{wirr} characteristics between the two sets are obvious (Figure 5.12). Judging from the wettability comparison between the two sets (Figure 5.15a), different strength in wettability is likely to be the main cause, even though it is thought that different strength in oil-wettability is less effective—compared to water-wettability—in influencing the K - S_{wirr} trend.

Comparisons on wettability composition for the other two cases are slightly different. For the two cases (Figures 5.15b and 5.15c), the two sets of samples are of opposite wettability. Tapus and Semberah samples are preferentially oil-wet, whereas E Kayuara and Attaka samples are definitely water-wet. The three cases show that contrasting K - S_{wirr} trends is not only governed by opposing wetting tendencies but also, to somewhat lesser degrees, by different strength in oil-wettability.

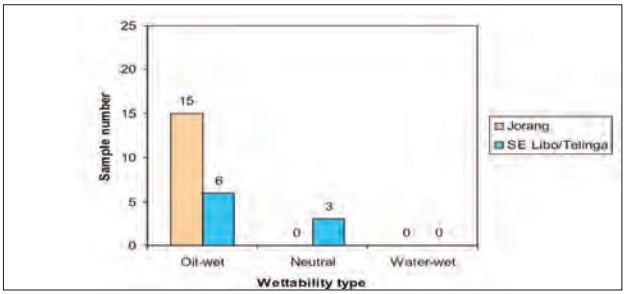

(a)

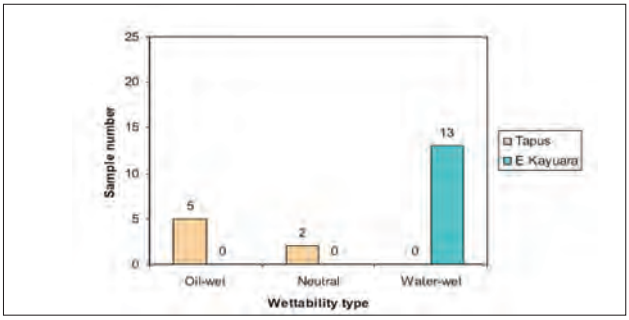

(b)

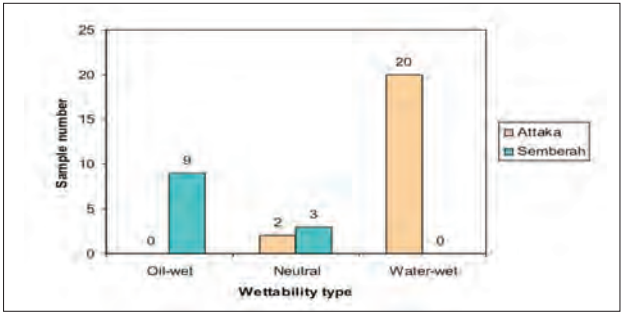

(c)

Source: Widarsono (2011a)

Figure 5.15 Wettability composition of the two most contrasting K - S_{wirr} gradients: (a) SE Libo/Telinga and Jorang for Central Sumatra Basin, (b) E Kayuara and Tapus for South Sumatra Basin, and (c) Attaka and Semberah for Kutai Basin. Difference in wettability composition appears to play a pivotal role in shaping K - S_{wirr} characteristics (note: numbers on top of histogram represent number of samples).

At macro scale, as shown on Figures 5.12 to 5.14, all fields appear to have each of its K - S_{wirr} gradient uniform regardless of wettability. At lower scale, the meso scale, the picture could be different. To investigate this possibility, a more meticulous investigation was made on the gradients for individual fields. Four sets of samples, having complete wettability types needed, are selected. Figures 5.16, 5.17, 5.18, and 5.19 present plots for Tanjung Tiga (South Sumatra Basin), Bajubang (Central Sumatra Basin), Handil (Kutai Basin), and East Kayuara (South Sumatra Basin) fields. The first two examples (Figures 5.16 and 5.17) show that separation is indicated between samples with opposing wettability, of which neutral and water-wettability samples are commonly represented by a single K - S_{wirr} gradient. This occurrence shows that in the case of Tanjung Tiga and Bajubang fields, neutral and water-wettabilities behave similarly, leaving the oil-wet samples to yield K - S_{wirr} characteristics that are markedly lower in values. This explains that, despite its supposedly limited effect on K - S_{wirr} characteristics, samples with oil-wettability may differ from samples with either neutral or weak water-wettability.

The case is rather different for Handil field samples (Figure 5.18), which exhibit three apparent K - S_{wirr} gradients representing all three wettabilities. This case presents full influence of wettability K - S_{wirr} characteristics. In a completely different case, Figure 5.19 depicts a case—East Kayuara field, South Sumatra Basin—in which all samples with the three wettabilities are represented by a common single gradient. This appears that there is no effect of wettability on K - S_{wirr} tendency. However, a more thorough investigation had revealed that the oil-wet and water-wet samples are of weak in nature, hence leading to no noticeable difference when compared to neutral-wettability. Observation over the four cases put above suggests that variation in the K - S_{wirr} characteristics of a reservoir is very much influenced by the level of wettability variation and heterogeneity.

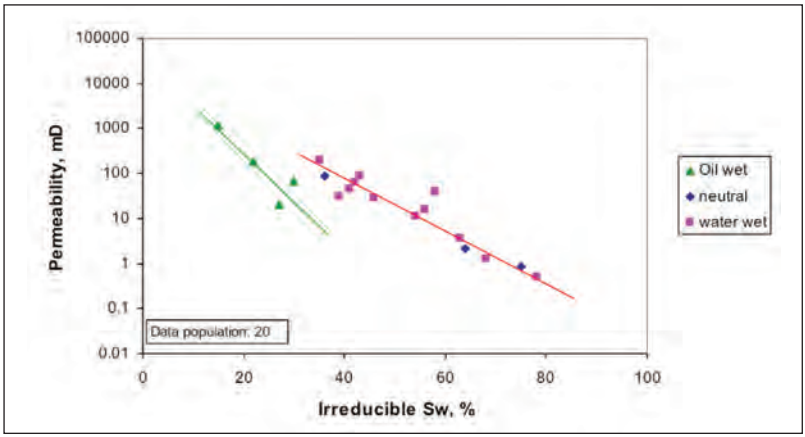

Source: Widarsono (2011a)

Figure 5.16 K - S_{wirr} data plot for Tanjung Tiga Field, South Sumatra Basin. Combined neutral and water-wet samples are in certain deviation from the oil-wet samples.

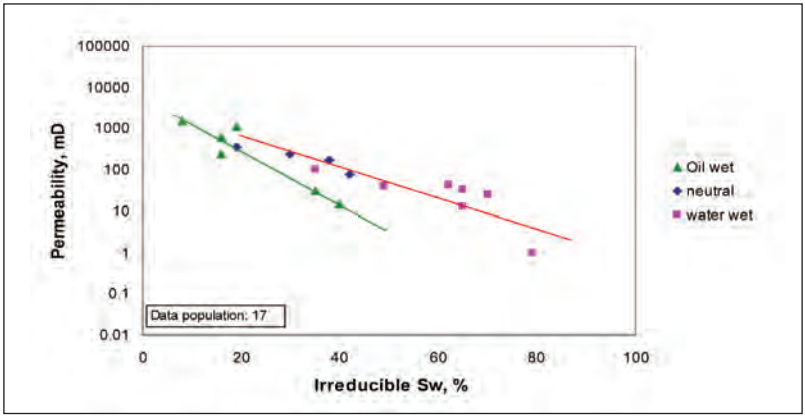

Source: Widarsono (2011a)

Figure 5.17 K - S_{wirr} data plot for Bajubang Field, Central Sumatra Basin. Oil-wet samples tend to have lower S_{wirr} values than ones belong to neutral and water-wet samples.

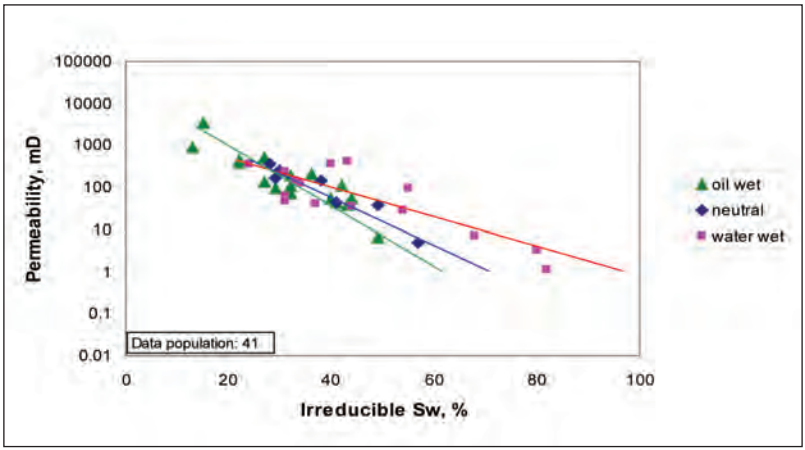

Source: Widarsono (2011a)

Figure 5.18 K - S_{wirr} data plot for Handil field, Kutai Basin. Three slopes belonging to oil-wet, neutral, and water-wet characteristics are visible.

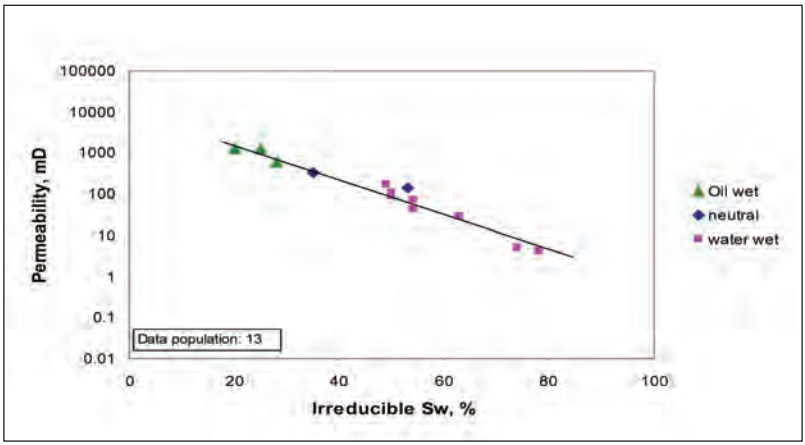

Source: Widarsono (2011a)

Figure 5.19 K - S_{wirr} data plot for E Kayuara Field, South Sumatra Basin. All samples with three different wettabilities are in one slope. A closer investigation shows that the oil and water wettability are classified as 'very weak' (i.e. close to neutral numerically) leading to minimum effect on S_{wirr} characteristics.

4. S_{wirr} characteristics of individual rock formation

In any petrophysical evaluation, division and classification of properties are often based on geological rock formations due to the presumption that they represent distinctive geological uniqueness caused by specific factors such as depositional environment, source rocks, diagenetic events, and age. Rock formations in the Central Sumatra sedimentary basin are taken as an example due to its detailed data available to the study. Manifestation of heterogeneity is often illustrated using correlation between porosity and permeablity. Figure 5.20 presents the correlations for some of the rock formations in the Central Sumatra Basin.

The K - S_{wirr} plot for the Central Sumatra rock formations are presented on Figure 5.21. The plot exhibits two big clusters having trends by Bangko and Pematang samples (Group A) and by Bekasap,

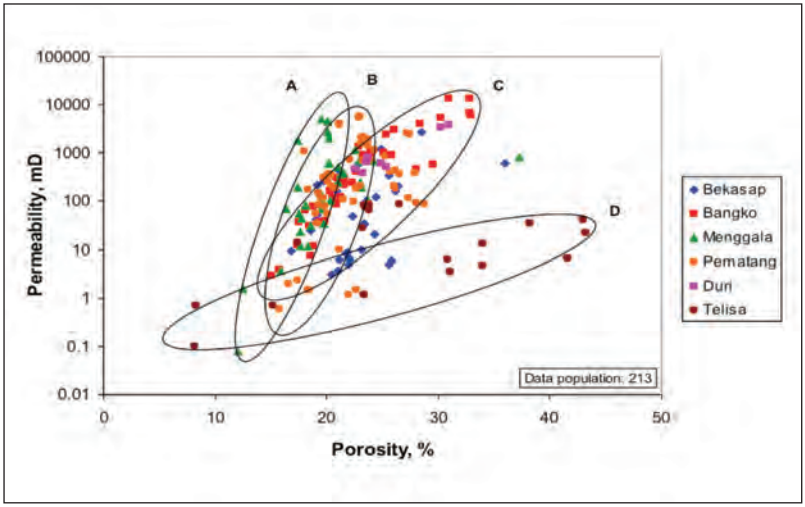

Source: Widarsono (2011a)

Figure 5.20 Porosity-permeability correlations for some rock formations in Central Sumatra Basin. Clusters A represents Menggala Formation, B for Pematang Formation, C for Bekasap – Bangko – Duri Formations, and D for Telisa Formation.

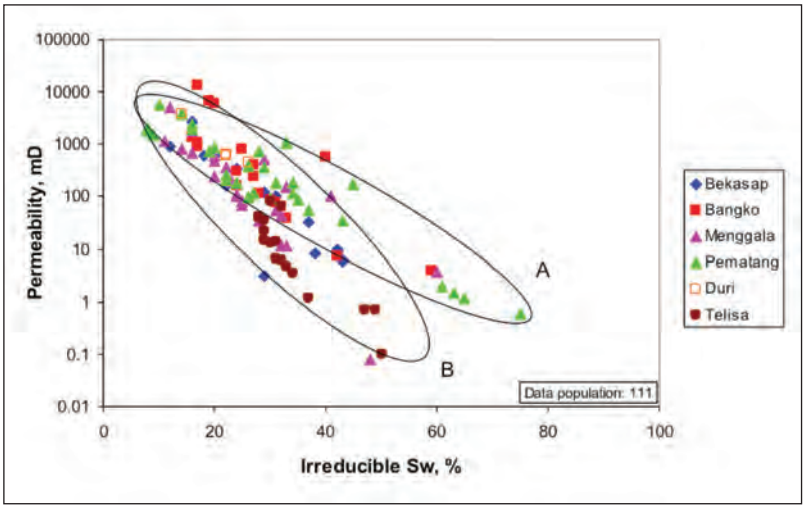

Source: Widarsono (2011a)

Figure 5.21 K - S_{wirr} plots for six rock formations in Central Sumatra Basin. Samples from Bangko and Pematang formations (cluster A) are apparently different in characteristics from the rest of the data population (cluster B), except Duri samples that are too few for cluster inclusion.

Menggala, and Telisa samples (Group B). Duri samples (only 4 samples) are included in Group A for no specific reason. Note that the data used for the plot are only data that are specifically known to belong to certain rock formations. Having no identity regarding their rock formations, the other Central Sumatra data are not included in the plot.

When K - S_{wirr} plots presented on Figure 5.21 are coincided with the hydraulic heterogeneity indicators presented on Figure 5.20, it has become noticeable that the rock formation's heterogeneity, represented by porosity-permeability characteristics, is not the governing factor for the formation's K - S_{wirr} characteristics. There are at least four clusters indicated: A (Menggala Formation), B (Pematang Formation), C (Bekasap, Bangko, and Duri Formations), and D (Telisa Formation). This grouping is certainly not in agreement with the

grouping on Figure 5.21. Bangko and Bekasap samples fall in the same porosity-permeability cluster even though having different K - S_{wirr} characteristics, while the opposite is the case for samples from Menggala and Telisa Formations.

Upon observing the disagreement between the rock formations' rock hydraulic heterogeneity and their corresponding K - S_{wirr} characteristics, observations were made on the wettability composition of the two clusters shown on Figure 5.21 (i.e. Clusters A and B). Figure 5.22 presents the result, in which it is obvious that Cluster A is characterized by stronger oil-wettability tendency than the one exhibited by Cluster B. This occurrence, again, explains that wettability plays a predominant factor in influencing S_{wirr} characteristics of reservoir rocks.

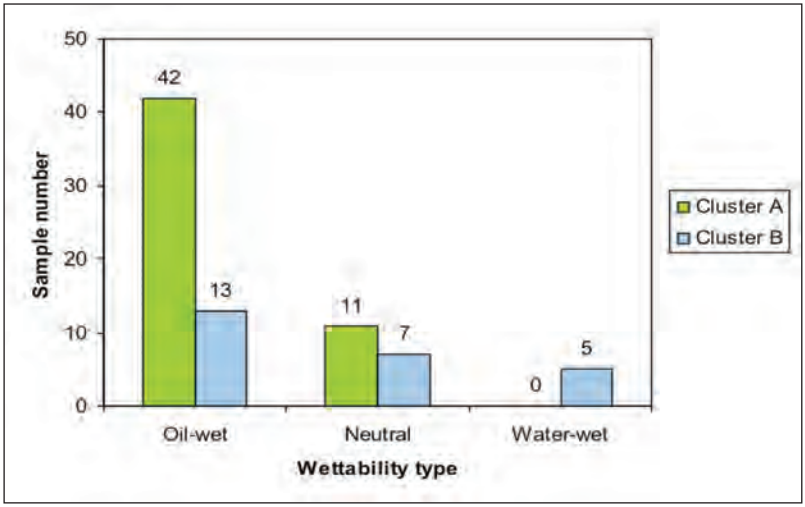

Source: Widarsono (2011a)

Figure 5.22 Wettability composition of some samples representing rock formations in Central Sumatra Basin. Cluster A includes samples from Bangko, Pematang, and Duri Formations whereas Cluster B covers Bekasap, Menggala, and Telisa samples.

E. Irreducible Water Saturation and Geological Similarity

As in the case of all empirical studies, quantity of data used in the study determines the validity of any conclusion drawn. The data quantity used in this study varies significantly among the sedimentary basins investigated. The data quantity for three top sedimentary basins, Central Sumatra, South Sumatra, and Northwest Java Basins, is far larger than the others like Sunda-Asri and West Natuna Basins (Tables 5.1 through 5.3). This is not to mention that, considering the large number of fields in those three sedimentary basins, the data quantity available for the three basins is probably insufficient for a credible representation. This is even worse for the other seven sedimentary basins with their more limited data quantity. However, since the primary objective of this study is to investigate the factor(s) that govern S_{wirr} characteristics, then it is thoughtfully considered that geological representativeness should not be of a major concern. Sedimentary basins merely represent places of origin for the samples, which data are used in the study. Consequently, any mathematical correlations presented in this chapter have to be viewed and used with considerations.

Characteristics of irreducible water saturation in reservoir rocks are certainly not determined by geological similarity, let alone geographical proximity. For instance, Central Sumatra and South Sumatra Basins are located nearby geographically and similar geologically. Nonetheless, observations on the data has clearly revealed that the Central Sumatra samples used are predominantly oil-wet whereas the South Sumatra samples are largely water-wet. The factors affecting S_{wirr} that matter, and wettability appears to be the most crucial one. Other factors, including porosity and permeability characteristics, are likely to influence in more minor ways.

F. Effects of Other Petrophysical Properties

Irreducible water saturation tends to increase with decrease in permeability. This occurs for all of the sandstones. However, from all K - S_{wirr} plots made in the study on irreducible water saturation, one rather uniform occurrence readily visible is that rock wettability does not affect S_{wirr} much at high permeability levels. For rocks with differing wettability, this occurs at permeability higher than roughly 100 mD. Over this permeability value, the S_{wirr} values converge into a single big cluster. From physical point of view, this occurrence is indeed logical. High permeability rocks have larger pore throats and usually also larger pore chambers. In this condition, the pore radius element in the capillary force (Equation 5-1) is lessened, hence reducing difference in total capillary forces between differing wettabilities. Moreover, in large pore chambers and throats, any irreducible water volumes are likey to be less distinctive relative to the large volume of the pore chambers/throats themselves.

Rock wettability appears to be a major factor in determining irreducible water saturation. Variation in wettability strongly influences variation in irreducible water saturation characteristics, whereas variation in rock porosity-permeability relationship does not have specific influence. Irreducible water saturation tends to be higher for rocks with water-wettability compared to ones for rocks with oil-wettability. However, this difference is not only exhibited in rocks with opposing wettabilities but also in rocks with different strength of wettability even though both are belonging to the same wettability type (i.e. water-wet or oil-wet). The influence of wettability on irreducible water saturation takes place in all scales of observation: sedimentary basin, field, and rock formation.

CHAPTER VI
ROCK COMPRESSIBILITY – LIMESTONES CHARACTERISTICS

A. General

As reservoir pressure declines and effective stress increases during production, reservoir rocks also tend to shrink in its pore volume. The shrinkage, and expansion due to decrease in effective stress, is known to be represented by a rock property named rock compressibility. There are actually three type of rock-related compressibility: pore volume compressibility, matrix compressibility, and bulk compressibility (rock compressibility). A bulk compressibility is by principle a combination between pore volume compressibility and matrix (grain) compressibility. However, since pore volume compressibility is much larger than matrix compressibility, a rock compressibility is therefore much more controlled by pore volume compressibility, and accordingly the term of rock compressibility is simply interchangeable with pore volume compressibility. In overpressured oil, and especially gas, reservoirs rock compressibility can often be regarded as even the most important source of driving energy (Fetkovitch et al., 1991).

The effect of changes in effective stress on reservoir rock porosity, and permeability, has long been acknowledged and various studies have been performed in order to investigate its impact on various

aspects. Rock compressibility is an important data required for cross-checking hydrocarbon in place and reserves in relatively mature fields using material balance method (e.g. Dake, 1978; Bradley, 1987). Study over the use of material balance method is further studied through incorporating fracture rock compressibility (Aguillera, 2008) and its application for an Indonesian case (Widarsono, 2009). The application has confirmed difficulties due to the lack of representative rock compressibility data but proved accurate in determining original gas in place when the right data is being used.

Studies in other areas of reservoir characterization have also shown various facts, such as dependence of rock compressibility on production-related stress path (Ruistuen et al., 1999), uncertainties in well test-derived rock compressibility that needs comparison with real data from laboratory (Cox et al., 2000), and the important role of rock compressibility data for determination of well drainage radius from well test data (Pinzon et al., 2001). In broader scales of reservoir evaluation through reservoir simulation, Gutierrex (1998) recognised the relation between geomechanics and reservoir productivity, and stated that it is only rock compressibility that can be used to compensate the lack of coupling between the two mechanisms in most reservoir simulators. In a later study, Tran et al. (2004) described various ways possible for coupling the two mechanisms but they nonetheless stated the still considerable role played by rock compressibility.

Reservoir shrinkage due to hydrocarbon production also affects other areas of activities indirectly related to the production itself. Subsidence is an example, in which as early as in 1920s, its occurrences in oil fields were felt and observed (Geertsma, 1973). More recent studies of some fields confirmed the subsidence in Valhall field (North Sea) (Ruddy et al., 1989) due to massive production from its soft chalk reservoir, and subsidence in Ekofisk field (also North Sea) that led to a conclusion over the importance of rock compressibility information

for helping pressure maintenance operation (Sulak and Danielsen, 1988). The difference between field and laboratory-measured rock compressibility due to non-linearity in rock behavior was reported by deWall and Smits (1988), prompting to a more thorough understanding over a field's rock compressibility.

The importance of rock compressibility led various investigators spent attention on the rock property's underlying theory and its relations with other properties. Early studies like ones reported by Hall (1953), Geertsma (1957), Fatt (1958), and Newman (1973) resulted in some important conclusions, as well as correlations attempted to provide practicians with practical sets of equations for predicting rock compressibilities. Latter studies by Yale et al. (1993), Harari et al. (1995), Li et al. (2004), Liu et al. (2009), Betts et al. (2011), Myers & Hatton (2011), and Bakhtiari et al. (2011) attempted to produce some correlations based on the samples they used in the study. Most of the studies reported inaccurate predicted values using past correlations and yielding discussions over various factors that may serve as the cause of the misprediction.

Rock compressibility studies for Indonesian rock samples are very limited, to author's knowledge. Pathak and Wirya (2007) successfully used rock compressibility data from laboratory to explain pressure anomaly in NSO field-Aceh, and Fardiansyah et al. (2010) studied rock compressibility data from outcrop samples for the purpose of analogy. The rarity of such study and a complete absence of comprehensive studies on reservoir rocks in Indonesia have underlined the need of such studies. A study on Indonesian reservoir limestone rocks was carried out accordingly and the report of the study is presented in Widarsono (2014a). The article, which presented aspects such as characteristics, general trends, relation with rock types, and correlations with other properties, makes up the bulk of this chapter.

B. Rock Compressibility

Under constant temperature condition, compressibility of a rock formation is defined as a ratio of an amount of change in volume with change in pressure to its original volume, or can be expressed as (Zimmerman, 1991):

$$C_f = \frac{1}{V_P}\left(\frac{\partial V_P}{\partial P}\right)_T \tag{6-1}$$

with C_f, V_p, and P are formation compressibility (usually in psi^{-1}), pore volume (in cu-ft), and pressure exerted on the formation (in psi). T is to mark that the condition is under constant temperature. In reality in the formation, when a reservoir is being produced for its hydrocarbon, the reservoir pressure declines resulting in—while overburden pressure remains constant—increase in effective stress. The formation's contraction characteristics in response to the increasing (or decreasing) effective stress reflects the formation's compressibility. Different pore types and structures may respond differently toward compression, and their pores and permeability may also decrease in different manners. However, for most reservoir rocks, the volume change is actually small, in the magnitude of 10^{-6} psi^{-1}, and normally within the range of $2x10^{-6}$ to $15x10^{-6}$ psi^{-1} at initial reservoir pressure (Satter, 2007).

Similarly to its relation to pore structure, rock compressibility also relates closely with porosity. However, there is a wide range in compressibility for a particular porosity, and furthermore, rock compressibility may behave differently for rocks with different porosities. This led to the need to understand the relationship and seek correlation(s) that link the two. In 1953, Hall established a general empirical correlation of

$$C_f = 1.87\times10^{-6}\,\phi^{-0.415} \tag{6-2}$$

where ϕ is porosity, usually at atmospheric or overburdened conditions. Since the correlation was established based on a certain number of samples only and is unlikely to be valid for reservoir rocks in general, other latter investigators attempted to establish other correlations. Newman (1973) established general hyperbolic correlations for both sandstones and limestones based on 79 samples put in the study. For limestones, the correlation is

$$C_f = \frac{0.8535}{\left[1+2.367\phi\right]} \times 10^{-6} \tag{6-3}$$

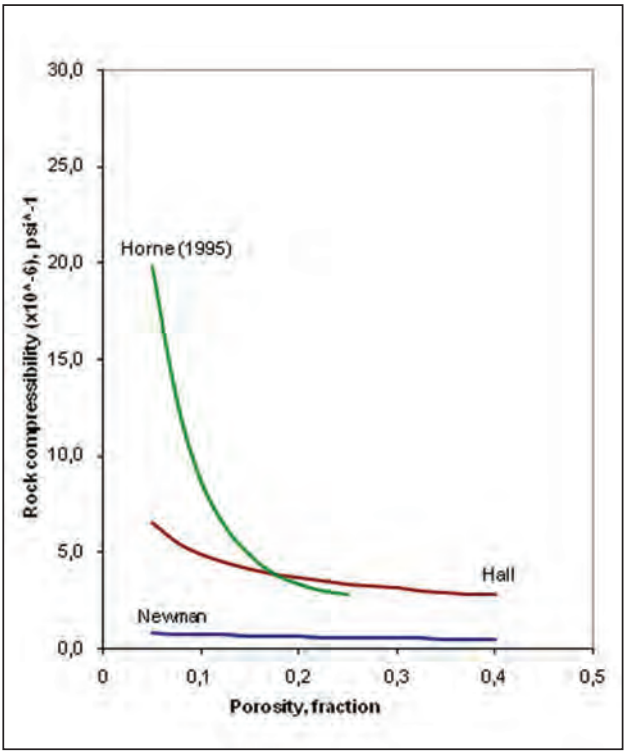

Source: Widarsono (2014a)

Figure 6.1 The Existing Rock Compressibility Correlations for Limestones

Results of a more recent study also yielded correlations of (as shown in Horne, 1995)

$$C_f = \exp\left(4.026 - 23.07\phi + 44.28\phi^2\right) \times 10^{-6} \quad (6\text{-}4)$$

for limestones. Figure 6.1 shows the three ϕ-C_f existing correlations. All three correlations infer lower compressibility for higher porosity rocks. Using the correlations presented above, comparisons are to be made on the rock compressibility characteristics of Indonesian reservoir sandstones.

C. Data Inventory

Tests on core samples in Widarsono (2014a) were initiated by core plugging and cleaning, after which samples underwent geological visual description and basic properties measurements of porosity and permeability. The PVC test itself was performed by evacuating and fully saturating the samples with brine and then both pore and confining pressures were elevated up to a certain pressure level (i.e 200 psig). Using this as a starting point, the overburden pressure was raised further up to pre-determined pressure levels while the pore pressure was kept constant. After estimating changes in pore volume at each pressure level, the rock compressibility was calculated using Equation 6-1. For converting hydrostatic loading condition into uniaxial condition, that is more representing reservoir under overburden loading, theoretical formula proposed by Teeuw (1971) was used. Figure 6.2 presents an exemplary set of measurement results, in the standard form of rock compressibility versus effective overburden pressure.

As many as 84 limestone samples were used in the study (Tables 6.1 to 6.6). The samples were taken from 11 productive oil and gas fields in Indonesia, located in four productive sedimentary basins (Figure 6.3). They represent various limestone types, and belong to five

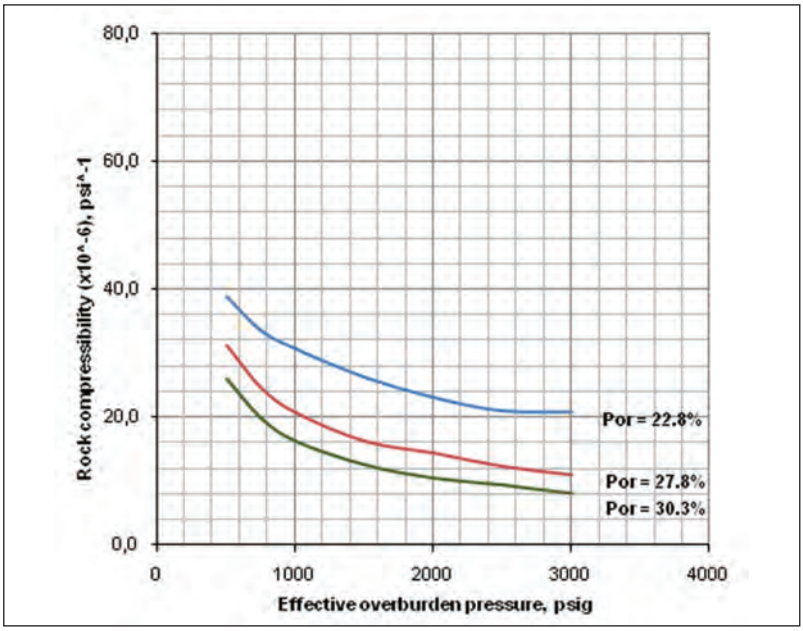

Source: Widarsono (2014a)

Figure 6.2 Example of Pore Volume Compressibility Results (Kujung)

important limestone formations in Indonesia: the Baturaja of South Sumatra Basin, Belumai and Peutu of North Sumatra, Minahaki of Banggai Basin, and Kujung of Northeast Java Basin. Through the use of these representative samples, valuable information is expected to be revealed about the compressibility characteristics of carbonate rocks of Indonesian reservoirs.

D. Rock Compressibility Characteristics

In performing evaluation over the results of measurement, Widarsono (2014a) took two angles of approach are adopted; evaluation through rock type grouping and evaluation through their geological place of origin (i.e rock formation). For rock type grouping, Dunham clas-

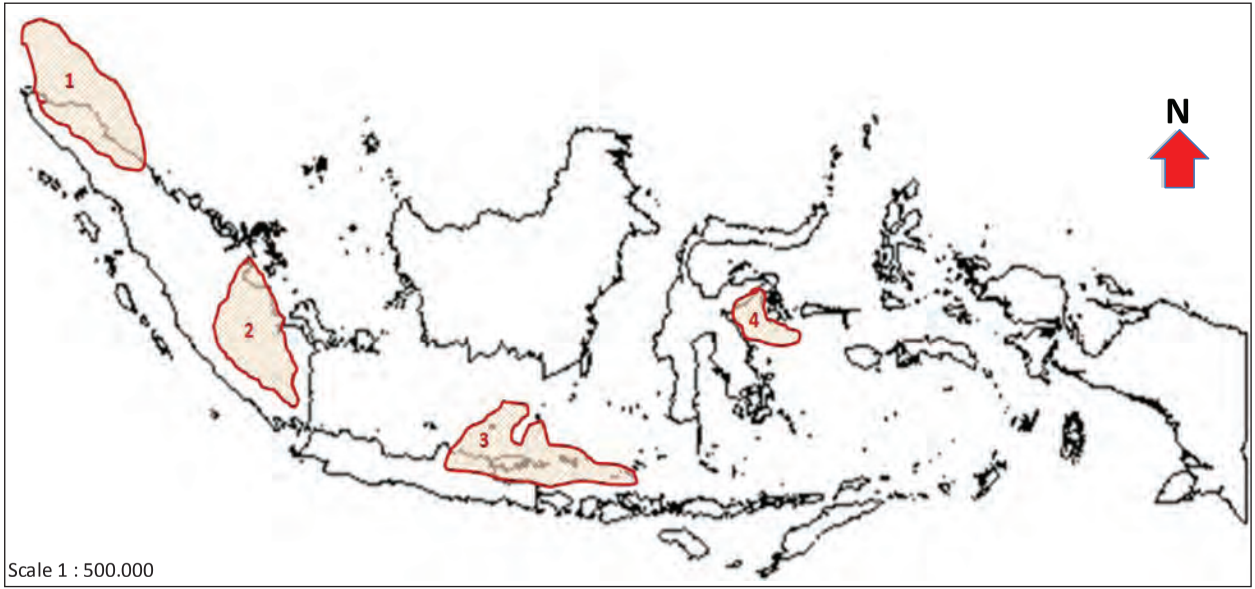

Figure 6.3 Tertiary Sedimentary Basins, the Place of Origin of the Limestone Core Samples Used in the Rock Compressibility Study: (1) North Sumatra Basin, (2) South Sumatra Basin, (3) Northeast Java Basin, and (4) Banggai Basin

Table 6.1 Number of Limestone Core Samples per Rock Type and Their Field of Origin, North Sumatra, South Sumatra, Northeast Java, and Banggai Basins

Basin	Field/structure (no. of wells)	Number of samples			
		Wacke-stone	Pack-stone	Grain-stone	Bound-stone
North Sumatra Formation(s): Peutu, Belumai	NSO (3), South Lhok Sukon (4), Total wells = 7	6	26	-	3
South Sumatra Formation Baturaja	ASDJ (2), Karangdewa (1), Musi (1), Prabumenang (1), Sopa (1), Suban Barat (1) Total wells = 6	6	6	-	4
Northeast Java Formation Kujung	Bukit Tua (1) Total wells = 2	-	13	-	-
Banggai Formation Minahaki	Matindok (1), Senoro (2) Total wells = 3	4	10	4	-

sification is used. Dunham (1962) established a stratified classification starting from the top by recognising 'crystalline' and 'non-crystalline', dividing the 'non-crystalline' into 'components bound' and components not bound', dividing further the 'components not bound' into 'containing mud' and not, down to division of the rocks classified as 'containing mud' into 'mud dominated' and 'grain dominated'. These definitions, based clearly on rock fabric, classify carbonate rocks into rocks types of crystalline, boundstone, grainstone, packstone, wackestone, and mudstone. In this study, only data of rock samples

Table 6.2 Basic Data of Core Samples from Baturaja Formation (South Sumatra Basin)

No.	Type	Porosity (fraction)	Permeability (mD)	Description
1	Packstone	0.245	49	hd,sli vug, for
2	Packstone	0.16	2.1	hd,for,OM streak
3	Packstone	0.233	111	hd, for,OM streak
4	Packstone	0.218	132	hd,sli vug, for
5	Packstone	0.188	9.7	hd,sli vug, for
6	Packstone	0.227	117	hrd,form
7	Wackestone	0.05	3.4	hd,vug,for
8	Wackestone	0.053	3	hd, vug, foram
9	Wackestone	0.228	11	hd, sty, foram
10	Wackestone	0.14	1	hd,for, styl
11	Boundstone	0.217	14.5	hd,coral
12	Boundstone	0.159	33	hd, styl
13	Boundstone	0.045	6.8	hd,coral, styl
14	Boundstone	0.129	119	hd,coral, sli vug
15	Wackestone	0.228	11	hd,for,vug
16	Wackestone	0.14	1	hd,for,vug drusy

Source: Widarsono (2014a)

Table 6.3 Basic Data of Core Samples from Minahaki Formation (Banggai-Sula Basin)

No.	Type	Porosity (fraction)	Permeability (mD)	Description
1	Grainstone	0.252	7.3	hd, sli vug,foram
2	Grainstone	0.23	10	hd, for, pp-vug
3	Grainstone	0.3	13	hd,sli foss frag
4	Grainstone	0.314	18	hd, vug
5	Packstone	0.23	33	hd, vug
6	Packstone	0.229	8.6	hd, vug
7	Packstone	0.283	34	hd, vug
8	Packstone	0.219	6.3	hd, vug
9	Packstone	0.2	2.4	hd, sli vug
10	Packstone	0.216	8.4	hd, vug
11	Packstone	0.181	14.2	hd, vug
12	Packstone	0.237	14.5	hd, vug
13	Packstone	0.221	5.6	hd, vug
14	Wackestone	0.269	3.2	hd, vug
15	Packstone	0.284	11	hd, for, pp-vug
16	Wackestone	0.287	2	hd,sli foss frag
17	Wackestone	0.247	4.9	hd-vhd
18	Wackestone	0.23	6	hd, foss, pp-vug

Source: Widarsono (2014a)

Table 6.4 Basic Data of Core Samples from Peutu Formation (North Sumatra Basin)

No.	Type	Porosity (fraction)	Permeability (mD)	Description
1	Packstone	0.096	0.55	hd, for, algae, ppv
2	Packstone	0.031	1	hd, for, alg, styl
3	Wackestone	0.154	5.4	hd, for, alg, styl
4	Packstone	0.151	1.7	hd, for, algae, ppv
5	Packstone	0.121	1	hd, for, algae, ppv
6	Wackestone	0.119	0.3	hd, algae
7	Wackestone	0.14	0.76	hd, aggregate
8	Packstone	0.016	0.04	hd, aggr, styl
9	Packstone	0.126	1	Hd, for, pp-vug
10	Packstone	0.144	0.8	hd, for, mot-vug
11	Packstone	0.164	3.5	hd,for,pp-vug
12	Packstone	0.113	0.9	hd,for,alg,pp-vug
13	Packstone	0.096	1.1	hd,for,alg,cor,motv
14	Packstone	0.14	6.5	hd,for,alg,mot v
15	Packstone	0.16	5.6	as above
16	Packstone	0.124	1.1	hd,cor,loc xlin
17	Packstone	0.124	1.5	hd,cor,alg,for,ppv
18	Packstone	0.145	1.6	hd,for,ppvug
19	Packstone	0.147	1.6	hd,cor,alg,loc xlin
20	Packstone	0.169	0.8	hd,cor,alg,

Source: Widarsono (2014a)

belonging to boundstone, grainstone, packstone, and wackestone are available for evaluation.

For data presentation, compressibility values at reservoir initial pressure, hence minimum effective overburden presure. By assuming uniform overburden pressure (P_{OB}) and reservoir pressure (P_{res}) gradients of 1 psi/ft and 0.5 psi/ft, respectively, an effective overburden pressure of 0.5 psi/ft is used as following $effective\, P_{OB} = P_{OB} - \mathrm{P}_{res}$.

As effective overburden pressure has been determined, the needed compressibility values are obtained from the rock compressibility curves. Figure 6.2 depicts an example result from a measurement.

The tendency of relation between rock compressibility and porosity for the 84 rock samples are depicted on Figure 6.4. Although

no clear trend can be observed, the data population still provide a semblance of decrease in initial rock compressibility for higher porosity limestones. The lack of sharp, a general trend is also still visible, trend is also shown and reinforced by their porosity-permeability relationship (Figure 6.5). This lack of obvious trend is expected and analysis on lower levels is required.

1. Rock compressibility of different rock types

As rock typing has been established through visual description, samples and the corresponding data are grouped into rock type-based groups. For boundstone (9 samples), the data are presented on Figure 6.6. In this limited amount of samples, no sharp trend is indicated and none of the correlations can represent all data population, even though Horne (1995) model appears to be the closest model to fit some of the data points. Apart from the limited sample number, this inconclusive data plot probably reflects the reefal nature of boundstone along with its associated heterogeneity.

Despite the similarly limited sample number (9 samples), data for grainstone samples are clearly different compared to the boundstone group (Figure 6.7). Hall model appears to agree well with the data. Interestingly, the nine samples are actually from five fields and three formations located in three different sedimentary basins: North Sumatra, South Sumatra, and Banggai (Sulawesi). The good agreement between data and the Hall model reflects the less variation in pore structures among the samples classified as grainstones, all characterized by presence of forams and pin-point vugs.

Packstone make the bulk of the sample population with its 48 samples. Plot in Figure 6.8 presents a fair degree of scatter even though the general trend shows decrease or at least constant in compressibility with the increase in porosity. However, a more careful analysis may

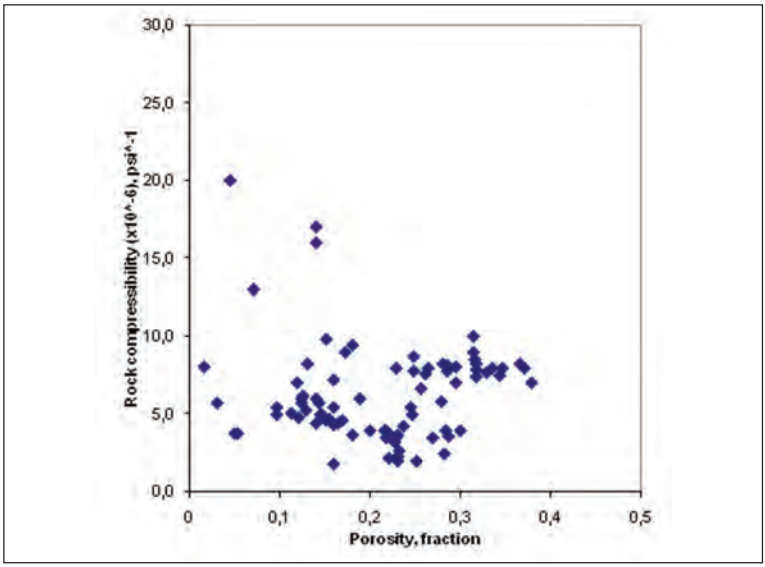

Source: Widarsono (2014a)

Figure 6.4 Plot between Rock Porosity and Rock Compressibility of All Data (84 Samples)

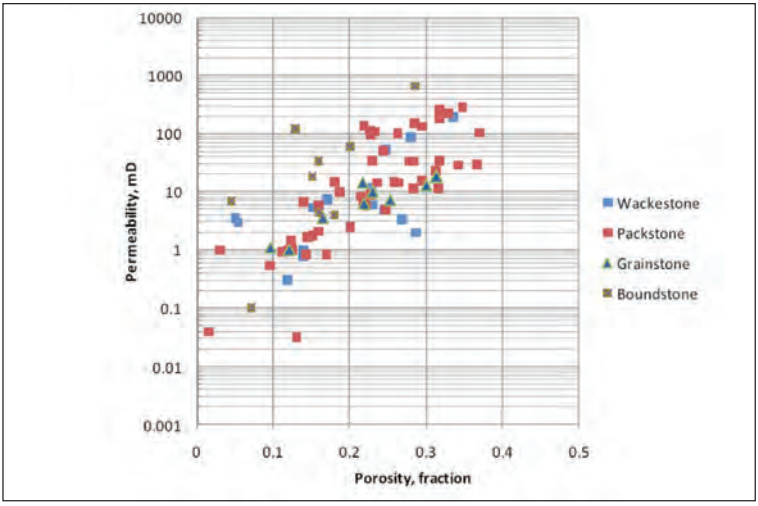

Source: Widarsono (2014a)

Figure 6.5 Porosity-Permeability Plot for All Limestone Samples (84 Samples)

show that the lower part of the data cluster agree well with both correlations with Hall model appears to represent better. On the other hand, the data on the upper cluster of the data is likely to be represented by other model other than the three existing models. A closer look on the data with regard to physical features shows differences between the two clusters. The lower cluster is predominantly Arun limestone that are characterized by presence of forams, algae, stylolites, and pin-point vugs at most, while the upper cluster's Kujung limestones show presence of larger vugs. Different environment and development during the rock forming may have some relation to the place of origin.

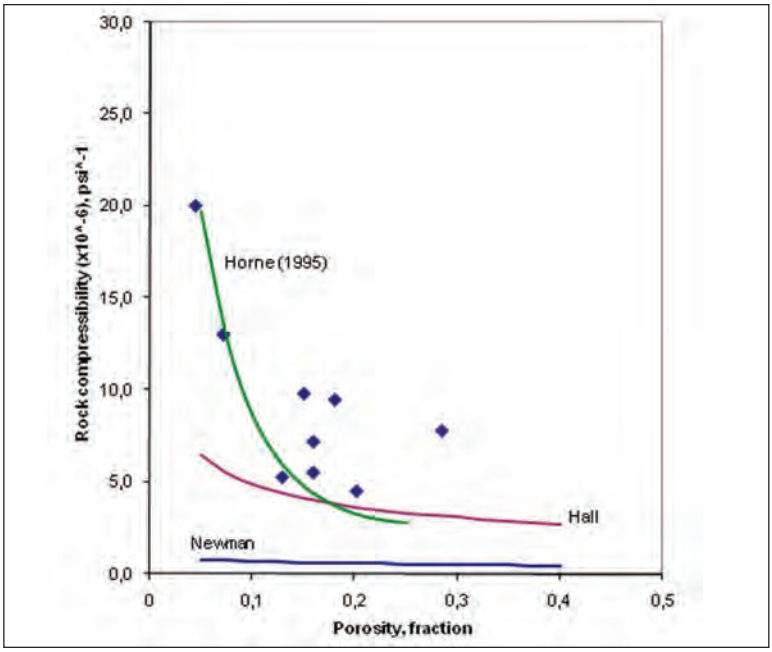

Source: Widarsono (2014a)

Figure 6.6 Rock compressibility data for boundstone (9 samples). Most of the data fall beyond the three corelations.

In a way similar to packstone, data showing for the wackestone group (18 samples) yields agreement between either Hall (1953) or Horne (1995) model and only a part of the data populations (Figure 6.9). In this case, this is also apparent that the lower and upper data come from different place of origin, Banggai and North Sumatra Basins, respectively. Overall evaluation over data based on rock typing have shown that some of the data agree with Hall (1953) and/or Horne (1995) models, while Newman model for limestones predicts too low compressibility values for the same porosity range. The fact that some of the data do not fit with the models also leads to the need for an alternative of evaluation approach.

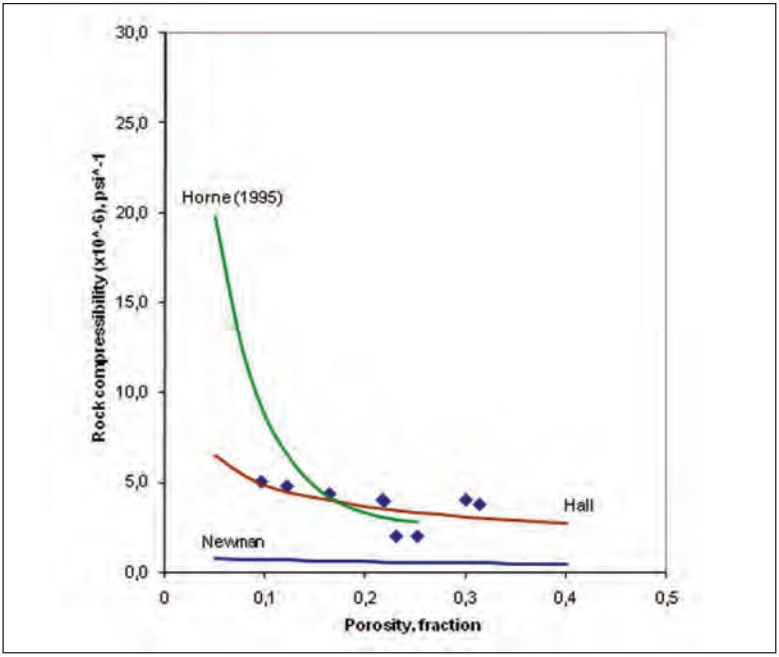

Source: Widarsono (2014a)

Figure 6.7 Rock Compressibility Data for Grainstone (9 Samples) Showing Good Agreement with Hall Correlation

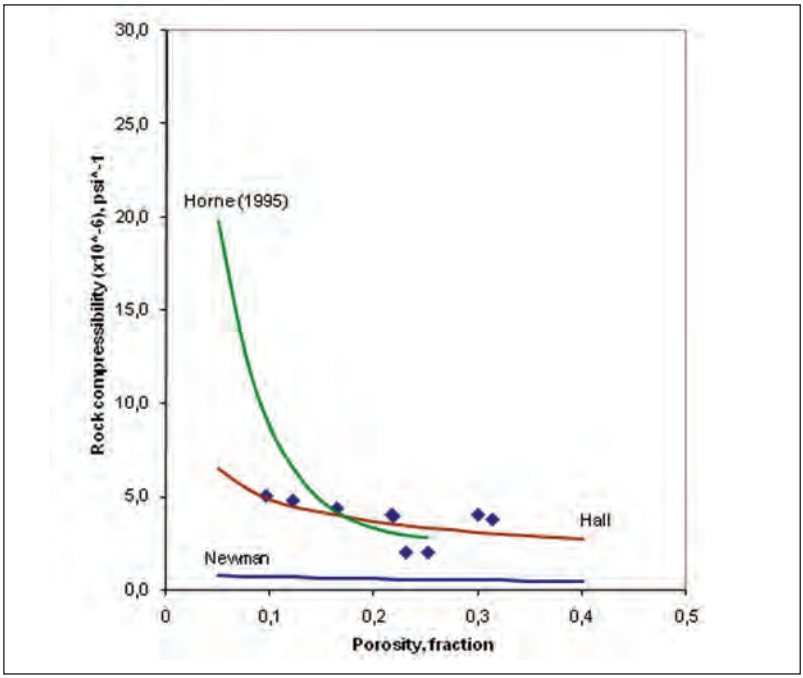

Source: Widarsono (2014a)

Figure 6.8 Rock Compressibility Data for Packstone (48 Samples) Showing Two Clusters of Data, with the Lower Cluster Tends to Agree with Hall Correlation

2. Rock compressibility and rock formations

As put earlier, the 84 limestones used in the study have been taken from four limestone formations in four productive sedimentary basins. Each locations may have different environment and rock forming path that affect rock compressibility characteristics. Figure 6.10 depicts plot for the Baturaja Limestones (South Sumatra). The ϕ-C_f plot (17 samples) some degree of scatter even though agreement with Hall model (or Horne (1995)?) is evident for most of the data. When compared to data plot for Minahaki Limestones (18 samples), a stronger agreement to the Hall (1953) correlation is indicated under a much better degree of tolerance (Figure 6.11). This agreement to

Hall correlation has to be underlined since the Horne (1995) model is valid only up to porosity of 23%. The two data shown from two places of origin strongly indicate that the existing models, derived using samples from other places, can be proved valid for some Indonesian limestones belonging to some specific places, in this case Baturaja (South Sumatra) and Minahaki formations.

For the limestone samples (36 samples) from North Sumatra Basin, the plot between rock compressibility and porosity is presented on Figure 6.12. From the data, a separation into two groups is visible. The lower cluster, all from Peutu formation, appears to reasonably agree with either Hall (1953) or Horne (1995) models. A more care-

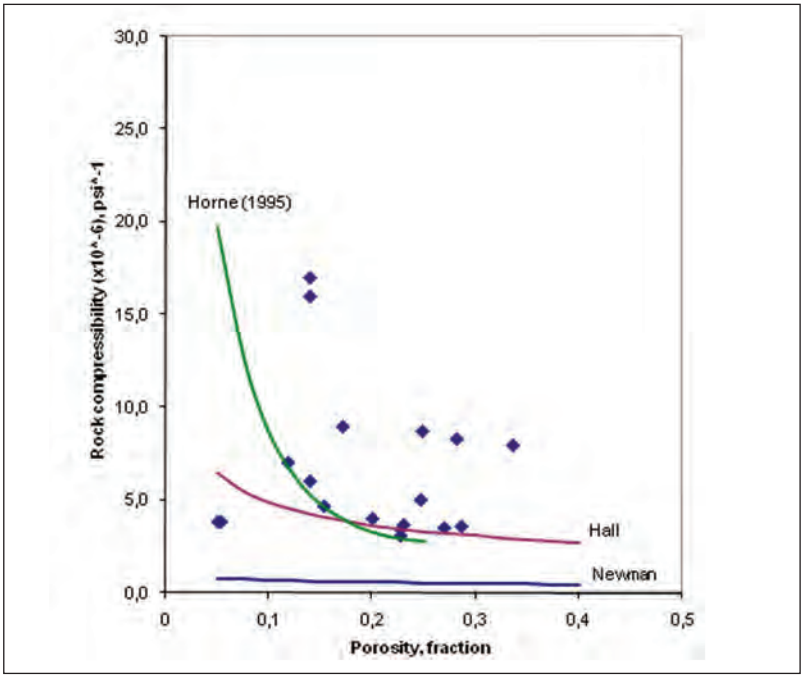

Source: Widarsono (2014a)

Figure 6.9 Rock Compressibility Data for Wackestone (18 Samples) Depicting Similar Trends to Packtone with Some of the Data in Reasonably Good Agreement with Hall Model

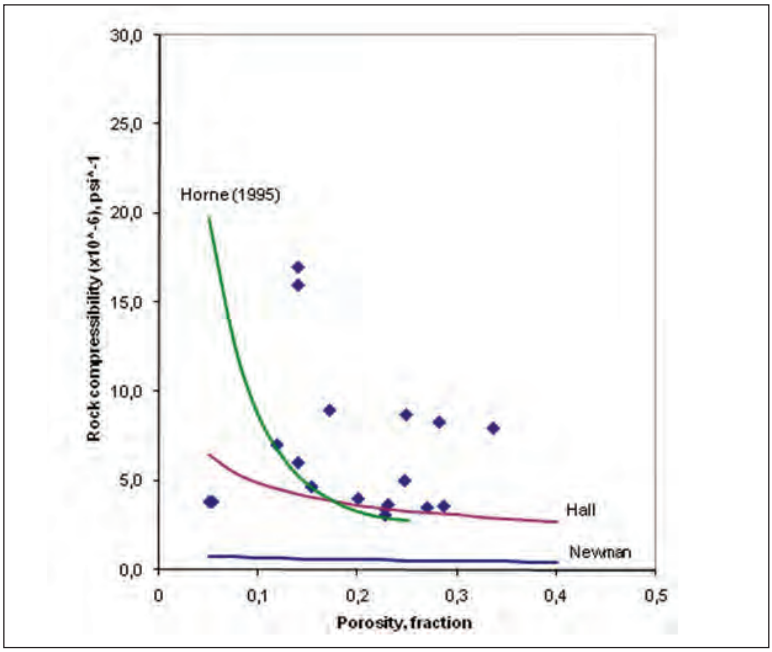

Source: Widarsono (2014a)

Figure 6.10 Rock Compressibility Data for Baturaja Formation Limestones (17 Samples) Presenting in Reasonably Good Agreement between Data and Hall and/or Horne (1995) Model(s)

ful examination, however, tend to lean on Hall model as the more representative correlation for the Peutu samples. On the other hand, the upper cluster, all samples from Belumai formation, apparently fall out of all three correlations. By observing the clear trend shown by the samples, it can be concluded that the data are not of false ones but they should be represented by other model. A new correlation is therefore required.

Through observing trend of the Belumai samples, the required correlation could bear a resemblance to any of the three empirical correlations. As reformulation of the three correlations have been

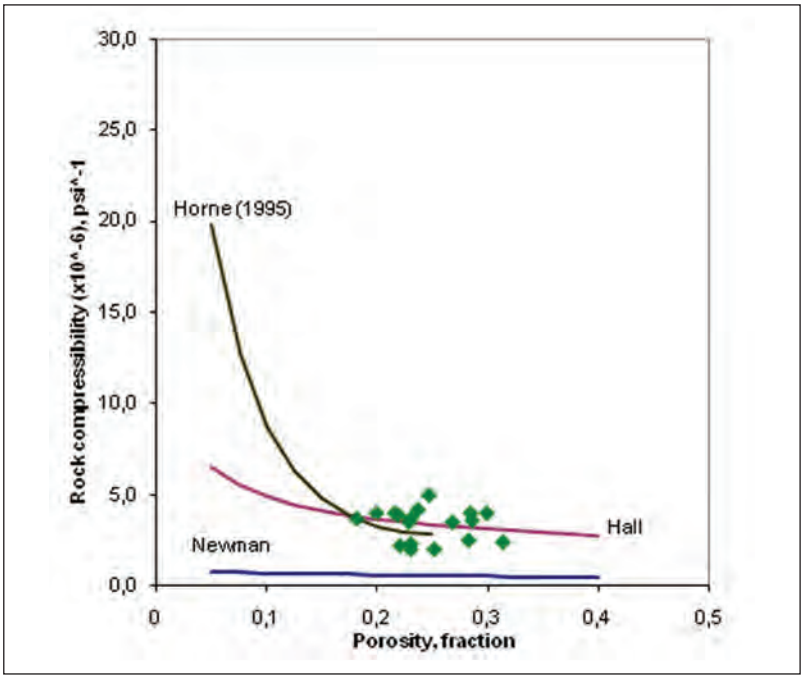

Source: Widarsono (2014a)

Figure 6.11 Rock compressibility data for Minahaki Formation Limestones (18 samples) Showing Good Agreement between Data and Hall Model. Presence of data with porosity higher than 24% defies association to Horne (1995) model.

undertaken, it came out that the most appropriate correlation for the Belumai samples is

$$C_f = \frac{85.35}{\left[1+15.35\phi^{0.385}\right]} \times 10^{-6} \qquad (6\text{-}5)$$

which is mathematically a modification of Newman model but with similar curve shape, except in the order of magnitudes, with Hall model. Upon observing the newly proposed ϕ-C_f empirical correlation, the presence of $\phi^{0.385}$ implies that effect of porosity difference

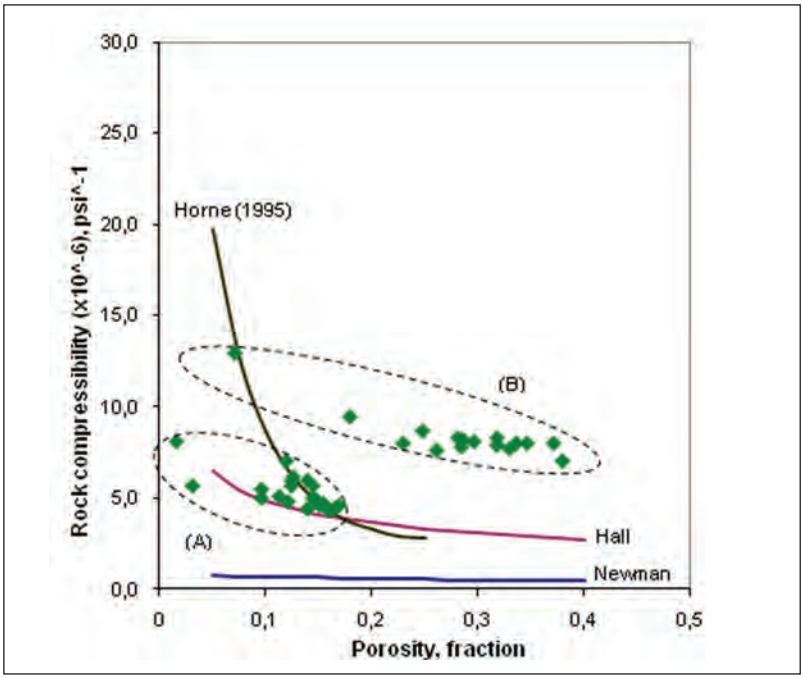

Source: Widarsono (2014a)

Figure 6.12 Rock compressibility data for North Sumatra Basin limestones (36 samples) depicting two data clusters of data from (A) peutu formation and (B) belumai formation. The Peutu data appears to agree more to Hall rather than to Horne (1995) model due to presence of some low porosity samples that tilt to the former model.

at higher porosity diminishes. In other words, the higher the porosity values the lesser the compressibility variation among them.

Application of Equation 6-5 on Belumai rock compressibility data is presented on Figure 6.13. The equation shows no limit of validity at least up to porosity of 50%. Agreement between the proposed correlations with the Belumai data appears very good, with gentler slope at higher porosity that well represents the less variation in rock compressibility within that porosity range.

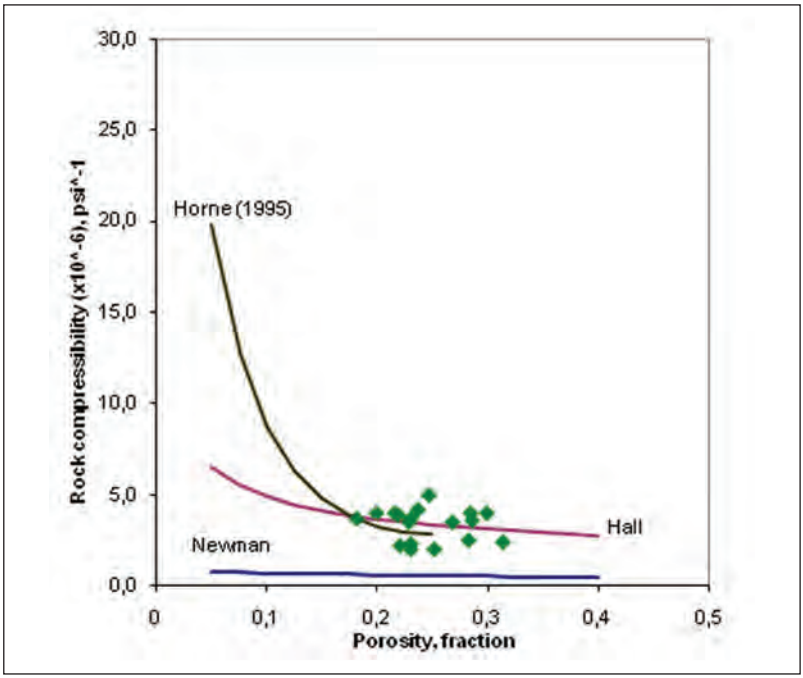

Source: Widarsono (2014a)

Figure 6.13 A Newly proposed model that fits very well with the medium hard – vuggy belumai limestones (15 Samples). The model has no porosity limit in the validity.

Plot for the Kujung Formation (Northeast Java Basin) data (13 samples) is shown on Figure 6.14. In the manner similar to Belumai samples, the Kujung samples also fall out of the three existing correlations. However, when the newly proposed correlation is applied, it fits the data reasonably well. Although the data comprises only data for higher porosity values, and no evidence whether the correlation is also valid for lower porosity values, the model works well for the available data. The newly proposed model can therefore be considered valid since it can represent two data groups taken from two far separated regions.

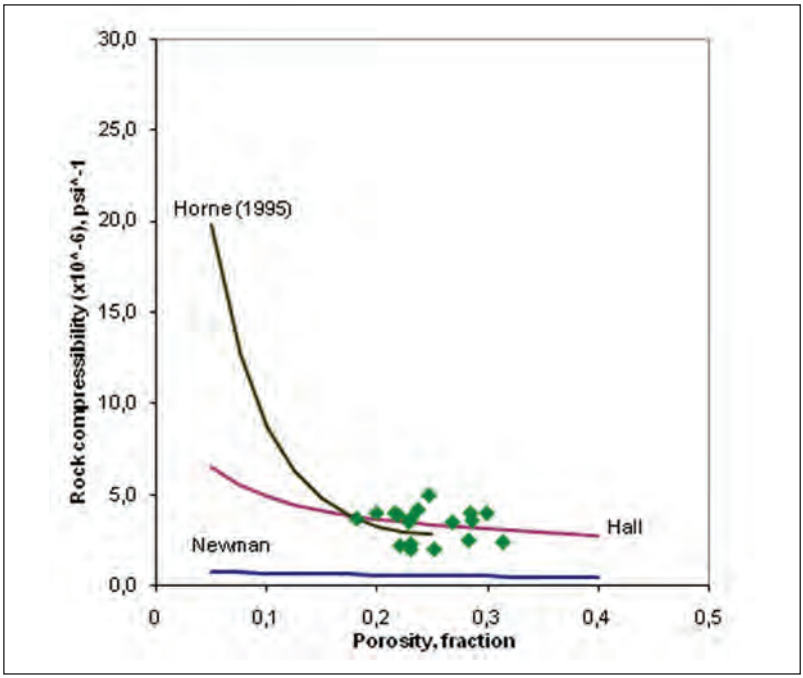

Source: Widarsono (2014a)

Figure 6.14 Rock compressibility plot showing good agreement between samples from Kujung Formation (13 samples) and the proposed model. Kujung formation (Northeast Java Basin) samples are also of medium-hard and vuggy limestones.

E. Model Assignment for Indonesian Limestones

As has been observed in the application of the new model, it agrees well with two sets of samples taken from two sedimentary basins that are not linked in every way. This leads to the need to compare aspects of the two sets of samples. Attempts to compare the two at scales larger than core scale—field or basin-scale depositional and diagenetic aspects—are simply too complicated and may be considered as irrelevant to the theme of this chapter.

Comparison between the physical nature of the two sets show that the Kujung samples are almost entirely medium hard packstone with porosity made mainly of vugs, while the Belumai samples are also mainly medium hard with 9 packstones, 3 wackestones, and 3 boundstones (Table 6.5). The samples' porosity is mainly made of pin-point to mottled vugs/med vugs. Considering the mostly medium hard nature of the limestone samples analysed, it is most likely that the hardness of the two sample sets provides the similarity in the rock compressibility characteristics. This becomes more underlined when comparison is made to all other samples from all other formations that are almost entirely of 'hard' hardness and less vuggy. Therefore, it can be said that the newly proposed correlation (Equation 6-5) is a ϕ-C_f correlation for medium-hard and vuggy limestones, regardless of rock types.

Table 6.5 Basic Data of Core Samples from Belumai Formation (North Sumatra Basin)

No.	Type	Porosity (fraction)	Permeability (mD)	Description
1	Packstone	0.318	253	mhd,for,alg,cor,ppv
2	Wackestone	0.281	85	mhd,aggr,pp-mot v
3	Wackestone	0.248	52	mhd,aggr,pp-mot v
4	Boundstone	0.071	0.1	vhd, coral
5	Boundstone	0.18	4	hd,cor,alg,for,ppv
6	Packstone	0.347	275	hd,for,alg,mot v
7	Packstone	0.329	214	mhd,for,alg,ppv
8	Packstone	0.318	176	mhd,for,alg,ppv
9	Packstone	0.262	98	mhd,for,alg,pp m-v
10	Packstone	0.296	136	mhd,for,alg,pp m-v
11	Packstone	0.286	147	mhd,alg,for,m-vug
12	Packstone	0.371	106	mhd,alg,for,m-vug
13	Wackestone	0.336	190	mhd,cor,alg,for,ppv
14	Boundstone	0.285	665	mhd,cor,alg,for,vug
15	Packstone	0.229	94	mhd,cor,alg,for,ppv

Source: Widarsono (2014a)

For the rest of hard limestones, on the other hand, the models of Hall (1953) and Horne (1995) appear to well represent them. However, caution should be taken in choosing the Horne (1995) model since it has limitation of validity. The Hall model is likely to be more appropriate for Indonesian hard limestones. For the Newman model, it is apparently at odd with all data population. No explanation whether or not it can be applied for any of Indonesian limestones. It can probably be applied for 'very hard' Indonesian limestones, which may no longer be considered as productive reservoir rocks.

Table 6.6 Basic Data of Core Samples from Kujung Formation (Northeast Java Basin)

No.	Type	Porosity (fraction)	Permeability (mD)	Description
1	Packstone	0.314	22	mhd,vug, styl, for
2	Packstone	0.317	11	mhd,vug, styl, for
3	Packstone	0.343	29	mhd,vug, corl, for
4	Packstone	0.367	28	mhd,vug, styl, for
5	Packstone	0.295	15	mhd,vug, styl, for
6	Packstone	0.318	33	mhd,vug calc, for
7	Packstone	0.279	34	mhd,vug calc, for
8	Packstone	0.248	4.8	mhd,vug, corl, for
9	Packstone	0.264	14.5	hard,vug, corl, for
10	Packstone	0.36	8	mhd,vug, corl, for
11	Packstone	0.35	7	mhd,vug, corl
12	Packstone	0.3	8	mhd,vug, styl, for
13	Packstone	0.26	9	hd,vug,for

Source: Widarsono (2014a)

REFERENCES

Aase, N. E., Bjorkum, P. A., & Nadeau, P. H. (1996). The effect of grain-coating microquartz on preservation of reservoir porosity. *AAPG Bulletin*, *80*, 1654–1673.

Aghighi, A. M., & Rahman, S. S. (2010). Horizontal permeability anisotropy: Effect upon the evaluation and design of primary and secondary hydraulic fracture treatments in tight gas reservoirs. *Journal of Petroleum Science and Engineering*, *4* (1–2), 4–13.

Aguilera R. (2008). Effect of fracture compressibility on gas-in-place calculations of stress sensitive naturally fractured reservoirs. *SPE Reservoir Evaluation & Engineering, 11(2)*: 307–310.

Akhoundzadeh, H., Mogadashi, J., & Habibnia, B. (2011), *Correlation of pore volume compressibility with porosity in one of the Iranian southern carbonate reservoirs*. Abadan: Petroleum University of Technology (PUT).

Al-Aulaqi, T., Grattoni, C., Fisher, Q., Musina, Z., & Al-Hinai, S. (2011). *Effect of temperature, oil asphaltene content, and water salinity on wettability alteration*. SPE-149071-MS, presented at the SPE/DGS Saudi Arabia Section Technical Symposium and Exhibition, 15–18 May, Al-Khobar, Saudi Arabia.

Al-Hadrami, H. K., & Teufel, L. J. (2000). *Influence of permeability anisotropy and reservoir heterogeneity on optimization of infill drilling in naturally fractured tight-gas mesaverde sandstone reservoirs*, *San Juan Basin*. Paper SPE-60295-MS, presented at the SPE Rocky Mountain Regional/ Low PermeabilityReservoirs Symposium and Exhibition, 12–15 March, Denver-Colorado.

Al-Hadhrami, H.S. & Blunt, M. (2001). Thermally induced wettability alteration to improve oil recovery in fractured reservoirs. *SPE Reservoir Evaluation & Engineering, 4*(3), 179–186

Alavi, M. F., Alavi, M .F., & Alavi, M. F. (2014). *Determination of reservoir permeability on irreducible water saturation and porosity from log data and FZI (flow zone indicator) from core data*. Proceeding, presented at the International Petroleum Technology Conference, 19-22 January, Doha–Qatar.

Al-Omair, O., & Garrouch, A. A. (2010). Classifying rock lithofacies using petrophysical data. *Journal of Geophysics and Engineering*, *7* (3), 302.

Alotaibi, M. B., Nasralla, R. A., & Nasr-El-Din, H. A. (2011). Wettability studies using low-salinity water in sandstone reservoirs. *SPE Reservoir Evaluation & Engineering*, *14* (6), 713–725.

Amott, E. (1959). Observation relating to the wettability of porous rock. *Trans. AIME*, *216*, 156–162.

Amyx, J. W., Bass Jr, D. M., & Whiting, R. L. (1960). *Petroleum reservoir engineering: Physical properties*. New York: McGraw-Hill.

Anderson, W. G. (1986a). Wettability literature survey–Part 2: Wettability measurement. *Society of Petroleum Engineer The Journal of Petroleum Technoogy*, *38*, 1246–1262.

Anderson, W.G. (1986b). Wettability literature survey—Part 3: The effects of wettability on the electrical properties of porous media. *J. Pet. Tech., 38*(12), 1371–1378.

Anderson, W.G. (1986c). Wettability literature survey—Part 5: The effects of wettability on relative permeability. *Soc. Petrol. Eng. JPT, 38*, 1453–1468.

Anderson, W. G. (1987). Wettability Literature Survey - Part 5: Effect of wettability on relative permeability. *Journal of Petroleum Technology*, *November*, 1453–1468.

Angeles, R., Lee, H. J., Alpak, F. O., & Torres-verdin, C. (2005). *Efficient and accurate estimation of permeability and permeability anisotropy from straddle-packer formation tester measurement using the physics of two-phase immiscible flow and invasion*. SPE Paper-95897, presented at the SPE Annual Conference and Exhibition, October, Dallas-TX.

Ansah, J., Proett, M. A., & Soliman, M. Y. (2002). *Advances in well completion design: A new 3-D finite element wellbore inflow model for optimizing performance of perforated completion*. Paper SPE-73760-MS, presented

at the International Symposium and Exhibition on Formation Damage Control, 20–21 February, Lafayette-Louisiana.

API. (1960). *Recommended practice for core analysis procedure – API RP 40*. The American Petroleum Institute.

API. (1998). *Recommended Practice 40: Recommended Practices for Core Analysis. Second Edition.* The American Petroleum Institute.

Archer, J. S., & Wall, C. G. (1986). *Petroleum engineering: Principles and practice*. London: Graham & Trotman Ltd, Sterling House.

Atkinson, J. H., & Bransby, P. L. (1978). *The mechanics of soil: An introduction to critical soil mechanics.* London: McGraw Hill.

Austad, T., Rezaei Doust, A., & Puntervold, T. (2010). *Chemical mechanism of low salinity water flooding in sandstone reservoirs*. SPE Paper #129767, presented at the 2010 SPE Improved Oil Recovery Symposium, 24–28 April, Tulsa - Oklahoma.

Austad, T., Shariatpanahi, S. F., Strand, S., Black, C. J. J., & Webb, K. J. (2011). *Condition for low salinity EOR-effect in carbonate oil reservoirs*. Proceeding, presented at the 32nd Annual IEA EOR Symposium and Workshop, 17–19 October, Vienna–Austria.

Austad, T., & Standnes, D. C. (2003). Spontaneous imbibition of water into Oil-wet carbonates. Journal of Petroleum Science and Engineering, 39.

Bakhtiari, A. H., Moosavi, S. A., Kazemzadeh, E., Goshtasbi, K., Esfahani, M. R., & Vall, J. (2011). The effect of rock types on pore volume compressibility of limestone and dolomite samples. *Geopersia*, *I* (1), 37–46.

Barclay, S. A., & Worden, R. H. (2000). Effects of reservoir wettability on quartz cementation in oil fields, in quartz cementation in sandstones (eds. R.H. Worden & S. Morad). *IAS Special Publication*, *29*, 147–161.

Barclays, S. A., & Worden, R. H. (2000). Effects of reservoir wettability on quartz cementation in oil fields. *Special Publications of the International Association of Sedimentologists*, *29*, 103–117.

Beard, D. C., & Weyl, P. K. (1973). Influence of texture on porosity and permeability of unconsolidated sand. *AAPG Bulletin*, *57*, 349–369.

Benson, P. M., Meredith, P. G., Platzman, E. S., & White, R. E. (2005). Pore fabric shape anisotropy in porous sandstones and its relation to elastic wave velocity and permeability anisotropy under hydrostatic pressure. *International Journal of Rock Mechanics and Mining Sciences, 42* (7–8), 890–899.

Besson, J. (1990). *Performance of slanted and horizontal wells on an anisotropic medium*. SPE Paper #20965, presented at Europec 90, The Hague – Netherlands, October 22 – 24.

Betts, W. S., Flemming, P. B., & Schneider, J. (2011). *Permeability and compressibility of resedimented gulf of Mexico Mudrock*. Paper # MR43A-2133, American Geophysical Union Fall Meeting.

Bjorkum, P. A., & Nadeau, P. H. (1998). Temperature controlled porosity/ permeability reduction, fluid migration, and petroleum exploration in sedimentary basins. *Australian Petroleum Production and Exploration Association Journal*, *38*, 453–465.

Bjorkum, P. A., Oelkens, E. H., Nadeau, P. H., Walderhaug, O., & Murphy, W. M. (1998). Porosity prediction in quartzose sandstone as a function of time, temperature, depth, stylolite frequency, and hydrocarbon saturation. *AAPG Bulletin*, *82*, 637–648.

Bloch, S., Lander, R. H., & Bonnell, I. (2002). Anomalously high porosity and permeability in deeply buried sandstone reservoir: Origin and predictability. *AAPG Bulletin*, *86*, 301–328.

Block, A., & Simms, B. B. (1967). Desorption and exchange of absorbed octadecylamine and stearic acid on steel and glass. *Journal of Colloid and Interface Science*, *25*, 514.

Bobek, J. E., & Mattax, C. C. (1958). Reservoir rock wettability - Its significance and evaluation. *Trans. AIME*, *213*, 155–160.

Bradley, H. B. (Ed.). (1987). Petroleum engineering handbook. *Society of Petroleum Engineers*, ISBN: 1555630103 9781555630102, p: 1842.

Brons, F., & Marting, V. E. (1961). The effect of restricted fluid entry on well productivity. *Journal of Petroleum Technology*, *February*, 172–174.

Buckles, R. S. (1965). Correlating and averaging connate water saturation data. *Journal of Canadian Petroleum Technology*, *9* (1), 42–52.

Buckley, J.S., Takamura, K., and Morrow, N.R. (1989). *Influence of electrical surface charges on the wetting properties of crude oils. SPE Reservoir Engineering, 4,* 332–340.

Buckley, J. S., Liu, Y., & Monsterleet, S. (1998). Mechanisms of wetting alteration by crude oils. *SPE Journal*, *3* (1), 54–61.

Bukar, M. (2013). *Does oil emplacement stop diagenesis and quartz cementation in deeply buried sandstone reservoirs*. (Doctor of Philosophy Thesis), University of Liverpool.

Burton, D., & Wood, L. J. (2013). Geologically-based permeability anisotropy estimates for tidally-influenced reservoirs using quantitative shale data. *Petroleum Geoscience*, *19* (1), 3–20.

Calhoun, J. C. Jr. (1953). *Fundamentals of reservoir engineering*. Norman, Oklahoma: University of Oklahoma Press.

Chapman, R. E. (1986). *Petroleum geology – I*. New York: Elsevier Science Pub.

Chilingarian, G. V., & Yen, T. F. (1983). Some notes on wettability and relative permeabilities of carbonate rocks. *Energy Sources*, *7* (1), 67–75.

Clennell, M.B., Dewhurst, D.N., Brown, K.M., & Westbrook, G.K. (1999). Permeability anisotropy of consolidated clays. In A.C. Aplin, A.J Fleet, & J.H.S MacQuacker (Eds.), *Geological society's special publication vol. 158–Muds and mudstones: Physical and fluid-flow properties* (pp: 79 – 96). London: Geological Society.

Coates, G. R., & Dumanoir, J. L. (1974). A new approach to improve log-derived permeability. *The Log Analyst*, *XV* (1), 17–29.

Cox, D. O., Stinson, S. H., & Stellavato, J. N. (2000). *Well testing in ultra high permeability formation*. SPE Paper #63279, presented at SPE Annual Technical Conference & Exhibition, October 1–4, Dallas-TX.

Craft, M., & Keelan, D. K. (1985). Coring, Part 7–Analystical aspect of sidewall coring. *World Oil*, *201*, 77–90.

Craig, F. F. (1971). *The reservoir engineering aspects of water flooding*, SPE Monograph Series, Richardson-TX, Chapter 2.

Crowell, E., Bennion, D. B., Shaw, D., & King, H. (1995). *Use of petrophysical measurements to determine by-passed pay potential*. Proceeding presented at the 1st Annual International Conference on Reservoir Conformance, Profile Control, and Gas Shutoff, 21–23 August, Houston-TX, USA.

Dake, L. P. (1978). *Fundamentals of reservoir engineering*. Amsterdam: Elsevier Science BV.

Datta Gupta, A., Pope, G. A., & Sepehrnoori, K**.** (1986). *Effects of reservoir heterogeneity on chemically enhanced oil recovery*. SPE/DOE 14889, Proceeding 5th Symposium on Enhanced Oil Recovery, Tulsa-Oklahoma, USA, April 20 – 23.

Denekas, M. O., Mattax, C. C., & Davis, G. T. (1959). Effect of crude oil composition on rock wettability. *Trans. AIME*, *216*, 330–333.

deWall, J. S., & Smits, R. M. M. (1988). Prediction of reservoir compaction and surface subsidence: Field application of a new model. *SPE Formation Evaluation*, *3* (2), 347–356.

Dicksen, T., Hirasaki, G. J., & Miller, C. A. (2002). Mobility of foam in heterogeneous media: Flow parallel and perpendicular to stratification. *SPE Journal*, *7* (2), 203–212.

Donaldson, E. C., Lorenz, P. B., & Thomas, R. D. (1969). Wettability determination and its effect on recovery efficiency. *Society of Petroleum Engineers Journal*, *9* (1), 13–20.

Dubey, S. T., & Doe, P. H. (1993). Base number and base wetting properties of crude oils. *SPE Reservoir Engineering*, *August*, 195–200.

Dunham, R. J. (1962). *Classification of carbonate rocks according to depositional texture*. In Ham, W. E., ed. Classification of Carbonate Rocks–A Symposium. AAPG Memoir, No. 1, 108–121.

Duquerroix, J-P. L., Lemouzy, P., Noetinger, B., & Romeu, R. K. (1993). *Influence of permeability anisotropy ratio on large-scale properties of heterogeneous reservoirs*. Paper SPE-26612-MS, presented at the SPE Annual Technical Conference and Exhibition, 3-6 October, Houston-TX.

East, L., Willett, R., Surjaatmadja, J., & McDaniel, B. W. (2004). *Application of new fracturing technique improves stimulation success for openhole horizontal completions*. SPE-86480-MS, presented at SPE International Symposium and Exhibition on Formation Damage Control, 18–20 February, Lafayette-Lousiana.

Economides, M. J., Brand, C. W., & Frick, T. P**.** (1996). Well configurations in anisotropic reservoirs. *SPE Formation Evaluation*, *December*, 257–262.

Ehrenberg, S.N., & Jakobsen, K. G. (2001). Plagioclase dissolution caused by biodegradation of oil in the Brent Group Sandstones (Middle Jurassic) of Gullfaks Field Northern North Sea. *Sedimentology*, *48*, 703–721.

Ehrenberg, S. N., & Nadeau, P. H. (2005). Sandstone vs carbonate petroleum reservoirs: A global perspective on porosity – depth and porosity – permeability relationships. *AAPG Bulletin*, *89* (4), 435–445.

Ehrenberg, S. N., Nadeau, P. H., & Steen, O. (2009). Petroleum reservoir porosity versus depth: Influence of geological age. *AAPG Bulletin*, *93* (10), 1281–1296.

Ennis-King, J., & Paterson, L. (2002). *Engineering aspects of geological sequestration of carbon dioxide*. SPE Paper-77809-MS, presented at the SPE

Asia Pacific Oil and Gas Conference and Exhibition, 8–10 October, Melbourne-Australia.

Fardiansyah, I., Budiman, A., & Prasetyadi, C. (2010). *Identifying rock compressibility influence on delta facies at Simpang Pasir Area, Samarinda Seberang, Kutai basin and its relation to reservoir characterization*. Paper IPA 10-SG-11, Proceeding, Indonesian Petroleum Association 34th Annual Convention and Exhibition, May.

Fatt, I. (1958). Volume compressibilities of sandstone reservoir rocks. *Journal of Petroleum Technology*, *10* (3), 64–66.

Fetkovich, M. J., Reese, D. E., & Whitson, C. H. (1991). *Application of a general material balance for high-pressure gas reservoirs*. SPE paper #22921, presented at 66th Technical Annual Conference and Exhibition of the Society of Petroleum Engineers, Dalas-Texas, October 6–9.

Furui, K., Zhu, D., & Hill, A. D. (2003). A rigorous formation damage skin factor and reservoir inflow model for a horizontal well. *SPE Production & Facillities*, *18* (3), 151–157.

Gatens, J. M., Lee, W. J., Hopkins, C. W., & Lancaster, D. E. (1991). *The effect of permeability anisotropy on the evaluation and design of hydraulic fracture treatments and well performance*. SPE Paper 21501, presented at the SPE Gas Technology Symposium, held in Houston-Texas, January 23–25.

Gautier, D. L., & Schmoker, J. W. (1989). *Evaluation of sandstone porosity from thermal maturity information*, in Short Course in Burial Diagenesis (Ed.: I.E. Hutcheon), Mineralogical Association of Canada, 15, 135–148.

Geertsma, J. (1957). The effect of fluid pressure decline on volumetric changes of porous rocks. *Petroleum Transaction AIME*, *210*, 331–340.

Geertsma, J. (1973). Land subsidence above compacting oil and gas reservoirs. *Journal of Petroleum Technology*, *25* (6), 734–744.

Geffen, T. M., Owens, W. W., Parrish, D. R., & Morse, R. A. (1951). Experimental investigation of factors affecting laboratory relative permeability measurements. *Trans. AIME*, *192*, 99–110.

Giles, M. R., & de Boer, R. B. (1990). Origin and significance of redistributioal secondary porosity. *Marine and Petroleum Geology*, *7*, 378–397.

Gratier, J-P., Dysthe, D. K., & Renard, F. (2013). The role of pressure solution creep in the ductility of the Earth's upper crust. *Advances in Geophysics*, *54*, 47-179. doi: 10.1016/B978-0-12-380940-7.00002-0.

Gluyas, J., & Cade, C. A. (1997) *Prediction of porosity in compacted sands*. In "Reservoir Quality Prediction in Sandstones and Carbonates" (Eds.: Kupecz, J.A., Gluyas, J.G., dan Bloch, S.), AAPG Memoir 69, AAPG Publisher, Tulsa – Oklahoma, USA 74101.

Gu, F., & Chalaturnyk, R. (2010). Permeability and porosity models considering anisotropy and discontinuity of coalbeds and applicaion on coupled simulation. *Journal of Petroleum Science and Engineering*, *74* (3), 113–131.

Gutierrex, M. (1998). *The role of geomechanics in reservoir simulations*. SPE Paper #47392, presented at the SPE/ISRM Rock Mechanics in Petroleum Engineering, 8–10 July, Trondheim – Norway.

Hamilton, E. L. (1976). Variations of density and porosity with depth in deep-sea sediments. *Journal of Sedimentary Petrology*, *46* (2), 280–300.

Hall, H. N. (1953). Compressibility of reservoir rocks. *Journal of Petroleum Technology*, *5* (1), 17–19.

Harari, Z., Wang, T. W., & Saner, S. (1995). Pore-compressibility study of arabian carbonate reservoir rocks. *SPE Formation Evaluation*, *10* (4), 207–214.

Harris, Jr, O. A. (1992). A relationship between critical and irreducible water saturations. *Gulf Coast Association of Geological Societies Transactions*, *42*, 809–809.

Harrison, B., & Jing, X. D. (2001). *Saturation height methods and their impact on volumetric hydrocarbon in place estimates*. Paper SPE #71326, presented at the 2001 SPE Annual Technical Conference and Exhibition held in New Orleans, Louisiana, 30 September–3 October.

Heidari, Z., Torres-verdin, C., Mendoza, A., & Wang, G. L. (2011). Assessment of residual hydrocarbon saturation with the combined quantitative interpretation of resistivity and nclear logs. *Petrophysics*, *52* (3), 217–237.

Heinemann, Z. E., Brand, C. W., Munka, M., & Chen, Y. M. (1991). Modeling reservoir geometry. *SPE Reservoir Engineering*, *6* (2), 225–232.

Hirasaki, G.J. (1991). Wettability: Fundamental and surface forces. *SPE Formation Evaluation, 6*(2), 217–226.

Hoeiland, S., Barth, T., Blokhus, A. M., & Skauge, A. (2001). The effect of crude oil acid fractions on wettability as studies by interfacial tension and contact angles. *Journal of Petroleum Science and Engineering*, *30*, 91–103.

Holmes, M., Holmes, A., & Holmes, D. (2009). *Relationship between porosity and water saturation: Methodology to distinguish mobile from capillary bound water*. Proceeding, presented at the AAPG Annual Convention and Exhibition, 7–10 June, Denver – Colorado.

Horne, R. N. (1995). *Modern well test analysis: A computer aided approach*. Petroway Publisher, 2nd edition, p: 257.

Hudson, J.A. & Cooling, C.M. (1988) In situ rock stresses and their measurement in the UK–Part 1: The current state of knowledge. *Int. J. Rock Mech. Min. Sci & Geomech. Abstr., 25*, 363–70.

Inameta. (2006). *Indonesia – Basin summaries*. Jakarta, Indonesia: PT Patra Nusa Data.

Jackson, M. D., Valvatne, P. H., & Blunt, M. J. (2003). Prediction of wettability variation and its impact on flow using pore- to reservoir-scale simulations. *Journal of Petroleum Science and Engineering*, *39*, 231–246.

Jadhunandan, P. P., & Morrow, N. R. (1995). Effect of wettability on waterflood recovery for crude-oil/brine/rock systems. *Soc. Pet. Eng. Res. Eng., 10*, 40– 46.

Landrum, B. L. & Crawford, P. B. (1960). Effect of directional permeability on sweep efficiency and production capacity. *Journal of Petroleum Technology*, *12* (11): 67–71.

LEMIGAS. (2006). *Kuantifikasi Sumber Daya Hidrokarbon-volume 1: Kawasan Barat Indonesia*. Jakarta: Pusat Penelitian dan Pengembangan Teknologi Minyak dan Gas Bumi.

Li, C., Chen., X., & Du, Z. (2004). A *new relationship of rock compressibility with porosity*. SPE Paper #88464, presented at the SPE Asia Pacific Oil and Gas Conference and Exhibition, 18–20 October, Perth-Australia.

Liu, H. H., Rutqvist, J., & Berryman, J. G. (2009). On the relationship between stress and elastic strain for porous and fractured rocks. *International Journal of Rock Mechanics and Mining Sciences*, *46* (2), 289–296.

Loucks, R. G., Bebout, D. G., & Galloway, W. E. (1977*).* Relationship of porosity, formation, and preservation to sandstone consolidation history–gulf coast lower tertiary frio formation. *Gulf Coast Association of Geological Societies Transactions*, *27*, 109–120.

Ma, S., Morrow, N. R., & Zhang, X. (1999). Characterization of wettability from spontaneous imbibition measurements. *Journal of Canadian Petroleum Technology (Special Edition)*, *38* (13), 56.

Manseur, S., Tiab, D., Berkat, A., & Zhu, T. (2002). *Horizontal and vertical permeability determination in clean and shally reservoirs uing in-situ measurement*. SPE Paper 75773, presented at SPE WR/AAPG Pacific Section Joint Meeting, Anchorage, Alaska, 20–22 May.

Marchand, A. M. E., Haszeldine, R. S., Smalley, P. C., Macaulay, C. I., & Fallick, A. E. (2001). Evidence for reduced quartz-cementation rates in oil-filled sandstones. *Geology*, *29*, 915–918.

Marechal, J. C., Dewandel, B., & Subramanyam, K. (2004). Use of hydraulic tests at different scales to characterize fracture network properties in the wheathered-fractured layer of a hard rock aquifer. *Water Resources Research*, *40* (11), November.

Masalmeh, S. K., Abu-Shiekah, I. M., & Jing, X. (2007). Improved characterization and modeling of capillary transition zones in carbonate reservoirs. *SPE Reservoir Evaluation & Engineering*, *10* (2), 191–204.

Mattax, C. D., & Kyte, J. R. (1962). Imbibition oil recovery from fractured water drive reservoir. *SPEJ*, 177–184.

McGuire, W. J., & Sikora, V. J. (1960). The effect of vertical fractures on wells productivity. *Trans. AIME*, *219*, 401–403.

Mennella, A., Morrow, N. R., & Xie, X. (1995). Application of the dynamic Wilhelmy Plate to identification of slippage at a liquid-liquid-solid three phase line of contact. *JPSE*, *13*, 179–192.

Meyer, R. (2002). Anisotropy of sandstone permeability. *CREWES Research Report*, *14*, 1–12.

Meyer, R., & Krause, F. F. (2006). Permeability anisotropy and heterogeneity of a sandstone reservoir analogue: An estuarine to shoreface depositional system in the Virgelle Member, Milk River Formation, Writing-on-Stone Provincial Park, southern Alberta. *Bulletin of Canadian Petroleum Geology*, *54* (04), 301–318.

Moncada, K. (2003). *Application of TDS technique to calculate vertical and horizontal permeabilities for vertical wells with partial completion and partial penetration, (*M.Sc. Thesis), University of Oklahoma.

Mondol, N. H., Jahren, J., Berre, T., Grande, L., & Bjorlykke, K. (2010). *Permeability anisotropy in mudstones - An experimental study*. Presented at AAPG Annual Convention and Exhibition, New Orleans, Louisiana, April 11–14.

Morrow, N.R. (1976), Capillary-pressure correlations for uniformly wetted porous-media. *J. Can. Pet. Technol., 15*(4), 49–69.

Morton, K., Thomas, S., Corbett, P., & Davies, D. (2002). Detailed analysis of probe permeameter and interval pressure transient test permeability measurement in a heterogeneous reservoir. *Petroleum Geoscience*, *8*, 209–216.

Morvan, M., Chabert, M., Tabary, R., & Bazin, B. (2011). *Fractured carbonates: A methodology to evaluate surfactant performance for wettability alteration*. Presented at the 32nd Annual Symposium and Workshop-IEA Collaborative Project on Enhanced Oil Recovery, 17–19 October, Vienna - Austria.

Myers, M. T., & Hatton, L. A. (2011). *Prediction of Rock Properties in the Gulf of Mexico*. American Rock Mechanics Association Paper #11-353, presented at the 45th U.S. Rock Mechanics/Geomechanics Symposium, June 26–29, San Francisco – California, USA.

Mwangi, P., Thyne, G., & Rao, D. (2013), *Extensive experimental wettability study in sandstone and carbonate-oil-brine systems: Part 1 – screening tool development*. Paper SCA #3013-84, presentated at the International Symposium of the Society of Core Analysts held in Napa Valley, California, USA, 16–19 September.

Nagtegaal, P. J. C. (1978). Sandstone framework instability as a function of burial diagenesis. *Journal of the Geological Society*, *135*, 101–105.

Newman, G. H. (1973). Pore-volume compressibility of consolidated, friable, and unconsolidated reservoir rocks under hydrostatic loading. *Journal of Petroleum Technology*, *25* (2), 129–134.

Nisle, R. G. (1958), The Effect of Partial Penetration on Pressure Build-Up in Oil Wells. *Trans. AIME*, *213*, 85–90.

Odeh, A. S., & Babu, D. K. (1990). Transient Flow Behavior of Horizontal Wells, Pressure Drawdown, and Buildup Analysis. *SPE Formation Evaluation*, *March*, 7–15.

Ogbe, O. B., Opatola, O. A., Wilson, I., & Azuka, O. (2013). Reservoir Quality Evaluation of Sand Bodies of K-Field, Onshore Niger Delta, Using Wireline Logs. *International Journal for Science and Emerging Technologies with Latest Trends*, *13* (1), 46–64.

Osborne, M. J., & Swarbrick, R. E. (1999). Diagenesis in North Sea HPHT Elastic Reservoirs – Consequences for Porosity and Overpressure Prediction. *Marine and Petroleum Geology*, *16*, 337–353.

Pan, Z., & Connell, L. D. (2012). Modeling Permeability for Coal Reservoirs: A Review of Analytical Models and Testing Data. *International Journal of Coal Geology*, *92*, 1–44.

Pathak, P., & Wirya, S. I. (2007). *Impact of Rock Compaction on NSO Gas Field Performance*. Paper #11238, presented at the International Petroleum Conference, 4 – 6 December, Dubai – UAE.

Paul, P. K., Zoback, M., & Hennings, P. (2011). A method to implement permeability anisotropy associated with fault damage zones in reservoir simulation. *Society of Petroleum Engineers, SPE Reservoir Evaluation & Engineering*, *14* (1), 138–152.

Peffer, M. A., & O'Callagan, P. J. (1997). *In-situ determination of permeability anisotropy and its vertical distribution – A case study*, SPE Paper #38942, Proceeding, SPE ATCE, San Antonio, Texas, 5–8 October.

Permadi, P., Kurnia, I., & Budiarto, A. (2011). *Rock typing and permeability prediction for water-wet and oil-wet rocks*. Proceeding, presented at the International Symposium of the Society of Core Analysts held in Austin, Texas, USA 18–21 September.

Pinzon, C. L., Chen, H. Y., & Teufel, L. W. (2001). *Numerical well test analysis of stress-sensitive reservoirs*. SPE Paper #71034, presented at the SPE Rocky Mountain Petroleum Technical Conference, 21 – 23 May, Keystone – Colorado.

Pittman, E. D., & Larese, R. E. (1991). Compaction of lithic sand: Experimental results and application. *AAPG Bulletin*, *75*, 279–299.

Qiao, C., Li, L., Johns, R. T., & Xu, J. (2014). *A mechanistic model for wettability alteration by chemically tuned water flooding in carbonate reservoirs*. SPE Paper #170966, presented at the SPE Annual Technical Conference and Exhibition held in Amsterdam, The Netherlands, 27–29 October.

Rajayi, M., & Kantzas, A. (2011). Effect of temperature and pressure on contact angle and interfacial tension of quartz/water/bitumen system. *Journal of Canadian Petroleum Technology*, *50* (6), 61–67.

Ramm, M., & Bjorlykke, K. (1994). Porosity/depth trends in reservoir sandstones: Assessing the quantitative effects of varrying pore pressure, temperature history and mineralogy, Norwegian Shelf Data. *Clay Minerals*, *29*, 475–490.

Ramm, M., Forsberg, A. W., & Jahren, J. (1997). *Porosity depth trends in deeply burried upper jurassic reservoirs in the Norwegian Central Graben: An example of porosity preservation beneath the normal economic basement*

by grain-coating micro-quartz. In "Reservoir Quality Prediction in Sandstones and Carbonates" (Eds.: Kupecz, J.A., Gluyas, J.G., dan Bloch, S.), AAPG Memoir 69, AAPG Publisher, Tulsa – Oklahoma, USA 74101.

Rao, D. N. (1999). Wettability effects in thermal recovery operations. *SPE Reservoir Evaluation.& Engineering*, *2*, 420-430.

Rao, D. N., & Girard, M. G. (1996). A new technique for reservoir wettability characterization. *Journal of Canadian Petroleum Technology*, 31-39.

Renard, F., Brosse, E., & Gratier, J. P. (2000). The different processes involved in the mechanism of pressure solution in quartz-rich rocks and their interactions. *International Association Sedimentologists Special Publication*, *29*, 67–78.

Renard, G., & Dupuy, J .M. (1991). Formation damage effects on horizontal well flow efficiency. *Journal of Petroleum Technology*, *43* (7), 786–869.

Ringen, J. K., Halvorsen, C., Lehne, K. A., Rueslaatten, H., & Holland, H. (2001). *Reservoir water saturation measured on cores: Case histories and recommendation*. Proceeding of the 6th Nordic Symposium on Petrophysics, 15–16 May, Trondheim -Norway.

Ruddy, I., Andersen, M. A., Pattillo, P. D., Bishlawi, M., & Foged, N. (1989). Rock compressibility, compaction, and subsidence in a high-porosity chalk reservoir: A case study of valhall field. *Journal of Petroleum Technology*, *41* (7), 741–746.

Ruistuen, H., Teufel, L. W., & Rhett, D. (1999). Reservoir stress path on deformation and permeability of weakly-cemented sandstone reservoirs. *SPE Reservoir Evaluation and Engineering*, *2* (3), 266–272.

Sahin, A., Ali, A. Z., Saner, S., & Menuoar, H. (2007). Permeability anisotropy distribution in an upper jurassic reservoir, Eastern Saudi Arabia. *Journal of Petroleum Geology*, *30* (2), 147–158.

Saleh, M., Vega, S., Prasad, M., & Sharma, R. (2009). *A study of permeability and velocity anisotropy in carbonates.* Paper SEG-2009-4238, presented at SEG Annual Meeting, 25–30 October, Houston-TX.

Saneifar, M., Nasr-El-Din, H.A., Nasralla, R.A., & Hill, D. (2011), *Effect of spent acids on the wettability of sandstones and carbonates at high temperature and pressure.* SPE-144132-MS, presented at the SPE European Formation Damage Conference, 7–10 June, Noordwijk, The Netherlands.

Satter, A., Iqbal, G. M., & Buchwalter, J. L. (2007). *Practical enhanced reservoir engineering*. PennWell Corporation, 1421 South Sheridan Road, Tulsa – Oklahoma 74112 – 6600 USA, p: 688.

Shapiro, S. A., Audigane, P., & Royer, J-J. (1999). Large-scale in situ permeability tensor of rocks from induced microseismicity. *Geophysical Journal International*, *137* (1), 207–213.

Sattler, U., Zampetti, V., Schlager, W., & Immenhauser, A. (2004). Late leaching under deep burial condition: A case study of the Miocene-Zhujiang carbonate reservoir, South China Sea. *Marine and Petroleum Geology*, *21*, 977–992.

Sayyouh, M.H., Dahab, A.S. & Omar, A. (1990), Effect of clay content on wettability of sandstone reservoir. *Journal of Petroleum Science, 4*(2), 119–125.

Sayyouh, M. H., Hemeida, A. M., Al Blehed, M. S., & Desouky, S. K. (1991). Role of polar compounds in crude oils on rock wettability. *Journal of Petroleum Science*, *6*, 225–233.

Scherer, M. (1987). Parameters influencing porosity in sandstones: A model for sandstone porosity prediction. *AAPG Bulletin*, *71* (5), 485–491.

Schlumberger. (1986). *Formation evaluation conference, Indonesia*. P.T. Ichtiar Baru – Van Hoeve Publishing, 2nd edition.

Shedid, S.A., & Ghannam, M. T. (2004). Factors affecting contact-angle measurement of reservoir rocks. *Journal of Petroleum Science and Engineering*, *44* (3-4), 193–203.

Smith, R. K., Sawyer, W. K., & Esposito, P. R. (1981). *The effect of anisotropy and vertical fracture penetration on production decline curves for low permeability gas wells*. SPE Paper 10369, presented at the 1981 Eastern Regional Meeting of the Society of Petroleum Engineers of AIME, held in Columbus – Ohio, November 4–6.

Straley, C., Rossini, D., Vinegar, H., Tutunjian, P., & Morriss, C. (1994), *Core analysis by low field NMR*. The Society of Core Analysts, SCA Paper#9404.

Sulak, A. M., & Danielsen, J. (1988). *Reservoir aspects of ekofisk subsidence*. SPE Paper #5618, presented at the Offshore Technology Conference, 2–5 May, Houston – TX.

Taktak, F., Rigane, A., Boufares, T., Kharbachi, S., & Bouaziz, S. (2011). Modeling approaches for the estimation of irreducible water saturation

and heterogeneities of the commercial Ashtart Reservoir from the Gulf of Gabes, Tunisia. *Journal of Petroleum Science and Engineering*, *78* (2), 376–383.

Tariq, S. M., Ichara, M. J., & Ayestaran, L. (1989). *Performance of perforated completion in the presence of anisotropy, laminations, or natural fractures.* SPE Paper 14320.

Teeuw, D. (1971). Prediction of formation compaction from laboratory compressibility data. *Society of Petroleum Engineering Journal*, *11* (3), 263–271.

Tiab, D., & Donaldson, E. C. (2004). *Petrophysics: Theory and practice of measuring reservoir rock and fluid transport properties*. MA: Gulf Professional Publishing.

Timmerman, E. H. (1982). *Practical reservoir engineering – Methods for improving accuracy or input into equations and computer programs*. Oklahoma: PennWell publishing Company.

Timur, A. (1968). An investigation of permeability, porosity, and residual water saturation relation for sandstone reservoirs. *Log Analysts*, *9*, 4.

Tissot, B. P., & Welte, D. H. (1978). *Petroleum formation and occurrence*. Heidelberg: Springer – Verlag Pub. Co.

Tixier, M. P. (1949). Evaluation of Permeability from Electric Log Resistivity Gradient. *Oil and Gas Journal*, *June 16*.

Torskaya, T., Jin, G., & Torres-Verdin, C. (2007). *Pore-level analysis of the relationship between porosity, irreducible water saturation, and permeability of clastic rocks.* SPE Paper #109878, presented at the SPE Annual Technical Conference and Exhibition, 11–14 November, Anaheim – California.

Tran, D., Settari, A., & Nghiem, L. (2004). New itterative coupling between a reservoir simulator and a geomechanics module. *SPE Journal*, *9* (3), 362–369.

Treiber, L. E., Archer, D., & Owens, W. W. (1972). A laboratory evaluation of the wettability of fifty oil producing reservoirs. *Society of Petroleum Engineering Journal*, *12* (6), 531–540.

Uguru, C., Udofia, A., & Oladiran, O. (2010). *Estimating irreducible water saturation and relative permeability from logs*. SPE-140623-MS, presented at the Nigeria Annual International Conference and Exhibition, 31 July–7 August, Tinapa-Calabar, Nigeria.

U.S. Geological Survey Geologic Names Committee. (2007). Divisions of geologic time-Major chronostratigrapic and geochronologic unit. *U.S. Geological Survey Fact Sheet 2007–3015*. Retrieved from pubs.usgs.gov/fs/2007/3015/ on March 2015

Vera, R. (2009). *Characterization of Roabiba Sandstone Reservoirs in Bintuni Field, Papua, Indonesia*. M.Sc Thesis, Graduate Studies – Texas A&M University, Texas-USA, p: 112.

Vesic, A. S., & Clough, G. W. (1968). Behaviour of granular material under high stresses. *Journal of Soil Mechanics Foundation Division*, *94*, 661–688.

Wang, Y., Bandal, M.S., Moreno, J.E., & Sakdilah, M.Z. (2006), *A systematic approach to incorporate capillary pressure-saturation data into reservoir simulation*. SPE-101013-MS, presented at the SPE Asia Pacific Oil & Gas Conference and Exhibition, 11–13 September, Adelaide-Australia.

Welge, H.J. & Bruce, W.A. (1947). The restored state method for determination of oil in place and connate water. *In Drilling and Production Practices*. New York: American Petroleum Institute.

Widarsono, B. (2008a). Ketidaktepatan dalam pemakaian model saturasi air dan implikasiny (Inaccuracy in the use of various water saturation models and the implications). *Lembaran Publikasi LEMIGAS*, *42* (2), 10–18.

Widarsono, B. (2008b). Perubahan sifat kebasahan fluida dan sifat kelistrikan batuan reservoir: Isu lama, problem aktual (Change in reservoir rocks' wettability and its influence on electrical characteristics: Old issue, ever present problem). *Lembaran Publikasi LEMIGAS*, *42* (1), 20-28.

Widarsono, B. (2009). Pengaruh dari kompresibilitas rekahan pada estimasi volume awal gas di tempat (Influence of fracture compressibility in the estimation of initial gas in place). *Lembaran Publikasi LEMIGAS*, *43* (1), 59-64.

Widarsono, B. (2010). An investigation over rock wettability and its alteration on some Indonesian sandstones. Accepted for publication in *Lemigas Scientific Contributions to Petroleum Science & Technology*.

Widarsono B. (2011a). Irreducible water saturation and its governing factors: Characteristics of some sandstones in Western Indonesia. *LEMIGAS Scientific Contributions to Petroleum Science & Technology*, *34* (1), 19–34.

Widarsono B. (2011b). Rock wettability characteristics of some indonesian limestones. Case study: Baturaja formation. *Scientific Contributions Oil & Gas*, *34* (2), 105–116.

Widarsono, B. (2014a). The Rock compressibility characteristics of some indonesian reservoir limestones. *Scientific Contributions Oil & Gas*, *47* (1), 1–14.

Widarsono, B. (2014b). Porosity versus depth characteristics of some reservoir sandstones in Western Indonesia. *Scientific Contributions Oil & Gas*, *37* (2), 87–104.

Widarsono, B., Muladi, A., & Jaya, I. (2006). *Permeability vertical-to-horizontal anisotropy in Indonesian oil and gas reservoirs: A general review*. SPE Paper 103315 PP, presented at the 2006 International Oil Conference and Exhibition, 31 August–02 September, Cancun – Mexico.

Widarsono, B., Muladi, A., & Jaya, I. (2007). *Vertical–horizontal permeability ratio in indonesian sandstone and carbonate reservoirs.* Proceeding, presented at IATMI National Symposium, Yogyakarta 25–28 July.

Wilkinson, M., & Haszeldine, R. S. (2011). Oil charge preserves exceptional porosity in deeply buried, overpressured, sandstones: Central North Sea, UK. *Journal of the Geological Society*, *168*, 1285–1295.

Wilkinson, M., Haszeldine, R. S., & Fallick, A. E. (2006). Hydrocarbon filling and leakage history of a deep overpressured sandstone, fulmar formation, UK North Sea, *AAPG Bulletin*, *90*, 483–491.

Wolcott, J. M., Groves Jr, F. R., Trujillo, D. E., & Lee, H. G. (1993). Investigation of crude-oil/mineral interactions: Factors influencing wettability alteration. *SPE Advanced Technology Series*, *April*, 117–126.

Worden, R. H., Oxtoby, N. H., & Smalley, P. C. (1998). Can oil emplacement prevent quartz cementation in sandstones? *Petroleum Geoscience*, *4*, 129–137.

Wu, J., Torres-Verdin, C., Sepehmoori, K., & Delshad, M. (2004). Numerical simulation of mud-filtrate invasion in deviated well. *SPE Reservoir Evaluation & Engineering, 7*(2), 143–154.

Wu, Y., Shuler, P., Blanco, M., Tang, Y., & Goddard, W.A. (2008). An experimental study of wetting behavior and surfactant EOR in carbonates with model compounds. *SPE Journal, 13*(1), 26–34.

Wyllie, M. R. J., & Rose, W. D. (1950). Some theoretical considerations related to the quantitative evaluation of the physical characteristics of reservoir rock from electric log data. *Trans. AIME*, *189*, 105–118.

Xiao, L., Mao, Z. Q., & Jin, Y. (2012). Calculation of irreducible water saturation (S_{wirr}) from NMR logs in tight gas sands. *Applied Magnetic Resonance*, *42* (1), 113–125.

Xu, C., & Torres-Verdin, C. (2012). *Saturation-height and invasion hydraulic rock typing using multi-well conventional logs.* Proceeding, Presented at the SPWLA 53rd Annual Logging Symposium, June 16-20.

Xu, C., Torres-Verdin, C., Yang, Q., & Diniz-Ferreira, E. L. (2013). *Connate water saturation - irreducible or not: The key to reliable hydraulic rock typing in reservoirs straddling multiple capillary windows*. SPE Paper #166082, presented at the SPE Annual Technical Conference and Exhibition held in New Orleans, Louisiana, USA, 30 September–2 October.

Yale, D. P., Nabor, G. W., Russell, J. A., Pham, H. D., & Yousef, M. (1993). *Application of variable formation compressibility for improved reservoir analysis*. SPE Paper #26647, presented at the 68th Annual Technical Conference and Exhibition of the Society of Petroleum Engineers, 3–6 October, Houston – TX.

Yang, Y., & Aplin, A. C. (1998). Influence of lithology and compaction on the pore size distribution and modelled permeability of some mudstones from the Norwegian margin. *Marine and Petroleum Geology*, *15*, 163–175.

Yetkin, C., Ramirez, B., Al-kobaisi, M., Kazemi, H., & Ozkan, E. (2009). *A Simple method to account for permeability anisotropy in reservoir models and multi-well pressure interference tests*. SPE Paper #122972-MS, presented at SPE Rocky Mountain Petroleum Technology Conference, 14–16 April, Denver, Colorado.

Zahaf, K., & Tiab, D. (2002). Vertical permeability from in-situ horizontal permeability measurements in Shaly-Sand Reservoirs. *Journal of Canadian Petroleum Technology, August*, 43–50.

Zhang, P. M., & Austad, T. (2006). Wettability and oil recovery from carbonates: Effects of temperature and potential determining ions. *Colloid and Surface Area*, *279*, 179–187.

Zhang, Y., & Morrow, N. R. (2006). *Comparison of secondary and tertiary recovery with change in injection brine composition for crude oil/sandstone combinations*. SPE Paper #99757, presented at the 2006 SPE/DOE Symposium on Improved Oil Recovery, 22–26 April, Tulsa – Oklahoma.

Zhou, X., Morrow, N. R., & Ma, S. (2000). Interrelationship of wettability, initial water saturation, aging time, and oil recovery by spontaneous imbibition and waterflooding. *SPE Journal*, 199–207.

Zimmerman, R. W. (1991). *Compressibility of sandstones*. New York: Elsevier Science.

NOMENCLATURE

A_T - adhesive tension

A_1 - area under the curve of oil displacing water (USBM wettability test)

A_2 - area under the curve of water displacing oil (USBM wettability test)

C - constant in Wyllie and Rose model, dimensionless (oil C=250, gas C=79)

C_f - formation compressibility, psi^{-1}

D - depth, m

D' - effective depth, m

g - gravity force. m/s2

I - USBM wettability index

I_O - oil index (Amott wettability)

I_W - water index (Amott wettability)

K - permeability, mD

K_H - horizontal permeability, mD

K_{ro} - oil relative permeability, fraction

K_{rw} - water relative permeability, fraction

K_V - vertical permeability, mD

P - pressure, psi

P_c - capillary pressure, psi

P_{OB} - overburden pressure, psi

P_{res} - reservoir pressure, psi

r - pore radius

S_w - water saturation, percent or fraction

S_{wirr} - irreducible water saturation, percent or fraction

S_{wor} - residual oil saturation, percent or fraction

u - overpressure (MPa)

V_{oi} - produced oil volume in slow imbibition process

V_{od} - volume of oil forcefully displaced by oil

V_p - pore volume, cu-ft

V_{wi} - displaced volume of water in slow imbibition

V_{wd} - volume of water forcefully displaced by oil

Z - depth, km

θ - contact angle (in rock wettability), degree

θ_{wo} - contact angle between water and oil (in rock wettability), degree

ρ_r - rock bulk density, kg/m3

ρ_w - formation water density, kg/m3

σ - interfacial tension

σ_{so} - interfacial tension between solid and oil

σ_{sw} - interfacial tension between solid and water

σ_{wo} - interfacial tension between water and oil

ϕ - porosity, fraction

INDEX

Petrophysical Characteristics

of Some Indonesian Reservoir Rocks

Indonesia has been facing a serious challenge in meeting its oil and gas demands. Indonesia's domestic consumption continues to grow, while oil and gas reserves are depleting. As non-renewable sources, their supplies will always be limited. Therefore, optimizing the productivity of current reservoirs is a good alternative besides finding new reservoirs through field exploration.

In order to maximize energy production, rocks' petrophysical properties are important in determining the characterization of reservoirs. Reservoir characterization is important for mapping further development of oil and gas fields. This book, *Petrophysical Characteristics of Some Indonesian Reservoir Rocks*, is the authoritative guide on the petrophysical properties of rocks and reservoirs in Indonesia.

As the only primary sources of petrophysical properties of Indonesian rocks, the book will be an invaluable asset for the future of Indonesia's energy stability.

LEMIGAS
Research and Development Centre for Oil and Gas Technology
The Ministry of Energy and Mineral Resources Republic of Indonesia
Jl. Cileduk Raya Kav. 109, Cipulir, Kebayoran Lama
Jakarta Selatan 12230, Indonesia.
Phone. +62-21-7394422, 7394778
Fax. +62-21-7246150
www.lemigas.esdm.go.id

LIPI Press
ISBN 978-979-799-840-0